UNIVERSITY OF THE WITWATERSRAND
JOHANNESBURG

MSc Thesis

Application of Process Synthesis for the Recovery of Valuable Chemicals from an Industrial Waste Stream

Submitted by: Moratwe Molote

Supervisor: Prof Jean Mulopo

Date: 14/February/2018

Declaration

I declare that this thesis is my own unaided work. It is being submitted for the degree of Master of Science in Engineering at the University of the Witwatersrand, Johannesburg. It has not been submitted before for any degree or examination at another university.

Moratwe Molote

Abstract

This work aims at designing and simulating on Aspen Plus process simulator a process that can recover valuable chemicals from a High Organic Waste (HOW) stream produced at Sasol Secunda plant, South Africa. The waste is made up of low boiling point organic components such as pyridine, acetonitrile and Methyl Ethyl Ketone and water. Currently, the waste is incinerated without energy recovery. This practice serves to exacerbate the already high greenhouse gases emissions from the plant, but more importantly, it results in the missed opportunity to maximize revenues through resale of recycled valuable chemicals. The recovery of valuable chemicals from the HOW is made difficult by the formations of azeotrope between organic components and water; at least 6 azeotropes exist in the HOW stream. In this work the emphasis is on pyridine because of its established market value and demand. Pyridine market size is about 400 million USD in 2017 and is expected to increase to over 600 million USD by 2021 mainly due to increased usage in the agrochemical industry. Water integration strategy was also assessed demand because of the reported need to improve water utilization efficiency at Sasol Secunda plant.

The recovery was achieved in 2 separate steps: 1) water-pyridine mixture was separated from the rest of the HOW stream using fractional distillation and 2) pyridine enrichment section which was designed using thermodynamic tools such as residue curve maps and isovolatility curves. The rest of the HOW stream (light fractions) was sent to the currently used incinerator. Liquid-liquid extraction and azeotropic distillation were considered for the pyridine enrichment step. Results showed that the combination of liquid-liquid extraction and distillation offered the benefit of a lower entrainer to azeotropic mixture ratio (EA) compared to azeotropic distillation. This gave the lowest recorded EA at 0.320:1. The comparison between the proposed process and the incineration of the whole HOW stream showed that the implementation of the process proposed reduced the incineration load by 60wt% and CO and CO_2 emissions by 50%. Dividing Wall column process integration technique was implemented to reduce the number of distillation columns in the proposed process and 10% reduction in the reboiler and condenser duties was observed. Implementation of DWC further improved the purity of the recovered pyridine from 96mol% to over 99.9mol%. Preliminary economic evaluation carried out on Aspen Plus showed that the proposed recovery process was profitable with an Internal Rate of Return (IRR) of 20% and a payback period of 4.5 years.

Acknowledgements

I wish to express my sincere gratitude to the following people and organizations/institutions:

1. Prof Jean Mulopo (supervisor) for his guidance and patiently answering to my curiosities throughout my research. Moreover, thank you for assuming mentor position in my life and helping me deal with life challenges I encountered during my project, you are simply the best;
2. The school of Chemical and Metallurgical Engineering for affording me the opportunity to work on Aspen Plus process simulator;
3. My colleagues, Miss Lisa Shambare and Mr Jibril Abdulsalam for their advices and input in my research;
4. Sasol and National Research Foundation (NRF) for their financial support to carry out this work;
5. My mother (Kgomotso Molote) thank you for your unparalleled support and faith in me;
6. A big thank you to my life companion (Letlhogonolo Morake) for the support and encouragement you gave me throughout this journey, much love to you!
7. Finally, to God, the father of my Lord Jesus Christ for seeing me through this work.

Dedications

I would like to dedicate this thesis to my beautiful daughter (Realeboga Morake); I hope this mile stone will serve to inspire you to be the best version of yourself, reaching for the stars. I love you!!

I would like to further honor my late father (Letshwenyo Molote) with this work. You have always encouraged me unto academic excellence, thank you for that. Rest in eternal peace.

Table of Contents

List of Tables

List of Figures

Abbreviations List

Abbreviation	Explanation
DSTWU	Distillation Winn-Underwood
DWC	Dividing Wall Column
NRTL	Non-Random Two-Liquid
RCM	Residue Curve Map
UNIQUAC	Universal QuasiChemical

Chapter 1 : Introduction

1.1. Background

Recent economic expansion in developing countries such as South Africa and China has resulted in an increased waste generation [1]. If untreated, waste results in undesirable environmental impacts such as pollution and health associated issues [2]. The most widely used waste treatment is incineration [3]. While incineration can reduce the amount of solid waste by over 90mass% and can eliminate liquid waste [3], it is an energy intensive process and is prone to air pollution [4]. Recycling and reusing of waste has the potential to address some of the socio-economic issues such as unemployment; for instance, the South African waste industry is worth over 15 billion ZAR, employing over 29000 people and this is achieved with a recycle of only 10% of all waste produced [4]. This work considers the High Organic Waste (HOW) produced at Sasol Secunda plant, South Africa. The stream is composed of mainly low boiling point organic components such as pyridine, Methyl Ethyl Ketone (MEK), acetone and acetonitrile; its typical flowrate range is 20-30kton/year. Currently, the stream is incinerated without energy recovery. The HOW stream emanates from the coal gasification process.

Some of the components contained in the HOW are valuable chemical solvents. The formation of azeotropes renders the stream complex and deters recovery of valuable chemicals. Prime focus in this work will be the recovery of pyridine. Although pyridine has a low composition in the HOW (5mass%), its market size and demand justify the recovery. Pyridine market size is currently estimated at 400 million USD and growth projections indicate that the market size will increase to over 600 million USD by 2021 [5]. The growth is mainly attributed to the increased pyridine usage in the agrochemical industry [6]. Pyridine finds application in a wide variety of other industries such as the paint, pharmaceutical and spectrometry [5]. The recovery of pyridine has been a subject of many research studies [7-12]; however, most of the studies have mainly focused on its recovery from a binary mixture. The limitation with these studies is that pyridine is likely to be found in waste streams with many other organic components. The contribution of this study lies in the extension of known separation techniques to the recovery of valuable chemicals from a multicomponent waste stream.

Pervaporation and other novel separation techniques have been proposed for the recovery of pyridine and other valuable chemical solvents from azeotropic aqueous streams [13-16]. Pervaporation is a membrane based separation technique with advantages such as low energy consumption and low capital investment compared to traditional separation techniques such as distillation [17]. However, due to confidence and expertise in distillation based techniques, the chemical industry has shown more preference towards distillation [18,19]. Moreover, a lot of capital has been invested in distillation; it is reported that over 90% of separations taking place in the chemical industry occur in distillation columns [18]. On the other hand, fractional distillation cannot separate azeotropic mixtures into pure components. Nevertheless, other distillation techniques such as Pressure Swing Distillation (PSD) and azeotropic distillation are capable of separating azeotropic mixtures [9,20,21]. Although distillation is energy intensive, there are energy saving techniques that have been proposed and have not been implemented adequately in industry [22].

Dividing Wall Column (DWC) and diabatic distillation are examples of established energy saving distillation-based techniques. DWC is an integration of 2 or more thermally coupled distillation columns into 1 so that the integrated column has more than 2 product streams [23]. This is achieved by inserting a vertical wall in the midsection of the column [22-24]. DWC technique has been reported to reduce energy utilization by up to 30% [25]. By contrast, diabatic distillation involves the use of heat exchangers to enable tray wise heat exchange [26].

1.2. Problem Statement

The incineration of the High Organic Waste (HOW) stream signifies 2 main problems: 1) loss of opportunity to maximize revenues through the resale of the recovered valuable chemicals and 2) air pollution through emission of greenhouse gases; incineration may be eliminating the HOW, but this is done at the expense of air pollution. Moreover, incineration of the HOW is an energy intensive process, requiring consistent addition of liquid fuel. With all its drawbacks, incineration of waste may be inevitable as not all components contained in the HOW warrant recovery. Therefore, there is a need to reduce the incinerator load to mitigate pollution and the fuel consumption due to incineration. Ideally, this should be achieved through a recovery of valuable chemicals that can be resold. Sasol has reported water utilization inefficiency issue at their Secunda plant and implemented strategies to improve water utilization in 2011 which have not been able to reach the targeted efficiency [27]. Water constitutes 40-60% of the HOW; consequently, water integration assessment in addition to recovery of valuable chemicals is worth considering.

1.3. Aims and Objectives

1. Use of thermodynamic tools to assess different separation techniques for the recovery of pyridine from the HOW
2. Design and propose a cost-effective process flowsheet for the recovery of pyridine from the HOW stream produced at Sasol Secunda plant.
3. Simulation of the proposed process on Aspen Plus process simulator.
4. Assessment of water integration feasibility on the proposed process.
5. Evaluate economic performance using Net Present Value (NPV) and Internal Rate of Return (IRR).

1.4. Scope of Research

Computer simulations are well established in the chemical and petrochemical industry; they are used in process development, design of equipment and optimization of both new and old plants [28]. Moreover, simulations avoid costly and time-consuming processes of experimentation especially in the initial stages of design [28]. For this reason, simulation approach was chosen in this work. Aspen Plus was selected as the software package for this work because of its reported versatility [29]. It can be used for design, control, optimization, and monitoring processes. It is used extensively in fine chemicals. polymer, bulk and biochemical industries and has a wide-ranging, class leading database of pure components [29]. Most of process units in the chemical industry, i.e. reactors, distillation columns, absorbers and strippers are built-in within the

Aspen Plus library. For those units that are not part of the Aspen Plus library, it offers an option of building custom models; these include pervaporation and other membrane-based techniques which can be modelled on Aspen Custom Modeler (ACM) then imported to Aspen Plus.

1.5. Thesis Outline

Chapter 1: Introduction

Background to the work is given and the objectives of this study are presented.

Chapter 2: Literature Review

In Chapter 2, South African waste landscape is discussed. Furthermore, Sasol processes are briefly deliberated to better understand the source of waste. Potential techniques for azeotropic mixtures separations are reviewed.

Chapter 3: Recovery of Pyridine: Thermodynamic Constraints and Alternatives Analysis

In Chapter 3, different separation techniques are assessed using thermodynamic tools for the recovery of pyridine from the HOW. Pyridine recovery process is proposed and compared with a classical example of pyridine recovery from an aqueous stream.

Chapter 4: Integration of the Pre-concentration Stage using Dividing Wall Column Technique

In Chapter 4, the assessment of the integration of distillation columns using a principle of Dividing Wall Column (DWC) is made.

Chapter 5: Entropy Generation Analysis of the Regeneration Column

In Chapter 5, energy integration commenced in Chapter 4 is extended to other parts of the process and recommendation to improve energy utilization is made.

Chapter 6: Evaluation of the Incineration Process and Process Economics

In Chapter 6, the proposed process is compared with the current practice of incineration. Heat recovery from the incineration unit through water integration is proposed. Furthermore, economic evaluation of the proposed process is evaluated.

Chapter 7: Conclusions

Summary of all chapters is given, and recommendations are made for future work.

References

[1] D. Hoornweg, P. Bhada-Tata, and C. Kennedy, “Environment: waste production must peak this century,” *Nature*, vol. 502, pp. 615–617, Oct. 2013.

[2] B. Vrede, “Department of Geography and Environmental Studies petroleum waste disposal challenges in selected African contries - policy, practice and prospects,” November, 2014.

[3] “Environmental Outlook,” pp. 1987–1996, 2001.

[4] GreenCape, “Waste economy: market intelligence report 2016,” no. April, pp. 1–55, 2015.

[5] Marketsandmarkets, “Pyridine & amp; pyridine derivatives market worth 656.3 Million USD by 2021,” 2017. [Online]. Available: http://www.marketsandmarkets.com/PressReleases/pyridine-derivatives.asp. [Accessed: 13-Jul-2017].

[6] “Pyridine market: global industry size, share and forecast period 2015 -2025.” [Online]. Available: http://www.persistencemarketresearch.com/market-research/pyridine-market.asp. [Accessed: 28-Jun-2017].

[7] P. Sébastien, M. Silvère, G. Vincent, B. Olivier, B. Philippe, and J. Xavier, “Heterogeneous batch distillation processes: Real system optimisation,” *Comput. Aided Chem. Eng.*, vol. 20, pp. 1081–1086, 2005.

[8] W. L. Luyben and I.-L. Chien, *Design and control of distillation systems for separating azeotropes*, vol. 53, 2013.

[9] M. K. Mandal, S. B. Sant, and P. K. Bhattacharya, “Dehydration of aqueous acetonitrile solution by pervaporation using PVA-iron oxide nanocomposite membrane,” *Colloids Surfaces A Physicochem. Eng. Asp.*, vol. 373, pp. 11–21, 2010.

[10] E. Drioli, S. Zhang, and A. Basile, “Recovery of pyridine from aqueous solution by membrane pervaporation,” *J. Memb. Sci.*, vol. 80, pp. 309–318, 1993.

[11] N. R. Singha, P. Das, and S. K. Ray, “Recovery of pyridine from water by pervaporation using filled and crosslinked EPDM membranes,” *J. Ind. Eng. Chem.*, vol. 19, pp. 2034–2045, 2013.

[12] R. Cheng, C.-H. Cho, S. Kirby, and B. Lim, “Economic recovery of pyridine and 3-methylpyridine,” 2010.

[13] Z. Zhu, D. Xu, X. Liu, Z. Zhang, and Y. Wang, “Separation of acetonitrile/methanol/benzene ternary azeotrope via triple column pressure-swing distillation,” *Sep. Purif. Technol.*, vol. 169, pp. 66–77, 2016.

[14] S. Xia, X. Dong, Y. Zhu, W. Wei, F. Xiangli, and W. Jin, “Dehydration of ethyl acetate-water mixtures using PVA/ceramic composite pervaporation membrane,” *Sep. Purif. Technol.*, vol. 77, pp. 53–59, 2011.

[15] J. Bokhove, T. J. Visser, B. Schuur, and A. B. De Haan, “Selective recovery of a pyridine derivative from an aqueous waste stream containing acetic acid and succinonitrile with solvent impregnated resins,” *React. Funct. Polym.*, vol. 86, pp. 67–79, 2015.

[16] M. K. Mandal and P. K. Bhattacharya, “Poly(ether-block-amide) membrane for pervaporative separation of pyridine present in low concentration in aqueous solution,” *J. Memb. Sci.*, vol. 286, pp. 115–124, 2006.

[17] I. F. McConvey, D. Woods, M. Lewis, Q. Gan, and P. Nancarrow, “The importance of acetonitrile in the pharmaceutical industry and opportunities for its recovery from waste,” *Org. Process Res. Dev.*, vol. 16, pp. 612–624, 2012.

[18] C. Bravo-Bravo, J. G. Segovia-Hernández, C. Gutiérrez-Antonio, A. L. Durán, A. Bonilla-Petriciolet, and A. Briones-Ramírez, “Extractive dividing wall column: design and optimization,” *Ind. Eng. Chem. Res.*, vol. 49, pp. 3672–3688, 2010.

[19] M. Illner and M. R. bin O. Othman, “Modeling and simulation of a dividing wall column for fractionation of fatty acid in oleochemical industries,” *Iran. J. Chem. Eng.*, vol. 12, pp. 60–67, 2015.

[20] V. Julka, M. Chiplunkar, and L. O. Young, “Selecting entrainers for azeotropic

distillation," *Aiche*, no. March, pp. 47–53, 2009.

[21] Y. Wang, Z. Zhang, D. Xu, W. Liu, and Z. Zhu, "Design and control of pressure-swing distillation for azeotropes with different types of boiling behavior at different pressures," *J. Process Control*, vol. 42, pp. 59–76, 2016.

[22] K. Khushalani, A. Maheshwari, and N. Jain, "Separation of mixture by divided wall column using Aspen Plus," *Int. J. Emerg. Technol. Adv. Eng.*, vol. 4, pp. 563–571, 2014.

[23] V. K. Sangal, V. Kumar, and I. M. Mishra, "Optimization of a Divided Wall Column for the Separation of C4-C6 Normal Paraffin Mixture using Box-Behken design," *Chem. Ind. Chem. Eng. Q.*, vol. 19, pp. 107–119, 2013.

[24] A. A. Kiss and R. R. Rewagad, "Energy efficient control of a BTX dividing-wall column," *Comput. Chem. Eng.*, vol. 35, pp. 2896–2904, 2011.

[25] Y. C. Wu, H. Lee, H. Huang, and I. Chien, "Energy-Saving Dividing-Wall Column Design and control for Heterogeneous Azeotropic Distillation Systems Energy-Saving Dividing-Wall Column Design and Control for Heterogeneous Azeotropic Distillation Systems," 2014.

[26] G. M. De Koeijer and S. Kjelstrup, "Application of irreversible thermodynamics to distillation," *Int. J. Thermodyn.*, vol. 7, pp. 107–114, 2004.

[27] "Sustainability reporting, sasol," 2016.

[28] Z. Zhu, D. Xu, X. Liu, Z. Zhang, and Y. Wang, "Separation of acetonitrile/methanol/benzene ternary azeotrope via triple column pressure-swing distillation," *Sep. Purif. Technol.*, vol. 169, pp. 66–77, 2016.

[29] "Aspen Technology," 2017. [Online]. Available: http://home.aspentech.com/products/engineering/aspen-plus/. [Accessed: 22-Aug-2017].

Chapter 2 : Literature Survey

This chapter gives a background on South African waste landscape. A brief history about Sasol and its production processes is presented to give a better understanding of the origin of the High Organic Waste (HOW) stream under consideration. The basic properties of valuable chemicals found in the waste stream are also discussed, and the detailed discussion for pyridine and its market size is made. State of the art azeotropic mixtures separation techniques are then discussed in detail as well as analyzing their applications by different researchers for similar waste streams as the HOW. Advantages and disadvantages of each technique are outlined. A discussion about the application of thermodynamic tools for distillation design and synthesis is presented in this chapter.

2.1. Brief Background on the South African Waste Landscape

Recent economic and industrial expansion across the globe (Indonesia, China, South Africa and India), increasing population and the development of urban cities (megacities) has resulted in massive waste generation; a phenomenon which has grown to be one of the major challenges of the 21st century [1, 2]. Ineffective data collection, lack of policy enforcement capacities and thus lack of compliance from stakeholders are some of the challenges pertaining to effective waste management in South Africa [3]. The general waste composition in SA is depicted in Figure 2.1.

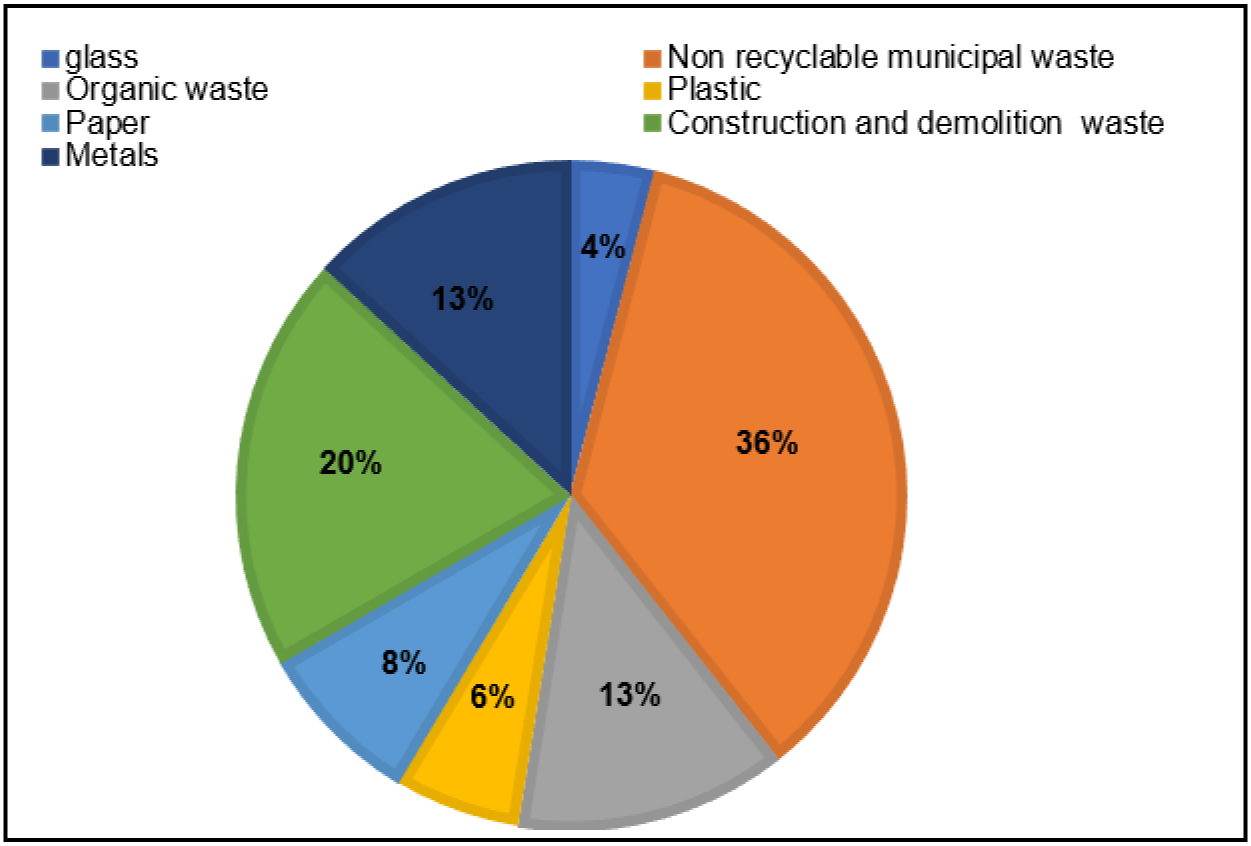

Figure 2.1. Waste composition in South Africa [1]

Dilute industrial waste streams are often discarded onto large water bodies by coastal firms and onto sewage systems for companies located inland [3]. The former results in the ecosystem disturbance and the latter results in difficulty in treating sewage waste. Recent research has shown that in SA, of the 108 million tons of waste (all types of waste) generated per annum, only 10% is recycled and the rest is landfilled [3]. Consequently, the development of sustainable waste management strategies remains a critical area of concern in South Africa. Waste valorization through implementation of appropriate waste management strategies has the potential to alleviate the socio-economic stresses such as unemployment and high resource consumption rate in South Africa [3]. For instance, the SA waste industry was reported to be worth 15.8 billion ZAR (0.51% GDP of the country) in 2012, employing over 29,000 people [1, 4]. It is estimated that a further 20% and 60% recycle of industrial waste and domestic waste respectively could result in a further 17 billion ZAR revenue and potential job creation for 30,000 more people [4]. In its entirety, the waste management sector can create over 100,000 jobs [4]. The main source of employment opportunity lies in recycling (Figure 2.2) [4].

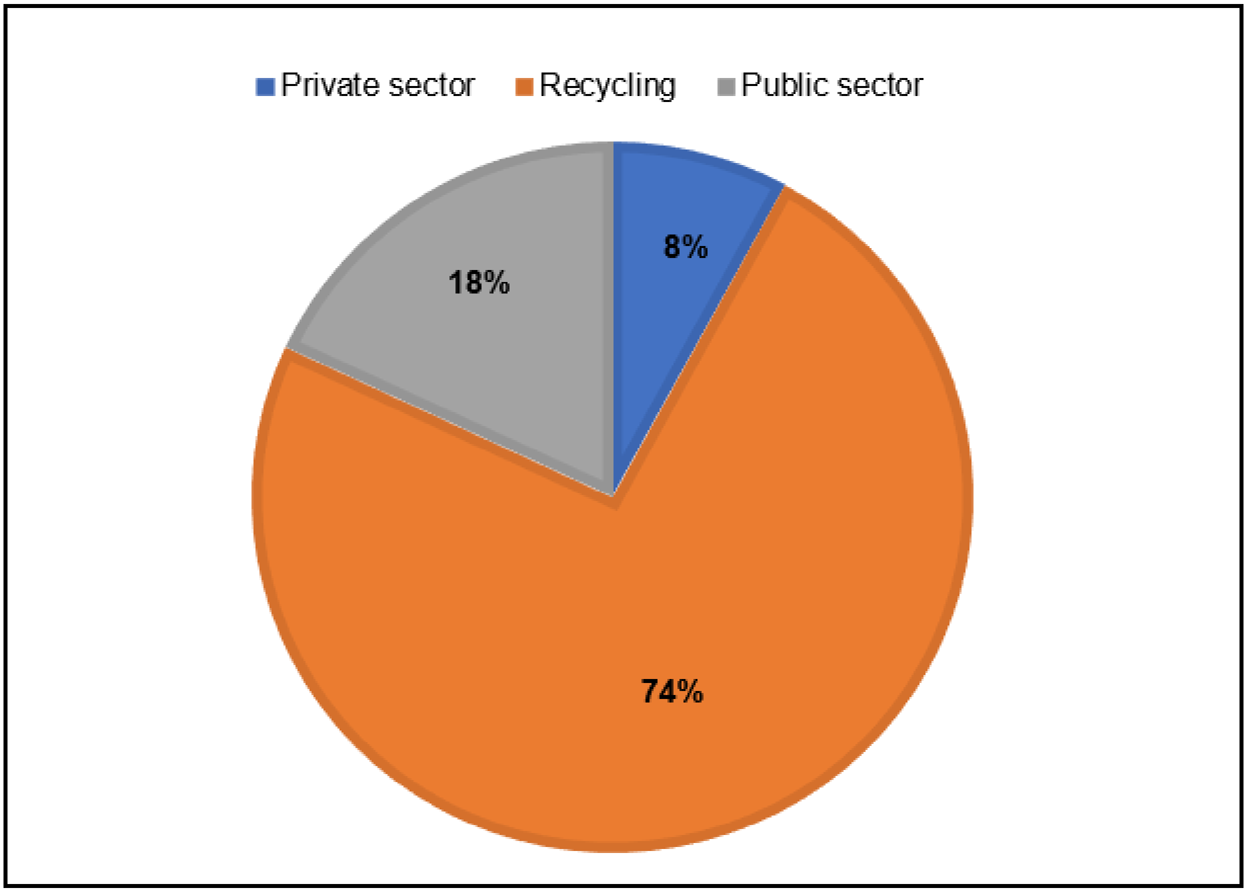

Figure 2.2. Employment opportunities in the waste management sector [1]

In response, the SA government developed a green policy and regulatory framework for waste management which emphasize minimization of waste production and resource consumption in 2008 [National Environmental Management: Waste Act (Act 59 of 2008))] [4]. This work focuses on the aqueous High Organic Waste (HOW) stream produced at Sasol Synthetic Fuels (SSF) in Secunda, South Africa.

2.2. Oil Production Processes at Sasol Secunda

In 1950, the South African government responded to a lack of crude oil and natural gas by sponsoring the South African Coal, Oil and Gas Ltd (Sasol) to produce crude oil from coal using the then new German technology referred to as the Fischer-Tropsch (FT) process [5]. Sasol's first production took place in 1955 in the plant situated in the Free State province, the town currently known as Sasolburg [5]. Owing to growth and increased need for a variety of chemicals due to population growth, Sasol set up 2 more plants in Secunda, Sasol 2 and Sasol 3 in 1980 and 1982 respectively [6]. Today, using the FT process, Sasol produces about 160,000 barrels of liquid fuel from coal which account for over 40% of the country's liquid fuel [7].

Sasol has contributed over 40 billion ZAR to the South African Gross Domestic Product (GDP) and employs over 170,000 people [6]. In its 50th year anniversary in the year 2005 it had produced over 1.5 billion barrels of liquid fuels from Coal since its inception [7]. Sasol produces over 200 liquid fuels including petrol, paraffin, diesel, jet fuel and wax. There are 3 main liquid fuels and chemicals production routes at Sasol: refinery of crude oil, Gas to Liquid (GTL) and Coal to Liquid (CTL) technologies [7].

Crude Oil Refinery

Crude oil consists of hydrocarbons ranging from C_5-C_{18} [8]. Like coal, it is acquired from nature. Due to the lack of crude oil in South Africa, Sasol imports it from West Africa, Gabon [8]. Production of liquid fuels and chemicals from crude oil is achieved through refining the oil in the Natref (National petroleum refiners of South Africa) plant; a plant jointly owned by Sasol and Total South Africa. This plant was commissioned in 1971 for the most part, to cater for the refinery needs of Sasol in Sasolburg [8].

Gas to Liquid Technology (GTL)

The raw materials used to produce liquid fuels at Sasol are natural gas imported from Mozambique, crude oil, and coal. Natural gas imported from Mozambique is reacted with steam and oxygen at temperatures as high as 1300˚C in an auto-thermal reactor to produce syngas [9]. The syngas then reacts in the Sasol Slurry Phase (SSP) reactor in the presence of iron catalyst. Fischer-Tropsch process takes place in this reactor [9].

Coal to Liquid Technology (CTL)

The process of converting coal to liquid fuels occurs in 4 main steps: coal mining, coal gasification, gas purification, and Fischer-Tropsch process [9]. Coal gasification results in the gas which is mainly composed of carbon monoxide and hydrogen, referred to as synthesis gas (syngas) [10]. The Fischer-Tropsch process takes place in a Sasol Synthol Reactor (SAS) wherein carbon monoxide and hydrogen (syngas) react at elevated temperature and pressure in the presence of an iron catalyst. The reaction temperature in the Sasol Slurry Phase (SSP) is much higher than the temperature in the SSF reactor [9]. The product of the SAS reactor are different hydrocarbon chains and water; the general reaction of which is given by equation (2.1), where n represents the number of carbon atoms [8]. The waste emanating from the coal gasification unit as shown in Figure 2.3, is of interest in this research work.

$$(2n+1)H_2 + nCO \rightarrow C_nH_{2n} + nH_2O \qquad (2.1)$$

Where:

n denotes the number of carbon atoms in a chain.

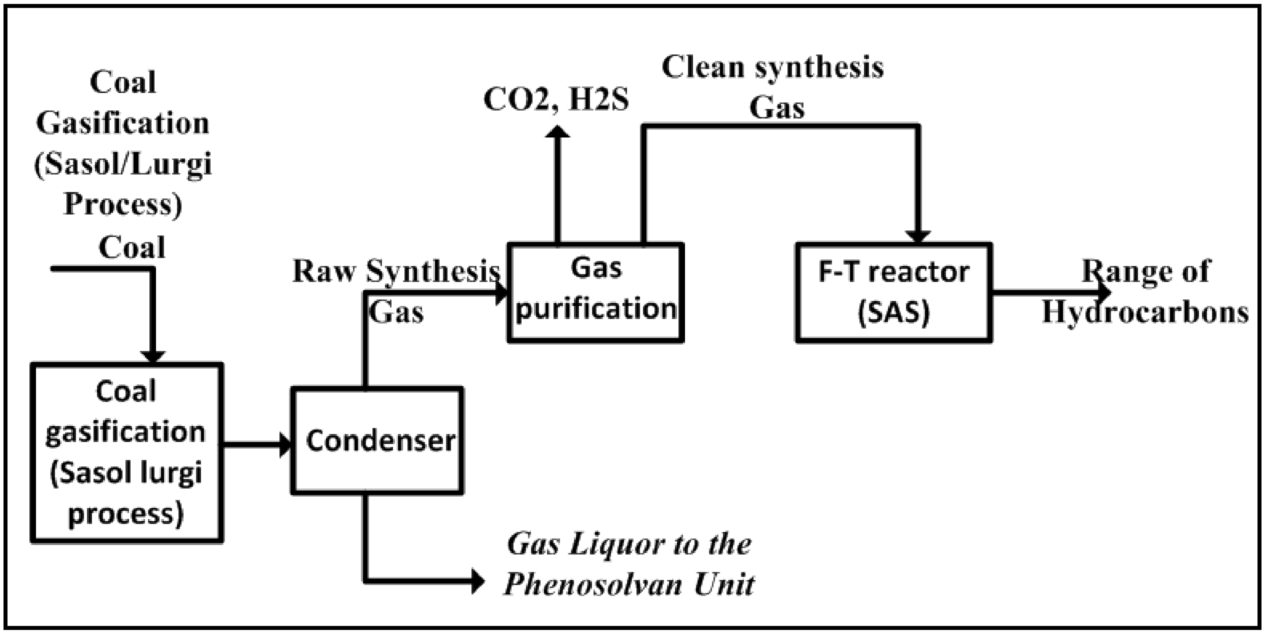

Figure 2.3.Coal to Liquid simplified process flow diagram [9]

Coal Gasification

In coal gasification, the coal is subjected to temperatures as high as 1300˚C [8]. The products of this process are ash and raw gas where ash is collected by an intermittent collection unit. The raw gas is comprised of carbon monoxide, tar, oils and phenols amongst other things. The raw gas is cooled to condense and remove the gas liquor which is mainly water and dissolved impurities (phenols, tar, organic acids etc.) from the raw gas. The raw gas concentrated with CO and H_2 is finally taken to an absorber referred to as the Rectisol unit. In the Rectisol unit, methanol is used to remove CO_2 and H_2S [8]. The gas liquor from the condenser is passed to the gas liquor separation unit in which phenols, dissolved gases and oils are removed from the gas liquor. The product of this unit is referred to as the clean gas liquor gas. The clean gas liquor is then passed to the Phenosolvan process where ammonia and High Organic Waste (HOW) stream are separated (Figure 2.4) [9].

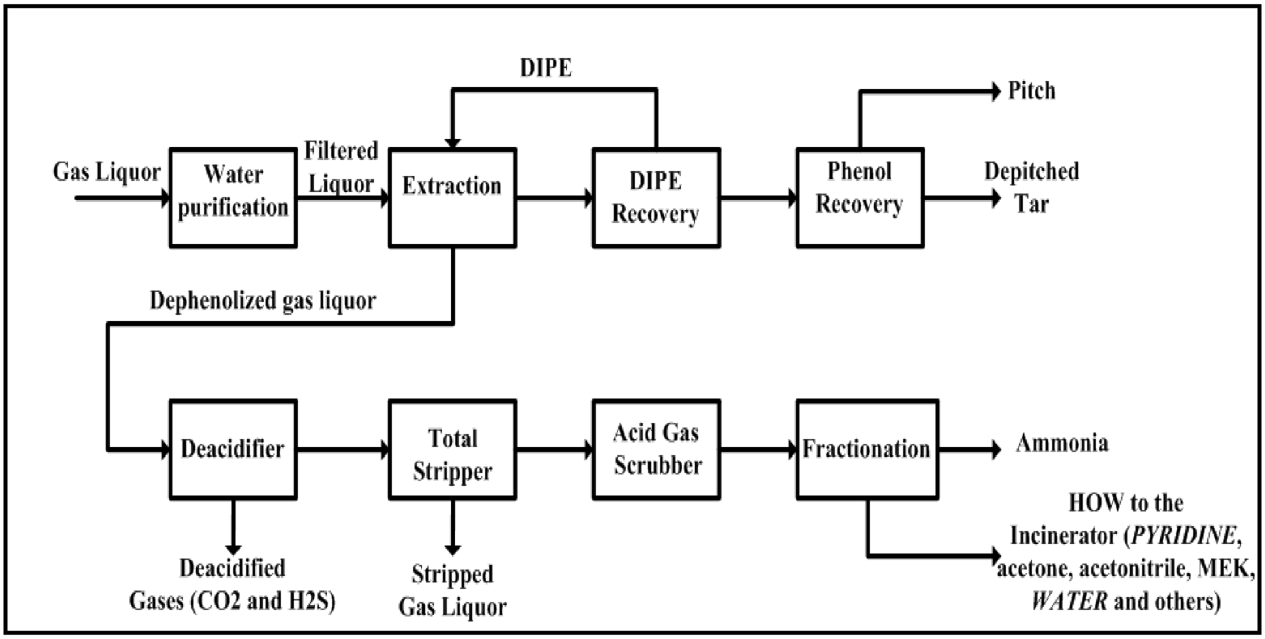

Figure 2.4. Phenosolvan unit: Origin of the HOW stream [9]

2.2.1. Background of the HOW

The high organic waste stream is composed mainly of low boiling components (Table 2.1). Some of the components from the HOW are valuable chemical solvents and find applications in a variety of fields. Brief discussion about the application of acetone, acetonitrile and pyridine is given in this section.

Table 2.1. HOW stream typical average composition and components properties

Component	**Mass Fraction**
Pyridine	0.05
Acetone	0.02
Water	0.62
Acetonitrile	0.15
Methyl Ethyl Ketone	0.04
Methyl Iso Propyl Ketone	0.12

Acetone

Acetone, also known as propanone is a colorless liquid ketone with characteristic odor and taste. It has proven itself as multipurpose solvent and is applied extensively in the manufacturing of paints and nail polish. Furthermore, it is used an intermediate chemical to produce other chemicals such as methylmethacrylate and bis-phenol-A [10]. Sasol uses acetone as a raw material in the production of Methyl Isobutyl Ketone (MIBK) over an impregnated ion exchange catalyst in the presence of hydrogen [11].

Acetonitrile

Acetonitrile is a toxic, clear liquid with a sweet-like smell. Acetonitrile is used in the making of pharmaceuticals, rubber products, nail polish and batteries [12]. Although acetonitrile is a polar solvent (miscible with water in all proportions), it also possesses hydrophobic properties, enabling its application in liquid chromatography and as photosensitive material [13]. In petrochemical industries it is used in the separation of ole-diolefin as an extracting solvent [14]. There are 2 main sources of acetonitrile;

reaction of acetic acid in the excess of ammonia and as a byproduct of the production of acrylonitrile in the Sohio process [14]; nonetheless the latter is a major source of acetonitrile. Upon heating, acetonitrile emits harmful gases such as hydrogen cyanide which can have adverse health effects to humans and the environment in general; if inhaled, acetonitrile can cause mucous irritation [15]. The toxicity of acetonitrile and its broad range of applications serve as incentives for its recovery from a spent stream.

Pyridine

Pyridine is a colorless chemical with an unpleasant odor which is structurally related to benzene; the only difference between the molecular structure of benzene and pyridine is that one of the C-H groups in the benzene is replaced by a nitrogen atom N. Pyridine has a broad range of applications and is used in most industries. Its application ranges from alcohol denaturation, use as a chemical solvent in paint and rubber preparation and extraction of plant hormones. It is also renowned for its use in HNMR spectrometry [16]. Moreover, pyridine is used in colometric determinations of cyanide in aqueous solutions, as a dyeing agent in the textiles industry, and a precursor to agrochemicals and pharmaceuticals [17,18]. Separation of pyridine from water and other components is an ongoing research topic. This can be attributed to the fact that pyridine is currently in high demand with a market size of over 450 million USD [19]. It is also projected that the pyridine market size will grow by at least 200 million USD by 2021 [16].

Recovery of pyridine from waste has been investigated since early 1990s. A case study by Crew & Schafer [20] refers to a project that was undertaken to recover pyridine from a waste stream; this project was forecasted to have the potential to save a drug a manufacturing company (Burroughs Co.) up to 1.5 million USD pa . The motivation behind the need to recover pyridine from a waste was mainly economical; firstly, the recovery of pyridine would reduce the disposal costs since the waste in this plant was incinerated without energy recovery and secondly the cost of virgin pyridine was high and the recovery of used pyridine could then abate such costs [20].

Water

South Africa is currently faced with a water crisis and has been listed as one of the 30 driest countries in the world [5]. In 2016, the Vaal dam which supplies the Gauteng province, South African economic hub and the most populated province with water was reported to have hit an all-time low, below 30% of its capacity, resulting in water supply interruption. This affected the industrial and agricultural activities adversely, exacerbating the already strained economic performance of the country. Furthermore, water is one of the key raw material to Sasol for steam generation purposes and it is also used for other purposes such as heat exchanger medium and in cooling towers; an average of 167,000,000m^3 is consumed per annum [8]. As such, in 2011, Sasol initiated a voluntary water efficiency usage in their water intensive plants (Sasol Synfuels and Sasol Infrachem) [21]. In alignment with the implemented water efficiency strategy, water recovery will also be assessed in this work.

The successful recovery of pyridine and water from the HOW will reduce the stream by 50mass% and thus the incinerator load. Consequently, less steam and liquid fuel will be required to incinerate the remaining fraction of the HOW. The main hindrance of pyridine or any of the valuable chemicals recovery from the HOW stream is the complexity introduced by azeotropic formations between the organic components and water and between organic components themselves. The stream comprises at least 6 main azeotropes (Table 2.2).

Table 2.2. Main azeotropes found in the HOW stream

Type	Components	Mole Fraction	Temperature (°C)
Binary	Pyridine	0.25	93.71
	Water	0.75	
Binary	Acetonitrile	0.33	76.53
	Water	0.67	
Ternary	Water	0.37	76.32
	Acetonitrile	0.50	
	MIPK	0.13	
Binary	MEK	0.64	73.65
	Water	0.36	
Binary	Water	0.56	77.61
	MIPK	0.44	
Binary	Acetonitrile	0.29	79.09
	MEK	0.71	

Non-ideal intermolecular interactions between two or more dissimilar components may lead to an azeotropic phenomenon [22]. This causes the mixture to exhibit equal compositions between the liquid phase and vapor phase at equilibrium. The interactions may be repulsive or attractive in which case the azeotrope is a minimum boiling azeotrope or maximum boiling azeotrope respectively. Minimum boiling azeotrope means that the azeotrope has the lowest boiling point compared to all the components originally in the mixture and maximum boiling azeotrope means that the azeotrope has the highest boing point compared to original components of the mixture. Depending on the strength of the intermolecular interaction, the azeotrope may be homogenous or heterogeneous; stronger interactions result in the formation of heterogeneous azeotrope. At azeotropic composition the relative volatility of an azeotropic composition is unity [23]. Relative volatility of a binary mixture is given by equation (2.2).

$$\alpha_{AB} = \frac{\gamma_a P_a}{\gamma_b P_b} \tag{2.2}$$

Where:

α_{AB}: relative volatility of component A and B.

$\gamma_{:}$ Activity coefficient

P: Vapor pressure of component

To avoid dealing with azeotropic formation, the steam is currently incinerated without energy recovery.

2.2.2. Current HOW Stream Treatment

Currently, the HOW stream is incinerated without energy recovery. Incineration is a thermal treatment in which waste is combusted at elevated temperatures. It is the most preferred waste treatment technique globally [24]. Incineration temperature is controlled at 1300˚C at Sasol Secunda [21]. The HOW incineration unit at Sasol use 2 main utilities: steam and fuel gas [21]. The steam serves to atomize the HOW and the fuel gas is used to ignite the waste (Figure 2.5).

Incineration of the HOW stream serves to exacerbate the CO_2 emissions from Sasol operations; the greenhouse gases emissions (measured in CO_2 equivalent) for the year 2016 was reported as 69.3 million tons [21]. On the other hand, National Environmental Air Quality Act and Minimum Emissions Standards (MES) which were introduced in 2004, dictate that Sasol adhere to more stringent emission standards by the year 2020 [21]. This has put Sasol under pressure to reduce emissions and as a result in the last decade, it has spent over 20 billion ZAR in environmental improvement projects [21]. Potential techniques that can be used to recover valuable chemicals from the HOW despite the azeotropic formations of components are presented in section 2.3.

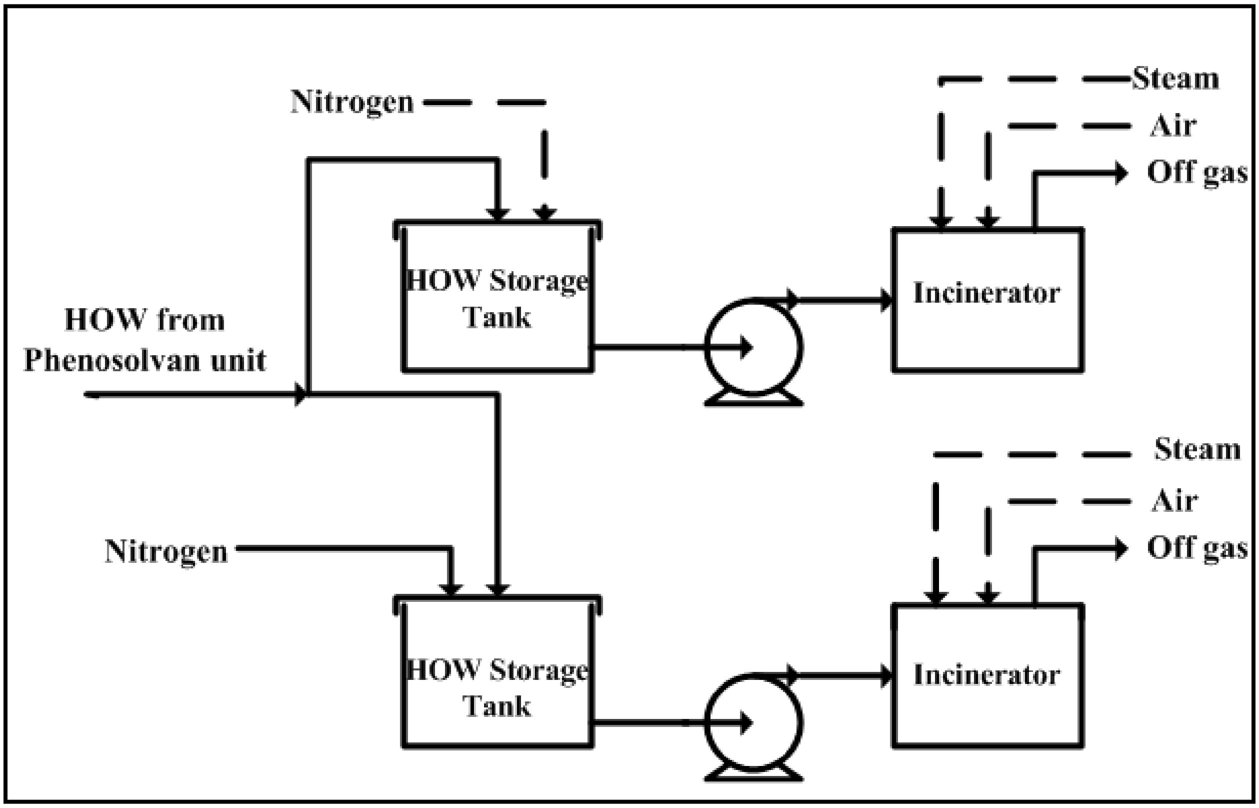

Figure 2.5. Schematic diagram of the incineration unit for High Organic Waste [21]

2.3. Azeotropic Mixtures Separation

The aim of a separation process is to separate a mixture of components into its distinctive constituents; the performance of such a process is evaluated on the purity of respective components from a mixture. There are several separation technologies for azeotropic mixtures currently in use in industry today. Separation processes exploit the difference in physical and chemical characteristics. Characteristics such as boiling point, size, shape, density, solubility and magnetic properties are used to separate mixtures [25].

Liquid-liquid Extraction

Liquid-liquid extraction (LLE), also referred to as solvent extraction, is a separation technique based on the difference of solute solubility in a solvent and the aqueous solution. The liquids are brought into contact either in a counter current or cross current manner to cause mass transfer of solute, usually from an aqueous phase to the solvent phase [26] (Figure 2.6). For this mass transfer to be possible, the solute has to be more soluble in the solvent phase than in the aqueous phase. Some of the factors that are considered upon choosing a solvent are: favorable partition coefficient, high selectivity towards the solute and easy separation of the solvent from the solute. The advantages of liquid-liquid extraction are: low energy intensity [27], ability to extract solutes present in smaller concentrations and separate heat sensitive chemicals [26].

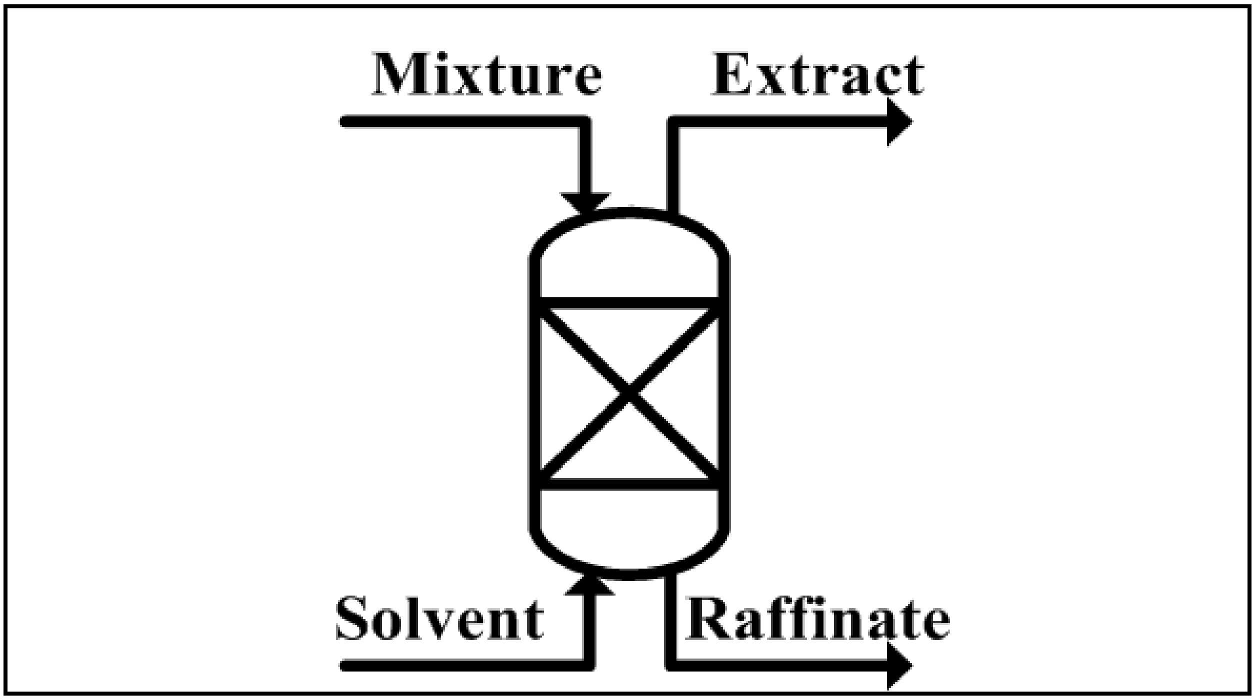

Figure 2.6. Liquid-liquid extraction unit

Liquid-liquid extraction has been traditionally used extensively in the separation of aliphatic-aromatic mixtures [26]. Like the waste stream considered in this work, these mixtures are made up of components with close boiling points and some of them form azeotropes with each other. Kaewchada et al. [26] conducted an experimental investigation of the effect of temperature, contact time and solvent to feed ratio on the separation efficiency of toluene from heptane using a micro tube contactor. It was found in this study that increasing contact time between 2s and 6s resulted in the reduction of extraction efficiency (Figure 2.7); this phenomenon was sensibly ascribed to the fact that contact time was controlled by flowrates of the solvent and the mixture respectively, therefore, higher flow rates (lower contact time) resulted in finer liquid droplets, which implied larger mass transfer interfacial area; a very important factor for any mass transfer operation. It was also observed that beyond 6s, extraction efficiency started increasing. This may be because of sufficiently higher contact time allowed for adequate mass transfer despite the interfacial area being relatively smaller.

These results show that interfacial area is a more influential parameter than contact time. Owing to diffusion coefficient being directly proportional to temperature [26], the separation efficiency was also found to increase with increasing temperature (Figure 2.8). The temperature was increased only up to 60˚C and this was taken as the operating temperature. Temperature could not be increased indefinitely due to several reasons: some chemicals degrade at elevated temperatures, but most importantly in liquid-liquid extraction the state of the solvent and the mixture to be separated needs to be in liquid phase; these factors limited the extent to which temperature could be increased.

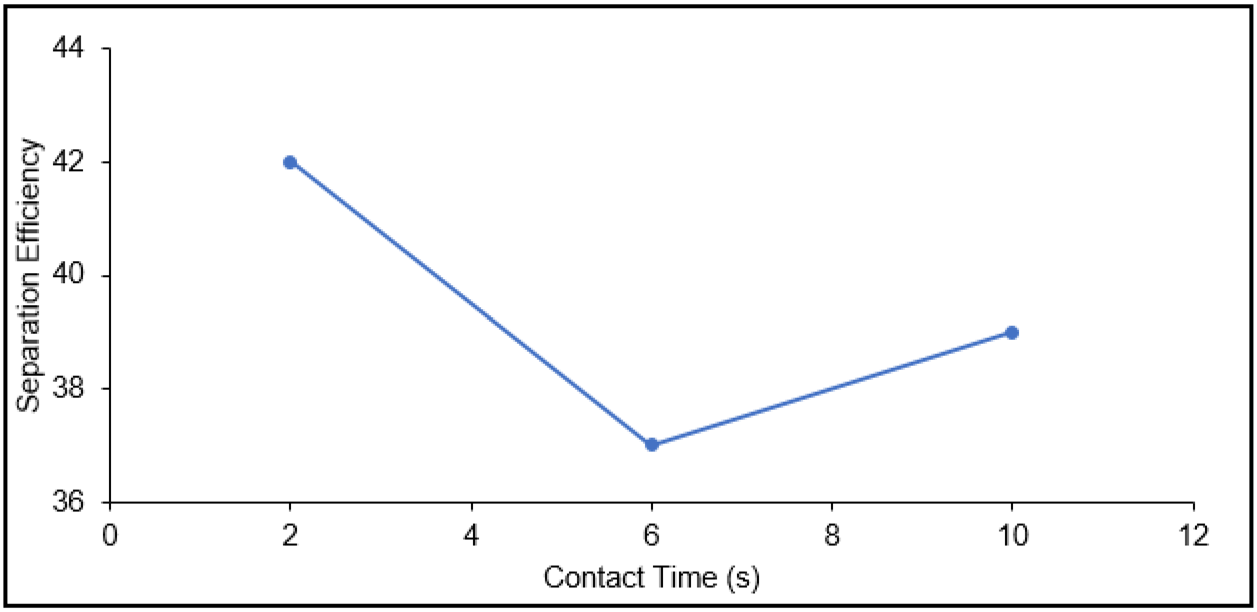

Figure 2.7. Effect of contact time on separation efficiency [26]

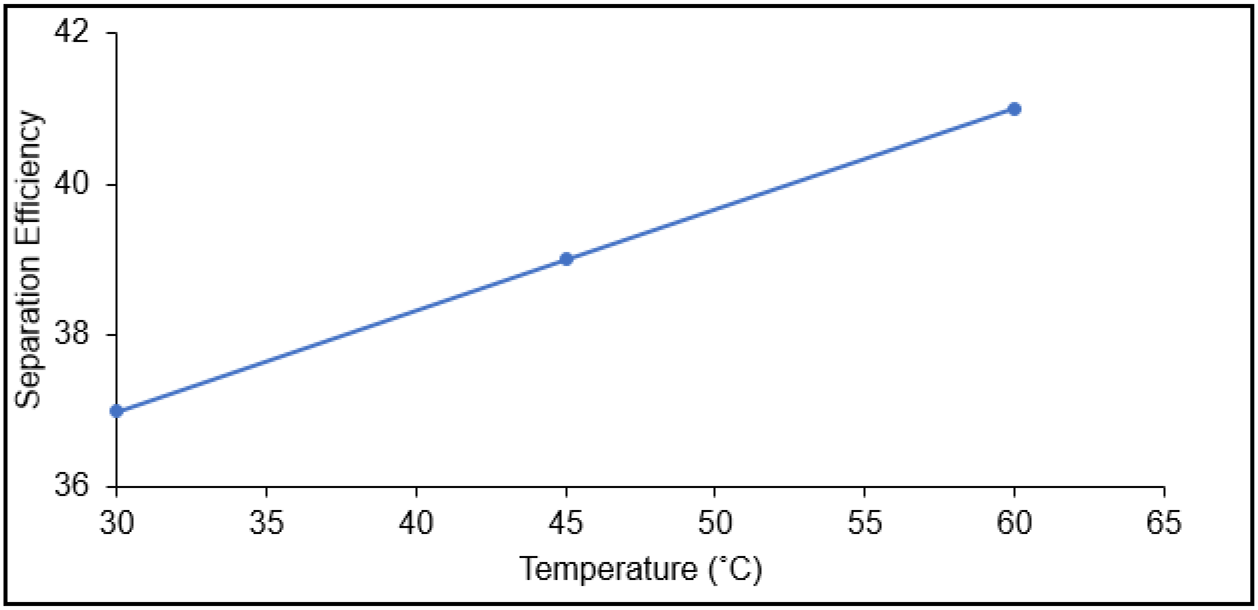

Figure 2.8. Effect of temperature on separation efficiency [26]

Since the early 2000s, novel approaches have been proposed for the breaking of azeotropes using liquid-liquid extraction. One such approach is replacing the organic solvent with ionic liquid. The argument with ionic liquid is that they enable easier regeneration and are less volatile unlike most of the organic solvents, and therefore losses to the environment can be minimized [27]. However, the problem with ionic liquids is that there is no exhaustive data around their toxicity and hence their environmental impact is not adequately known [28]. Also, the research of the use of ionic liquids is still in early development, there may be a need for further research to investigate their application for different azeotropic mixtures. Work by Pereiro & Rodriguez [27] proved the applicability of ionic liquids as extractants for the separation of propanol and ethyl acetate for liquid-liquid extraction. A study by Królikowski [28] aimed at investigating the separation of p-xylene (aromatic compound), octane and decane (aliphatic compounds) using ionic liquids in liquid-liquid extraction revealed that an increase in aliphatic chain length significantly increase selectivity of the ionic liquid. Furthermore, the experimental liquid-liquid equilibrium data was compared to the correlated Non-Random Two-Liquid (NRTL) and Universal QuasiChemical (UNIQUAC) liquid-liquid equilibrium data. A satisfactory representation was established between the correlated and experimental values, however NRTL was found to be a better representative of the experimental liquid-liquid equilibrium. The study also found that to acquire satisfactory separation, large amounts of ionic liquid(s) were required [28].

A drug manufacturing, pharmaceutical company (Burroughs Wellcome Co.) assessed liquid-liquid extraction for the recovery of pyridine from an industrial organic waste stream in 1993 [20]. The waste mixture was pre-concentrated to the water-pyridine azeotropic composition using fractional distillation and the azeotrope was broken using solvent extraction. The process used caustic soda as a solvent. Successful recovery of pyridine at purity over 99mass% was achieved. This resulted in the reduced need for virgin pyridine by 30mass% for drug production in the company. The reduction in the need for virgin pyridine corresponded to a 1.5 million USD savings per annum for the drug manufacturing company. This work showed that recovery of pyridine and perhaps any other valuable chemical may be economically viable.

Pervaporation

Pervaporation is a membrane based technique used to separate liquid mixtures by partial vaporization of a single component in a mixture [29]. The liquid feed is kept in contact with the membrane and the component to be removed is sucked through the membrane by a vacuum pump [30]. The vapor permeate leaving the membrane is condensed before being pumped to the product storage (Figure 2.9). The rejected liquid is referred to as the retentate. The membrane must have high selectivity towards the component that is being targeted. The membrane may be hydrophilic, hydrophobic or organoselective [18]. Hydrophilic membranes, which are more common than the other 2 excrete water as the permeate whereas hydrophobic membranes produce water as a retentate.

Hydrophobic membranes are not to be confused with organoselective membranes; separation in organoselective membranes is based on permeability of organic components of the mixture while separation in hydrophobic membranes is based on the rejection of water by the membrane. Hydrophobic membranes that have been tested in experiments show poor selectivity and they tend to allow the permeation of water [18]. Because the separation using pervaporation is independent of the vapor-liquid equilibrium, the technique is usually used for the separation of azeotropic mixtures, mixtures containing close boiling points and recovery of trace amounts [15]. Areas of application include: dehydration of organic mixtures, separation of organics and recovery of organics from aqueous solutions [30].

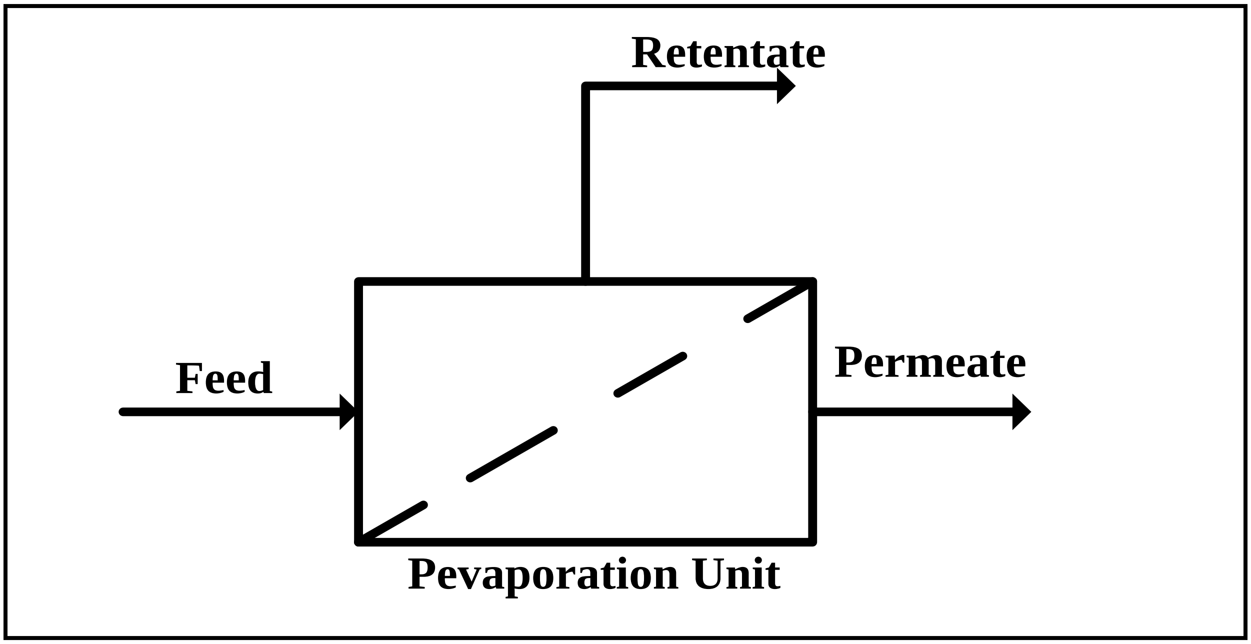

Figure 2.9. Schematic diagram of a pervaporation unit [31]

Some of the advantages of this process over the conventional methods of separation include: low energy consumption and low capital investment [30, 31]. Moreover, pervaporation is in accordance with green chemical processing as it does not require additional solvent to induce separation in case of azeotropic mixtures as is with azeotropic distillation and liquid extraction. The fact that only the diffusing component(s) experience phase change contribute to the low energy consumption of this process [10]. The synthesized membrane must be both chemically and structurally resistant; usually this is achieved through crosslinking. Crosslinking presents a dilemma; low level crosslinking results in swelling in a dilute mixture, whereas high level crosslinking causes membrane stiffness and comes in at the expense of reduction of flux and selectivity of the membrane. Reduction in flux is undesirable, particularly at industrial level because it means low throughput, and thus lower separation rate.

Various studies have undertaken to overcome the issues associated with crosslinking and few suggestions have been made. One of the explored avenues has been the use of PVA (Poly Vinyl Alcohol) based membranes reinforced with metal oxides. PVA is preferred due to its hydrophilicity and good chemical resistivity [15]. The purpose of the metal oxides nanocomposites is mainly reinforcement of the structure of the membrane. Work by Mandal et al. [15] established that using PVA based nanocomposite iron oxide membranes improved general performances of the membrane without the need for crosslinking. This study was aimed at comparing pervaporative performances of the PVA based commercial membrane with special crosslinking (Pervap 2202) and PVA based nanocomposite iron oxide membranes for the separation of water and acetonitrile. For pervap 2202, there was a direct relationship between flux and water mass% in the feed. The increase of flux with water mass% was faster between 5 and 10mass% and then slowed down approaching a plateau at about 130 g/m2/s (Figure 2.10(b)). Separation factor (equation (2.3)) on the other hand decreased linearly with increasing water composition in the feed.

$$\alpha_{i/j} = \frac{Y_i/Y_j}{X_i/X_j} \tag{2.3}$$

Where:

$\alpha_{i/j}$: Separation factor

$Y_{i/j}$: The vapor composition of component i or j.

$X_{i/j}$: The liquid phase composition of component i or j.

i: Component which the membrane is selective toward.

j: Component to be rejected by the membrane.

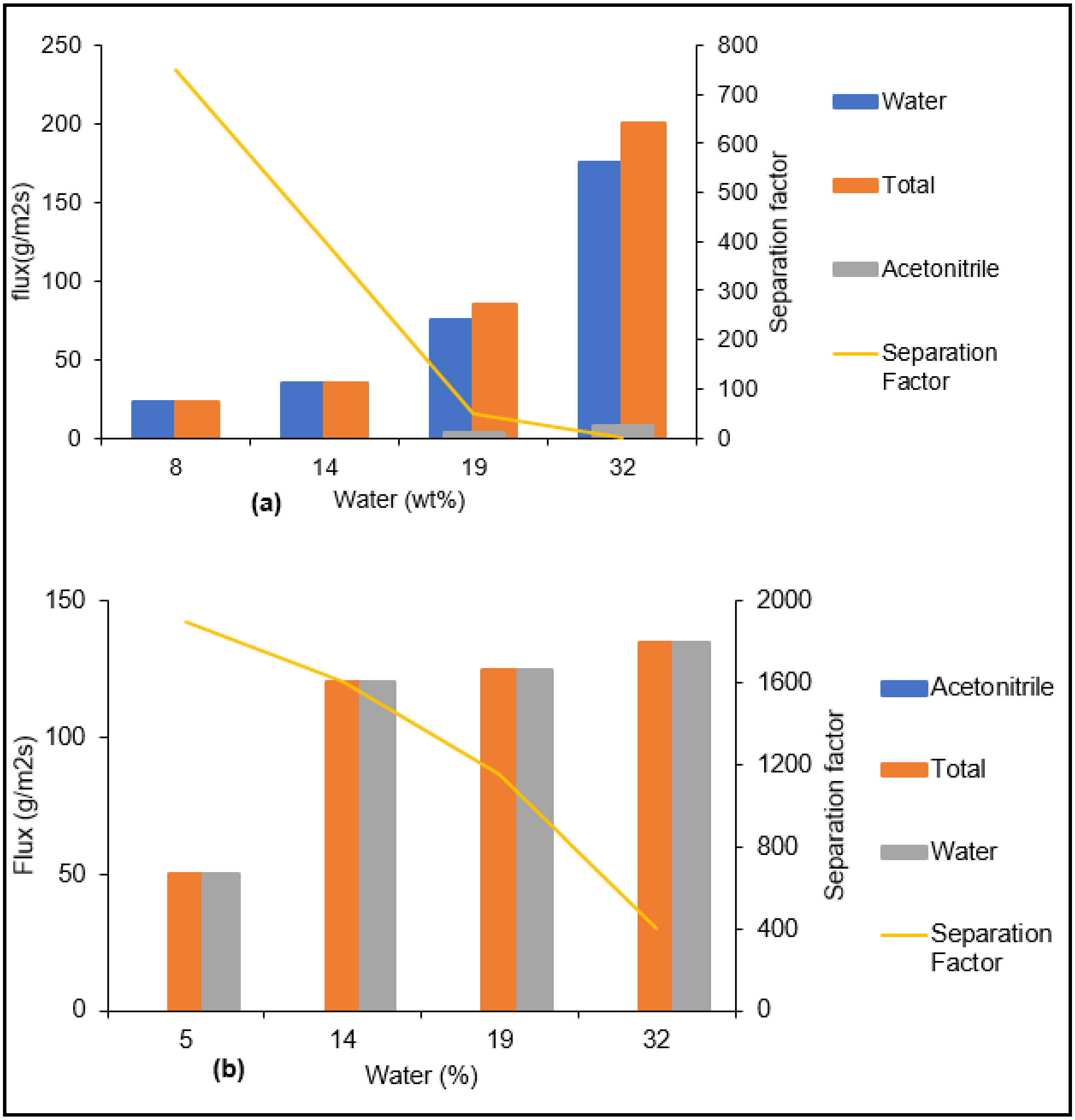

Figure 2.10. Effect of water concentration feed on flux (a) for in the PVA based membrane and (b) Pervap 2202 (commercial membrane) [15]

Due to the nature of the membranes (hydrophilic), water was meant to be recovered as the permeate and acetonitrile as the retentate, therefore, according to equation (2.3), the decrease of separation factor with increasing water feed composition is an undesirable phenomenon implying that some of the acetonitrile is lost to the permeate for the in-situ membrane (Figure 2.10 (a)). This is evident in Figure 2.10 (a) which shows acetonitrile flux increases with increasing water feed composition. For the commercial membrane (Pervap 2202), the decrease in separation factor as water feed composition increases implies that some of the water reported to the retentate, which is equally an undesirable phenomenon as the latter.

A concept of Pervaporative Separation Index (PSI) given by equation (2.4) was also considered. This parameter encompasses both flux and separation factor [35]. For both membranes, PSI peaked around 13mass% water composition, but the PSI for PVA-Fe based membrane was over 2 times higher than the one observed in the commercial membrane (Figure 2.11). The peak on the PVA-Fe membrane was followed by a sharp decrease with increasing water composition. Be that as it may, below and at azeotropic composition the PVA-Fe based membrane had a higher PSI showing that it is more suitable for the separation of water and acetonitrile as an azeotrope breaking membrane than the commercial membrane.

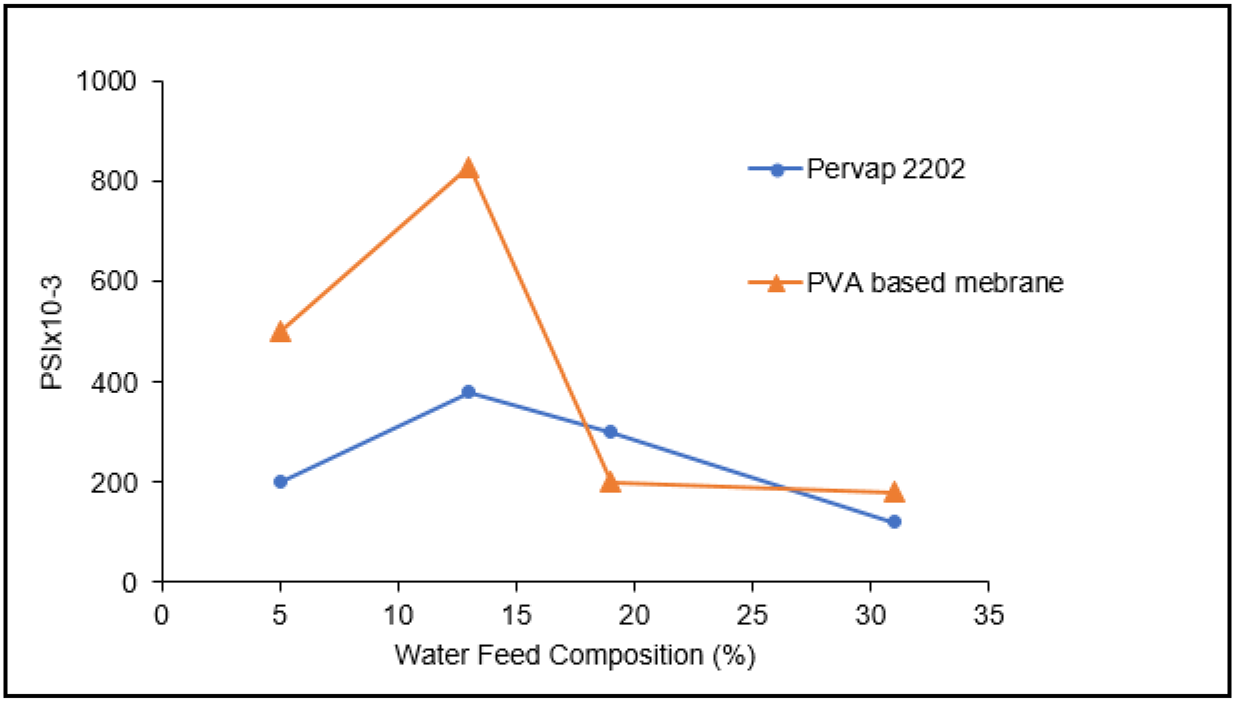

Figure 2.11. Effect of composition on PSI of Water-Acetonitrile membranes at 35˚C [15]

$$PSI = J(\alpha - 1) \tag{2.4}$$

Where:

PSI: Pervaporative Separation Index.

α: Separation factor

J: Permeate flux

Das & Kumar [15] also overcame the need for crosslinking. They used acrylonitrile and itaconic acid copolymer for the separation of water and pyridine. The acrylonitrile part of the polymer provided structural and chemical resistance whereas the itaconic acid provided hydrophilicity due to its bi-carboxylic acid nature [15]. The result was a hydrophilic membrane that does not need crosslinking.

A study to investigate the pervaporative performance of a commercial organoselective membrane (pervap 4060) was undertaken by Khayet et al. [31]. The effects of organic feed concentration and feed temperature on pervaporation performance (permeation flux and selectivity) were studied. Three binary mixtures were considered separately: acetone-water, acetonitrile-water and ethanol-water and then wastewater solution containing the combination of these organics was also studied. A peculiar phenomenon was spotted in the investigation of the effect of temperature on the pervaporative performance; it was found that the concentration of acetone in the permeate decreased with increasing feed temperature even though the concentration of the same acetone decreased rapidly in the feed (Figure 2.12). This was ascribed to the fact that the water permeation increased with increasing temperature thereby reducing the concentration of acetone in the permeate. Furthermore, results reported in this work show that water had a higher composition in the permeate for the acetonitrile-water and ethanol-water binary mixtures at different feed compositions. Even though acetone had a higher composition in the permeate at higher feed composition, it still had a substantial amount of water, about 13mass% of the permeate was water (Figure 2.13). All these indicate that the commercial organoselective membrane (Pervap 4060) may not be good for the separation of the mixtures considered.

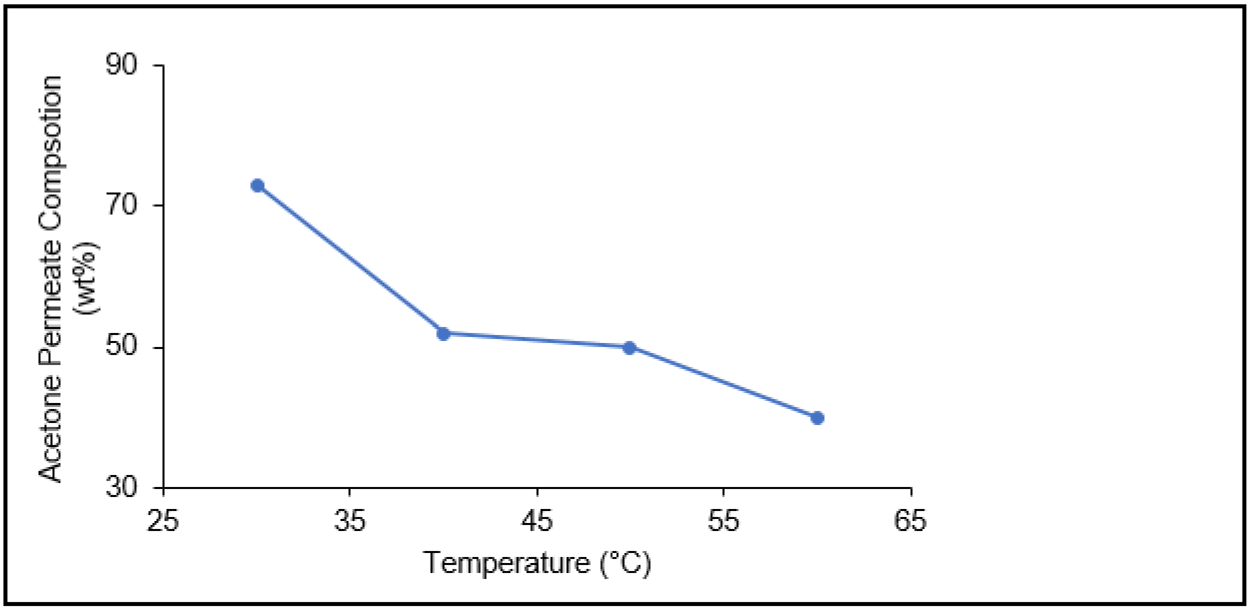

Figure 2.12. Effect of feed temperature on the permeate acetone composition [31]

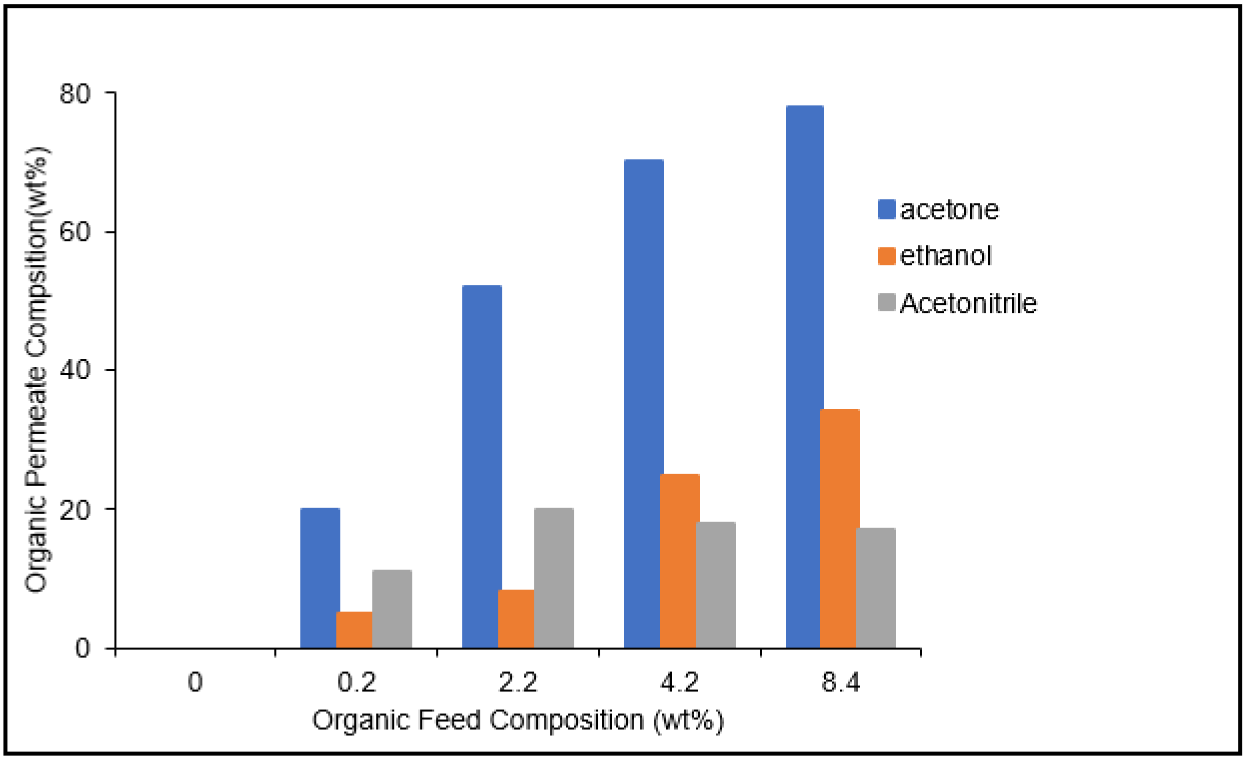

Figure 2.13. Effect of Organic feed composition on permeate organic composition for component-water binary mixture [31]

Singha et al. [18] used organoselective membrane in their experiment for the for the selective recovery of pyridine from water. Ethylene propylene diene monomer filled with N330 carbon filler was the employed membrane. Three of such membranes were synthesized and compared. The differences in the compared membranes were the composition of the filling; the compositions of the fillings were 2, 4 and 6wt% respectively. All these fillings showed a similar recovery of pyridine when the effect of feed concentration of pyridine on the concentration of pyridine in the permeate was investigated.

Admittedly the compositions were relatively high, showing a greater selectivity of pyridine. However, the concentration in the permeate which can be linked to purity was found to be satisfactory at 98mass% pyridine at feed compositions of pyridine of around 25mass%. For pyridine feed concentration of 5-15wt%, the concentration of pyridine in the permeate was not as good at 86wt% (Figure 2.14). It is unlikely that the composition of pyridine could be greater than 20wt% in a waste stream. Typical pyridine composition is about 10mass% in aqueous waste streams [22]. As such, this membrane would be more suitable as a purification technique as opposed to a separation technique.

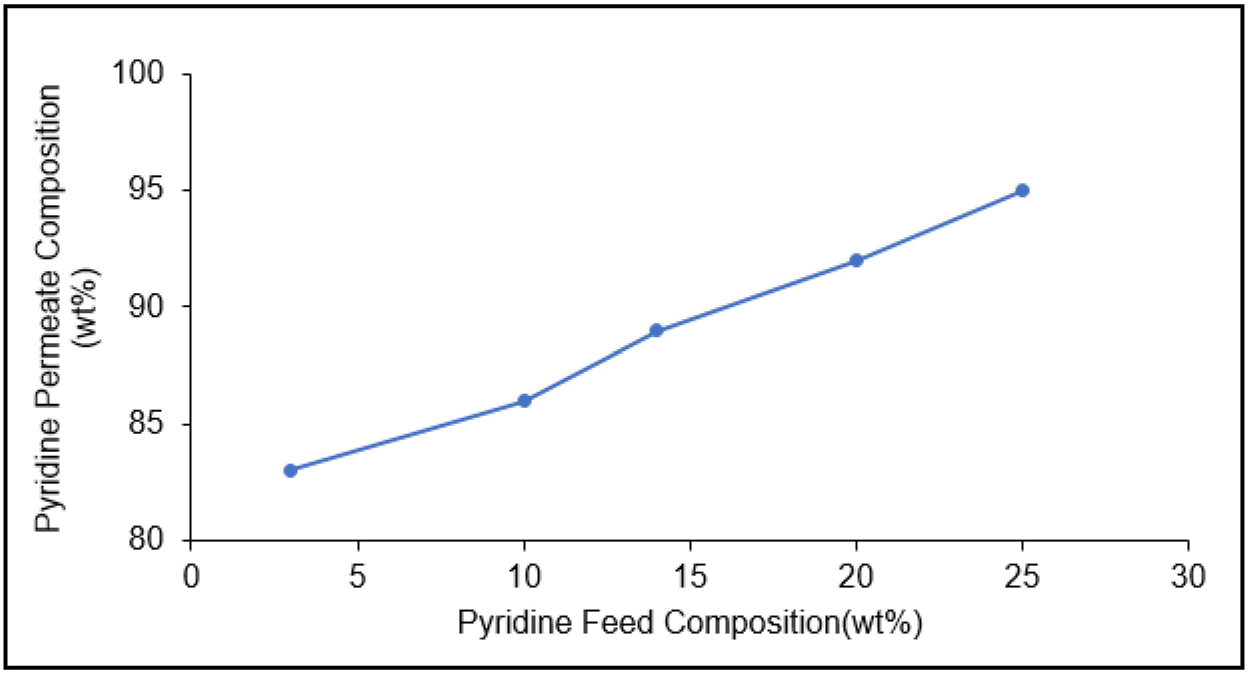

Figure 2.14. Effect of pyridine composition on pyridine permeate composition [18]

Another study by Mandal & Bhattacharya [29] endeavored to recover pyridine from an aqueous solution using an organoselective membrane. This pair utilized Poly (Ether-Block-Amide) membrane to recover pyridine from a pyridine-water binary mixture. They also studied the impact of pyridine feed composition on the permeate flux and permeate pyridine composition amongst other things. It was found that both partial fluxes of pyridine and water increased with increasing pyridine feed concentration, thereby also increasing the total flux. The composition was varied up to 7wt% and it was found that at lower compositions (around 1-5wt%) of pyridine in the feed, the water had a higher flux compared to pyridine. The pyridine permeation flux increased substantially with increasing feed pyridine composition and water permeation flux only increased slightly; this resulted in pyridine flux exceeding water flux beyond feed concentration of 6mass% (Figure 2.15). It followed that the composition of pyridine in the permeate increased with increasing feed concentration (Figure 2.16). These results conform with the ones reported by Singha et al. [18] in terms of the trends observed upon investigating the impact of pyridine feed composition on the permeate flux and pyridine concentration in the permeate. Separation factor decreased with increasing pyridine feed composition (Figure 2.15), implying that some of the pyridine reported to the retentate stream, thereby impacting recovery negatively. This observation is in agreement to results obtained by Mandal et al. [15].

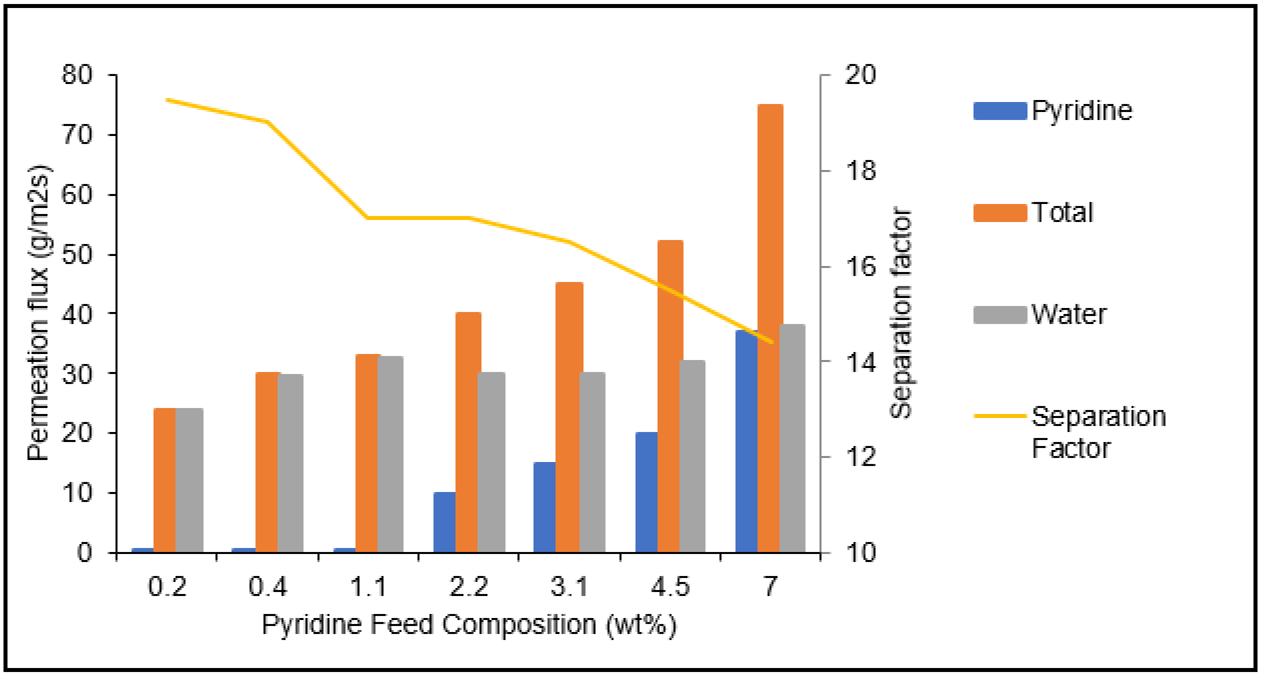

Figure 2.15. Effect of pyridine feed composition on separation factor and permeation flux [29]

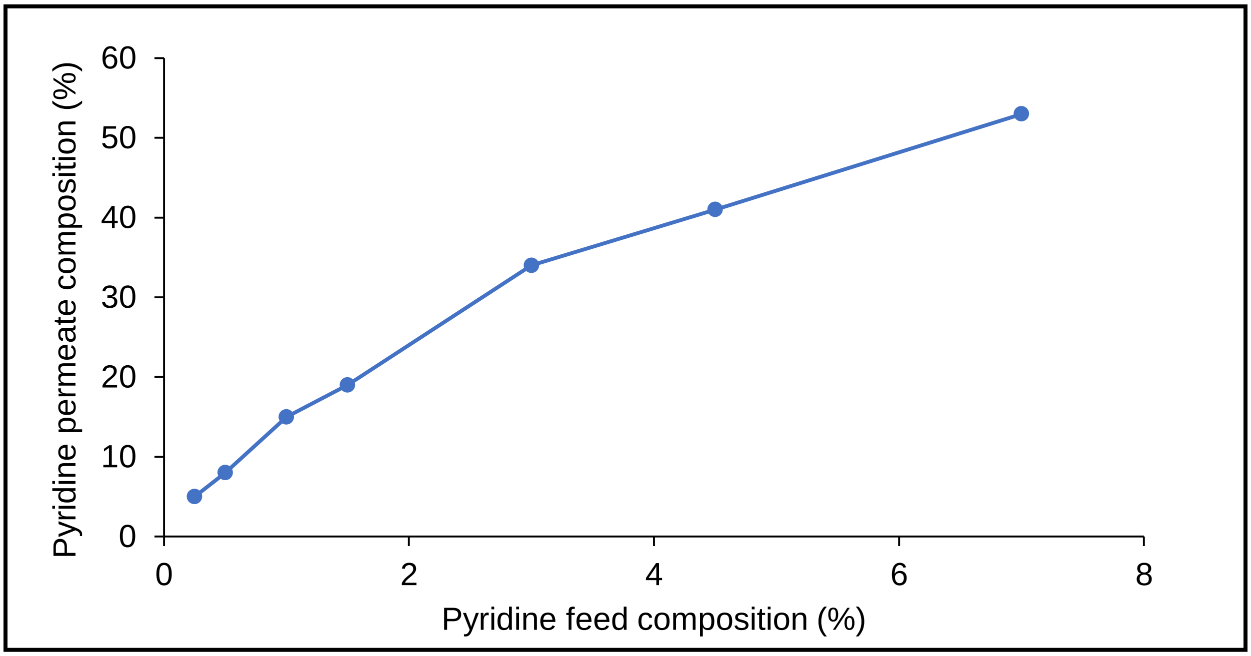

Figure 2.16. Effect of pyridine feed composition on pyridine composition in the permeate [29]

Pervaporation has also been tested for the recovery of acetone from a binary mixture of water and acetone. Samanta & Ray [10] synthesized an organoselective membrane of polyvinyl chloride (PVC) filled with polystyrene (PS) to investigate the effect of acetone feed concentration on acetone concentration in the permeate. The results were similar to the ones reported by Mandal et al. [15] and Mandal & Bhattacharya [29]. It was found that the concentration of acetone in the permeate increased with increasing acetone feed concentration. The composition of acetone in the permeate was between 20-35mass% for feed concentration range of 0-15mass%. The different membrane filling composition had little impact on the acetone concentration in the permeate. In fact, it was deduced by Mandal & Bhattacharya [29] that Vapor Liquid Equilibrium (VLE) separation would yield higher composition of acetone in the permeate than the suggested membrane technology.

Pulyalina et al. [32] studied the purification of methanol/ethanol mixture through pervaporation using polybenzoxazinoneimide (PBOI) membrane using organoselective membrane. The effect of temperature and methanol feed concentration ranges (5-20mass%) was investigated on flux, permeability, selectivity and permeate purity. It was found that the membrane was more permeable to methanol. The increase in temperature was found to increase the total flux through the membrane. This was attributed to the increase in free volume of the membrane at higher temperatures, thereby allowing more passage of methanol [32]. Moreover, the total flux was almost equal to the methanol flux, showing the high selectivity toward methanol in all composition ranges (Figure 2.17). As observed in the previous studies, an increase in the target component feed composition was inversely proportional to the separation factor (Figure 2.18). This was also confirmed by Pulyalina et al. [32].

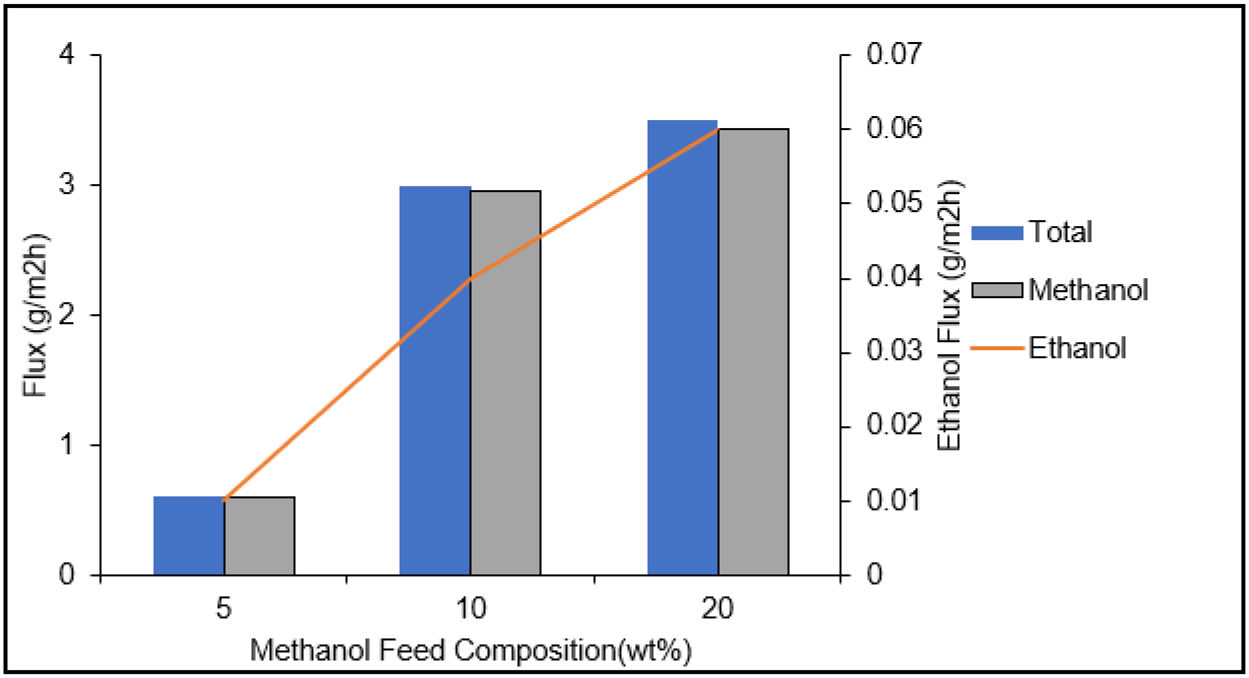

Figure 2.17. Effect of methanol composition on flux [32]

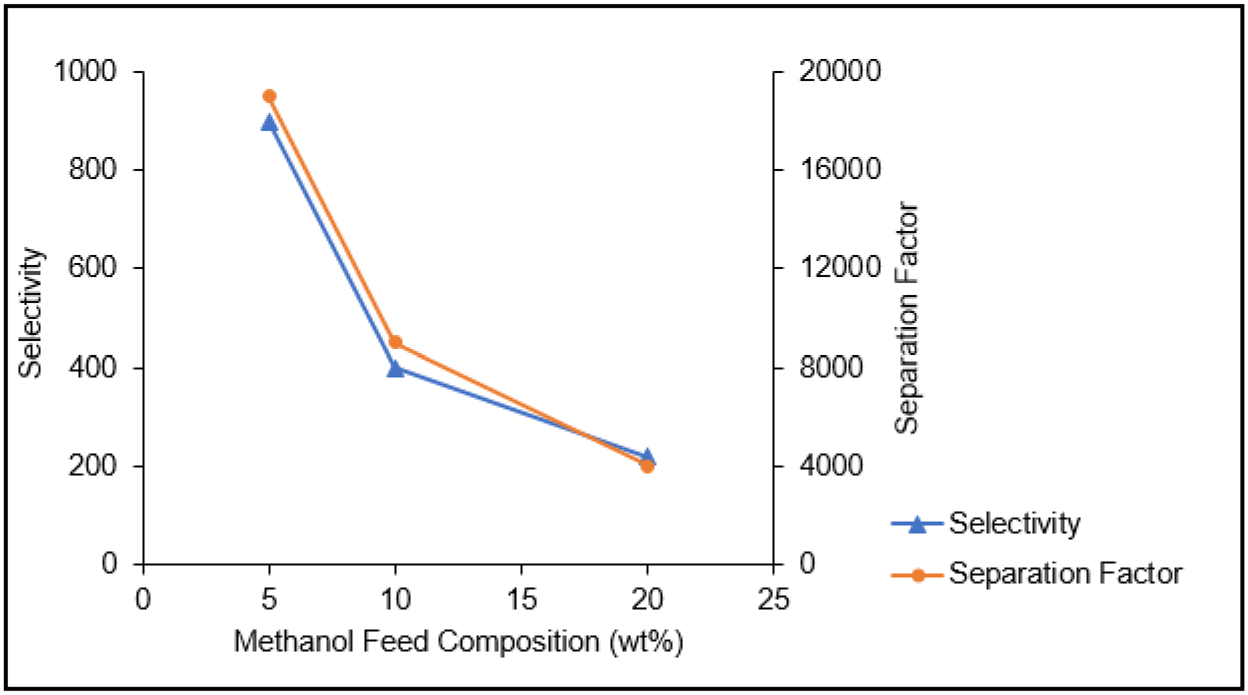

Figure 2.18. Effect of methanol composition on separation factor [32]

Effect of temperature, feed flow rate and water composition in the feed on the pervaporation performance was also investigated during the dehydration of ethyl acetate using PVA/ceramic composite membrane [33]. It was observed that temperature and flux were directly proportional. It was argued that this was caused by the fact that an increase in temperature resulted in increased free volume fraction [32]. Inherently, increased free volume fraction resulted in the passage of larger molecules that were initially hindered, hence decreased separation factor and selectivity (Figure 2.19). Nonetheless, this phenomenon was valid for a specific temperature range; an increase of temperature between 50 and 70˚C resulted in the increased separation factor.

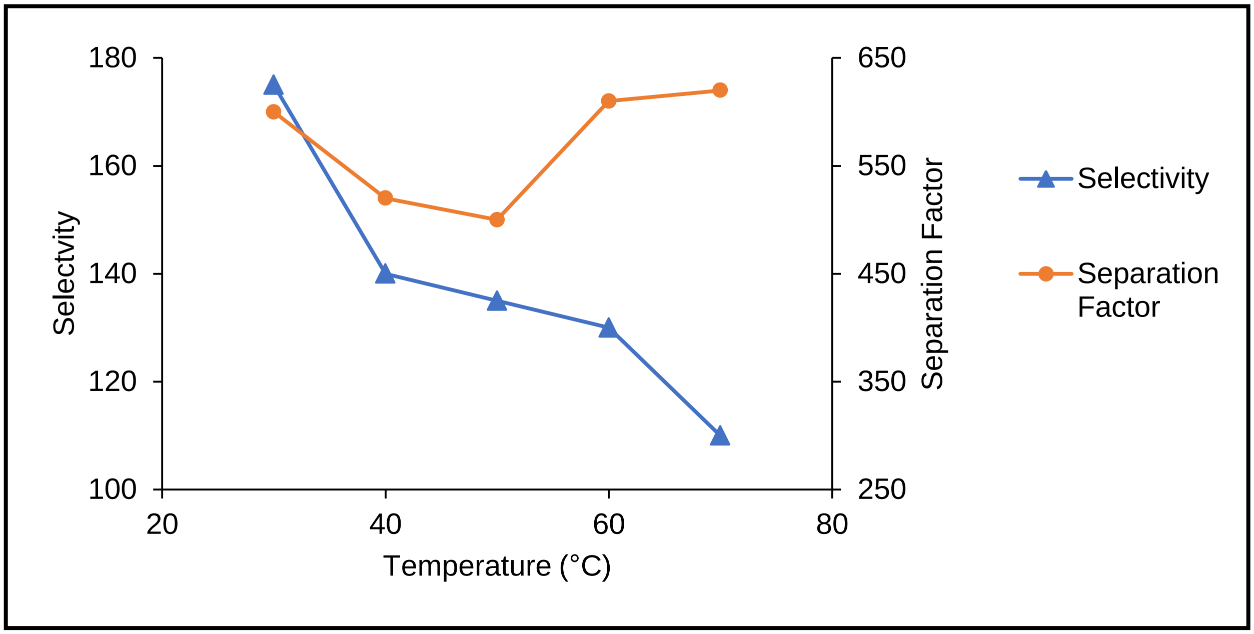

Figure 2.19. Effect of temperature on selectivity and separation factor [33]

Pulyalina et al. [33] deduced that, an increase in the water content of the feed resulted in the overall flux increase but had negative effect on selectivity as the ethyl acetate flux was also increased. This is an undesirable phenomenon as it results in the loss of the targeted product. It is noteworthy that this observation is contrary to Mandal et al. [15] who reported insignificant difference on the selectivity of the hydrophilic membrane upon increasing water content of the feed. This discrepancy can be attributed to the different membranes that were used, but more importantly to the fact that Mandal et al. [15] observed these improved results using a commercial membrane.

Distillation

Despite the advancement in research of other separation techniques and the energy intensity associated with distillation, it remains the most preferred technique in industry today [34-40]. The reluctance to move away from distillation may be due to the investment that has already been made by the chemical industry to the technology both in terms capital and expertise; it is reported that distillation is responsible for over 90% of the recovery/separation systems in the US [40]. Some of the advantages associated with distillation are: high purity of products and the ability to separate complex mixtures.

The basis of separation in distillation is the difference in volatility [41, 42]. There are 2 types of splits that can take place in distillation: direct and indirect. A direct split of a two or more components mixture implies that a pure low boiling component is recovered from the first distillation column, whereas an indirect split suggests that the highest boiling component is recovered as a pure bottoms product in the first column (Figure 2.20). Fractional cannot separate azeotropic mixtures, however, other distillation techniques such as extractive/azeotropic, reactive and pressure swing distillation are well suited for separation of azeotropic and other complex mixtures [17,23].

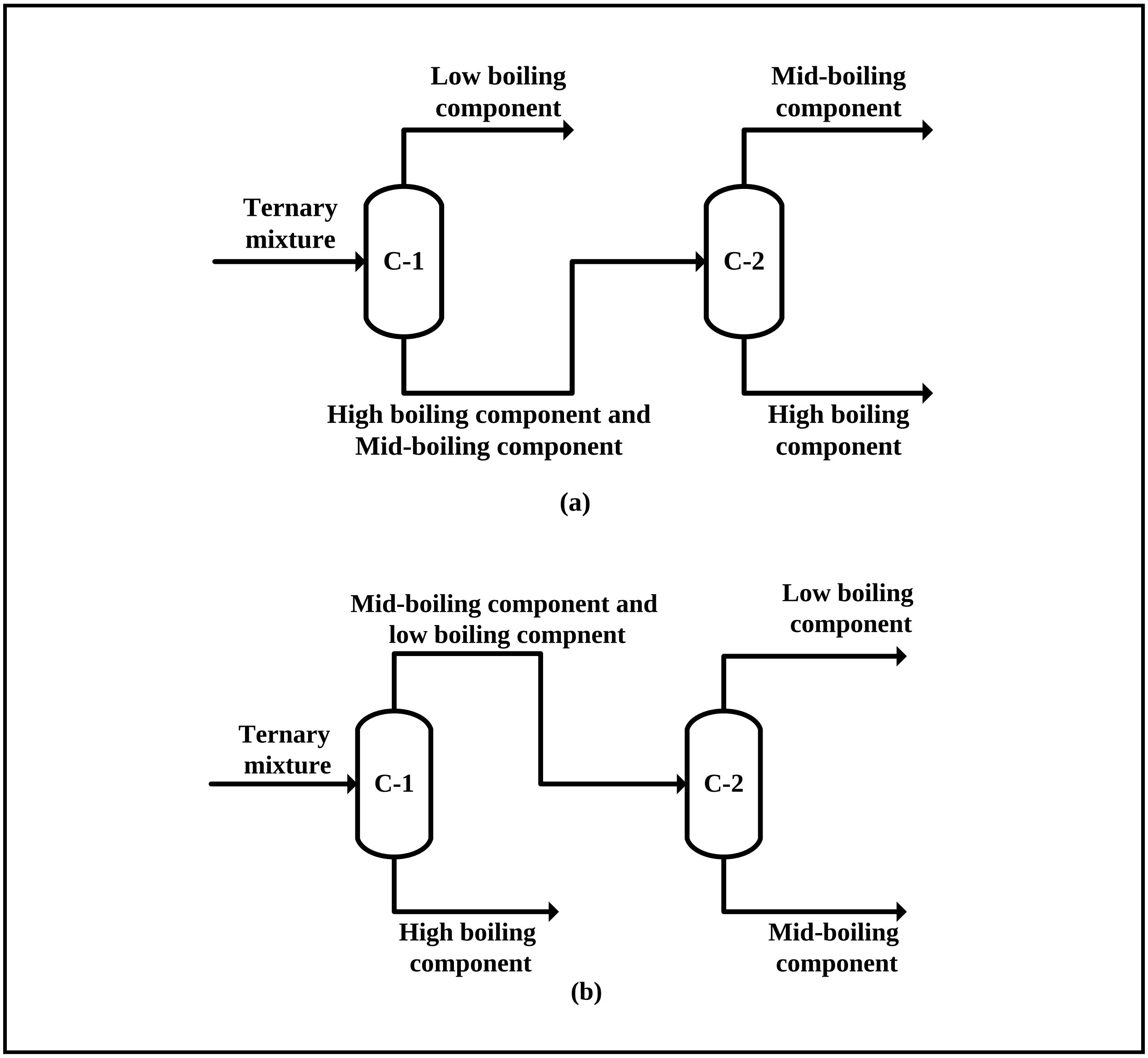

Figure 2.20. Ternary mixture separation (a) Direct split and (b) Indirect split [17]

Pressure Swing Distillation

Pressure swing distillation (PSD) is a technique in which 2 or more columns operating at different pressures are used to separate a homogeneous azeotropic mixture [43]. It may be appropriate if the azeotropic composition and temperature of a mixture are pressure sensitive. Pressure swing distillation may be perceived as being more environmentally friendlier than the other azeotrope breaking distillation techniques because it does not require the addition of a solvent/entrainer to effect separation. This eliminates the need for solvent regeneration column and cuts costs of raw materials. Furthermore, PSD configuration is relatively simpler [44]. Due to these advantages, some have suggested the evaluation of the feasibility of using pressure swing distillation before considering any other distillation types [43].

Cutting on regeneration and entrainer costs does not always translate to economically viable processes; in some instances, it has been shown that PSD is more energy intensive than azeotropic distillation which may render it expensive to operate [25]. Lladosa et al. [25] looked at the separation of di-n-propyl ether and n-propyl alcohol. They compared the use of extractive distillation and pressure swing distillation and concluded that pressure swing distillation was a more economical process for this application with total annual costs amounting to 557,157 USD as opposed to 796,933 USD required for extractive distillation. Pressure swing distillation system was composed of 2 columns operating at different pressures, 30kPa and 101.325kPa for the first and second column respectively. Both systems attained over 99mol% purity of di-n-propyl ether and n-propyl alcohol. However, it may be not entirely objective to conclude that in this case pressure swing distillation was more economical than the extractive distillation since the efficiency and hence the economy of the extractive distillation is largely dependent on the type of entrainer used.

Working on the separation of n-heptane and isobutanol, Wang et al. [44] aimed at assessing the economic viability and controllability of different types of PSD. In their preliminary studies, they discovered that the n-heptane and isobutanol azeotrope exhibited a minimum boiling azeotrope below 6atm and a maximum boiling azeotrope from around 7atm. This was accordingly referred to as an unusual phenomenon and hence was termed Unusual Pressure Swing Distillation (UPSD). UPSD was then defined as the pressure swing distillation in which a mixture displayed a minimum boiling azeotrope at low-pressures column and a maximum boiling azeotrope on the high-pressures. In the Conventional Pressure Swing Distillation (CPSD) the mixture showed minimum boiling azeotrope in both columns.

UPSD and CPSD could attain 99.9mol% purity of both n-heptane and isobutanol, but it was found that CPSD was more economical having Total Annual Cost (TAC) of 653,130 USD pa. UPSD proved to be more expensive to run with TAC reaching 897,690 USD pa. These results are not surprising when the dynamics of the UPSD are considered in detail. Firstly, the high-pressure column in the UPSD was operated at 12atm, whereas the high-pressure column in the CPSD was operated at 4atm. It is known high pressures are directly proportional to high energy consumption resulting in high energy costs. Moreover, higher pressures require that the columns be made of high strength material which do not come cheap either. Interestingly, the group reported that the control of UPSD was easier than that of the CSPD [44].

Zhu et al. [43] used a refined PSD referred to as Triple Column Pressure Swing Distillation (TCPSD) to separate acetonitrile-methanol-benzene into its distinct products. The system was made up of three sequential distillation columns operating at different pressures. The mixture considered in this work comprises 3 azeotropes, namely: methanol/acetonitrile, methanol/benzene and acetonitrile/benzene. The group reasoned that the use of one or two columns for the separation of the ternary azeotrope-based mixture would be impractical and hence the use of the TCPSD. The system was modelled on Aspen plus software. 99.9mass% purity of each recovered component was reported. The first column which was operated at 607.95kPa was used to seclude acetonitrile as a bottoms product. The recovery of methanol was made on the second column at 101.33kPa and lastly benzene was recovered on the last column at a pressure of 607.95kPa. The pressure for each column was determined using Sequential Iterative Optimization. All the papers reviewed agree that configuration plays a significant role in the economics of a PSD, thus it is important for one to optimize the sequencing of columns. The mostly used technique for this purpose has been iterative sequential optimization.

Azeotropic Distillation

Azeotropic distillation involves the addition of a solvent referred to as an entrainer to enhance the relative volatility of an azeotropic mixture or a mixture of components with close boiling points [22]. There are 2 types of azeotropic distillation: homogeneous and heterogeneous. Homogeneous azeotropic distillation is usually referred to as extractive distillation and heterogeneous azeotropic distillation is referred to as azeotropic distillation. This standard of naming will be followed in the sections that follow. The difference in the setup of the 2 techniques is shown in Figure 2.21 (a) and (b). Usually the entrainer in extractive distillation does not introduce any more azeotropes to the system and is often heavier than all the components originally in the mixture. For easier regeneration of the entrainer there must be at least 20ºC temperature difference between the entrainer and the higher boiling component in the mixture [45]. In heterogeneous azeotropic distillation on the other hand, the added entrainer is meant to form a low boiling, heterogeneous azeotrope with one of the constituents of the original mixture. This azeotrope would be recovered as a distillate in the azeotropic column and is usually separated using a decanter due to its immiscibility.

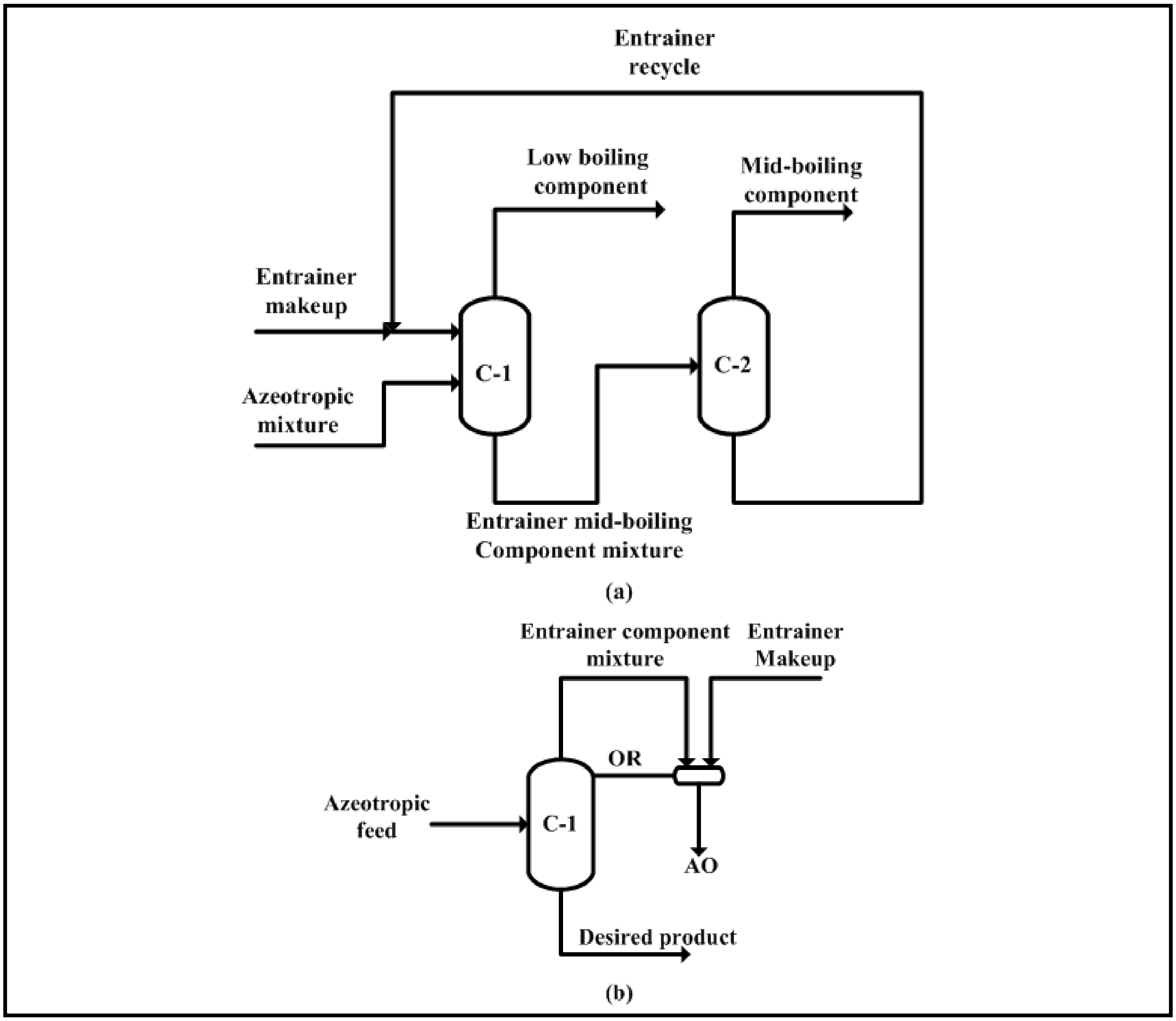

Figure 2.21. Typical setup of: (a) Extractive distillation and (b) Azeotropic distillation

Sazonova & Raeva [13] endeavored to recover acetonitrile from a waste aqueous solution using extractive distillation technique. They investigated the effect of an entrainer on the purity of acetonitrile produced, energy consumption and purity of the water recovered in the regeneration unit. They reported that glycerol was the most economical entrainer. The purity of the acetonitrile obtained by Sazonova & Raeva [13] was 99% which was neither adequate for acetonitrile to be used in HPLC (High Performance Liquid Chromatography) nor in pharmaceutical applications which are the major markets for acetonitrile. With further optimization of distillation conditions, the purity required for industrial application (99.5%) may be attained. The study nonetheless gives good insight into the relevant entrainers for extractive distillation.

Cheng et al. [17] considered several options for the recovery of pyridine and 3-methylpyridine from a stream of low boiling point organics stream but explored only 2 in detail. The explored processes were pervaporation and azeotropic distillation. Both processes could recover pyridine of industrial specifications, but it was found that the azeotropic distillation route was more economical. The conclusion reported in their work was contrary to what has been previously reported in literature that pervaporation is more economical than any type of distillation [17, 18].

One of the key studies done on the extractive distillation technique was by Hilal et al. [23]. Their study evaluated the factors that could reduce the solvent requirement in extractive distillation. The impact of solvent feed stage and splitting the solvent into 2 streams on the consumption of the solvent were investigated. Although the results found in this work were characteristic of the mixture being studied (methanol-acetone), the study addressed some of the key issues against extractive distillation i.e., the environmental concerns raised by the addition of an entrainer and the large amounts of entrainer required at times to effect separation where the solvent requirement may be up to 2 times the mixture in each stage [46].

Large entrainer requirements increase process costs in terms of entrainer procurement. The reduction of entrainer could further reduce the energy requirement of the extractive distillation column [23]. It was further reported by Hilal et al. [23] reported that that the solvent consumption was reduced by up to 35% due to moving the solvent feed stage from 3 to 8 when the mixture was fed at stage 2. An additional 28% reduction was experienced upon splitting the solvent feed into streams entering the column at stage 5 and 8 respectively in equal amounts.

Furthermore, Langston et al. [47] showed that the feed conditions of the extractive distillation column may impact the performance of the column on the methanol-acetone mixture. In their work, the effect of entrainer feed stages relative to the mixture feed stage, entrainer stream split as well as solvent feed conditions on the column performance were investigated. It was observed in this work that the purity of the distillate improved with increasing entrainer feed stage; this implied that sufficient distance between binary feed mixture and entrainer feed stages was required for efficient separation. This phenomenon can be ascribed to the fact that the solvent and the mixture have enough contact time to effect separation when the respective feed stages are far apart. Binary feed temperature as well as solvent feed temperature had no significant impact on the separation efficiency of the column [47]. In a typical distillation column, there is sufficient heat to induce separation of the mixture, therefore, it is sensible to learn that the feed temperature had negligible effect of the separation efficiency; if anything, feeding the mixtures near their boiling points should help reduce the heat duties of the column.

Upon reviewing technologies that can be used and have been used for the recovery of acetonitrile from acetonitrile-water azeotropic system, Mcconvey et al. [12] conducted a case study on the acetonitrile-water-toluene system; 4 azeotropes were said to exist in this system: acetonitrile-water, acetonitrile-toluene, water-toluene and water-acetonitrile-toluene. This study considered different azeotrope breaking agents and key issues with each were pointed out. The agents discussed were; ionic liquids, aromatics, ketones, esters and alcohols. Ionic liquids show a lot of potential for the recovery of acetonitrile but the problem with them as pointed out by Mcconvey et al. [12] is that there is no exhaustive data around their toxicity and thus their usage should be carried out with caution.

Summary of Recovery Technologies

The summary of the discussed separation techniques is given in Table 2.3. According to the summary, pervaporation has more merits to it than any other separation technique. However, the understanding of this process is still at elementary level. More research is still needed to fully understand the dynamics of pervaporation, especially the synthesis of suitable membranes with high recoveries. From the literature reviewed, it was established that membrane performance was sensitive to feed conditions. Liquid-liquid extraction on the other hand, is well understood in industry however, it has not been applied to separation of azeotropic mixtures, yet it is more economical than distillation techniques that can be used for azeotropic separations. Industry is well equipped with distillation-based techniques separation expertise. Moreover, a lot of capital has been invested in distillation equipment; it is reported that distillation is responsible for over 90% of all industrial separation in the United States [40]. Furthermore, distillation-based techniques have massive untapped potential such as the reduction of energy consumption using dividing wall column and diabatic operation.

Table 2.3. Summary of separation techniques considered

		Distillation		
Technique	**Pervaporation**	**Azeotropic**	**PSD**	**LLE**
Separation Basis	Membrane Permeability	Vapor Liquid Equilibrium(VLE)		Solubility
Industrial Application	Still at lab scale	Common		Common
Capital Investment	Low	High		Mid-Range
Energy Intensity	Low	High		Low
Solvent Addition	No	yes	no	Yes
Separation Efficiency	Sketchy	High		High

2.4. Energy Saving Techniques for Distillation Processes

Entropy minimization

The energy intensity associated with distillation remains a concern. It has been reported that distillation processes can account for up to over half of the energy consumption in a typical plant [25, 41, 48]. It has also been reported that distillation accounts for 5 million Ton Joules per year in the United States which is about 43% of the total net installed capacity [40]. Not only is distillation energy intensive, but it also generally has a low energy efficiency; i.e. thermodynamic second law efficiencies of 10-25% are typical in industry [49]. Entropy generation of a distillation column is directly proportional to its energy consumption and it is inversely proportional to the second law of thermodynamic efficiency [50].

Shen et al. [48] showed that entropy generation is a function of design variables such as reflux ratio and entrainer to feed ratio. The main source of entropy generation however, was found to be the cooler and the reboiler. Shen et al. [48] and Langston et al. [47] concur that the feed temperature is not an important variable in distillation design. It was also observed that reflux ratio had a more pronounced effect than solvent feed to feed ratio and as a result, it was recommended that to minimize entropy generation, entrainer to feed ratio should be increased and reflux ratio be decreased to a minimum possible value [48]. This may be sensible from a thermodynamic perspective but pose a problem from a material balance perspective as it will increase the amount of energy required to regenerate the solvent downstream. Moreover, the solvent costs would also increase. The use of a concept of entropy generation for energy analysis of a separation process has the advantage that it can identify areas of significant energy loss and can thus enable designers to selectively increase overall energy utilization [48].

To combat the high-energy consumption associated with distillation the concept of diabatic distillation has also been revisited by Koeijer & Kjelstrup [49]. This type of distillation is believed to have a higher thermodynamic second law efficiency (lower entropy generation) and to have a higher economic feasibility than its counter-part; adiabatic distillation [50]. This increased efficiency may be attributed to the supply or removal of heat at various stages of the column [51]. Koeijer & Kjelstrup [49] showed that entropy generation in an adiabatic distillation column can be reduced by 30-50% by using and optimizing a diabatic distillation column. It is of no surprise to learn of these results because in a diabatic distillation column, heat exchangers are used within trays to maximize energy utilization and replace the traditional reboiler and condenser in an adiabatic distillation column [51]. This is also in agreement with the observation by Shen et al. [48] that reboiler and condenser are the major sources of entropy generation. The use of heat exchangers at various levels within the column gives rise to the ability to provide exact heat where it is required.

Energy efficiency in a diabatic distillation column implies reduced operating costs because of reduced quantity of steam and cooling water requirement. However, this may be counteracted by the technical complexity of trays that demands expensive instrumentation and control [51]. The need to add an entrainer to overcome the azeotrope using extractive/azeotropic distillation has also been a point of major concern; this has been so because generally a solvent to feed ratio of at least 2:1 would be required for effective separation. However, recent studies have endeavored to reduce solvent consumption. Some of the suggestions that have been made are to split the solvent feed into 2 and to increase solvent feed and mixture feed distance.

Petlyuk Column and Dividing Wall Columns

The most promising technique to reduce the energy consumption of distillation columns for a multicomponent mixture separation is the thermal coupling of the distillation columns. This is referred to as Petlyuk column. It is reported that the implementation of this technique can save up to 20-40% of the reboiler duty [37, 52]. This may be due to the fact that Petlyuk column setup eliminates the need for a condenser and reboiler on every column and instead distillate vapor in one column is taken to the next distillation column without condensing thereby providing heat to that column (Figure 2.22).

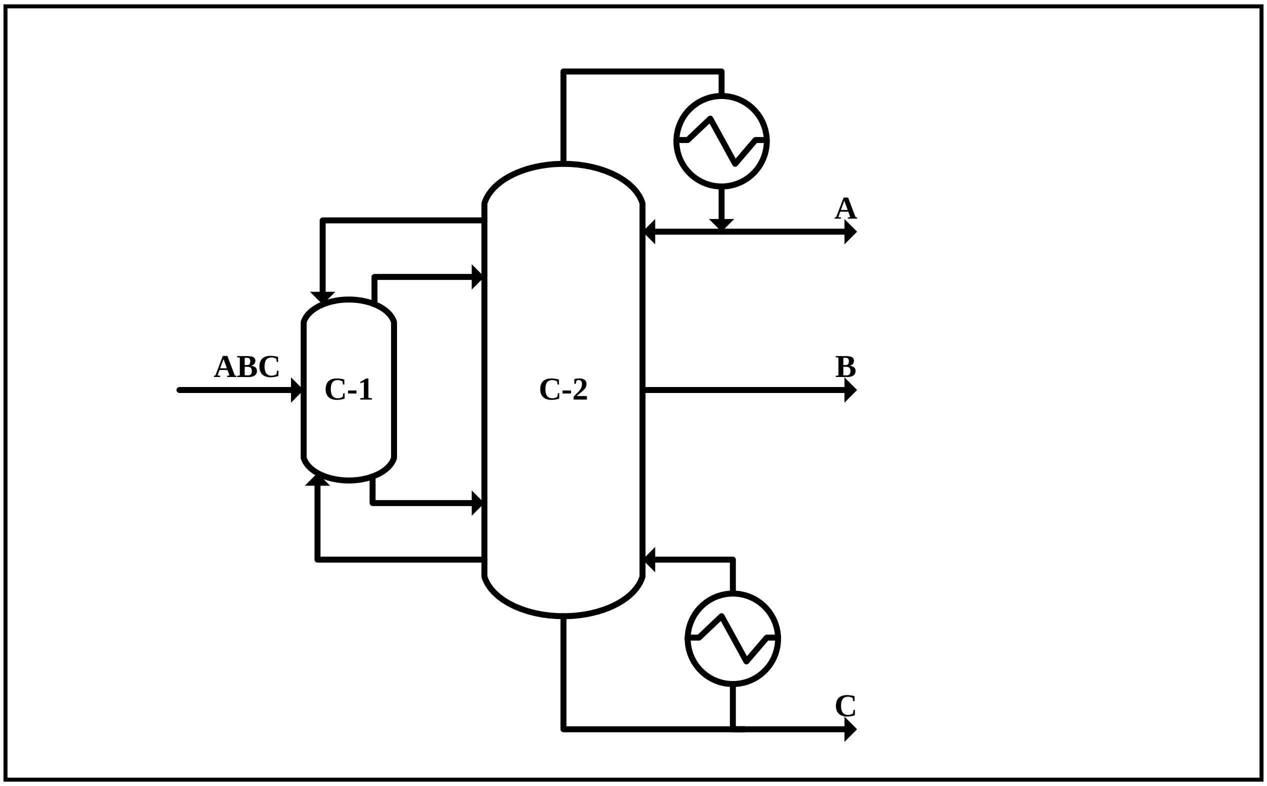

Figure 2.22. Petlyuk column setup [37]

The Petlyuk column can be further integrated into a single thermodynamically equivalent column referred to as the Dividing Wall Column (DWC) (Figure 2.23). In its basic form, DWC has a vertical wall that divides the column into 2 compartments that act as a pre-fractionator or post-fractionator and the main column (**I** and **II** in Figure 2.23 (a)). For a ternary mixture, the feed deflects against the wall; then the low boiling component moves upward along with some of the mid-boiling component. At the top stages, the mid-boiling component is separated from the low boiling component and goes down on the opposite side of the wall and the light component is recovered as the distillate. The rest of the mid-boiling component goes down with the high boiling component, separating in the lower stages of the column, then going upward on the opposite side of the wall while the heavy component is removed as the bottoms product. The mid-boiling component is then recovered as the midsection product of the column [36, 53].

Advantages of DWC over Petlyuk column include reduced capital investment due to equipment integration, reduced maintenance and control costs [53]. Both Petlyuk and DWC arrangements can reduce energy consumption of the distillation sequence by up to 30% [36]. Illner & Othman [53] illustrated the application of DWC for the fractionation of fatty acids in the oleochemical industries. The study is not comprehensive regarding the energy consumption of the DWC versus using 2 distillation columns in series. Bravo et al. [40] extrapolated the concept of DWC to extractive distillation claiming an improved thermodynamic efficiency from 21.42% to 23.70% compared to the conventional configuration.

Usually the Petlyuk equivalent of DWC (Figure 2.23 (b)) is used for simulation purposes since most of the commercial simulation software do not have the DWC unit in their libraries [35]. The Petlyuk column setup in Figure 2.23 (b) is referred to as the four-column model [54]. To mimic the DWC setup using the four-column model, 1 stripper, 2 absorbers and 1 rectifier are required. Because the stripper only has a reboiler and no condenser (column (**O**) in Figure 2.23 (b)), it is used to represent the bottom section of the DWC and the rectifier (column (**M**)) is used to represent the top section of the DWC since it only has a condenser and no reboiler. Lastly, 2 absorbers (columns (**L** and **N**)) are used to represent to represent the midsection of the column. The four-column is the closest representation of DWC in terms of practicality. Two more Petlyuk models for DWC representation and a more thorough discussion are presented in **Chapter 4**.

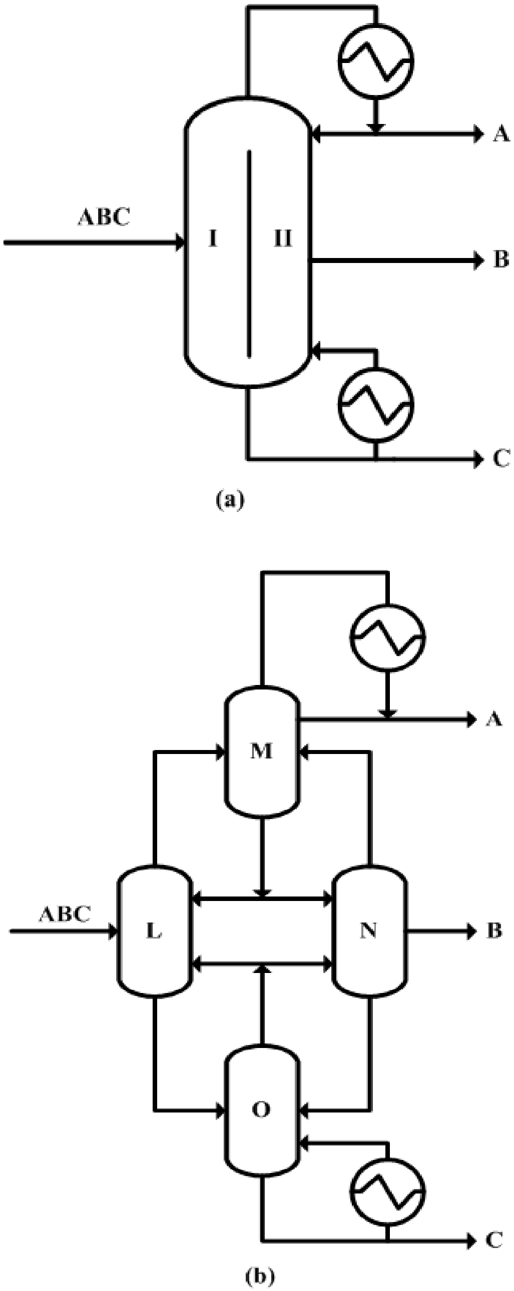

Figure 2.23. (a) Dividing Wall Column (DWC) configuration; (b) Equivalent Petlyuk column [54]

Entrainer selection is of utmost importance in the synthesis of azeotropic distillation since it determines feasible sequence and number of columns required to achieve the desired separation and consequently influences the economics of the distillation system [25, 41]. Thermodynamic tools can be used for distillation synthesis including entrainer screening for new/novel separation sequences.

2.5. Thermodynamic Tools for Separation Systems

Residue Curve Maps

A residue curve represents a change in composition of the liquid phase during continuous evaporation in a batch distillation [42]. The residue curve can be expressed mathematically as shown in equation (2.2). Alternately, residue curve can be determined experimentally by subjecting a mixture of certain composition to heat and recording the changing concentration of the liquid mixture remaining in the vessel. A collection of such curves with different starting compositions is referred to as the Residue Curve Map (RCM) (Figure 2.24). Detailed discussion of the topology of the residue curve maps and its implications on the separation sequence is given in **chapter 3**.

$$\frac{dx_i}{d\xi} = x_i - y_i \qquad (2.2)$$

Where

x_i: Liquid composition of component i

y_i: Vapor composition of component i

ξ: Dimensionless time

In addition to the assessment of feasibility of separation, flowsheet development and preliminary design, Residue Curve Maps (RCMs) can be used for the assessment of novel entrainers [41]. Prayoonyong [46] illustrated the use of RCMs for the assessment of novel entrainers when she was evaluating 1-butanol as a potential replacement for benzene (1-butanol was deemed as environmental friendlier than benzene) for the dehydration of ethanol. She concluded in this work that the use of 1-butanol was not economical compared to that of benzene which could be attributed to the large entrainer consumption of the 1-butanol system [46]. As such, RCMs are a valuable tool in distillation design.

Residue curve maps can also be used for entrainer selection for azeotropic distillation [41, 55, 56]. Julka et al. [41] summarized the process of using the residue curve maps for entrainer selection as: 1) plot RCM of each entrainer and the binary mixture being separated, 2) synthesize a distillation sequence by plotting material balance lines on the RCM and 3) make a decision on a suitable entrainer based on the feasibility and the number of columns required for separation using the entrainer [41]. The RCM approach may not always be effective for entrainer selection. For instance, when all the entrainers considered offer feasible separations with the same number of columns, then the method fails. It is rather useful for discarding entrainers that cannot work. So, it may be profitable to use it as an entrainer screening as opposed to entrainer selection process. Isovolatility curves are more suitable to assess the effectiveness of potential entrainers for the separation of azeotropic mixtures (more on this in **Chapter 3**). A complete residue curve map superimposed with the isovolatility curve, liquid-liquid immiscibility region and tie lines is depicted in Figure 2.24.

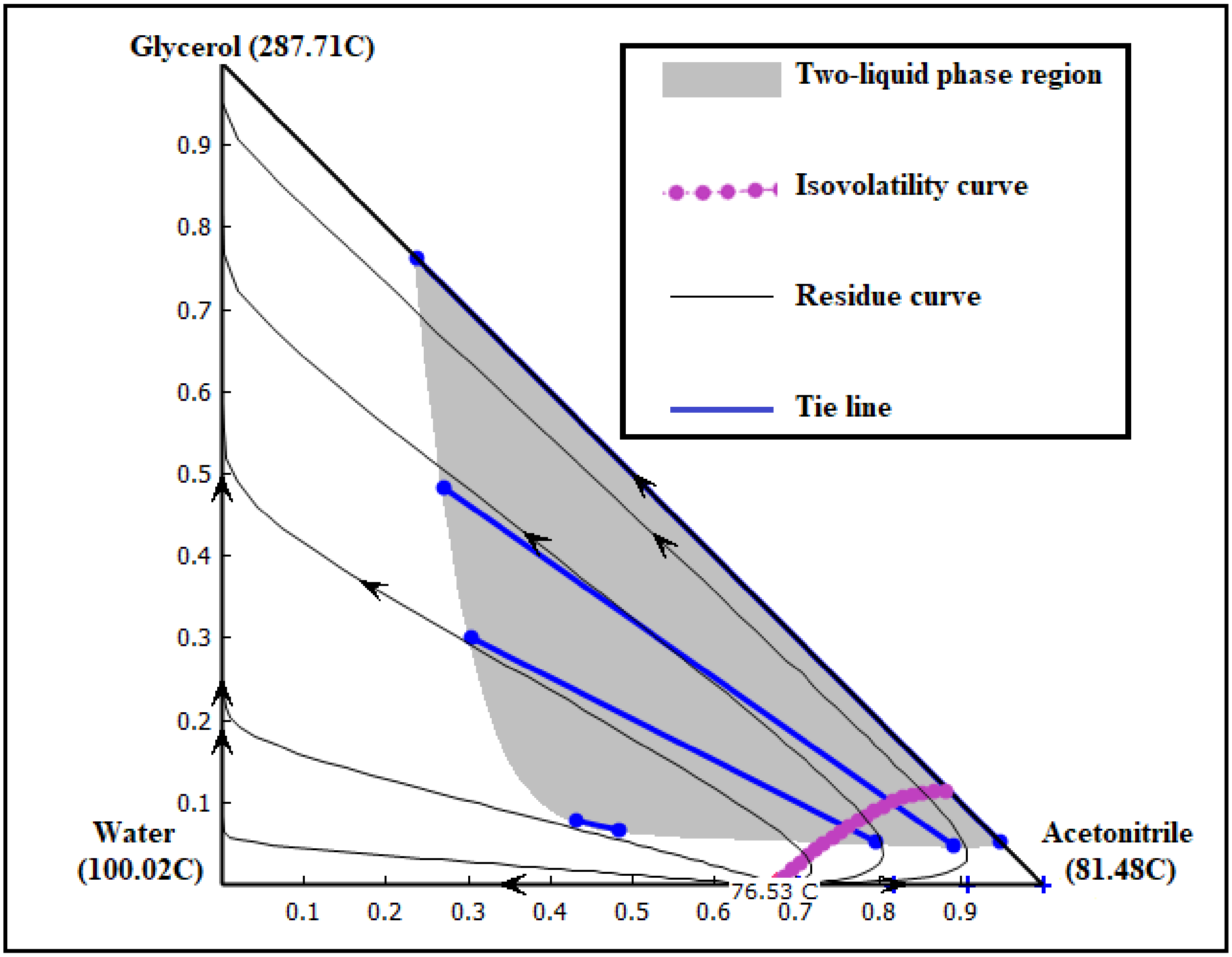

Figure 2.24. Residue curve map superimposed with isovolatility curve

Liquid-liquid immiscibility region represents a range of compositions in which there are 2 phases of liquids in the ternary mixture due to immiscibility of mixture components. The end of the tie lines within the liquid-liquid envelope denotes feasible products of liquid-liquid separation techniques such as decanting and liquid-liquid extraction (Figure 2.24). Wu & Chien [57] proposed the use of heterogeneous azeotropic distillation for the separation of pyridine and water using toluene as the entrainer. The use of RCM for the synthesis of distillation sequence was illustrated in their work. Using the residue curve maps enabled the authors to improve the initial design they proposed (Figure 2.25). The economic analysis of the 2 systems showed that by implementing the strategy presented in Figure 2.26 reduced the total annualized costs by 1.59 million USD, which was equivalent to about 40% reduction [57].

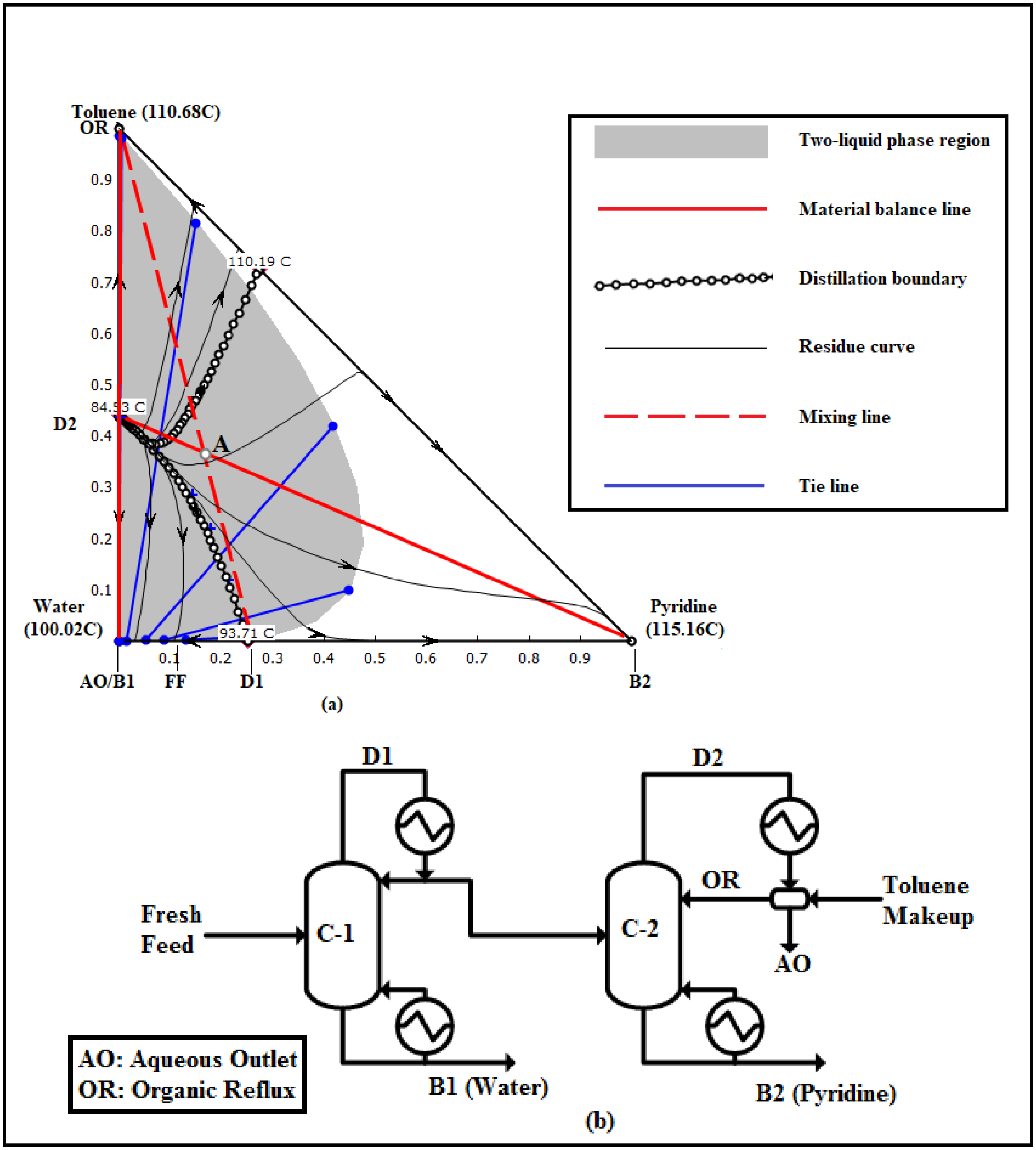

Figure 2.25. Pyridine-water RCM with material balances lines, liquid-liquid envelope and boundary lines; (b) Corresponding distillation sequence [57]

The feed is first preconcentrated to azeotropic composition in column C-1 by removing excess water which is collected as the bottoms product. The distillate (water-pyridine azeotrope) is mixed with toluene in column C-2. Then pyridine is collected as the bottoms product of C-2; the distillate of this column (water-toluene azeotrope) is cooled in a condenser and separated in a decanter into an organic rich phase and an organic lean phase. The organic rich phase is recycled into C-2 in the form of reflux. This is first mapped on the residue curve map using material balances. The problem with the design is that for it to be feasible, the material balance line must go through the distillation boundary which may require many stages which is in turn energy intensive (Figure 2.25) [57]. This is where the strength of RCM is shown as it enables process engineers to improve on poor distillation sequences design even before simulation stages.

Figure 2.26 depicts the improved version of the design in Figure 2.25. Instead of insisting the distillate to be the water-toluene azeotrope composition, the distillate is allowed to approach this composition without crossing the distillation boundary. This was a more realistic and sensible design. The water-pyridine mixture is very common azeotropic mixture occurring in industrial waste streams, however not much work has been done around its separation using azeotropic (homogeneous and heterogeneous alike). Although there has been patent work on the applicability for azeotropic distillation of this mixture, toluene is the only recorded entrainer which has been assessed in detail. Its application was assessed by Wu & Chien [57] and Sébastien et al. [58]. Moreover, these patents are old.

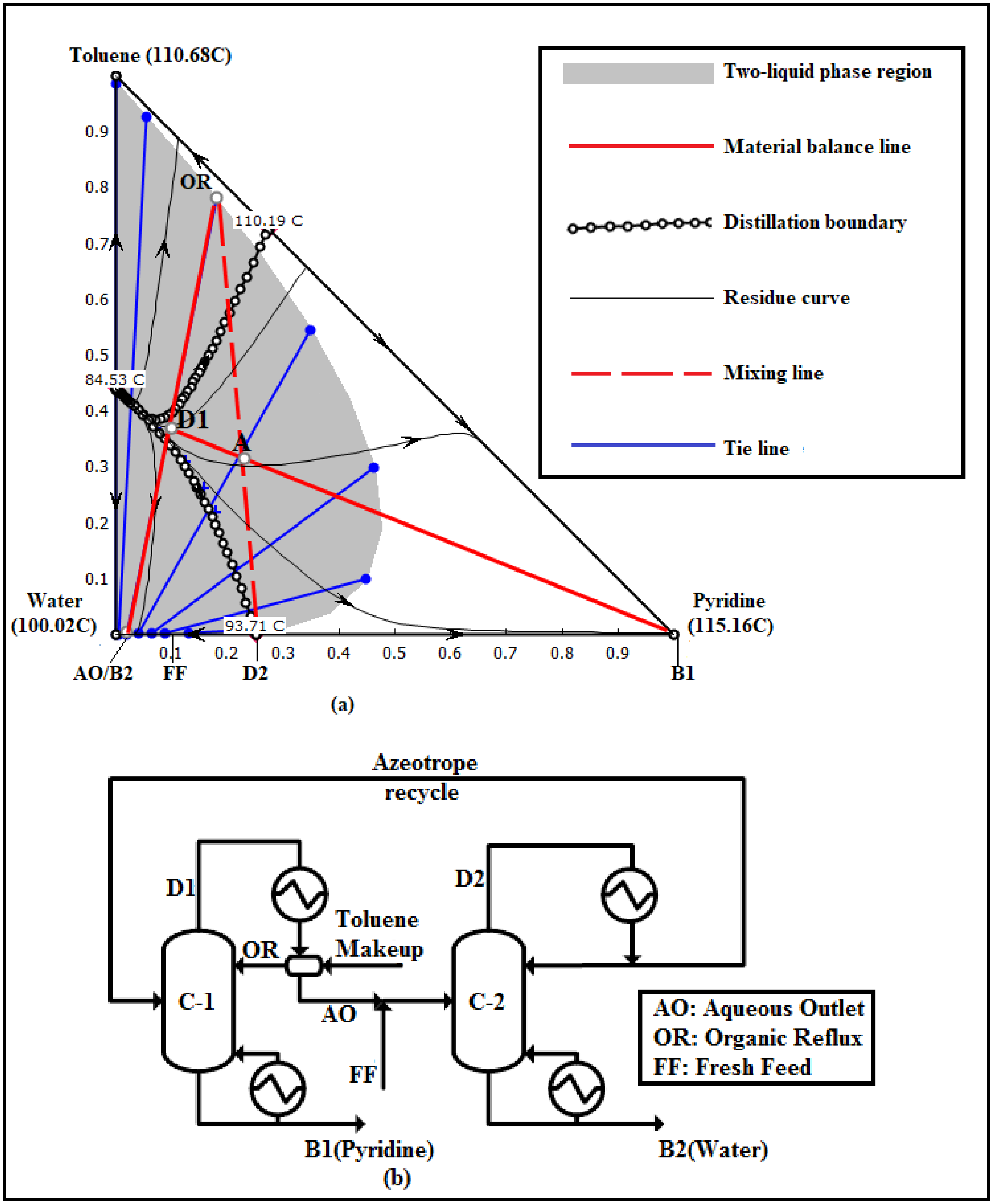

Figure 2.26. Improved pyridine-toluene-water system: (a) Residue curve maps; (b) Corresponding process flow diagram [57]

2.6. Aspen Plus

According Lladosa et al. [25] computer simulations are well established in the chemical and petrochemical industry as they are used in process development, design of equipment and optimization of both new and old plants. They are preferred because they avoid costly and time consuming processes of experimentation especially in the design of separation processes [25]. The major challenge in the simulation approach is finding reliable and consistent data [25]. Thermodynamic model chosen in the simulation determines the reliability and quality of the results obtained.

Aspen Plus is the industry leading chemical process simulation package that can be used for the design, control, optimization, and monitoring processes. It is used extensively in fine chemicals polymer, bulk and biochemical industries [59]. It has a wide-ranging, class leading database of pure components. Most of process units in the chemical industry, i.e., reactors, distillation columns, absorbers, strippers are built-in with Aspen Plus. For those units that are not part of the Aspen Plus library, it offers an option of building custom models which include pervaporation and other membrane-based techniques which can be modelled on the Aspen Custom Modeler (ACM) and then imported to Aspen Plus. Its reliability is corroborated by extensive use in industry. World class chemical processing companies such as Sasol make use of Aspen Plus in their operations. Moreover, the application of Aspen Plus is very commonly used in the simulation-based academic research.

References

[1] Department of Environmental Affairs, “National Waste Information Baseline Report,” 2012.

[2] D. Hoornweg, P. Bhada-Tata, and C. Kennedy, “Environment: waste production must peak this century,” *Nature*, vol. 502, pp. 615–617, Oct. 2013.

[3] E. C. S. Nunes and A. N. Haddad, “Waste Management in the Oil and Gas Industry by Brazilian Guideline for Environmental Audits - DZ-056-R.3,” *Am. J. Environ. Prot.*, vol. 2, p. 170, 2013.

[4] GreenCape, “Waste economy: market intelligence report 2016,” April, pp. 1–55, 2015.

[5] T. Majozi and P. Veldhuizen, “The chemicals industry in South Africa,” *Am. Inst. Chem. Eng.*, pp. 46–51, 2015.

[6] “Sasol produces 1,5 billion barrels of synthetic fuel from coal in fifty years | Sasol,” 2005. [Online]. Available: http://www.sasol.com/media-centre/media-releases/sasol-produces-15-billion-barrels-synthetic-fuel-coal-fifty-years. [Accessed: 22-Aug-2017].

[7] “Operations / Locations | Sasol.” [Online]. Available: http://www.sasol.com/about-sasol/regional-operating-hubs/southern-africa-operations/secunda-synfuels-operations. [Accessed: 28-Aug-2017].

[8] “The chemical industry: Sasol.” [Online]. Available: http://archive.cnx.org/contents/4733ff32-a845-42bb-b98d-37a346da5cce@1/the-chemical-industry-sasol. [Accessed: 28-Aug-2017].

[9] Sasol, “Sasol 50 years of Innovation,” *Sasol Ltd. 50th Anniv. J.*, 2000.

[10] H. S. Samanta and S. K. Ray, “Pervaporative recovery of acetone from water using mixed matrix blend membranes,” *Sep. Purif. Technol.*, vol. 143, pp. 52–63, 2015.

[11] L. Burger, R. von Gruenewaldt, and T. Bird, “Atmospheric impact report : Sasol

Secunda facility," vol. 27, 2014.

[12] I. F. McConvey, D. Woods, M. Lewis, Q. Gan, and P. Nancarrow, "The importance of acetonitrile in the pharmaceutical industry and opportunities for its recovery from waste," *Org. Process Res. Dev.*, vol. 16, pp. 612–624, 2012.

[13] A. Y. Sazonova and V. M. Raeva, "Recovery of acetonitrile from aqueous solutions by extractive distillation – effect of entrainer," *Int. J. Chem. Mol. Nucl. Mater. Metall. Eng.*, vol. 9, pp. 288–291, 2015.

[14] P. Das and S. Kumar, "Synthesis of highly water selective copolymer membranes for pervaporative dehydration of acetonitrile," *J. Memb. Sci.*, vol. 507, pp. 81–89, 2016.

[15] M. K. Mandal, S. B. Sant, and P. K. Bhattacharya, "Dehydration of aqueous acetonitrile solution by pervaporation using PVA-iron oxide nanocomposite membrane," *Colloids Surfaces A Physicochem. Eng. Asp.*, vol. 373, pp. 11–21, 2010.

[16] Marketsandmarkets, "Pyridine & amp; pyridine derivatives market worth 656.3 Million USD by 2021," 2017. [Online]. Available: http://www.marketsandmarkets.com/PressReleases/pyridine-derivatives.asp. [Accessed: 13-Jul-2017].

[17] R. Cheng, C.-H. Cho, S. Kirby, and B. Lim, "Economic recovery of pyridine and 3-methylpyridine," 2010.

[18] N. R. Singha, P. Das, and S. K. Ray, "Recovery of pyridine from water by pervaporation using filled and crosslinked EPDM membranes," *J. Ind. Eng. Chem.*, vol. 19, pp. 2034–2045, 2013.

[19] "Pyridine market: global industry size, share and forecast period 2015 -2025." [Online]. Available: http://www.persistencemarketresearch.com/market-research/pyridine-market.asp. [Accessed: 28-Jun-2017].

[20] C. Crew and T. Schafer, "Recovery of pyridine saves $1.5 million per year," 1993.

[21] Sasol, “Sasol online sustainable development information: responding to environmental challenges,” 2015.

[23] W. L. Luyben and I.-L. Chien, *Design and control of distillation systems for separating azeotropes*, vol. 53, 2013.

[24] N. Hilal, G. Yousef, and P. Langston, “The reduction of extractive agent in extractive distillation and auto-extractive distillation,” *Chem. Eng. Process.*, vol. 41, pp. 673–679, 2002.

[25] E. Lladosa, J. B. Montón, and M. Burguet, “Separation of di-n-propyl ether and n-propyl alcohol by extractive distillation and pressure-swing distillation: computer simulation and economic optimization,” *Chem. Eng. Process. Process Intensif.*, vol. 50, pp. 1266–1274, 2011.

[26] A. Kaewchada, S. Tubslingkra, and A. Jaree, “Separation of toluene from heptane via liquid–liquid extraction in microtube contactor using triethylene glycol,” *Chem. Eng. Res. Des.*, vol. 117, pp. 784–791, 2017.

[27] A. B. Pereiro and A. Rodríguez, “Ternary (liquid + liquid) equilibria of the azeotrope (ethyl acetate + 2-propanol) with different ionic liquids at T = 298.15 K,” *J. Chem. Thermodyn.*, vol. 39, pp. 1608–1613, 2007.

[28] M. Królikowski, “Liquid-liquid extraction of p-xylene from their mixtures with alkanes using 1-butyl-1-methylmorpholinium tricyanomethanide and 1-butyl-3-methylimidazolium tricyanomethanide ionic liquids,” *Fluid Phase Equilib.*, vol. 412, pp. 107–114, 2016.

[29] M. K. Mandal and P. K. Bhattacharya, “Poly(ether-block-amide) membrane for pervaporative separation of pyridine present in low concentration in aqueous solution,” *J. Memb. Sci.*, vol. 286, pp. 115–124, 2006.

[30] M. Khayet, C. Cojocaru, and G. Zakrzewska-Trznadel, “Studies on pervaporation separation of acetone, acetonitrile and ethanol from aqueous solutions,” *Sep. Purif. Technol.*, vol. 63, pp. 303–310, 2008.

[31] E. Drioli, S. Zhang, and A. Basile, “Recovery of pyridine from aqueous solution by

membrane pervaporation," *J. Memb. Sci.*, vol. 80, pp. 309–318, 1993.

[32] A. Y. Pulyalina, G. A. Polotskaya, K. Y. Veremeychik, M. Y. Goikhman, I. V. Podeshvo, and A. M. Toikka, "Ethanol purification from methanol via pervaporation using polybenzoxazinoneimide membrane," *Fuel Process. Technol.*, vol. 139, pp. 178–185, 2015.

[33] S. Xia, X. Dong, Y. Zhu, W. Wei, F. Xiangli, and W. Jin, "Dehydration of ethyl acetate-water mixtures using PVA/ceramic composite pervaporation membrane," *Sep. Purif. Technol.*, vol. 77, pp. 53–59, 2011.

[34] A. A. Kiss and R. R. Rewagad, "Energy efficient control of a BTX dividing-wall column," *Comput. Chem. Eng.*, vol. 35, pp. 2896–2904, 2011.

[35] R. K. Dohare, K. Singh, and R. Kumar, "Modeling and model predictive control of dividing wall column for separation of Benzene–Toluene- *o* -Xylene," *Syst. Sci. Control Eng.*, vol. 3, pp. 142–153, 2015.

[36] K. Khushalani, A. Maheshwari, and N. Jain, "Separation of mixture by divided wall column using Aspen Plus," *Int. J. Emerg. Technol. Adv. Eng.*, vol. 4, pp. 563–571, 2014.

[37] W. T. Chang, C. T. Huang, and S. H. Cheng, "Design and control of a complete azeotropic distillation system incorporating stripping columns for isopropyl alcohol dehydration," *Ind. Eng. Chem. Res.*, vol. 51, pp. 2997–3006, 2012.

[38] V. K. Sangal, V. Kumar, and I. M. Mishra, "Optimization of structural and operational variables for the energy efficiency of a divided wall distillation column," *Comput. Chem. Eng.*, vol. 40, pp. 33–40, 2012.

[39] Ö. Yildirim, A. A. Kiss, and E. Y. Kenig, "Dividing wall columns in chemical process industry: A review on current activities," *Sep. Purif. Technol.*, vol. 80, pp. 403–417, 2011.

[40] C. Bravo-Bravo, J. G. Segovia-Hernández, C. Gutiérrez-Antonio, A. L. Durán, A. Bonilla-Petriciolet, and A. Briones-Ramírez, "Extractive dividing wall column: design and optimization," *Ind. Eng. Chem. Res.*, vol. 49, pp. 3672–3688, 2010.

[41] V. Julka, M. Chiplunkar, and L. O. Young, “Selecting entrainers for azeotropic distillation,” *Aiche*, pp. 47–53, 2009.

[42] J. Gmehling and C. Mollman, “Synthesis of Distillation Processes Using Thermodynamic Models and the Dortmund Data Bank,” *Am. Chem. Soc.*, vol. 5885, pp. 3112–3123, 1998.

[43] Z. Zhu, D. Xu, X. Liu, Z. Zhang, and Y. Wang, “Separation of acetonitrile/methanol/benzene ternary azeotrope via triple column pressure-swing distillation,” *Sep. Purif. Technol.*, vol. 169, pp. 66–77, 2016.

[44] Y. Wang, Z. Zhang, D. Xu, W. Liu, and Z. Zhu, “Design and control of pressure-swing distillation for azeotropes with different types of boiling behavior at different pressures,” *J. Process Control*, vol. 42, pp. 59–76, 2016.

[45] L. Berg and Z. Yang, “Separation of pyridine from water using extractive distillation,” 1992.

[46] P. Prayoonyong, “Conceptual design of heterogeneous azeotropic distillation process for ethanol dehydration using 1-butanol as entrainer,” *Maejo Int. J. Sci. Technol.*, vol. 8, pp. 334–347, 2014.

[47] P. Langston, N. Hilal, S. Shingfield, and S. Webb, “Simulation and optimisation of extractive distillation with water as solvent,” *Chem. Eng. Process. Process Intensif.*, vol. 44, pp. 345–351, 2005.

[48] W. F. Shen, H. Benyounes, and J. Song, “Thermodynamic topological analysis of extractive distillation of maximum boiling azeotropes,” *Brazilian J. Chem. Eng.*, vol. 32, pp. 957–966, 2015.

[49] G. De Koeijer and S. Kjelstrup, “Minimizing entropy production rate in binary tray distillation,” *Int. J. Thermodyn.*, vol. 3, pp. 105–110, 2000.

[50] P. Salamon, G. Siragusa, M. Schaller, and K. H. Hoffmann, “Comparison of entropy production rate minimization methods for binary diabatic distillation,” pp. 5826–5834, 2002.

[51] R. Rivero, “Exergy simulation and optimization of adiabatic and diabatic binary distillation,” vol. 26, pp. 561–593, 2001.

[52] R. Delgado-Delgado, S. Hernández, F. O. Barroso-Muñoz, J. G. Segovia-Hernández, and V. Rico-Ramírez, “Some operational aspects and applications of dividing wall columns: energy requirements and carbon dioxide emissions,” *Clean Technol. Environ. Policy*, vol. 17, pp. 657–665, 2015.

[53] M. Illner and M. R. bin O. Othman, “Modeling and simulation of a dividing wall column for fractionation of fatty acid in oleochemical industries,” *Iran. J. Chem. Eng.*, vol. 12, pp. 60–67, 2015.

[54] M. T. D. Nguyen, “Conceptual Design, Simulation and Experimental Validation of Divided Wall Column: Application for Nonreactive and Reactive Mixture,” Toulouse Institute of Technology, 2015.

[55] M. A. Schultz, D. G. Stewart, J. M. Harris, S. P. Rosenblum, M. S. Shakur, and D. E. O’Brien, “Reduce costs with dividing-wall columns,” *Chem. Eng. Prog.*, vol. 98, pp. 64–71, 2002.

[56] W. E. De Villiers, R. N. French, and G. J. Koplos, “Navigate phase equilibria via residue curve maps,” *Chem. Eng. Prog.*, vol. 98, pp. 66–71, 2002.

[57] Y. C. Wu and I. L. Chien, “Design and control of heterogeneous azeotropic column system for the separation of pyridine and water,” *Ind. Eng. Chem. Res.*, vol. 48, pp. 10564–10576, 2009.

[58] P. Sébastien, M. Silvère, G. Vincent, B. Olivier, B. Philippe, and J. Xavier, “Heterogeneous batch distillation processes: Real system optimisation,” *Comput. Aided Chem. Eng.*, vol. 20, pp. 1081–1086, 2005.

[59] “Aspen Technology,” 2017. [Online]. Available: http://home.aspentech.com/products/engineering/aspen-plus/. [Accessed: 22-Aug-2017].

Chapter 3 : Recovery of Pyridine-Thermodynamic Constraints and Alternatives Analysis

The summary of this chapter was submitted as a conference paper and presented orally at the International Research Conference on Sustainable Energy, Engineering, Materials and Environment (IRCSEEME), United Kingdom, England, Northumbria University, 26-28 July 2017. The submitted paper can be found in Appendix A.

In this chapter**,** the recovery of pyridine from the High Organic Waste (HOW) produced at Sasol Secunda plant is discussed. This chapter is concerned with the recovery of pyridine from the High Organic Waste (HOW) produced at Sasol Secunda plant. Water recovery from the HOW is also assessed to add to the already implemented water utilization efficiency strategies at Sasol Secunda. The recovery is divided into 2 sections. The first section is about separation of water-pyridine mixture from the HOW and the second section is concerned with pyridine enrichment using thermodynamic tools.

3.1. Introduction

Pyridine is a versatile chemical solvent with application in a variety of industries [1]. It is used in the paint, spectrometry, and pharmaceutical industries [2]. A recent surge in pyridine usage in the agrochemical industry has contributed to its increased demand [1]. The pyridine market size is estimated around 400 million USD in 2017 and it is projected that the market size will increase by 50% in the next five years [1,2]. Consequently, pyridine recovery from water and other components is an ongoing research topic [3]. Luyben & Chien [3] proposed the use of heterogeneous azeotropic distillation using toluene as an entrainer; Burroughs Wellcome Co implemented liquid-liquid extraction for the recovery of pyridine from a waste stream and made 1.5 million USD worth of savings per annum in the early 1990s [4]. Although novel separation techniques such as pervaporation have been proposed for the separation of azeotropic mixtures such as water-pyridine, water-ethanol and water-acetonitrile [5-8], distillation remains the most widely used separation technique in industry today [9]. Distillation processes are well understood and are continuously improved [9-12].

In its ordinary form, distillation cannot separate azeotropic mixtures. As a result, modified distillation techniques such as azeotropic distillation (homogeneous and heterogeneous) and pressure swing distillation (PSD) are used for this purpose [13,14]. Pressure swing distillation involves using 2 or more columns operating at different pressures and may be suitable if the azeotropic mixture is pressure sensitive [3]. Since pyridine-water azeotrope is not pressure sensitive, this technique cannot be used [10,15].

Homogeneous azeotropic distillation (usually referred to as extractive distillation) involves the addition of a heavy entrainer (heavier than all the components originally in the mixture). Preferably, the entrainer should not introduce a new azeotrope onto the system for extractive distillation [13,16]. In contrast, heterogeneous azeotropic distillation entrainer introduces one or more azeotrope(s) and liquid-liquid immiscibility to the original mixture [12]. The new azeotrope must have the lowest boiling point of all components and azeotropes originally present in the mixture [3].

The addition of an entrainer in azeotropic distillation is a cause for concern especially for the application of waste minimization. In some applications, the entrainer to mixture ratio (EA) can be as high as 8:1, as in the dehydration of ethanol using 1-butnaol [12]. The higher the entrainer demand, the more redundant the waste treatment becomes since the chief aim is to reduce waste while the recovery of valuable chemicals serves as motivation. The entrainer reduction techniques including increasing the distance between entrainer and azeotropic mixture feed points and splitting the entrainer feed were studied by Hilal et al. [17], but entrainer consumption reduction has generally not been addressed adequately in the past, therefore, this chapter aims to expand on the subject as well.

The objective in this chapter was to assess the economic pyridine enrichment from the High Organic Waste (HOW) stream produced at Sasol Secunda plant using known separation techniques. The assessment was done through the combination of thermodynamic tools and Aspen plus process simulator. Hitherto, no other solvent apart from toluene has been studied in detail for the separation of water and pyridine azeotrope. In this chapter, Methyl Isobutyl Ketone (MIBK) and chloroform were compared as potential entrainers for the same. The assessment of MIBK and chloroform as potential entrainers was informed by the mentioned literature [4,18]. Solvent demand in the proposed process was then compared with the classical example of toluene-water-pyridine system proposed by Wu & Chien [19].

3.2. Separating Water-Pyridine Mixture from the HOW

A large fraction of the stream is made up of water. The stream composition is given in Table 3.1. As can be seen from Table 3.2, water is common in all the azeotropes formed except for the acetonitrile-Methyl Ethyl Ketone azeotrope. Azeotropic compositions were obtained from Aspen Plus using the “distillation synthesis” function. Pyridine is the highest boiling component, followed by water and Methyl Isopropyl Ketone (MIPK). Also, water-pyridine azeotrope is the highest boiling azeotrope in the feed mixture. The difference between the boiling points allows for the isolation of water-pyridine azeotrope using fractional distillation (Figure 3.2). This can be done without the loss of pyridine because pyridine forms azeotrope with water only. From these observations, the generic process flow diagram is depicted in Figure 3.1.

Table 3.1. Waste stream composition, existing azeotropes and boiling points

Component	**Mass Fraction**	**BP(°C)**	**Azeotropes Formed**	**Azeotrope BP(°C)**
Pyridine	**0.05**	**115.16**	**W-P**	**93.71**
Acetone	0.02	56.14	W-A	76.53
Water	**0.62**	**100.02**	**W-A-MIPK**	**76.32**
Acetonitrile	0.15	81.48	W-MEK	79.34
Methyl Ethyl Ketone	0.04	79.34	W-MIPK	77.61
Methyl Iso Propyl Ketone	0.12	94.08	A-MEK	79.09

Table 3.2. Nomenclature for Table 3.1 and azeotropic compositions

Abbreviation	**Explanation**	**Azeotropic composition (Mass fraction)**
W-P	Water-Pyridine	0.596 Pyridine
W-A	Water-Acetonitrile	0.825 Acetonitrile
W-A-MIPK	Water-Acetonitrile-Methyl Isopropyl Ketone	0.5353 Acetonitrile, 0.2887 MIPK
W-MEK	Water-Methyl Ethyl Ketone	0.875 MEK
W-MIPK	Water-Methyl Isopropyl Ketone	0.792 MIPK
A-MEK	Acetonitrile-Methyl Ethyl Ketone	0.712 MEK

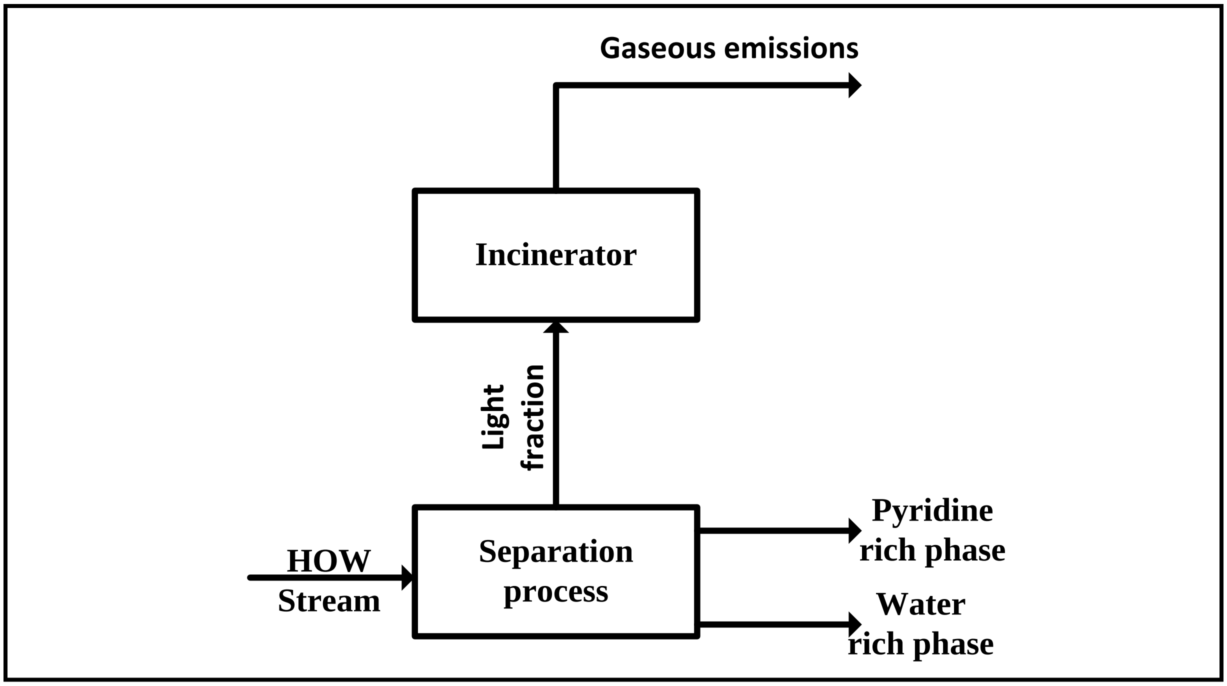

Figure 3.1. Generic layout of the separation process

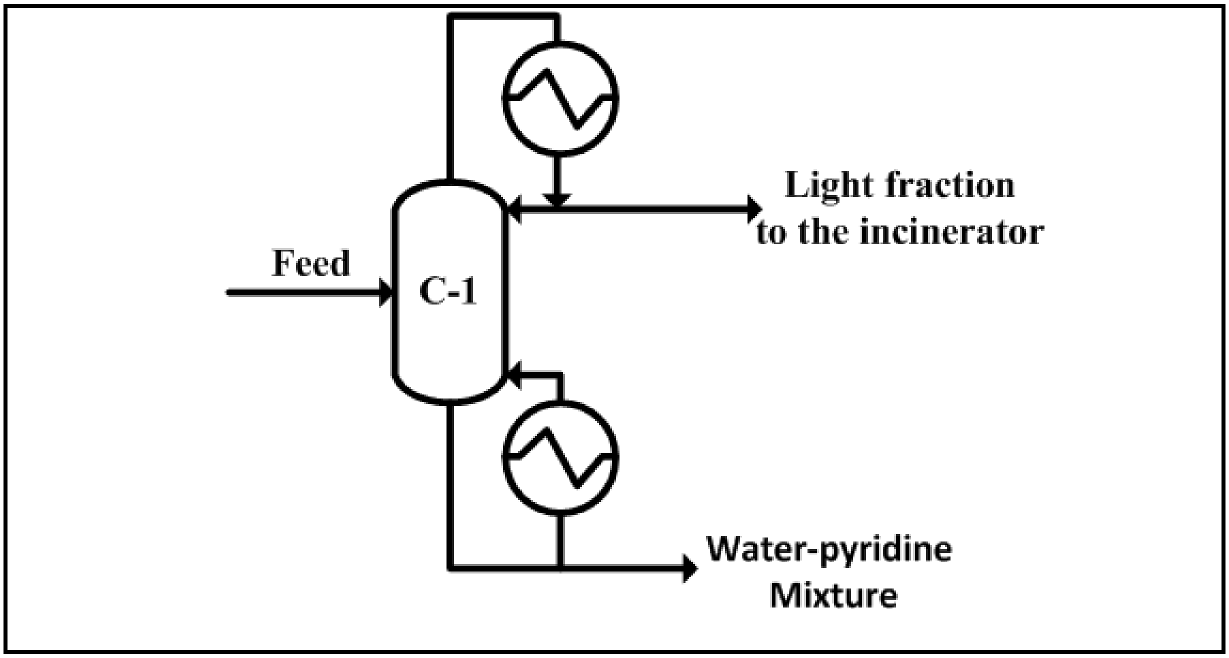

Figure 3.2. Separation of the water-pyridine mixture from the HOW

Assumptions

1. The waste stream flow rate is 20kton/year.
2. Pressure drop is insignificant in all distillation columns.
3. NRTL property method was used across all process units: Aspen plus uses the modified Antoine equation (3.1) to calculate the liquid activity coefficients using binary parameters. The binary parameters used can be found in Appendix D, Table D.1.

$$\ln \gamma_i = \frac{\sum_j x_j \tau_{ji} G_{ji}}{\sum_k G_{ki}} + \sum_j \frac{x_j G_{ij}}{\sum_k G_{kj}} \left[\tau_{ij} \frac{\sum_m x_m \tau_{mj} G_{mj}}{\sum_k x_k G_{kj}} \right] \qquad (3.1)$$

Where:

$$G_{ij} = \exp\left(-\alpha_{ij} \tau_{ij}\right) \qquad (3.2)$$

$$\tau_{ij} = a_{ij} + \frac{b_{ij}}{T} + e_{ij} lnT \qquad (3.3)$$

$$\alpha_{ij} = c_{ij}, \qquad \tau_{ii} = 0, \qquad G_{ii} = 1 \qquad (3.4)$$

3.2.1. Shortcut Model to determine Distillation Parameters for the Rigorous Simulation

Using the Distillation-Winn-Underwood (DSTWU) column in its model library, Aspen Plus uses the Winn Underwood Gilliland shortcut design method to determine the minimum number of stages given the reflux ratio and vice versa. The method also determines the optimum feed stage along with the reboiler and condenser duties (ASPEN Plus help function). The summary of the use of each correlation is given in Table 3.3.

Table 3.3. Summary of the Winn Underwood Gilliland shortcut design calculation (Aspen Plus help function)

DSTWU uses this method/correlation	**To estimate**
Winn	Minimum number of stages and optimum feed location at total reflux
Underwood	Minimum reflux ratio
Gilliland	Required reflux ratio and optimum feed location for the specified number of stages, or the required number of stages and optimum feed location for the specified reflux ratio

The Winn method is simply a modification of the Fenske equation (equation (3.5)).

$$N_{min} = \frac{ln\left[\frac{X_{LK,D}}{X_{LK}}\left(\frac{X_{HK,B}}{X_{HK,D}}\right)^{\theta_{LK}}\right]}{\ln \beta_{LK/HK}} \tag{3.5}$$

Where:

B: Bottoms rate

D: Distillate rate

LK: Light Key

HK: Heavy Key

$\beta_{LK/HK}$ and θ_{LK} are constants at fixed pressure determined using K values for the Light Key and Heavy Key at the bottom temperature.

Gilliland [20] produced a plot that correlated the minimum number of stages to the actual number of stages. In his plot (N-N_{min})/(N+1) and (R-R_{min})/(R+1) were plotted as the Y-axis and X-axis respectively. The mathematical expression of the plot has since been the subject of many studies, however the most famous expression was presented in 1972 by Molokanov and colleagues (3.6) [21].

$$\frac{N-N_{min}}{N+1}=1-exp\left[\left(\frac{1+\frac{54.4(R-R_{min})}{R+1}}{11+\frac{117.2(R-R_{min})}{(R+1)}}\right)\left(\frac{\frac{R-R_{min}}{R+1}-1}{[(R-R_{min})(R+1)]^{0.5}}\right)\right] \tag{3.6}$$

Where:

R: Reflux ratio

R_{min}: Minimum reflux ratio

N: Number of stages

N_{min}: Minimum number of stages

On the other hand, the Underwood equation is given by (3.7).

$$R_{min}+1=\sum_{1}^{n}\frac{X_D}{(\alpha-\theta)/\alpha} \tag{3.7}$$

Where:

n: Number of components

α: Relative volatility

These methods assume constant overflow and that the relative volatility does not change in the mean column temperature. An example of the shortcut model specifications on Aspen Plus can be found in Appendix B.1. The results obtained from the shortcut simulation model are presented in Table 3.4.

Table 3.4. Shortcut model results for column (C-1)

Parameter	**C-1**
Number of Stages	20
Reflux Ratio	7
Feed stage	7

3.2.2. Rigorous simulation of the Water-Pyridine Mixture from the HOW

In this section the specifications as input on Aspen Plus are illustrated and where needed explained; for instance, the choice of distillate rate and the calculations for such are shown and the assumptions made are stated. The results (material balance) are also discussed.

Aspen plus specifications and explanations

Distillation column C-1

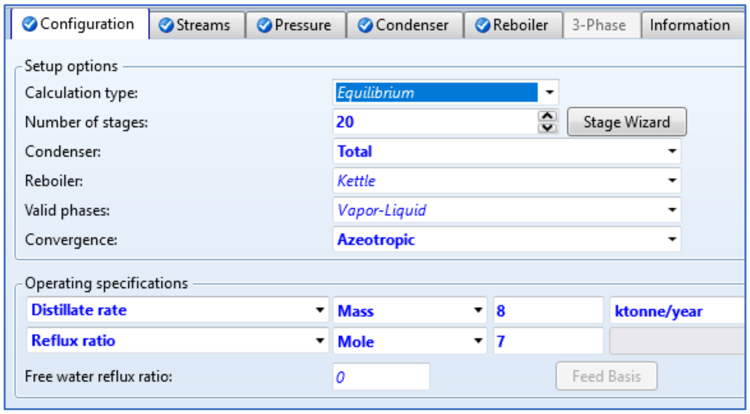

Setup options
Calculation type: Equilibrium
Number of stages: 20
Condenser: Total
Reboiler: Kettle
Valid phases: Vapor-Liquid
Convergence: Azeotropic

Operating specifications
Distillate rate: Mass 8 ktonne/year
Reflux ratio: Mole 7
Free water reflux ratio: 0

Figure 3.3. Specification for the configuration of column C-1

To get a good initial estimation of the distillate rate in column C-1, it was assumed, due to large presence of water (over 60mass% (Table 3.1)), that all water-component azeotrope forming components were consumed into forming water-component azeotropes. This suggested that they did not exhibit individual properties but displayed water-component azeotropic properties depicted in Table 3.1 and Table 3.2. Feed component flowrate was used along with component-water azeotropic composition to determine the component-water azeotropic flowrate. For instance, acetonitrile flowrate in the feed is 3kton/year and composition of acetonitrile in the acetonitrile-water azeotrope is 0.825 (Table 3.2). Therefore, the water-acetonitrile azeotrope flowrate was determined by dividing 3kton/year by 0.825.

The same procedure was followed to determine the flowrates of all other component-water azeotrope flowrate and the total was calculated to be 7.580kton/year as shown in Table 3.5. However, when this value was specified as the distillate rate, the simulation resulted in errors. Therefore, from this value, the 8kton/year specified on Aspen Plus (Figure 3.3) was found by trial and error. The error can be attributed to the fact that the water-acetonitrile-MIPK azeotrope was not accounted for in these calculations (Table 3.2). However, the assumption provided a good initial estimate for simulation and it will be further validated or disqualified by the simulation results discussed in the sections to follow.

Table 3.5. Component-water azeotrope flowrate

Name of component	**Mass flowrate (kg/hr)**	
Component	Pure component	Component-water azeotrope
Acetonitrile	3.000	3.635
MEK	0.800	0.915
MIPK	2.400	3.030
Total	**6.200**	**7.580**

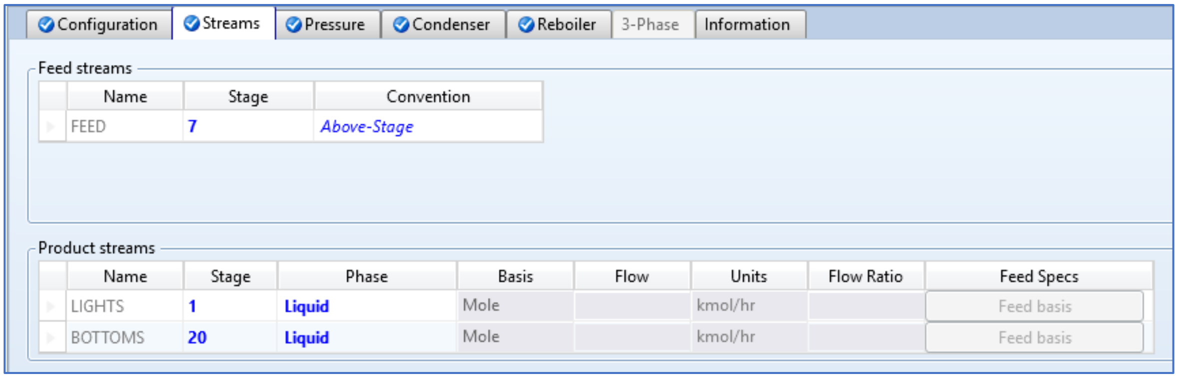

Feed streams

Name	Stage	Convention
FEED	7	Above-Stage

Product streams

Name	Stage	Phase	Basis	Flow	Units	Flow Ratio	Feed Specs
LIGHTS	1	Liquid	Mole		kmol/hr		Feed basis
BOTTOMS	20	Liquid	Mole		kmol/hr		Feed basis

Figure 3.4. Feed stage specifications for column C-1

The material balance around column C-1 is depicted in Figure 3.5. The simulation results are in line with the assumption made regarding the behavior of components in the mixture. On the other hand, the acetonitrile presence in the water-pyridine mixture stream was not expected (Figure 3.5). However, it is noteworthy that over 99mol% of acetonitrile was recovered to the distillate and its composition in the water-pyridine mixture stream is only 0.1mol% (Figure 3.5). The impact of the presence of acetonitrile in this stream will be evaluated in the subsequent sections.

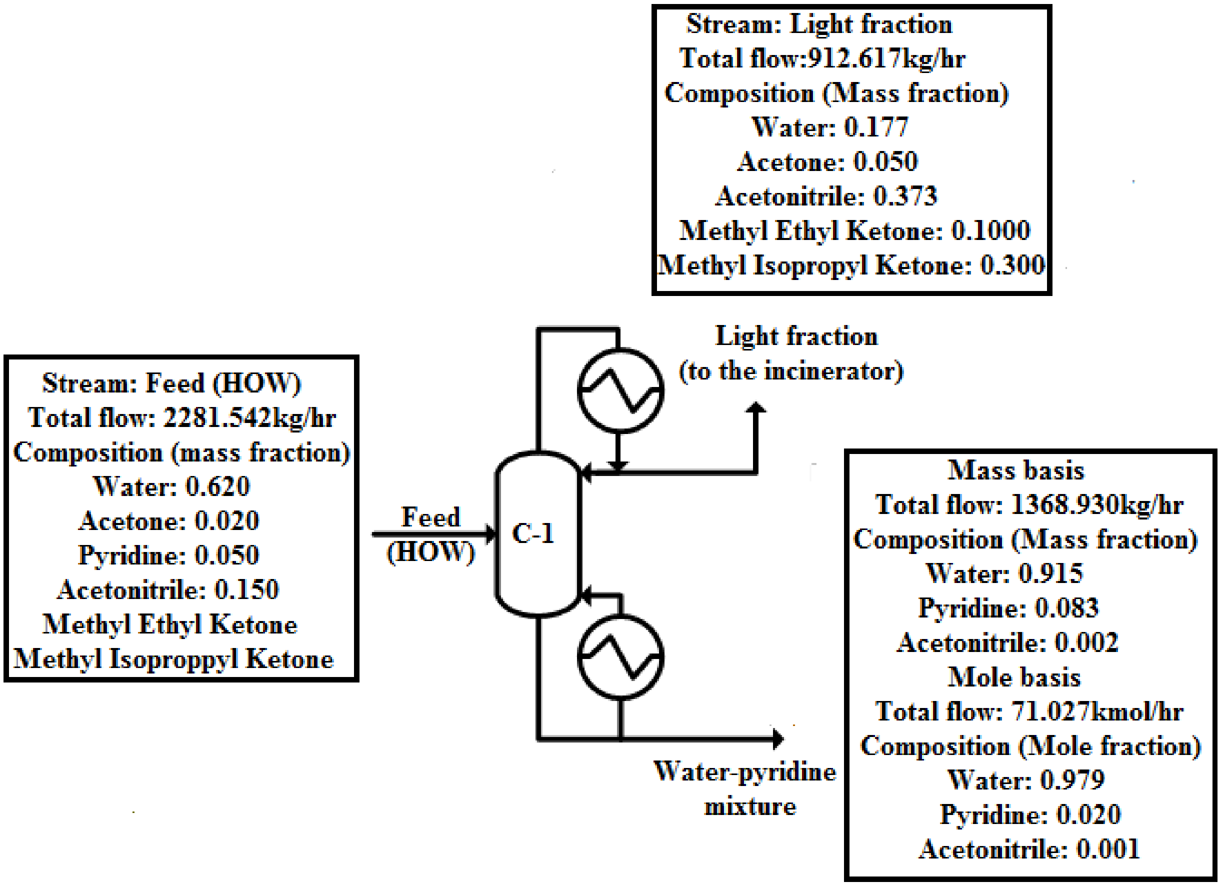

Figure 3.5. Material balance for water-pyridine mixture separation from the HOW

3.3. Pyridine Enrichment

3.3.1. Thermodynamic Analysis

Thermodynamic analysis of separation processes has been proposed to gain insight of the processes. The most used thermodynamic tools used for separation processes are residue curve maps and isovolatility curves. These are commonly applied to distillation based techniques [16, 22, 23].

Residue Curve Maps (RCMs)

Residue curve maps (RCMs) are primarily used for the preliminary design of distillation sequence and to assess the feasibility of separation [15, 16]. Other uses include column troubleshooting and control [16]. Although the RCMs are useful, their use have been extremely limited in the past due to the tedious process of producing them mathematically [16]. Today, computer software such as Aspen Plus and Matlab can generate these curves with relative ease. In this work, Aspen Plus was used to generate the residue curve maps. A residue curve represents composition of a liquid remaining in the vessel during simple batch distillation process [23]. This can be represented mathematically by equation (3.8) [12].

$$\frac{dx_i}{d\xi} = x_i - y_i \tag{3.8}$$

Where:

x_i: Liquid composition of component i

y_i: Vapor composition of component i

ξ: Dimensionless time

A residue curve starts at a lowest boiling component represented as the unstable node (**M**) and approaches the intermediate boiling component (Figure 3.6). The mid-boiling component appears as the saddle node (**L**) in the residue curve map. Finally, the residue curve ends up at the stable node (**N**) which corresponds to the high boiling component (Figure 3.6). Residue curve maps generated for azeotropic distillation will typically have at least one distillation boundary (**A, M**) (Figure 3.6).

The distillation boundary divides the RCM into regions and represents a thermodynamic limitation. For instance, a ternary mixture found in region **I** (**A, L, M**) can only be separated into **component 1**, **component 3** and **the azeotrope** (**A**) (Figure 3.6). The recovery of pure **component 2** from region **I** can only be achieved by crossing the distillation boundary, which cannot be done using ordinary distillation. Material balance lines are used to synthesize and assess different distillation sequences. The material balance line must start and end on the same residue curve as shown in Figure 3.6 (**X, Y**). One end of the material balance line represents the distillate and the other represents the bottoms product.

Isovolatility Curves

The isovolatility curve tracks the composition in which the relative volatility of the mixture is 1 [3]. Below the isovolatility curve (**A, B**) (Figure 3.6), the relative volatility of the mixture is less than unity and is thus more difficult to separate [39]. On the contrary, above the isovolatility curve, the relative volatility of the mixture is greater than unity and it is relatively easier to separate. The superimposition of the isovolatility curve on the residue curve map can help with the comparison of the effectiveness of potential entrainers for azeotropic distillation [3]. The isovolatility curve starts at the azeotrope (**A**) and ends at the intersection where the composition of one of the components in the original binary mixture is zero (**B**) (Figure 3.6). The entrainer whose point **B** (Figure 3.6) is farther from the entrainer is regarded as the most effective entrainer for enhancing the relative volatility of the mixture [3]. The isovolatility curve also gives insight about feasible distillate product of the extractive distillation column [3]. The component with the lowest boiling point at the intersection (**B**) becomes a feasible distillate [3]. In the case of RCM presented in Figure 3.6, Component 3 is a feasible distillate product. This concept is reserved for extractive distillation with a heavy entrainer [3].

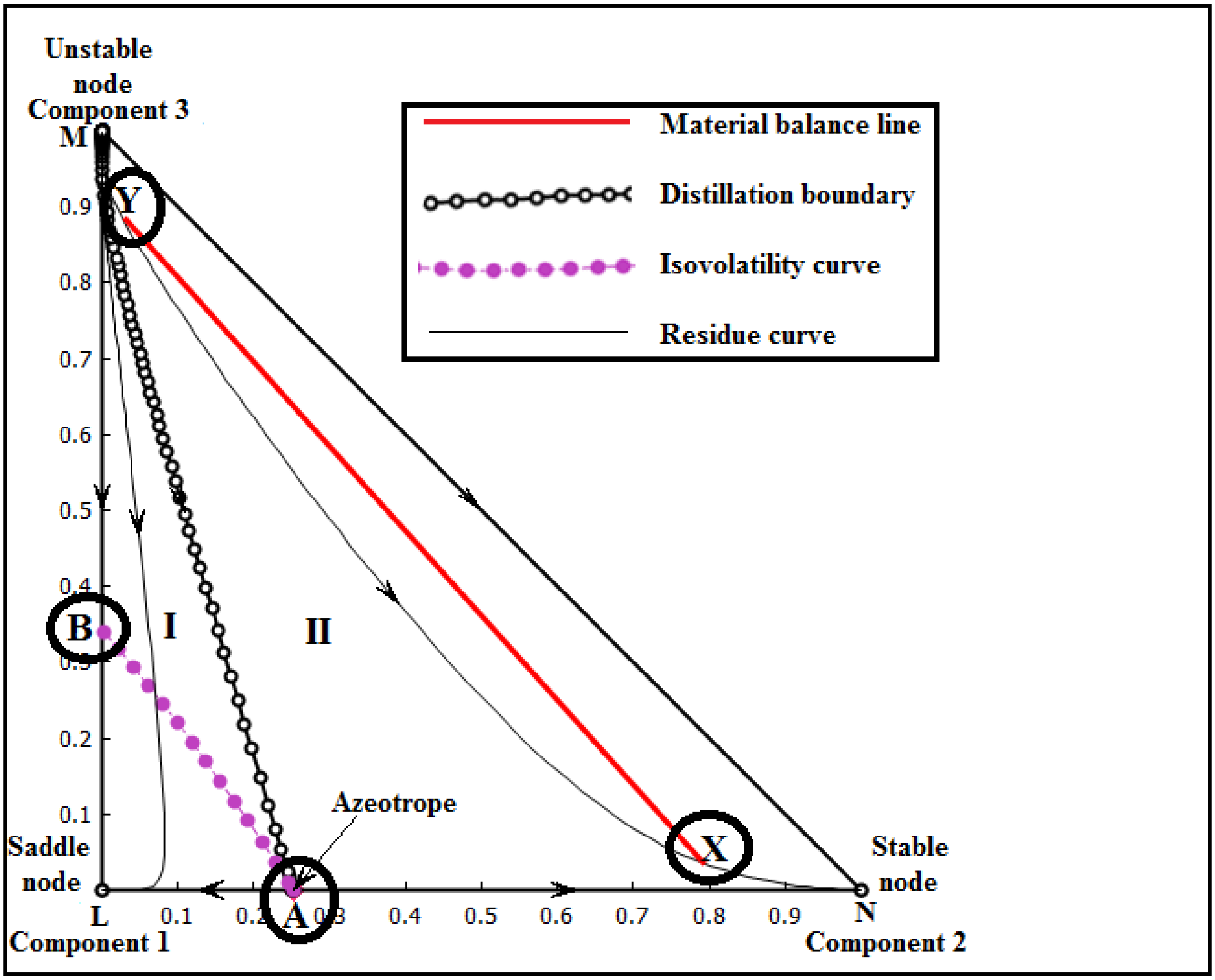

Figure 3.6. Superimposition of isovolatility curve on a residue curve map

The knowledge of feasible distillate product ahead of time is valuable because it is preferable to recover the desired component in the extractive column than the regeneration column. This is so because once the desired component has been recovered, the subsequent separation sections do not have to have high purity specifications which may be costly. Therefore, the entrainer whose RCM and isovolatility topology promotes the recovery of the desired component in the extractive distillation column will most likely be selected, assuming all other criteria are met.

3.3.2. Process Analysis Application

Entrainer selection is the single most crucial step in azeotropic distillation. This is because the entrainer dictates feasible separation sequence and number of columns required to realize the desired separation. Consequently, the entrainer plays a key role in the economics of the process and its energy consumption thereof. Any design made is within the constraints imposed by the entrainer, i.e. distillation boundaries. Some of the factors to consider when selecting the entrainer are: cost relative to the cost of the targeted chemical, availability within the area of the process and its toxicity. The most widely used entrainer for the separation of water-pyridine mixture is toluene [3, 19]. In this section, we assess chloroform and Methyl Isobutyl Ketone (MIBK) as potential entrainers and compare the selected entrainer with toluene.

Option I: Chloroform

The addition of chloroform to the water-pyridine mixture introduces one more azeotrope to the system (water-chloroform) as depicted in Figure 3.7. The resulting residue curve map is divided into 2 regions (**D2, B2, D3** (region **I**) and **D2, D3, OR, B3** (region **II**)) with a large liquid-liquid immiscibility region, thus allowing for natural liquid-liquid separation to take place (Figure 3.7). In both regions, the water-chloroform azeotrope is the lowest boiling point (unstable node). The feed is in region **I** (point **FM**) and the objective is to move into region **II** wherein pyridine (**B3**) is found. This can be achieved by pre-concentrating the mixture from feed composition (**FM**) to azeotropic composition (**D2**) in column C-2, then adding chloroform in the form of organic reflux (**OR**) in column C-3. In region **II,** pyridine is the stable node; therefore, it follows that once in region II, an indirect split approach will be followed to sample pyridine as a bottoms product (**B3**) of the distillation column.

The distillate of column C-3 is the water-chloroform azeotrope (**D3**); this azeotrope is separated using natural liquid-liquid separation in a decanter to get the aqueous outlet (**AO**) and the organic reflux (**OR**). The process flow diagram corresponding to this residue curve map analysis is depicted in Figure 3.8. It is important that the chloroform is added until its composition is 80mol% (point **A** in Figure 3.7). Any composition below point **A** will result in the loss of pyridine. For example, if point A is moved to 70mol%, the material balance line for sampling pyridine may not be able to cross the distillation boundary **(D2, D3)** at point **M (**Figure 3.7)**.** This results in the loss of pyridine since the pyridine is present at about 3mol% at point **M** (Figure 3.7). Further distillation of the mixture at point **M** will yield **D2** and **D3** as bottoms and the distillate respectively. Sometimes when the distillation boundary is closer to the edge, then the boundary could be crossed; however, this occurrence is very rare.

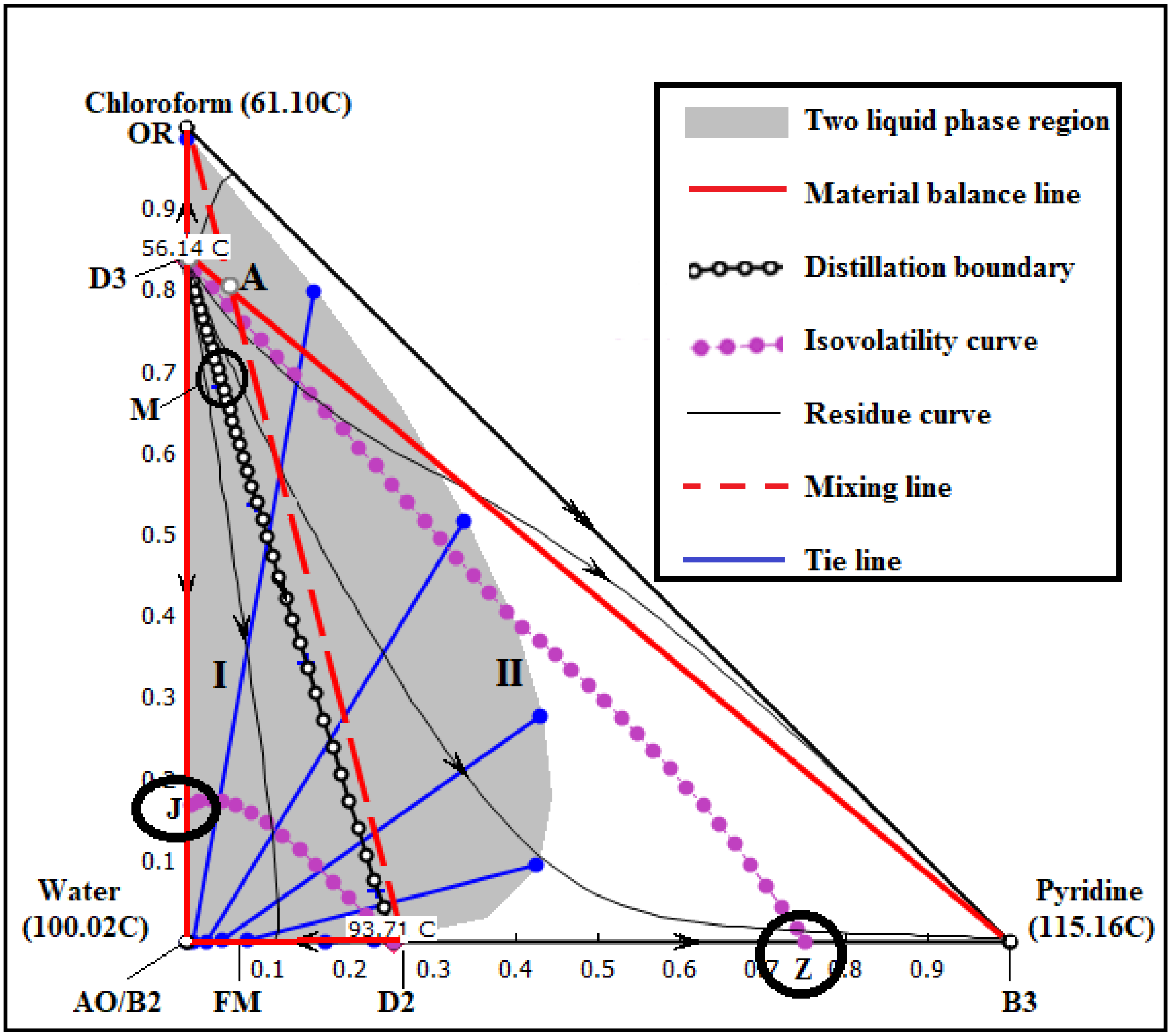

Figure 3.7. Water-pyridine-chloroform residue curve map showing liquid-liquid envelope, isovolatility curves, distillation boundary and material balance lines

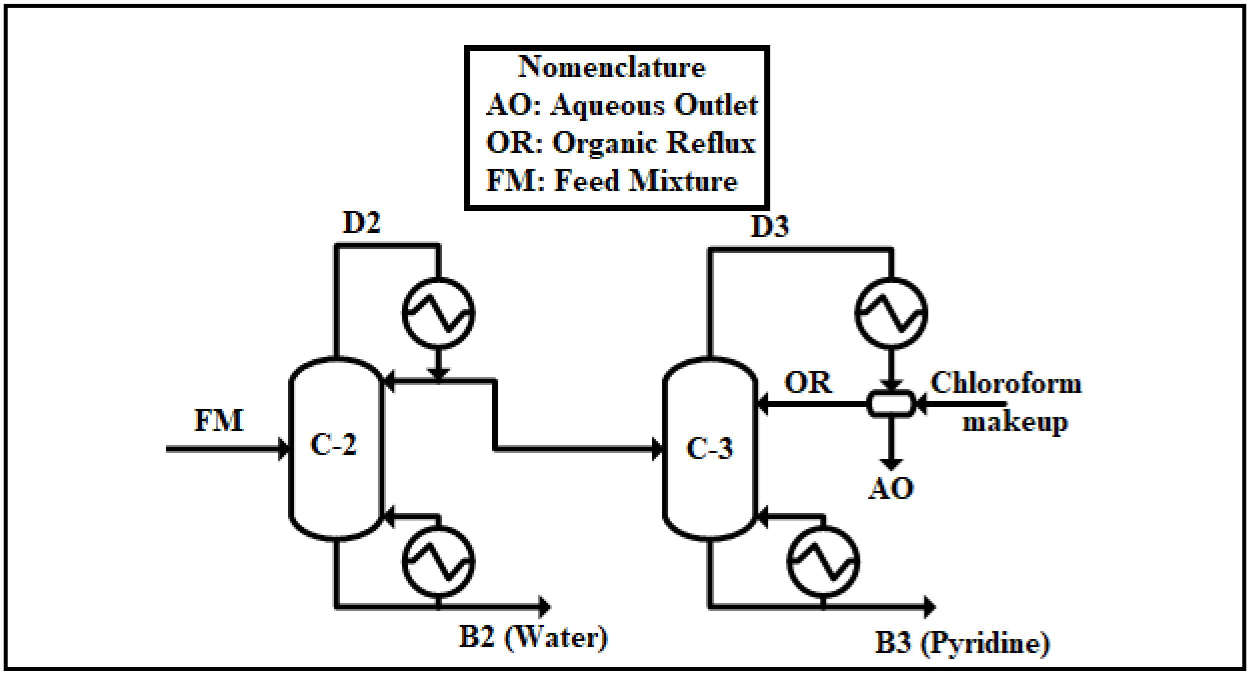

Figure 3.8. Process flow diagram for the water-pyridine-chloroform system

Option II: Methyl Isobutyl Ketone (MIBK)

The residue curve map is divided into 2 regions (**D2, B2, D3** (region **I**) and **D2, D3, B4, D4** (region **II**)) (Figure 3.9) by a single distillation boundary (**D2, D3**). The topology of the MIBK-water-pyridine system is similar to the one of chloroform-water-pyridine system; however, the former has a smaller liquid-liquid envelope thus limiting the effectiveness of the liquid-liquid separation (Figure 3.9). The feed is found in region **I** and as in the previous analysis the aim is to move to region **II** wherein pyridine is found. The feed is first concentrated to azeotropic composition (**D2**) in column C-2. The mixture at azeotropic composition (**D2**) leaves the first distillation column C-2 as a distillate and pure water leaves this column as the bottoms product (**B2**). **D2** is mixed with the organic reflux (**OR**) in the next distillation column (C-3) where the MIBK-water azeotrope (**D3**) is a distillate product and the mixture of pyridine and MIBK are sampled as a bottoms product (**B3**).

The bottoms product of C-2 is further distilled to separate it into pure pyridine and MIBK as a distillate (**D4**) and bottoms product (**B4**) respectively in distillation column C-4. The process flow diagram corresponding to this synthesis is depicted in Figure 3.10. The residue curve formed by the addition of methyl isobutyl ketone to the water-pyridine system necessitates the use of 3 distillation columns. Consequently, the operational costs will be much higher than the 2-column process on the chloroform system in terms of energy intensity and control costs. Moreover, the difference between boiling points of pyridine and MIBK is insignificant. This is undesirable because to achieve reasonable separation for components with close boiling points requires substantial number of stages and hence bigger columns thereby increasing capital costs. Furthermore, even with large number of stages, purity of the recovered pyridine is likely to be compromised.

Therefore, it follows that chloroform is the more suitable entrainer for the separation of pyridine-water azeotrope. Furthermore, the isovolatility curves also support the notion that chloroform may be a more effective entrainer (point **J,** Figure 3.7 and Figure 3.9 respectively); the isovolatility curve in the chloroform-water-pyridine intersects the water-chloroform axis at 0.18 whereas the intersection is at 0.30 for the MIBK system. Only the isovolatility curve originating from the water-pyridine azeotrope (**D2**, **J**) (Figure 3.7, Figure 3.9) is considered for this comparison. This is because the isovolatility curve emanating from the entrainer-water azeotrope (**D3, Z)** in Figure 3.7 and Figure 3.9 is concerned with the VLE limitations of the separation of the entrainer-water azeotrope and in this case, these azeotropes are separated using liquid-liquid separation which is independent of VLE limitations.

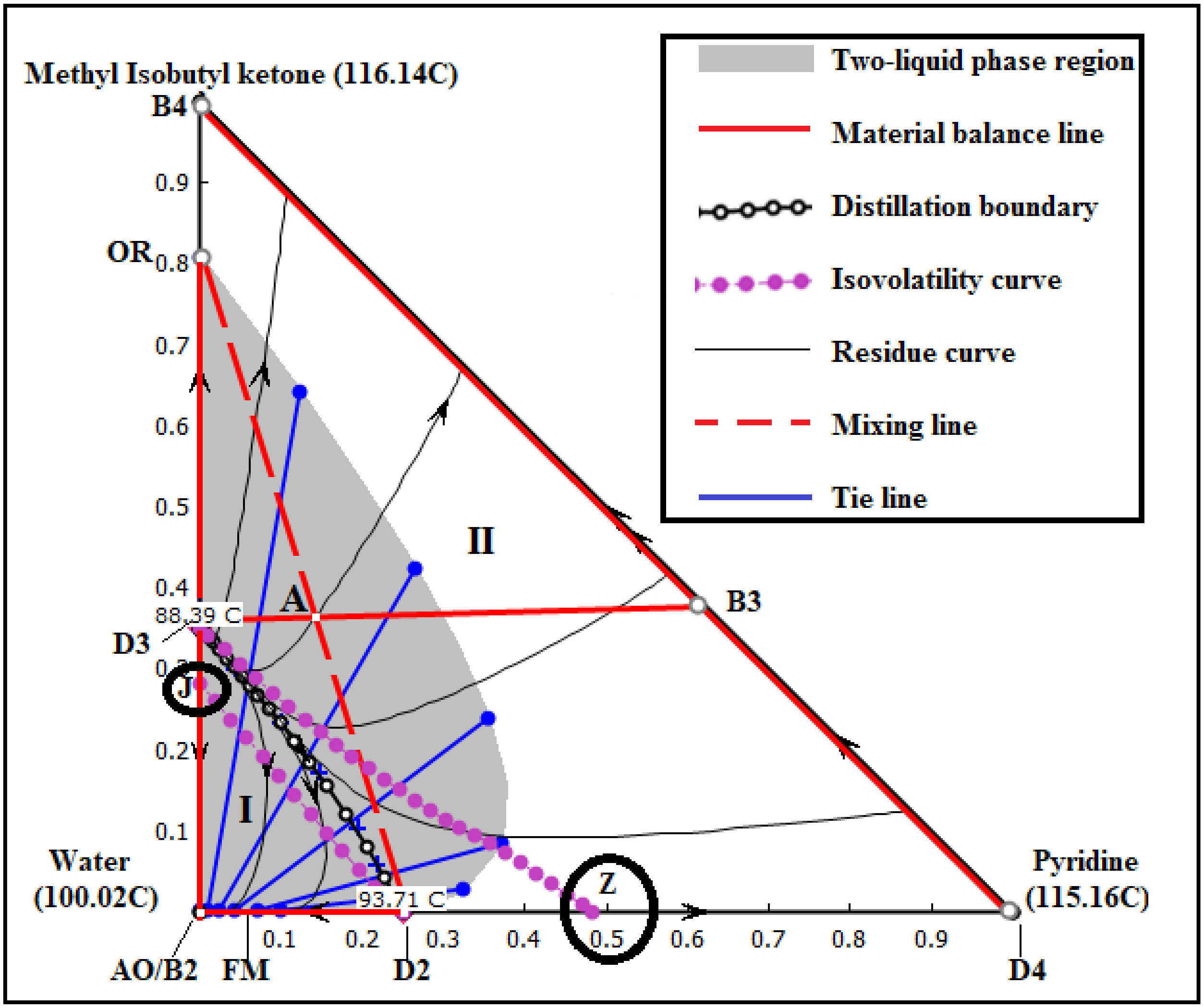

Figure 3.9. MIBK-water-pyridine residue curve map showing liquid-liquid envelope, isovolatility curves, distillation boundary and material balance lines

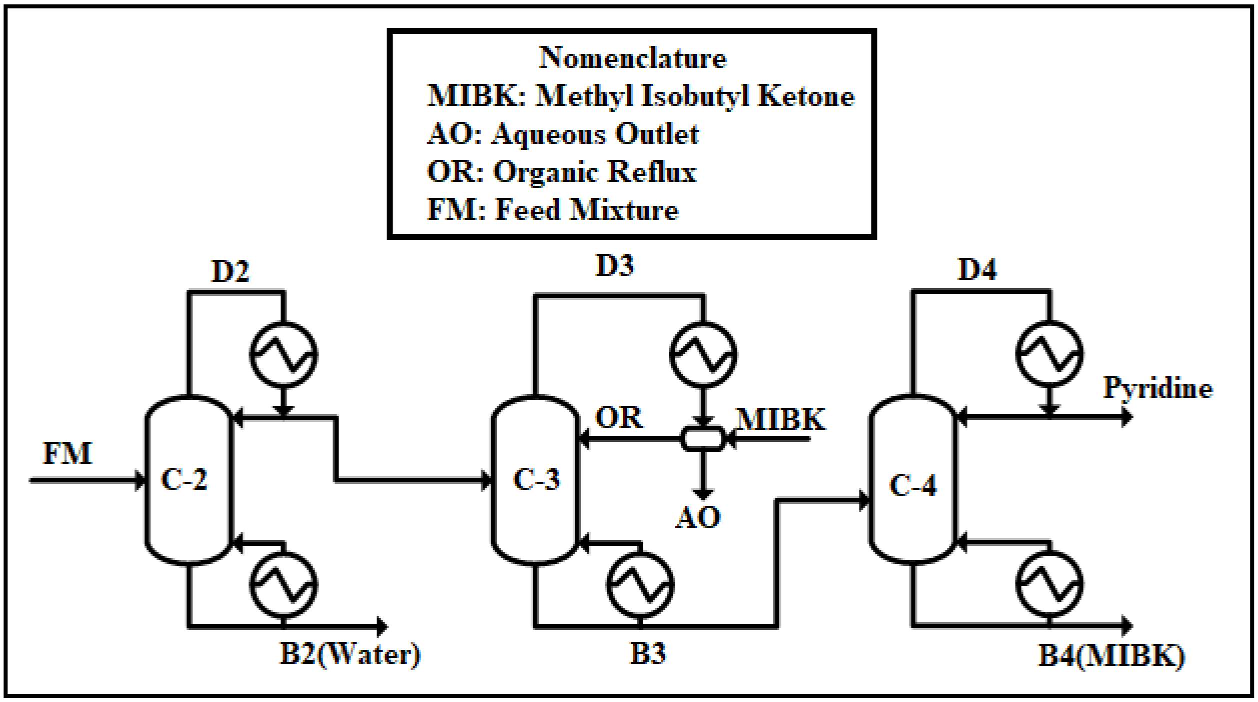

Figure 3.10. Process flow diagram for the water-pyridine-MIBK system

Although chloroform is a better than entrainer compared to MIBK, it has a very high entrainer to azeotropic mixture ratio (EA) (4:1). This ratio can be deduced from the RCM using equation (3.9) (sample calculation is presented in Appendix E, *calculation 1 (a)*). Higher entrainer to azeotropic mixture ratios may render the waste treatment redundant considering the overall objective of waste treatment. In the next section, reduction of entrainer consumption is assessed by altering separation sequence using RCM as a guide.

$$EA = \frac{Entrainer\ flowrate}{Azeotropic\ mixture\ flowrate} \tag{3.9}$$

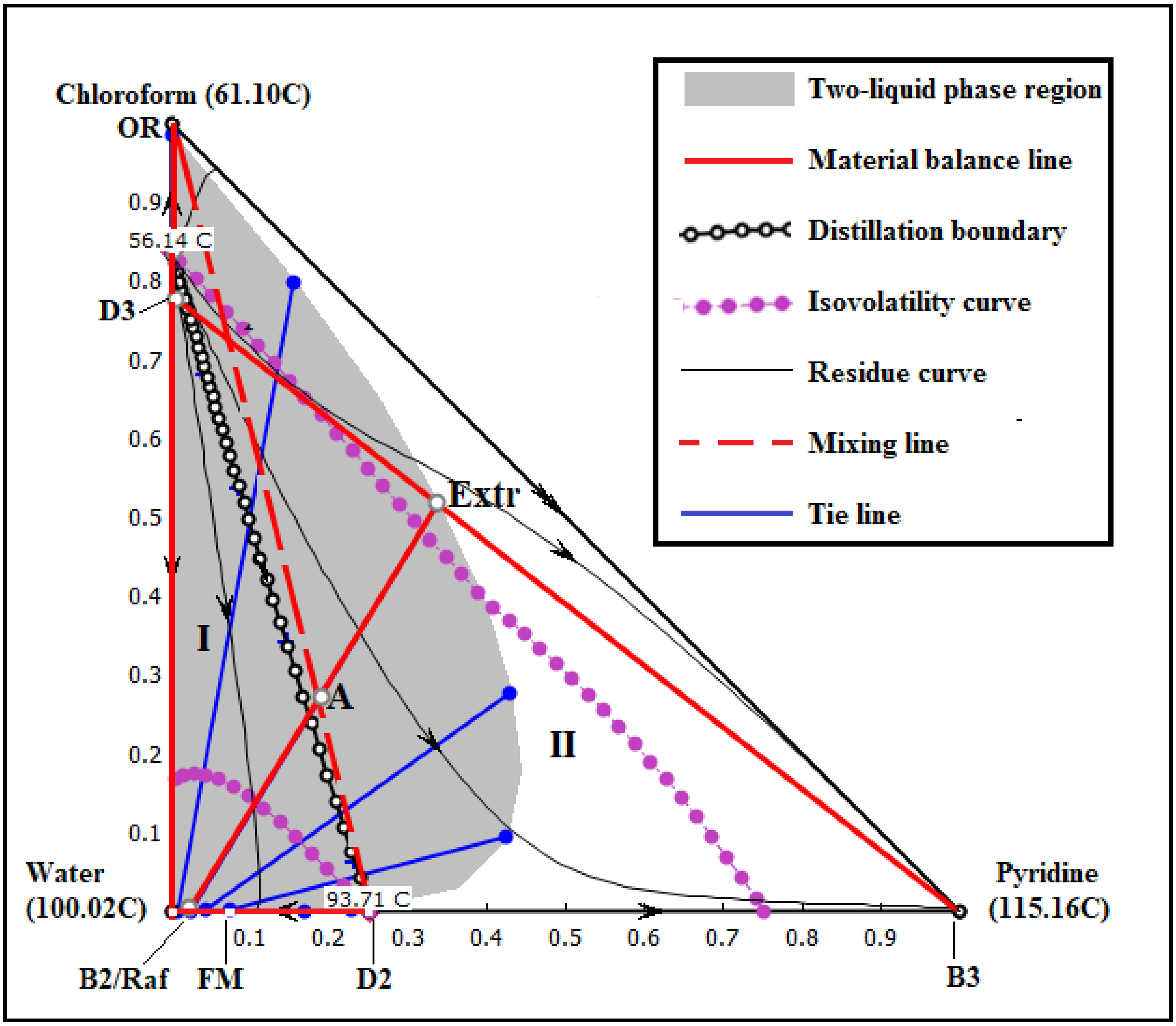

Figure 3.11. Improved pyridine-water-chloroform separation sequence

The idea is to add just enough entrainer to move point **D2** to point **A** (Figure 3.11) after the water-pyridine mixture is pre-concentrated to azeotropic level in column C-2 (Figure 3.12). Once the composition in **A** is attained, liquid-liquid extraction is used to separate the mixture into an organic rich phase (extract) and an organic lean phase (raffinate). The extract is a ternary mixture of pyridine, water and chloroform (**Extr** in Figure 3.11). This mixture is then taken to the azeotropic distillation column (C-3) where pyridine is sampled as a bottoms product (**B3**). Since the distillate of C-3 (**D3**) is composed of mainly chloroform (about 77mol%), and water (23mol%) (**D3** in Figure 3.11), it is recycled back to the liquid-liquid extraction column as it is to avoid the regeneration costs.

The main difference between the design in Figure 3.12 and the conventional analysis proposed in Figure 3.7 is that liquid-liquid separation in the conventional analysis is used for entrainer regeneration and water-pyridine separation takes place mainly in the distillation column, whereas in the improved design, separation of pyridine-water mixture takes place both in the liquid-liquid extraction column and the distillation column. This approach takes advantage of the both LLE (Liquid-Liquid Equilibrium) and VLE (Vapor Liquid Equilibrium) for separation of the same mixture. This results in the reduction of the entrainer to mixture mole ratio from 4:1 to 0.36:1 (sample calculation given in Appendix E, calculation 1). This is equivalent to over 90% reduction of the entrainer demand. Liquid-liquid extraction column (E-1) removes just enough water to enable distillation to sample pure pyridine from the ternary mixture. Therefore, distillation column C-3 serves 2 purposes: solvent regeneration as well as pyridine recovery. The former approach is equivalent to mixing the entrainer and the azeotropic mixture then distilling to sample the target component. That way, to move from **D1** to a point in region **II** where pyridine can be effectively sampled using distillation requires the addition of a large amount of entrainer. Separation would only be feasible if the entrainer makes up about 80mol% of the ternary mixture (point **A** in Figure 3.7).

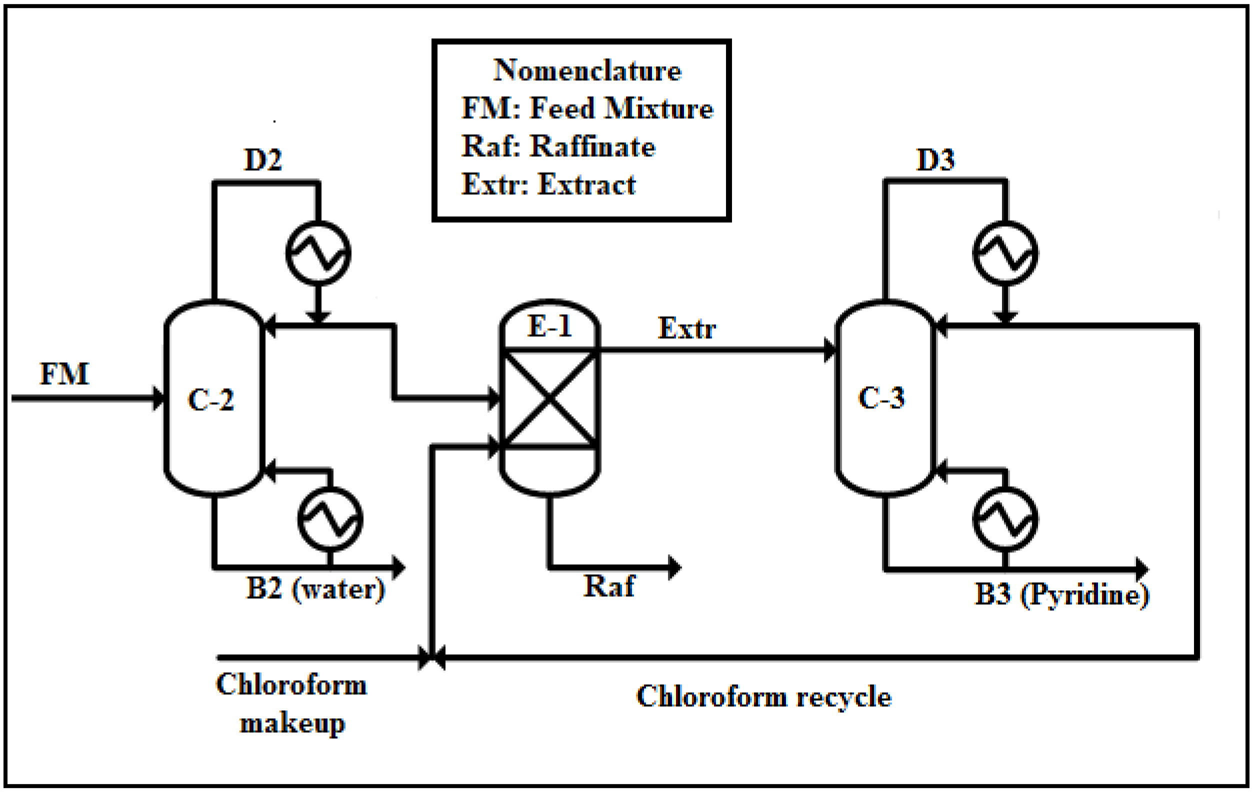

Figure 3.12. Process flow diagram for the improved water-pyridine-chloroform system

3.3.3. Simulation of the Chloroform Improved System

This process was simulated in Aspen Plus using NRTL property method. The binary parameters used are presented in Table D.2 of Appendix D. These parameters are built-in within Aspen Plus. Acetonitrile effect on the binary interaction was assumed to be negligible since it was only present in low concentration on this part of the process.

Shortcut model to determine distillation column parameters

The DSTWU shortcut model was used to determine the distillation parameters given in Table 3.6.

Table 3.6. Summary of columns used for pyridine dehydration

Parameter	C-2	C-3	E-1
Total number of stages	20.000	30.000	10.000
Reflux Ratio	2.000	2.500	-
Feed stage	7.000	7.000	1.000

Aspen Plus specifications and explanations for pyridine enrichment units

Distillation column C-2

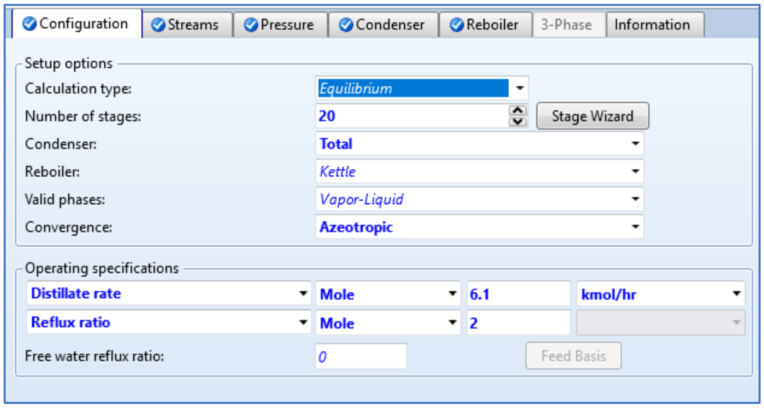

Setup options
Calculation type: Equilibrium
Number of stages: 20
Condenser: Total
Reboiler: Kettle
Valid phases: Vapor-Liquid
Convergence: Azeotropic

Operating specifications
Distillate rate Mole 6.1 kmol/hr
Reflux ratio Mole 2
Free water reflux ratio: 0

Figure 3.13. Configuration Specification for column C-2

Column C-2 was only simulated after the results for column C-1 were obtained. The distillate rate in this column was specified as 6.1kmol/hr (Figure 3.13). This included the water-pyridine azeotrope plus the acetonitrile impurity found in the bottoms product of column C-1. This flowrate was found by dividing the pyridine flowrate in the bottoms stream by 0.25 (pyridine composition in the water-pyridine azeotrope).

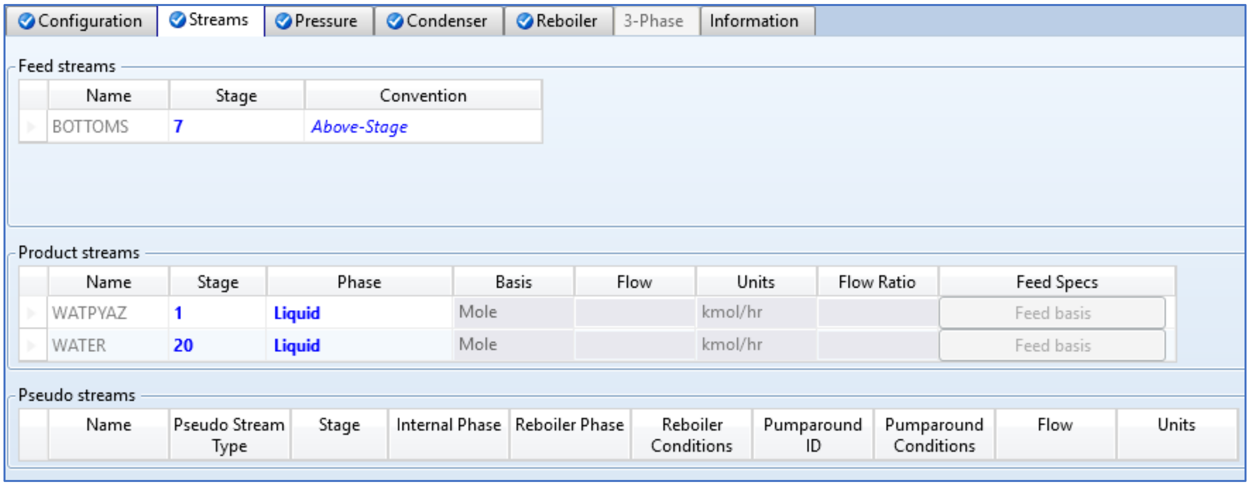

Feed streams

Name	Stage	Convention
BOTTOMS	7	Above-Stage

Product streams

Name	Stage	Phase	Basis	Flow	Units	Flow Ratio	Feed Specs
WATPYAZ	1	Liquid	Mole		kmol/hr		Feed basis
WATER	20	Liquid	Mole		kmol/hr		Feed basis

Pseudo streams

Name	Pseudo Stream Type	Stage	Internal Phase	Reboiler Phase	Reboiler Conditions	Pumparound ID	Pumparound Conditions	Flow	Units

Figure 3.14. Feed stream specification for column C-2

Extraction column (E-1)

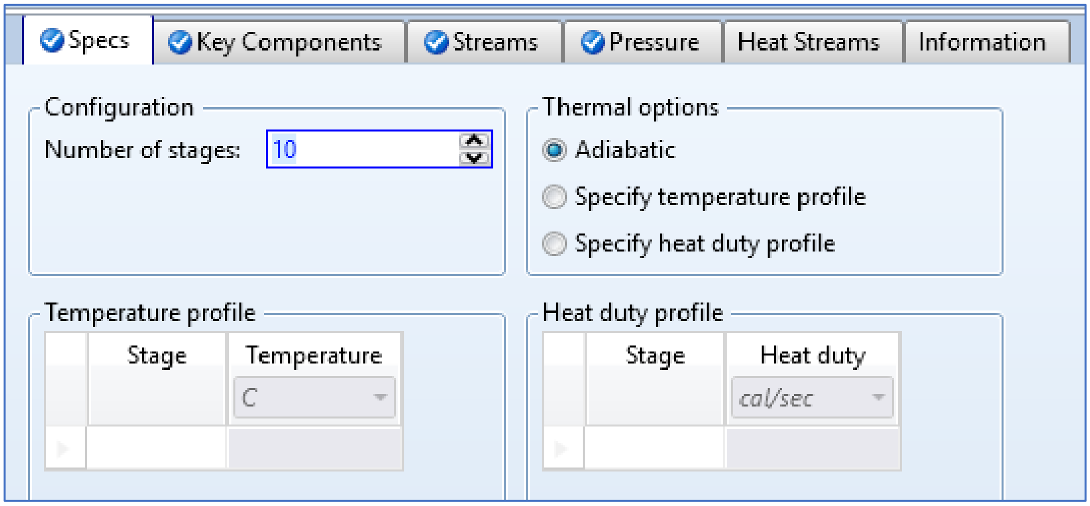

Configuration

Number of stages: 10

Thermal options

● Adiabatic

○ Specify temperature profile

○ Specify heat duty profile

Temperature profile

Stage	Temperature C

Heat duty profile

Stage	Heat duty cal/sec

Figure 3.15. Configuration for the liquid-liquid extraction unit

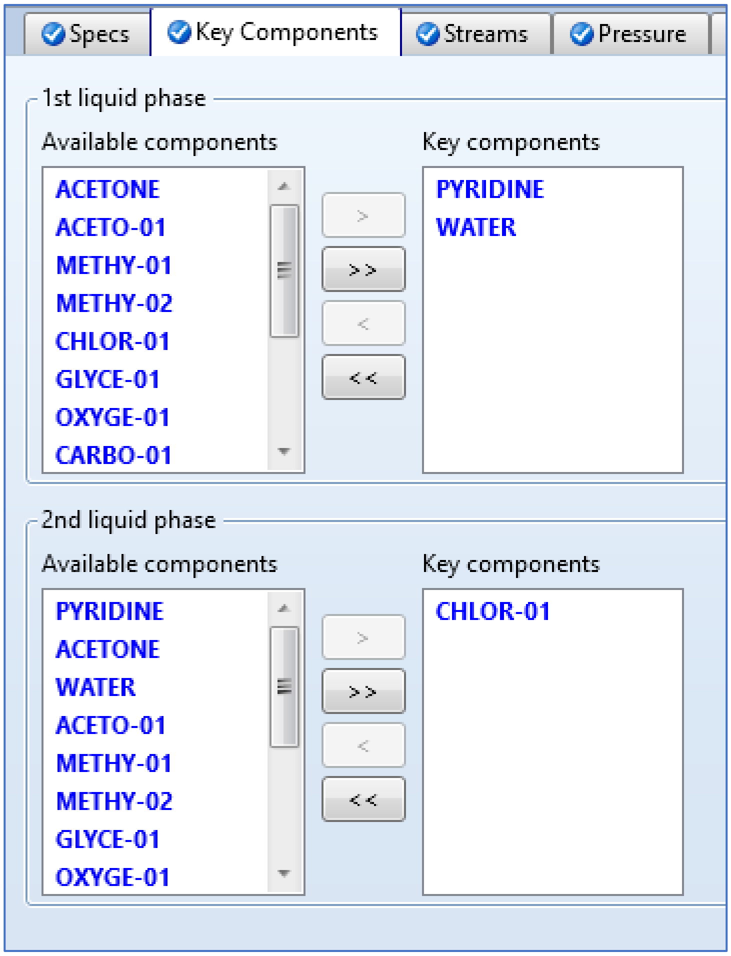

1st liquid phase

Available components
- ACETONE
- ACETO-01
- METHY-01
- METHY-02
- CHLOR-01
- GLYCE-01
- OXYGE-01
- CARBO-01

Key components
- PYRIDINE
- WATER

2nd liquid phase

Available components
- PYRIDINE
- ACETONE
- WATER
- ACETO-01
- METHY-01
- METHY-02
- GLYCE-01
- OXYGE-01

Key components
- CHLOR-01

Figure 3.16. Specification of the key components on the Extraction unit

The extraction column requires the user to specify key components in the 2 liquid phases (Figure 3.16). In liquid-liquid extraction, there are 2 phases: organic and aqueous. In this case, the organic phase (second liquid phase) is chloroform and the aqueous phase (first liquid phase) is made up of pyridine and water.

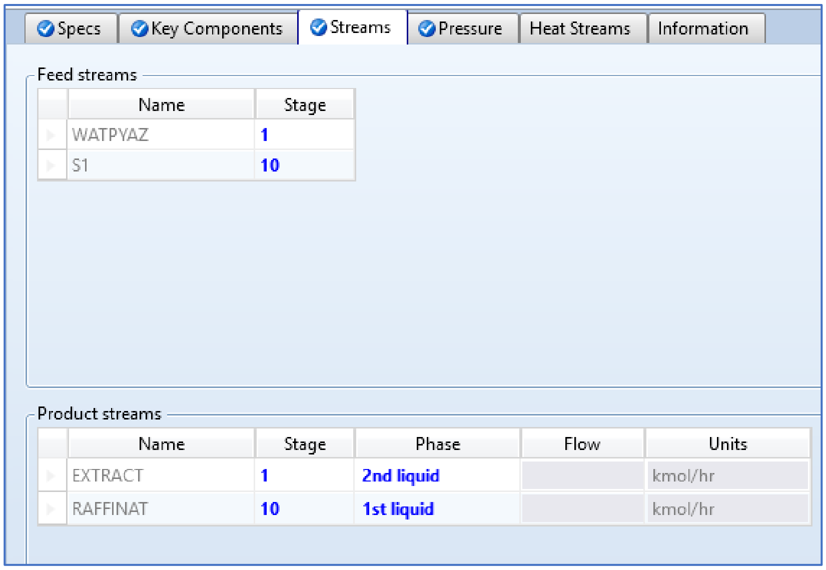

Feed streams

Name	Stage
WATPYAZ	1
S1	10

Product streams

Name	Stage	Phase	Flow	Units
EXTRACT	1	2nd liquid		kmol/hr
RAFFINAT	10	1st liquid		kmol/hr

Figure 3.17. Specification of the feed stages location on the extraction unit

Regeneration Distillation Column (C-3)

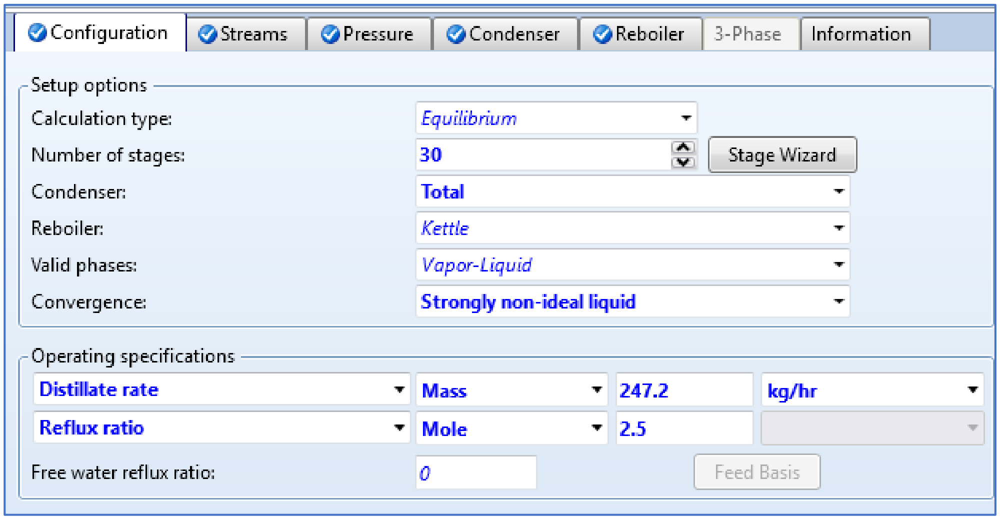

Setup options

Calculation type: *Equilibrium*
Number of stages: **30**
Condenser: **Total**
Reboiler: *Kettle*
Valid phases: *Vapor-Liquid*
Convergence: **Strongly non-ideal liquid**

Operating specifications

Distillate rate	**Mass**	**247.2**	**kg/hr**
Reflux ratio	**Mole**	**2.5**	

Free water reflux ratio: *0*

Figure 3.18. Configuration specification for the regeneration column

The separation in the regeneration column followed the indirect sequence (recovery of the heavy component first). To get the distillate rate in the regeneration column, simple arithmetic was made. Flowrate of pyridine was subtracted from the total of the stream and the balance was stated as the distillate rate. This is feasible because the liquid-

liquid extraction unit (E-1) has pushed the ternary mixture away from the boundary (**Extr** in Figure 3.11) and consequently, pyridine was the highest boiling component and was expected to report to the bottom of the regeneration column as a pure component when indirect separation sequence was employed in region II (**D2, D3, OR, B3**) in Figure 3.11.

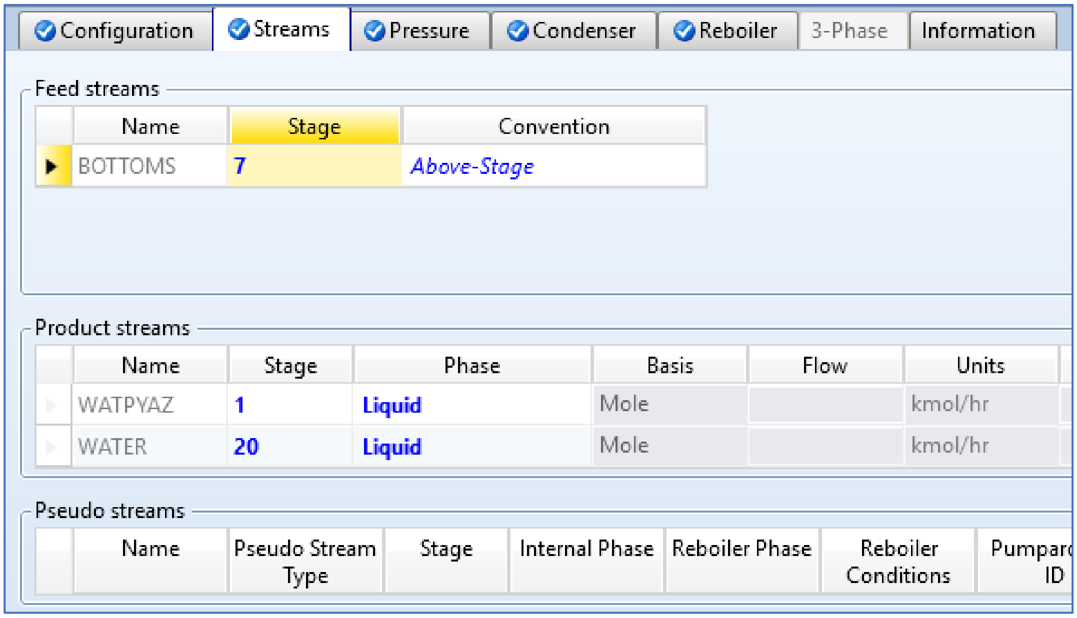

Feed streams

Name	Stage	Convention
BOTTOMS	7	Above-Stage

Product streams

Name	Stage	Phase	Basis	Flow	Units
WATPYAZ	1	Liquid	Mole		kmol/hr
WATER	20	Liquid	Mole		kmol/hr

Pseudo streams

Name	Pseudo Stream Type	Stage	Internal Phase	Reboiler Phase	Reboiler Conditions	Pumpar ID

Figure 3.19. Feed stream specifications in the regeneration column

Results Discussion

Pyridine recovery of over 99wt% at 98wt% (96mol%) purity is possible using the proposed design. Moreover, usable water at 99.99mass% purity was recovered from the HOW. The material balance summary for the pyridine enrichment section of the process is given in Figure 3.20 (detailed material balance is given Appendix C.1 and C.2). It is noteworthy that the main impurity in the pyridine stream (B2) is acetonitrile (Figure 3.20) and not water. This signifies that the proposed system is effective in breaking water-pyridine azeotrope in that in the absence of acetonitrile impurity, purity over 99mol% could potentially be attained.

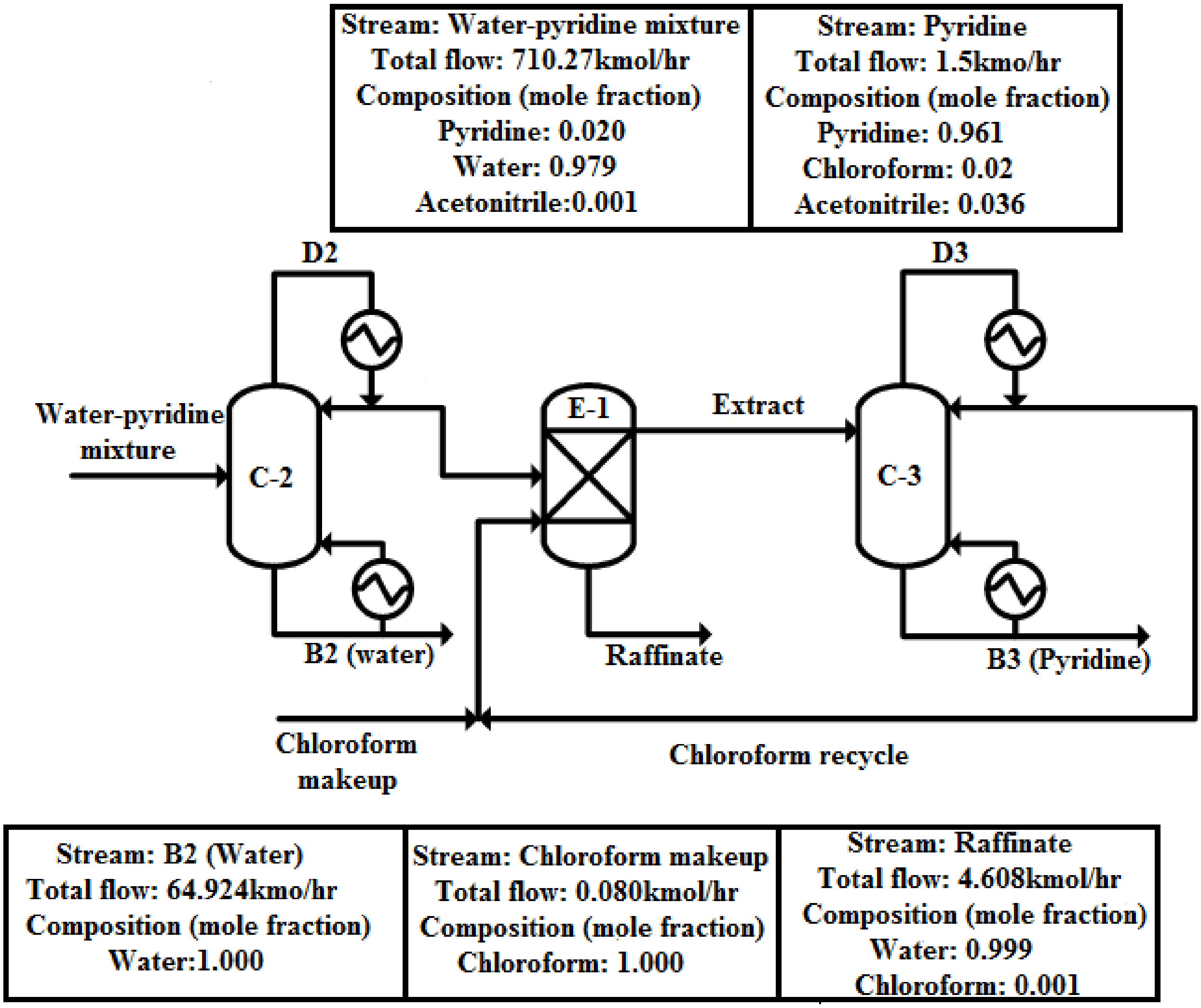

Stream: Water-pyridine mixture
Total flow: 710.27kmol/hr
Composition (mole fraction)
Pyridine: 0.020
Water: 0.979
Acetonitrile:0.001

Stream: Pyridine
Total flow: 1.5kmo/hr
Composition (mole fraction)
Pyridine: 0.961
Chloroform: 0.02
Acetonitrile: 0.036

Stream: B2 (Water)
Total flow: 64.924kmo/hr
Composition (mole fraction)
Water:1.000

Stream: Chloroform makeup
Total flow: 0.080kmol/hr
Composition (mole fraction)
Chloroform: 1.000

Stream: Raffinate
Total flow: 4.608kmol/hr
Composition (mole fraction)
Water: 0.999
Chloroform: 0.001

Figure 3.20. Overall material balance for the pyridine enrichment section

Sensitivity analysis depicted in Figure 3.21 to determine the amount of fresh chloroform that would realize the anticipated separation.

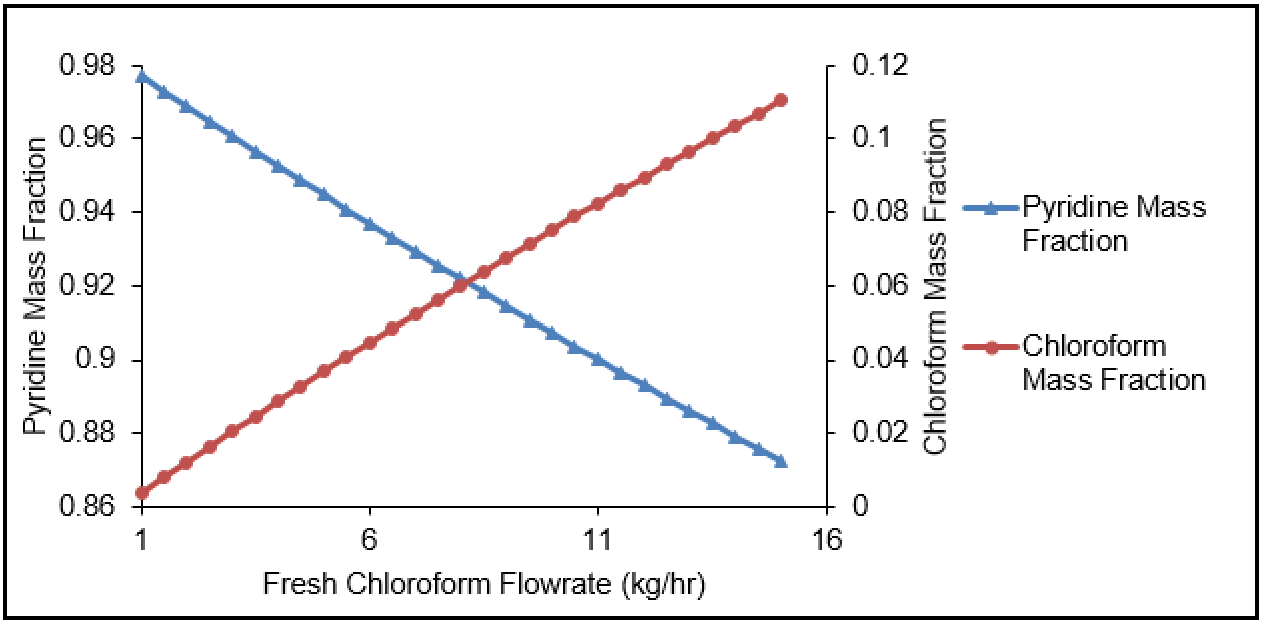

Figure 3.21. Effect of chloroform fresh feed on the pyridine purity in product stream

It can be deduced from Figure 3.21 which shows that the amount of fresh chloroform feed is indirectly proportional to the pyridine purity in the pyridine stream. The relation is sensible due to chloroform buildup in the recycle stream and the amount of water recovered to the raffinate can only take with it a certain amount of chloroform depending on solubility. Consequently, the chloroform that couldn't come out as the raffinate, report to the pyridine product stream. Below 1kg/hr of fresh chloroform the simulation resulted in errors.

The process using toluene as an entrainer proposed by Wu & Chien [19] and its mass balance are depicted in Figure 3.22 and Table 3.7 respectively. The residue curve produced for this system has 2 distillation boundaries resulting in 3 distillation regions. Fresh feed is mixed with the aqueous outlet from the decanter (Figure 3.23). The mixture is distilled to concentrate the mixture closer to azeotropic composition; this is done to avoid using excessive amounts of solvents in the azeotropic column [3]. The azeotropic mixture (**D2**) is recycled back to the heterogeneous azeotropic distillation column (C-1). From C-1, pure pyridine is recovered as the bottoms product as per material balance line shown in Figure 3.22. Liquid-liquid separation (decanter in this case) is used to cross the boundary to separate the organic rich phase from the organic lean phase (Aqueous Outlet). The organic rich phase is recycled back into the column.

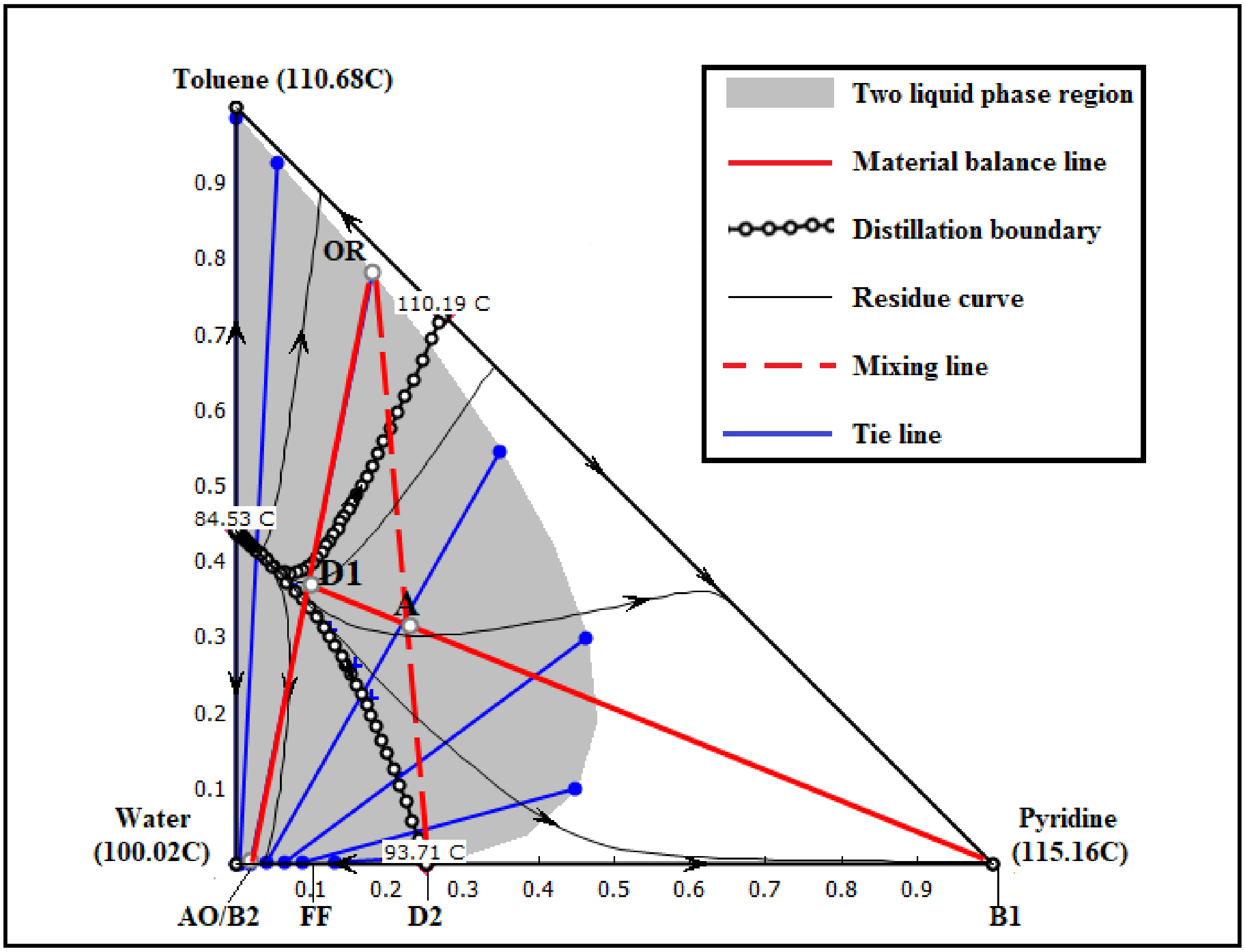

Figure 3.22. Water-pyridine-toluene system residue curve map [19]

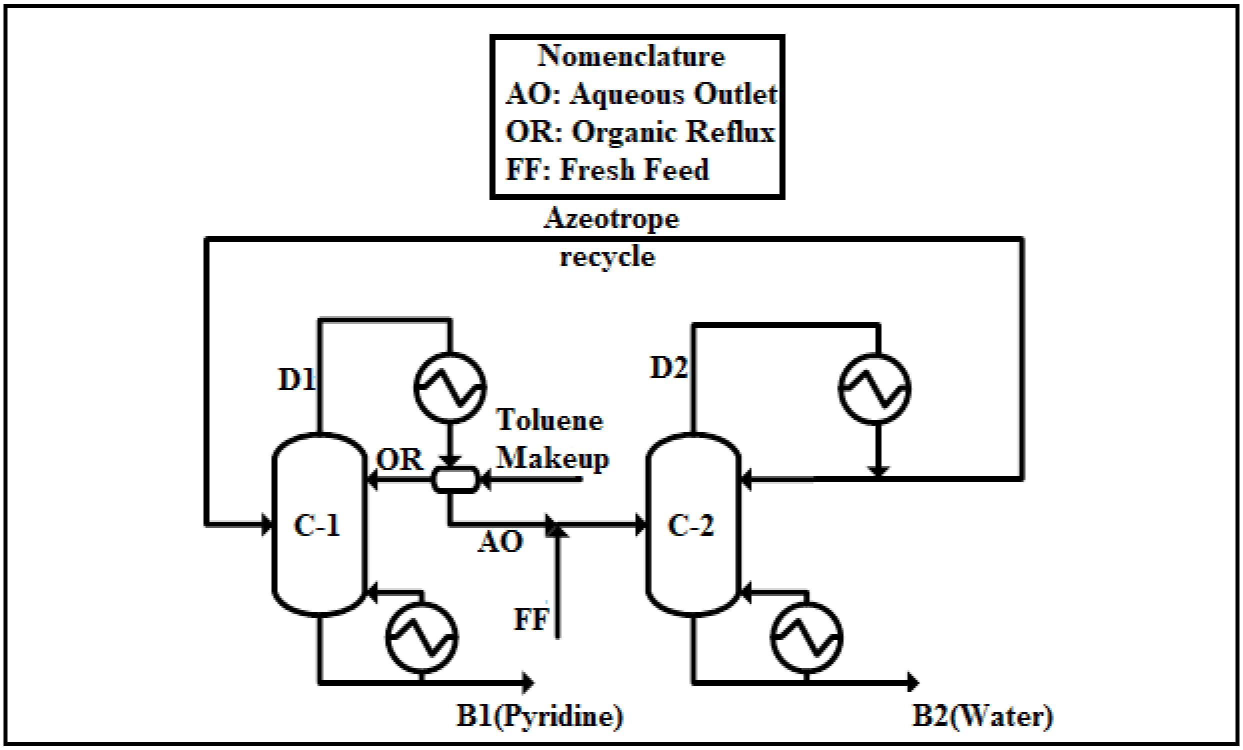

Figure 3.23. Water-pyridine-toluene process flow diagram for pyridine dehydration using toluene [19]

Table 3.7. Material balance for water-pyridine-toluene system [66]

	Fresh Feed	**AO**	**D2**	**B2**	**D1**	**B1**	**OR**
Total flow (kmol/hr)	1000.00	391.20	490.400	900.800	696.30	99.20	305.10
Mole fraction							
Pyridine	0.100	0.010	0.210	0.001	0.071	0.999	0.15
Water	0.900	0.999	0.790	0.999	0.561	0.001	0.011
Toluene	0.000	0.000	0.000	0.000	0.368	0.000	0.839

Toluene to water-pyridine azeotropic mixture ratio (EA) was first calculated from the residue curve map as plotted by Wu & Chien [19] to be 0.471:1 (sample calculation illustrated in Appendix E, *calculation 2 (a)*). The toluene to water-pyridine azeotropic mixture ratio was calculated as 0.522:1 from the material balance of the toluene-water-pyridine system given in Table 3.7 (sample calculation provided in Appendix E, *calculation 2 (b)*). On the other hand, the chloroform to water-pyridine azeotropic mixture ratio from the residue was calculated to be 0.360:1 (sample calculation given in Appendix E, *calculation 1 (a)*) and the ratio calculated from the simulation material balance was 0.320:1 (the calculation is illustrated in Appendix E, *calculation 1 (b)*). In both systems (chloroform-pyridine-water and toluene-pyridine-water) the predictive calculation of the EA from RCM was close to the one calculated from simulation material balance.

For the proposed chloroform system, the calculation made from the residue curve map had a percentage relative error of 12.500% (equation (3.10)); sample calculation provided in Appendix E, *calculation 1 (c)*) and for the toluene system, the percentage relative error was calculated to be 9.770% (sample calculation shown in Appendix E, *calculation 2 (c)*). It can be concluded that residue curve maps probably have a predictive percentage relative error of around 10% for entrainer performance evaluation. The results from the two systems serve to illustrate the reliability of residue curve maps in predicting entrainer performance for separation processes such as liquid-liquid extraction, decanting and distillation.

$$percentage\ relative\ error = \frac{|x - x_0|}{x} \times 100 \tag{3.10}$$

Where:

x: entrainer to mixture ratio from the simulation material balance

x_0: entrainer to azeotropic mixture ratio predicted from the RCM

The chloroform system has a lower EA of 0.320:1 versus 0.522: 1 of the toluene system. This translates to the chloroform system using 1.6 times less entrainer than the toluene system. Furthermore, the separation is achieved with the entrainer 3.1 times less than the azeotropic mixture. The reduced amount of entrainer means smaller equipment for storage and processing and thus lower capital costs. It can therefore be concluded that the chloroform process proposed in this work is better than the status-quo toluene azeotropic distillation system based on entrainer consumption. Chloroform has the added benefit of being cheaper than toluene at 0.5 USD/kg [24] versus 1 USD/kg [25]. The fact that separation of water and pyridine in the process proposed in this work takes place in both the liquid-liquid extraction column (E-1) and regeneration distillation column (C-3) (Figure 3.20), results in lower energy consumption compared to the instance whereby the entire load is processed by distillation. This is so because liquid-liquid extraction is less energy intensive than distillation [4].

Table 3.8. Comparison of toluene and chloroform as entrainers for dehydration of pyridine

Parameter	Chloroform	Toluene
Composition in the total mixture	0.270	0.321
Entrainer to mixture ratio	0.320	0.522

3.3.4. Further implications for the HOW stream

Currently the HOW stream is incinerated without energy recovery. With the proposed process, only 40% of the HOW is sent to the incinerator (Figure 3.5). The impact of the reduction of the incinerator load will be discussed in **Chapter 6**. The use of the recovered water (“recovered water” stream in Figure 3.24) will also be assessed in **Chapter 6**. The presence of acetonitrile on the recovered pyridine stream negatively impacts the reusability of pyridine for industry applications. In section 3.3.5, sensitivity analysis was made to determine the variables that affect the purity of the recovered pyridine and to also assess if acetonitrile composition in the pyridine stream could be reduced in the pyridine stream.

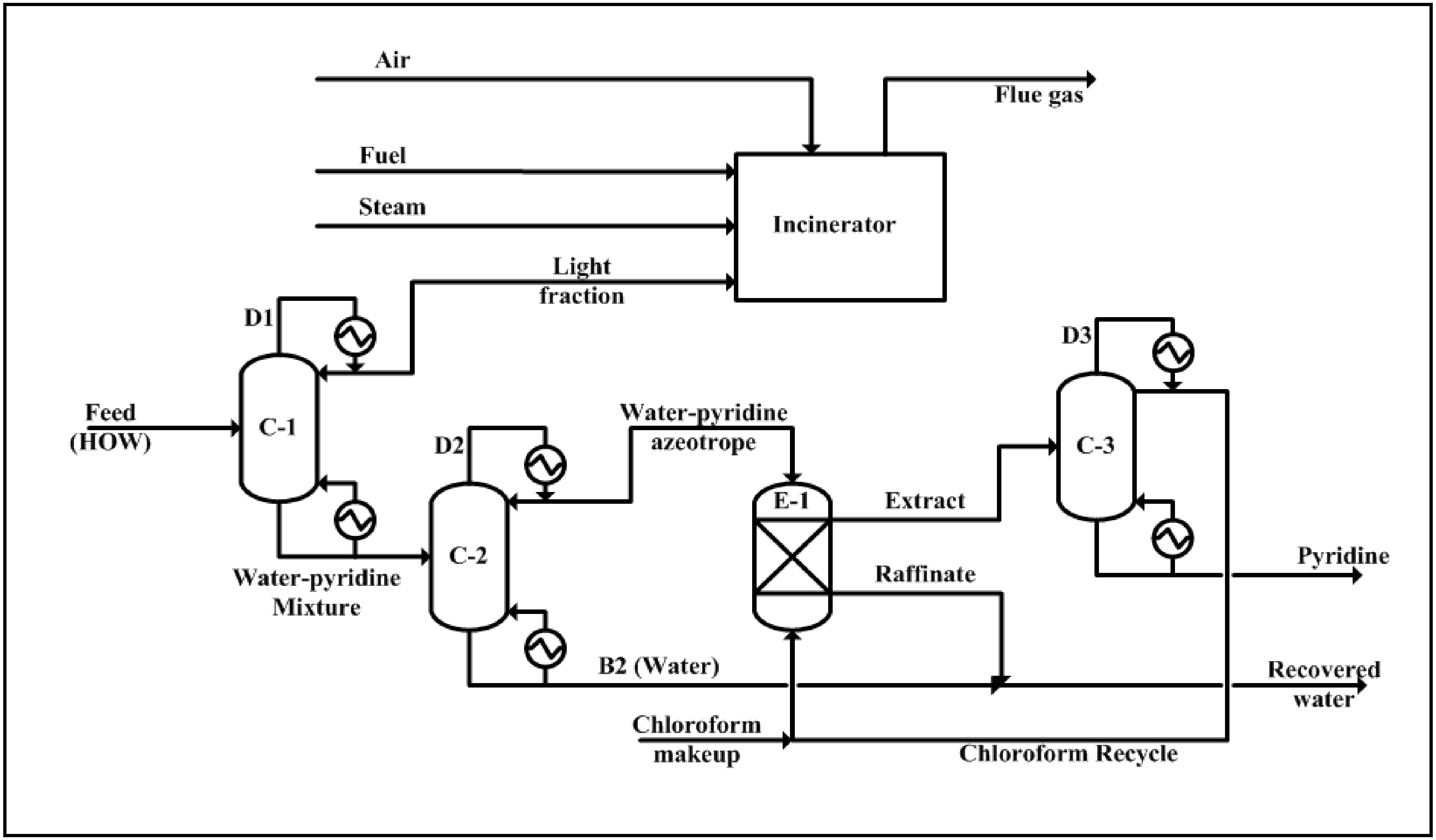

Figure 3.24. Proposed flowsheet for the recovery of pyridine from the HOW

3.3.5. Sensitivity Analysis to Assess Pyridine Purity Improvement

Acetonitrile is the main impurity in the pyridine stream. This undesirable phenomenon originates from the inefficient separation that occurred in the first pre-concentration column (C-1) (Figure 3.24). In this column, all the acetonitrile present in the feed should have reported to the distillate product but only a small amount of acetonitrile reported to the bottoms product and finally reports to the pyridine stream. The main consideration in column C-1 is to minimize the loss of pyridine to the distillate. Therefore, the sensitivity analysis focused on both acetonitrile and pyridine.

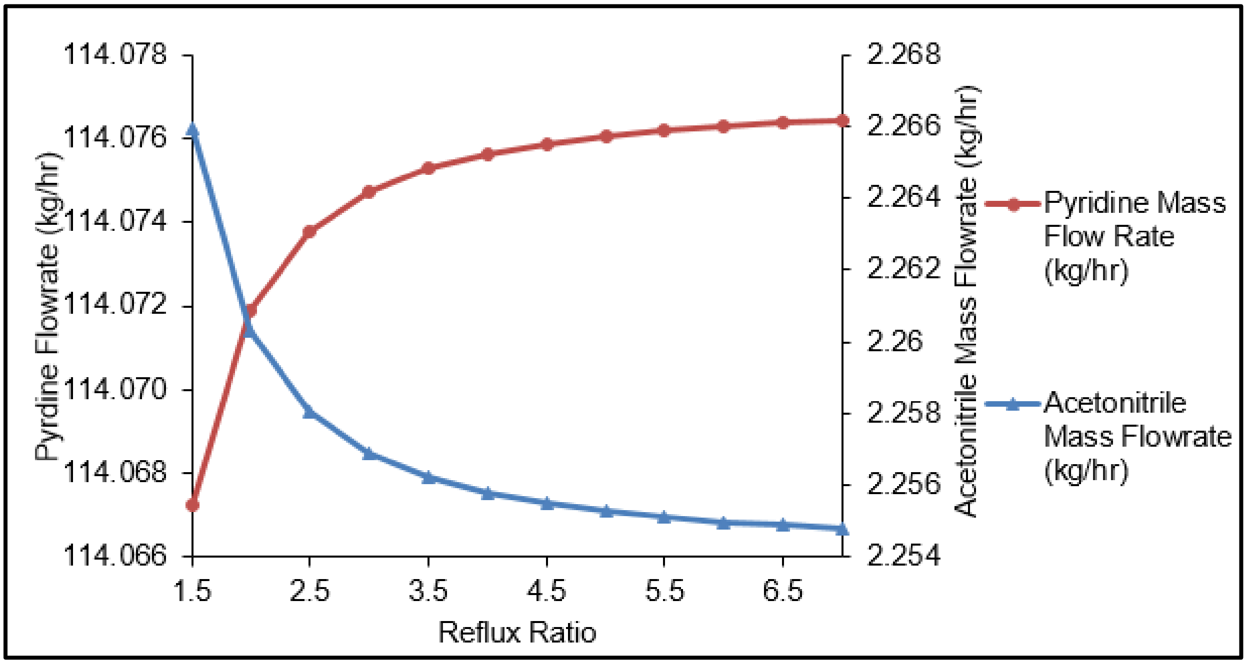

Figure 3.25. The effect of reflux ratio on the quantity of pyridine and acetonitrile that report to the bottoms product

An increase in reflux ratio resulted in a desirable decrease of acetonitrile in the bottoms product of column C-1 (Figure 3.25). The same is accompanied by an increase in pyridine flowrate in the bottoms product. However, the change is extremely small; in the 1.5-7 reflux ratio range the flowrate of acetonitrile and pyridine in the bottoms product have decreased by 0.0111kg/hr and increased by 0.0081kg/hr respectively. Since high reflux ratios are associated with high energy consumption, the increase of the reflux ratio does not seem justified in this case. This can however be confirmed or disproved by the slight change the increase has on the final pyridine purity in the pyridine stream. Figure 3.26 shows the impact of the reflux ratio in the column C-1 on the final product purity.

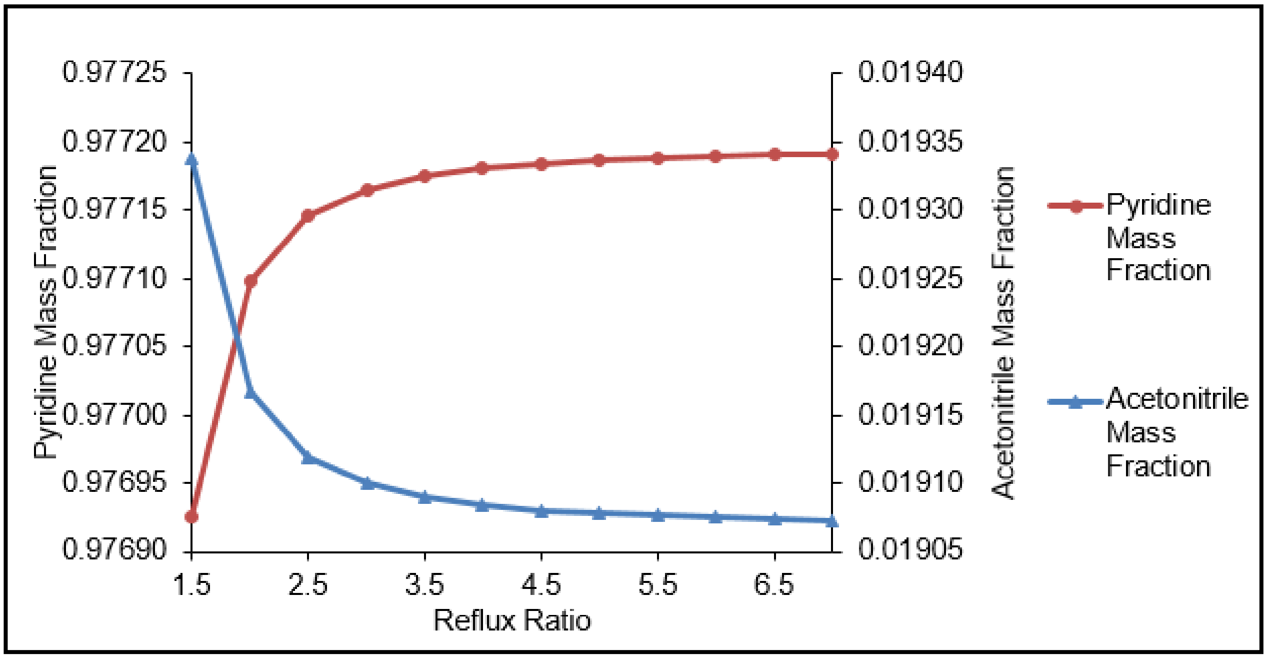

Figure 3.26. The effect of reflux ratio on the mass fraction of pyridine and acetonitrile in the pyridine product stream

As assumed in the previous discussion, the reflux ratio in the first column has negligible impact on the purity of the pyridine product. The increase in the reflux ratio in the range of 1.5-7 has negligible effect on the pyridine purity (Figure 3.26), and therefore, increasing the reflux ratio may not be the solution to the problem. In Chapter 4, the Dividing Wall Column (DWC) process integration technique is assessed to improve energy utilization in the pre-concentration columns (C-1 and C-2). This technique has also been reported to improve product quality from distillation [26].

3.4. Conclusions

The recovery of pyridine from the High Organic Waste (HOW) was assessed. Recovery was achieved in 2 steps: separation of water-pyridine mixture from the HOW and pyridine enrichment. The first step was realized using fractional distillation while the second step was achieved using residue curve maps to synthesize a feasible separation process for separating the water-pyridine azeotrope. The combination of liquid-liquid extraction and distillation using chloroform as an entrainer was proposed for the pyridine enrichment section and had the lowest recorded entrainer to azeotropic mixture ratio (EA=0.32:1) for the water-pyridine mixture. over 99mass% pyridine recovery at 96mol% purity was achieved. The obtained pyridine purity is not up to industry specification for resalable pyridine. In Chapter 4, we will be assessing the implementation of Dividing Wall Column (DWC) technique mainly for energy integration, but since it has been reported that DWC can improve quality of products, improvement of pyridine purity will also be assessed. From the pyridine enrichment section over 80mass% of the water originally present in the HOW was recovered at over 99mass% purity. Therefore, the water can be used for any process water requirements.

References

[1] “Pyridine market: global industry size, share and forecast period 2015 -2025.” [Online]. Available: http://www.persistencemarketresearch.com/market-research/pyridine-market.asp. [Accessed: 28-Jun-2017].

[2] R. Cheng, C.-H. Cho, S. Kirby, and B. Lim, “Economic recovery of pyridine and 3-methylpyridine,” 2010.

[3] W. L. Luyben and I.-L. Chien, *Design and control of distillation systems for separating azeotropes*, vol. 53,. 2013.

[4] C. Crew and T. Schafer, “Recovery of pyridine saves $1.5 million per year,” 1993.

[5] P. Das and S. Kumar, “Synthesis of highly water selective copolymer membranes for pervaporative dehydration of acetonitrile,” *J. Memb. Sci.*, vol. 507, pp. 81–89, 2016.

[6] A. Y. Pulyalina, G. A. Polotskaya, K. Y. Veremeychik, M. Y. Goikhman, I. V. Podeshvo, and A. M. Toikka, “Ethanol purification from methanol via pervaporation using polybenzoxazinoneimide membrane,” *Fuel Process. Technol.*, vol. 139, pp. 178–185, 2015.

[7] M. K. Mandal, S. B. Sant, and P. K. Bhattacharya, “Dehydration of aqueous acetonitrile solution by pervaporation using PVA-iron oxide nanocomposite membrane,” *Colloids Surfaces A Physicochem. Eng. Asp.*, vol. 373, pp. 11–21, 2010.

[8] S. Xia, X. Dong, Y. Zhu, W. Wei, F. Xiangli, and W. Jin, “Dehydration of ethyl acetate-water mixtures using PVA/ceramic composite pervaporation membrane,” *Sep. Purif. Technol.*, vol. 77, pp. 53–59, 2011.

[9] H. Benyounes, W. Shen, and V. Gerbaud, “Entropy Flow and Energy Efficiency Analysis of Extractive Distillation with a Heavy Entrainer,” *ACS*, pp. 4778–4791, 2014.

[10] E. Lladosa, J. B. Montón, and M. Burguet, “Separation of di-n-propyl ether and n-

propyl alcohol by extractive distillation and pressure-swing distillation: computer simulation and economic optimization," *Chem. Eng. Process. Process Intensif.*, vol. 50, pp. 1266–1274, 2011.

[11] G. M. De Koeijer and S. Kjelstrup, "Application of irreversible thermodynamics to distillation," *Int. J. Thermodyn.*, vol. 7, pp. 107–114, 2004.

[12] P. Prayoonyong, "Conceptual design of heterogeneous azeotropic distillation process for ethanol dehydration using 1-butanol as entrainer," *Maejo Int. J. Sci. Technol.*, vol. 8, pp. 334–347, 2014.

[13] J. Gmehling and C. Mollman, "Synthesis of Distillation Processes Using Thermodynamic Models and the Dortmund Data Bank," *Am. Chem. Soc.*, vol. 5885, pp. 3112–3123, 1998.

[14] S. Xia, X. Dong, Y. Zhu, W. Wei, F. Xiangli, and W. Jin, "Dehydration of ethyl acetate-water mixtures using PVA/ceramic composite pervaporation membrane," *Sep. Purif. Technol.*, vol. 77, pp. 53–59, 2011.

[15] V. Julka, M. Chiplunkar, and L. O. Young, "Selecting entrainers for azeotropic distillation," *Aiche*, March, pp. 47–53, 2009.

[16] W. E. De Villiers, R. N. French, and G. J. Koplos, "Navigate phase equilibria via residue curve maps," *Chem. Eng. Prog.*, vol. 98, pp. 66–71, 2002.

[17] N. Hilal, G. Yousef, and P. Langston, "The reduction of extractive agent in extractive distillation and auto-extractive distillation," *Chem. Eng. Process.*, vol. 41, pp. 673–679, 2002.

[18] L. Berg and Z. Yang, "Separation of pyridine from water using extractive distillation," 1992.

[19] Y. C. Wu and I. L. Chien, "Design and control of heterogeneous azeotropic column system for the separation of pyridine and water," *Ind. Eng. Chem. Res.*, vol. 48, pp. 10564–10576, 2009.

[20] E. R. Gilliland, "Multicomponent Rectification- Estimates of the Number of

Theoretical Plates as a Function of the Reflux Ratio," *Ind. Eng. Chem.*, vol. 32, pp. 1220–1223, 1940.

[21] M. A. Soliman, "A shortcut method for binary distillation column design," in *Towards Engineering Environment to Merge in a Competitive Global Economy*, 2007.

[22] G.-J. A. F. Fien and Y. A. Liu, "Heuristic synthesis and shortcut design of separation Processes using residue curve maps: A review," *Ind. Eng. Chem. Res.*, vol. 33, pp. 2505–2522, 1994.

[23] W. F. Shen, H. Benyounes, and J. Song, "Thermodynamic topological analysis of extractive distillation of maximum boiling azeotropes," *Brazilian J. Chem. Eng.*, vol. 32, pp. 957–966, 2015.

[24] "Chloroform Price, Chloroform Price Suppliers and Manufacturers at Alibaba.com." [Online]. Available: https://www.alibaba.com/showroom/chloroform-price.html. [Accessed: 18-Oct-2017].

[25] "Pyridine Price, Pyridine Price Suppliers and Manufacturers at Alibaba.com." [Online]. Available: https://www.alibaba.com/showroom/pyridine-price.html. [Accessed: 18-Oct-2017].

[26] M. T. D. Nguyen, "Conceptual Design, Simulation and Experimental Validation of Divided Wall Column: Application for Nonreactive and Reactive Mixture," Toulouse Institute of Technology, 2015.

Chapter 4 : Integration of the Distillation Columns using Dividing Wall Column (DWC) Technique

In this chapter, one of the renowned process intensification techniques referred to as the Dividing Wall Column (DWC) is being explored for the integration of the first 2 distillation columns in the proposed separation process in Chapter 3 (C-1 and C-2 in Figure 4.1). The following subtopics are covered: advantages and limitations of DWC, industrial applications, different simulation setups for DWC in Aspen Plus and other commercial process simulators. The application of DWC is then illustrated for our desired purpose with a step by step explanation of how it was implemented on Aspen Plus. The obstacles of simulation of DWC are discussed and troubleshooting recommendations are given. Furthermore, the results obtained are discussed vis-à-vis the results in **Chapter 3** where possible.

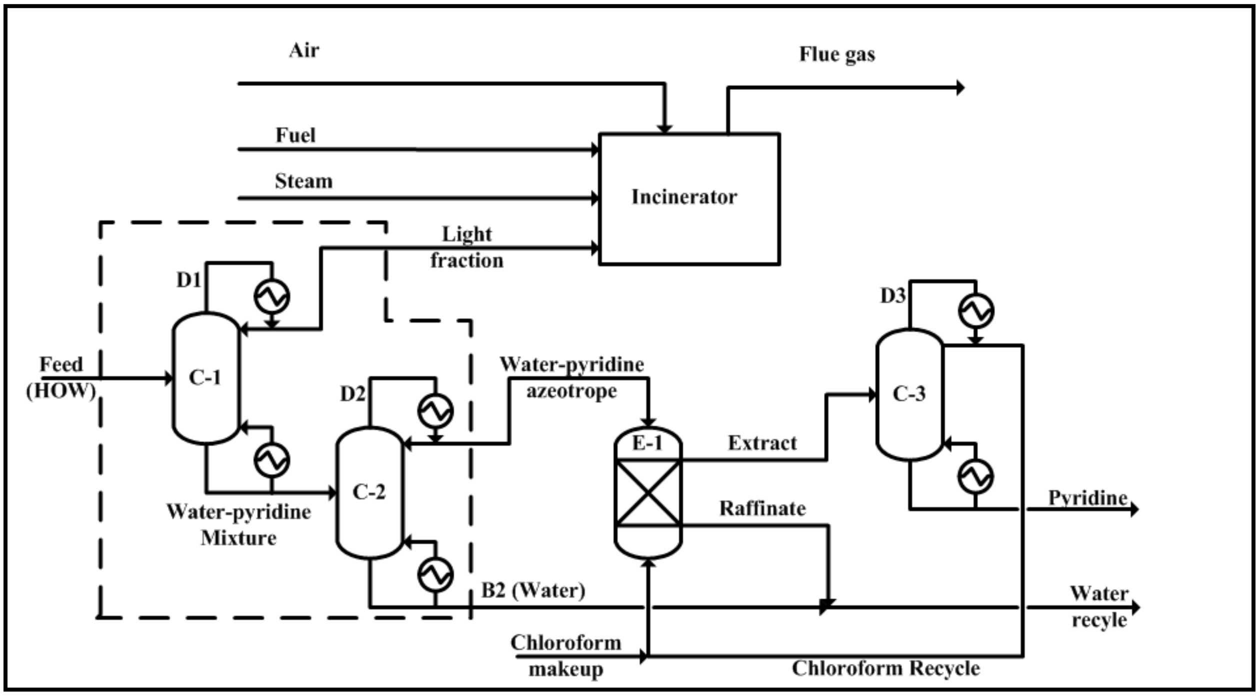

Figure 4.1. Proposed pyridine recovery process

4.1. Introduction

Process intensification consists in any effort to combine 2 or more chemical processes into 1 in order to reduce the size of the plant, reduce energy consumption or increase efficiency [1]. The key characteristic of process intensification is that production throughput is retained [2]. Some examples of process intensification are reactive distillation, membrane distillation and rotating packed beds [1]. The most common process intensification for distillation is the Dividing Wall Column. This technique combines 2 or more columns into 1 by dividing the core of the column into 2 parts using a vertical wall [3].

For a ternary mixture, the feed gets deflected by the wall and the low boiling component is propelled upward, while the heaviest component inherently flows downwards. The mid-boiling component on the other hand, is entrained with both the light and heavy components. At the bottom of the column, the mid-boiling component is separated from the heavy component and flows upwards on the opposite side of the wall. A similar phenomenon is observed at the top of the column whereby the mid-boiling component is again separated from the light component and flows downwards on the opposite side of the wall. Finally, the mid-boiling component is recovered as the middle product of the column [4] (Figure 4.2).

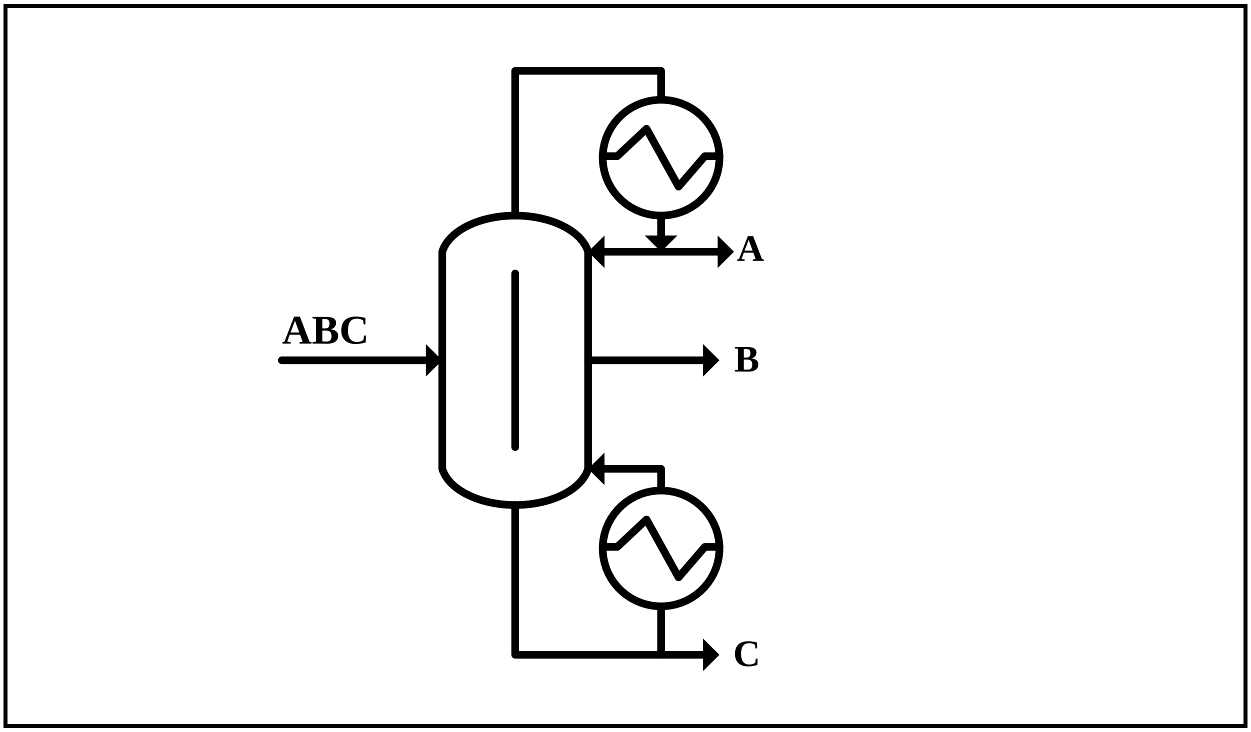

Figure 4.2. Dividing Wall Column [1]

Although distillation is the most preferred separation method, it has a low thermodynamic efficiency [3-5]. Sangal et al. [6] argued that over 50% of the total energy consumption in a chemical plant is typically due to distillation. In the US, distillation is reported to consume 3% of the total energy produced per annum [7]. Consequently, Petlyuk column or DWC technique has been proposed to curb the energy intensity of the distillation process. It has been reported in literature that process intensification through the application of the principle Petlyuk column or Dividing Wall Column can reduce the energy consumption of the distillation columns by up to 30% [3,4,6,7,8,9,10,11].. The reduced energy consumption is due to the reduced number of condensers and reboilers. In addition to economic gains, the reduction in energy consumption also benefits the environment through reduced burning of fossil fuels and hence abridged emissions [7]. Furthermore, the minimum equipment required for DWC results in the reduction of operational costs and capital investment [9]; it is argued that the operating costs can be reduced by up to 25% by employing the DWC technique [11]. It is further reported that the product streams from the DWC are of high purity compared to the conventional direct or indirect separation sequence [1]. Even with these advantages, the industrial application of DWC has been minimal mainly due to lack of expertise in its design and control [5,6].

Due to the complex nature of DWC, simulation work is a prerequisite. However, even its simulation is made difficult by the fact that many process simulators do not have a built-in column to simulate DWC. Therefore, the underlying thermodynamic principles must be understood to be able to simulate its equivalent. It is widespread practice to simulate the DWC as a Petlyuk column since the two are thermodynamically equivalent assuming that the heat transfer across the wall is negligible [7]. Petlyuk column is a process in which 2 or more columns are thermally coupled; its main objective being to minimize the energy consumption of distillation. In this way, the DWC is an integration of a Petlyuk column into one column [4]. The DWC configuration advantage over the Petlyuk are reduced number of equipment resulting in lower capital investment and low space consumption on the plant site. There are 3 ways to represent and simulate the DWC as a Petlyuk column [1]. These are:

- The pump around model (Figure 4.3) [1],
- Two-column model (Figure 4.4) [1] and;
- The four-column model (Figure 4.5) [1].

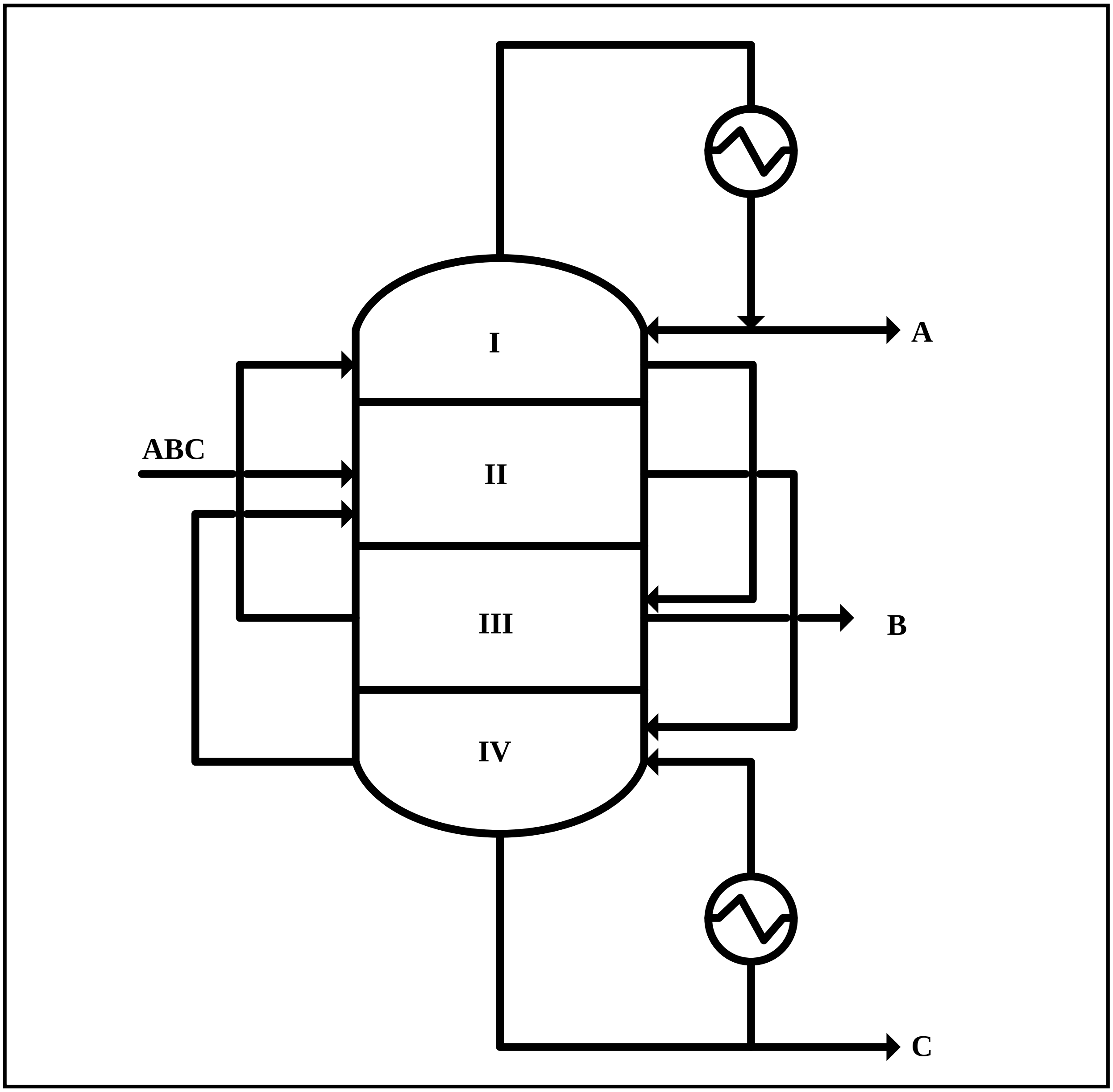

Figure 4.3. Pump around model for dividing wall column simulation [5]

In this model, the 4 sections found in the DWC are mimicked by placing different sections vertically above one another [5]. The regulation of vapor and liquid traffic is done through the vapor bypasses and liquid pump around as shown in Figure 4.3 [1]. This tends to result in convergence problems because of a stage in which all the liquid and vapor are drawn off [5].

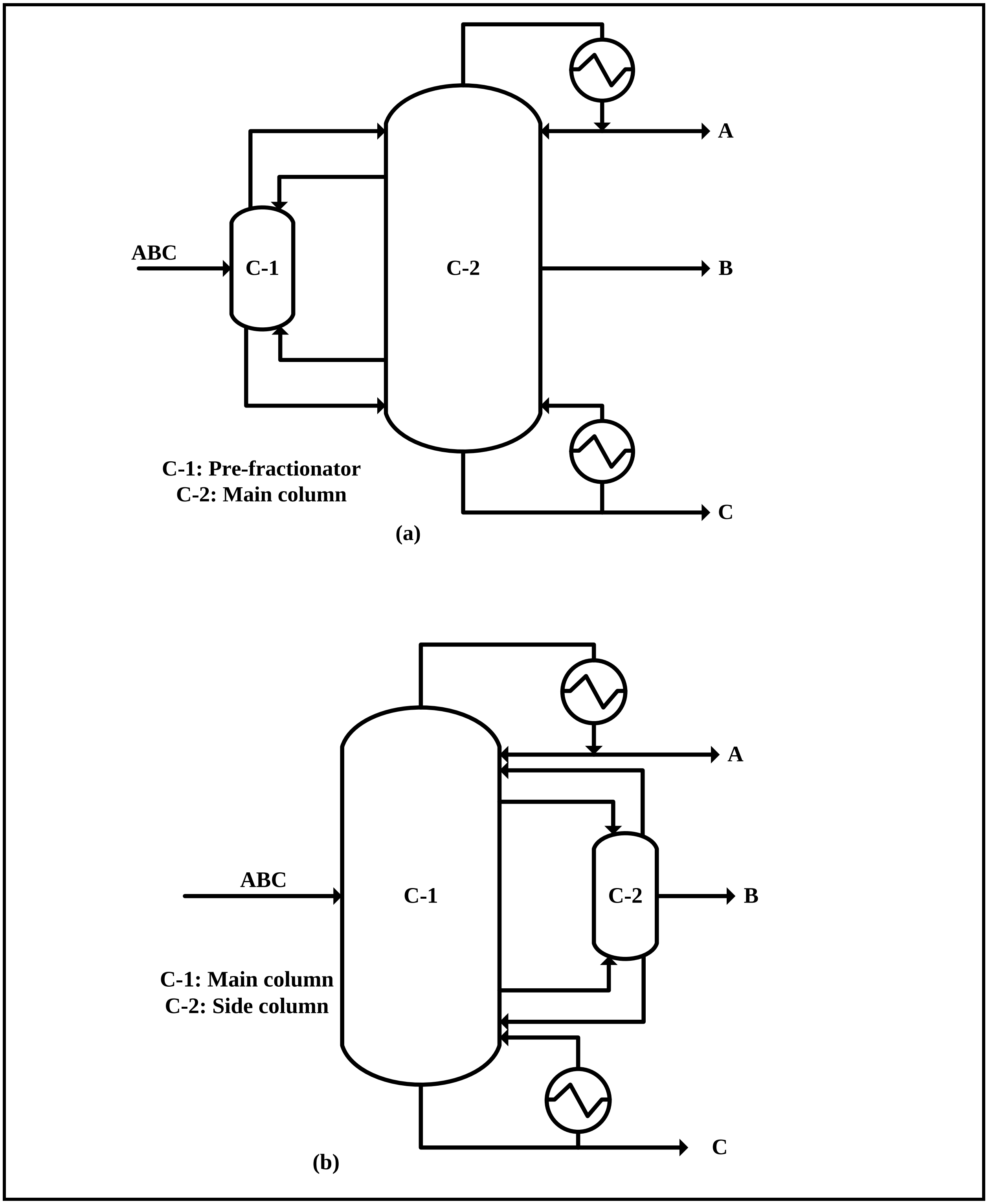

Figure 4.4. Two-column model for the representation of DWC: (a). Pre-fractionator and Main column (b). Main column and post fractionator [1]

There are 2 ways to simulate a two-column model. One way is to have a pre-fractionator and the main column (Figure 4.4 (a)) while the other is to have the main column and the post-fractionator (Figure 4.4 (b)). The former representation is the most commonly used for simulation design and optimization [1, 9].

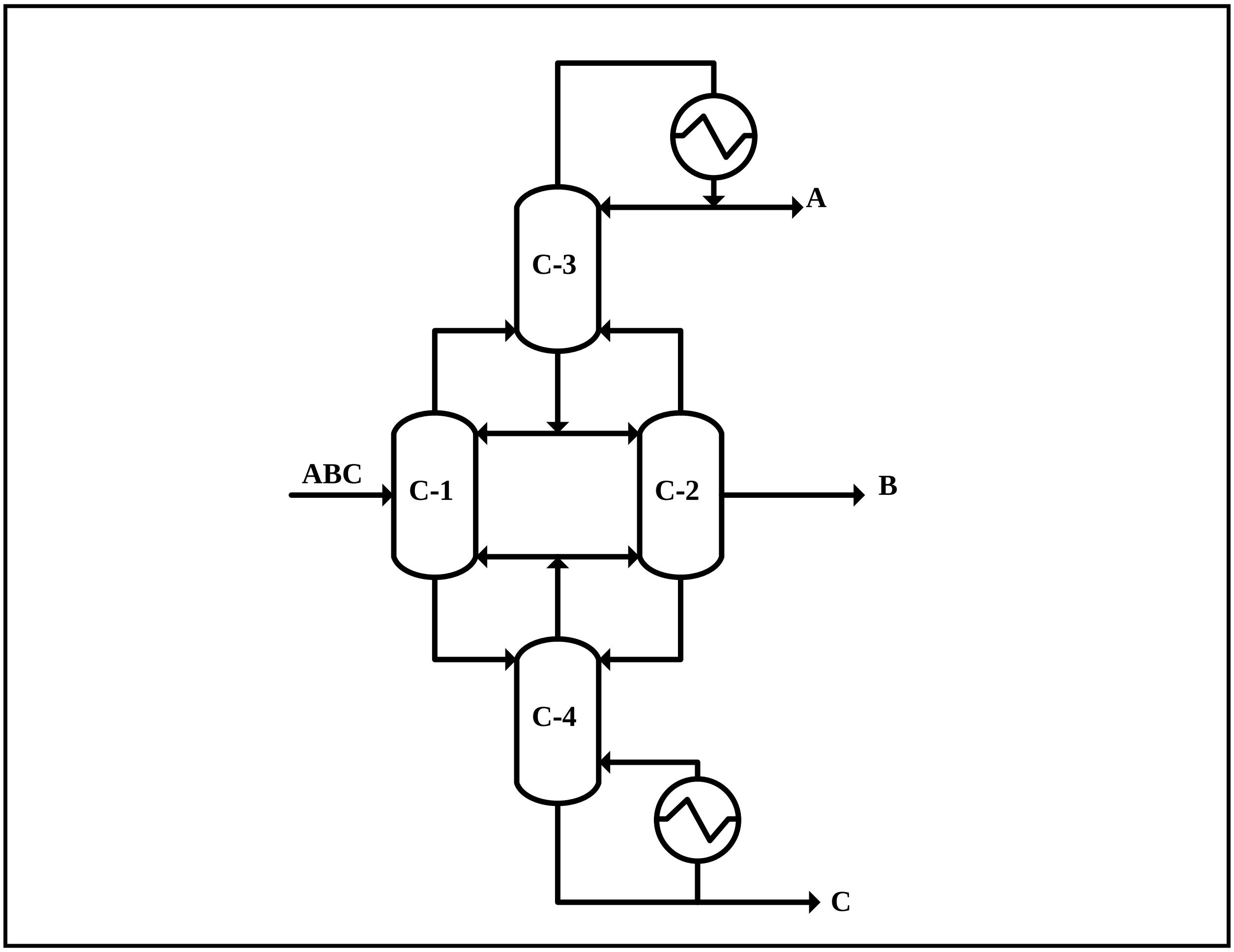

Figure 4.5. Four-column model for the DWC [7]

Although the two-column model is generally used for simulation, it is too simplified and does not capture the complexities within the DWC and to some extent nullifies the purpose of simulation which is to help overcome some of the complexities that may be encountered in a real setup. The four-column model on the other is the best representative of the actual real-life DWC [1] (Figure 4.5). This is so because the four individual columns represent each section found in the DWC. Moreover, the fluid transport around the model is aligned with the DWC concept. The four-column model is avoided because it is generally difficult to initialize and due to the potential convergence issues that may arise resulting from an increased number of recycles. In this chapter, the four-column approach is assessed for the integration of the first 2 distillation columns in the proposed recovery process. In the discussions sections (4.3), suggestions have been made on how to overcome some of the convergence problems. Aspen Plus and Aspen HYSYS process simulators have been preferentially used for the simulation and study of DWC [4, 9, 11]. In this work Aspen Plus has been chosen for its consistency with the results obtained in Chapter 3.

In 2010, there were 125 applications of DWC worldwide and the number was expected to increase to 350 applications by 2015 [1]. Sasol operates the largest DWC that is 107m tall and 5m wide which is used to separate Fischer-Tropsch products [4]. The areas of application of DWC throughout the world are summarized in Table 4.2. In 2010, there was only one application of DWC for azeotropic mixtures with most of the systems being about separation of ternary mixtures (Table 4.1) [12].In many systems, the pre-concentration of mixtures is often required to isolate mixtures containing desired components. For instance, in cases of azeotropic and extractive distillation, mixtures are often pre-concentrated to azeotropic composition to minimize entrainer quantity required to effect separation [13-15]. In complex mixtures, like the one considered in this work, two or more distillation units may be required to finally sample the desired mixture at azeotropic compositions. Because the pre-concentration units process higher loads of mixtures, their energy consumption tend to be substantial in the grand scheme of things. This is illustrated by the heat equation (4.1), which can be interpreted as: the higher the quantity of the mixture (M), the higher the heat (Q) required to raise the temperature by ΔT. As such, the application of DWC or any energy saving technique on the first 2 distillation columns in the proposed process is worth considering.

$$Q = MC_p\Delta T \tag{4.1}$$

Where

Q: Heat duty

M: Mass flow rate

C_p: Specific heat capacity

ΔT: Change in temperature

Therefore, this chapter aims to contribute to the application of DWC to azeotropic mixtures. In this work, the DWC concept is applied for the recovery of the water-pyridine azeotropic mixture (75mol% water and 25mol% pyridine) from the HOW by integrating Column C-1 and C-2 into 1 (Figure 4.6). To our knowledge, this type of application of DWC has not been conducted, as usually DWC is used for ideal mixtures like the fractionation of petroleum products (gasoline, diesel and naphtha) and the most prevalent application being the separation of benzene, toluene and xylene (BTX) [1, 3, 6, 10]. The azeotropic boiling points are tabulated in Table 4.3. The light, mid and heavy fractions are highlighted with assorted colors. The study of Table 4.3 shows that all the azeotropes have boiling points 80˚C except that of pyridine with water which boils at 93˚C and the boiling point of water is 100˚C. Therefore, the anticipation is that all the water containing azeotropes but water-pyridine are to be recovered as the distillate, water-pyridine azeotrope as the middle component and water recovered as the bottoms product (Figure 4.6).

Table 4.1. Applications of DWC in Industry as reported in 2010 [12]

System	Frequency
Mixtures with more than 3 components	2
Ternary mixtures	116
Azeotropic	1
Extractive	2
Revamps	4
Reactive	-

Table 4.2. DWC Industrial Applications [12]

Company	System	Constructor and Year	Features
Sasol, Johannesburg, South Africa	Separation of hydrocarbons from Fischer-Tropsch unit	1999	largest DWC column
BASF SE, diverse sites	Mostly undisclosed	1985	More than 70 DWCs
Veba Oel Ag, Münchs münster,Germany	Separation of benzene from pyrolysis gasoline	1999	140000 mt/year
Saudi Chevron Petrochemical Al Jubail, Saudi Arabia Al Jubail, Saudi Arabia	Undisclosed	2000	140,000 mt/year feed capacity
ExxonMobil Rotterdam, Netherlands	Benzene-Toluene-Xylene fractionation	2008	No data available

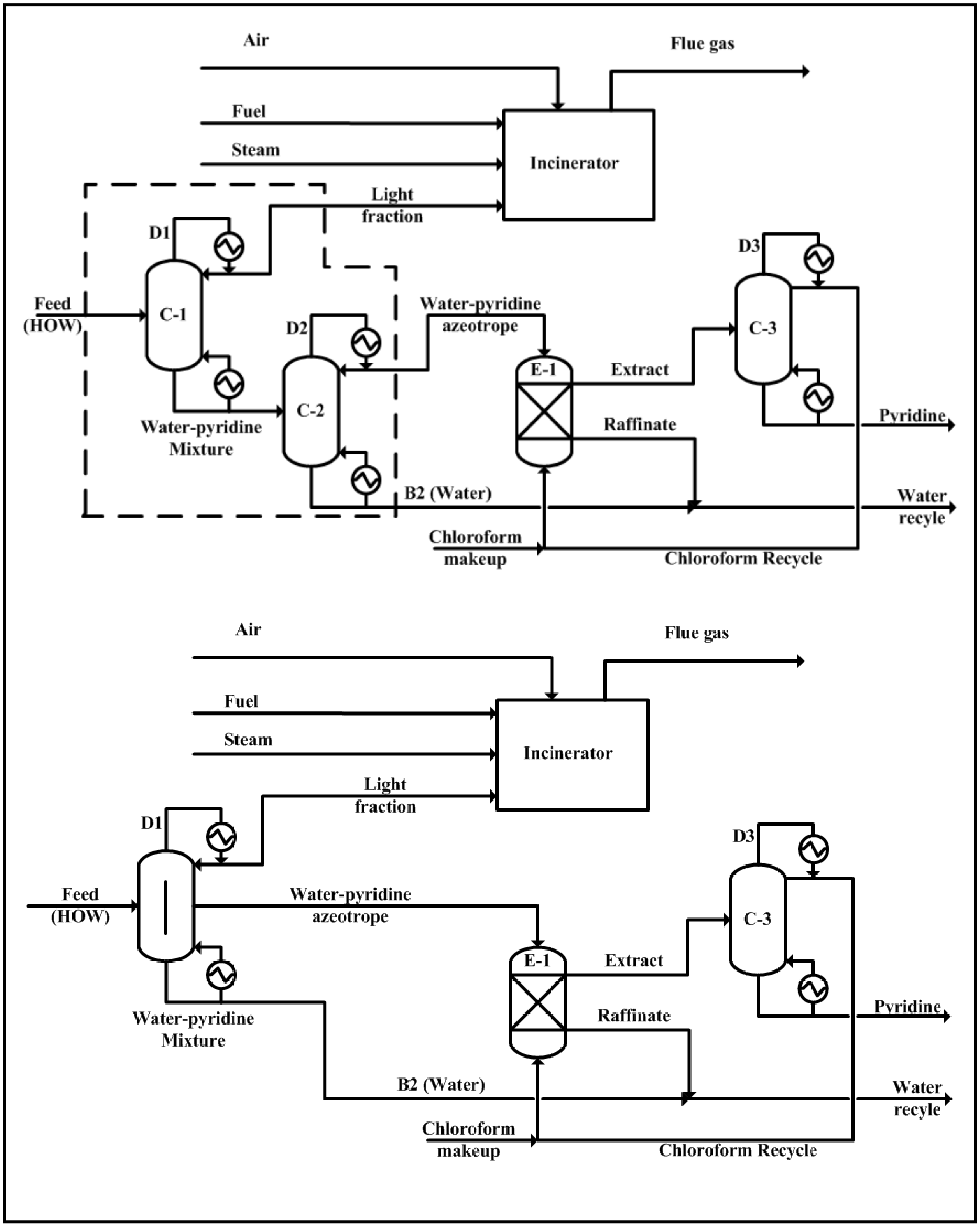

Figure 4.6. Integration of the first two distillation columns (C-1 and C-2) into 1

Table 4.3. Boiling points of pure components and azeotropes

Pure Components		**Azeotropic Components**	
Component	**Boiling Point(˚C)**	**Azeotrope**	**Boiling Point (˚C)**
Water	100.02	Water-MIK	77.61
Pyridine	115.16	Water-MEK	73.65
Acetone	56.14	Water-pyridine	93.71
Acetonitrile	81.48	acetonitrile-MEK	79.09
Methyl Ethyl Ketone (MEK)	79.34	Water-Acetonitrile	76.53
Methyl Isopropyl Ketone (MIK)	94.08	Water-MEK-Acetonitrile	76.32

🟧 High boiling
🟨 Mid-boiling
🟦 low boiling

4.2. Aspen Plus Simulation

The shortcut simulation model is used to get the operating parameters like number of columns, reflux ratio and feed stages of the columns C-1, C-2, C-3 and C-4 in Figure 4.7. The simulation is carried out using DSTWU column in the Aspen Plus library. It is noteworthy that column B and C represent the middle section of the DWC and thus have the same number of stages. For this reason, column C is not accounted for in the shortcut model (Figure 4.8). To get a good representation of the DWC, the mid-boiling composition for mid-boiling 1 and 2 must be close [3, 9]. This is achieved mainly by trial and error through adjusting light and heavy keys recoveries in the columns [16]. This illustration and other specifications for the shortcut model can be found in Appendix B.1.

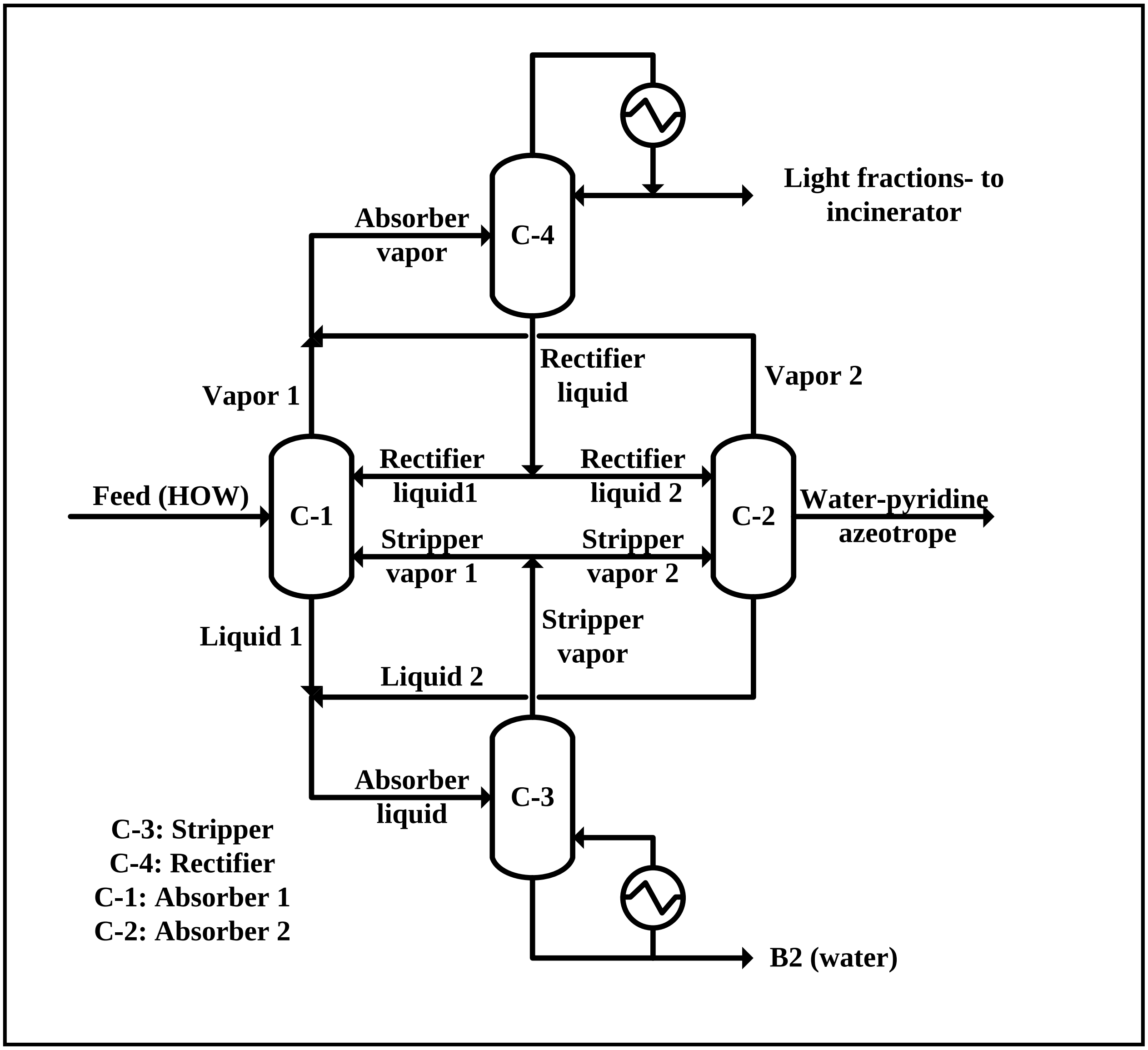

Figure 4.7. DWC model as depicted in Aspen Plus

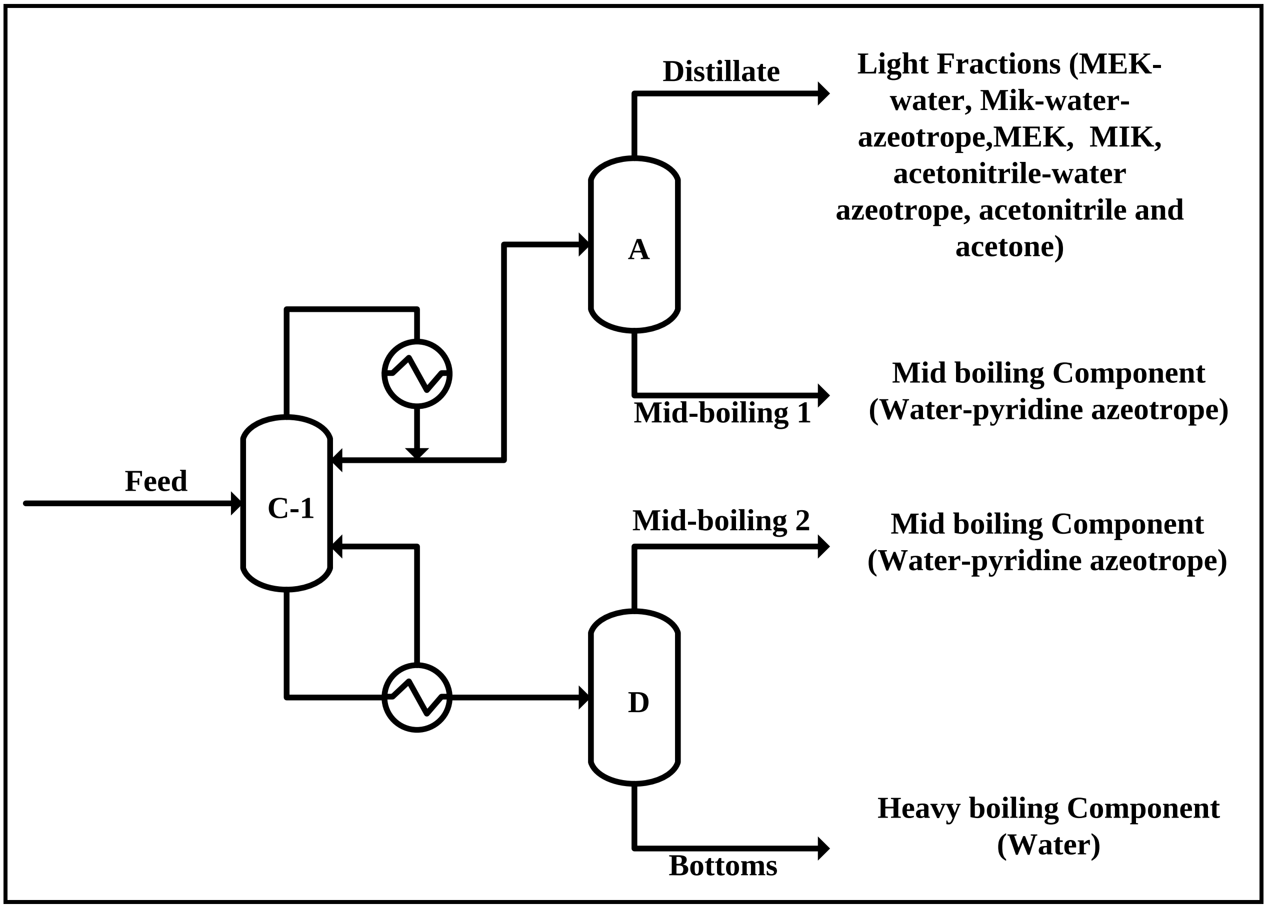

Figure 4.8. Shortcut model as shown on Aspen Plus

Table 4.4. Shortcut simulation results

Column	Number of stages	Reflux Ratio
C-1	40	7
C-4	20	4.5
C-3	10	2.2

The parameters obtained from the shortcut model were specified on the rigorous simulation model (Figure 4.9 to Figure 4.20). Due to the azeotropic nature of the waste the convergence type in all columns were changed from standard to azeotropic. As standard, the simulation resulted in severe errors.

Absorber 1 (column C-1)

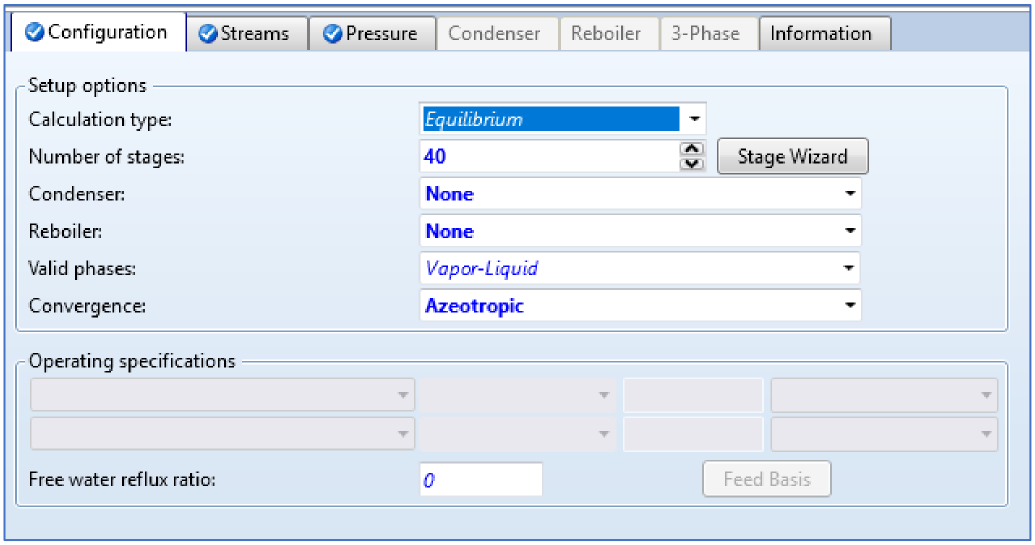

Setup options

Calculation type: Equilibrium

Number of stages: 40

Condenser: None

Reboiler: None

Valid phases: Vapor-Liquid

Convergence: Azeotropic

Operating specifications

Free water reflux ratio: 0

Figure 4.9. Configuration Specifications for Absorber 1

Since the absorber has got no reboiler and condenser, they are both specified as none in the specifications (Figure 4.9). The absorber is used to represent the middle part of the DWC because indeed in that section there is no heat exchange device.

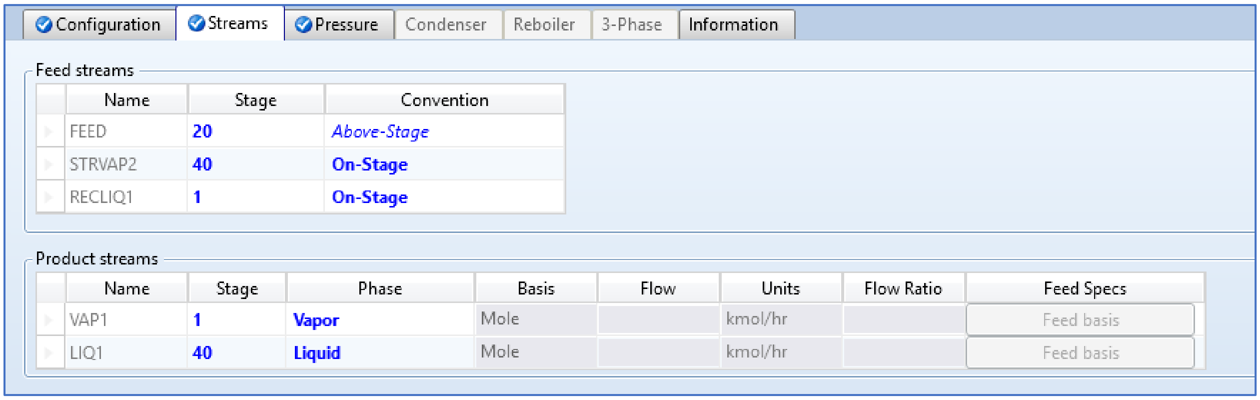

Feed streams

Name	Stage	Convention
FEED	20	Above-Stage
STRVAP2	40	On-Stage
RECLIQ1	1	On-Stage

Product streams

Name	Stage	Phase	Basis	Flow	Units	Flow Ratio	Feed Specs
VAP1	1	Vapor	Mole		kmol/hr		Feed basis
LIQ1	40	Liquid	Mole		kmol/hr		Feed basis

Figure 4.10. Streams Specifications for Absorber 1

Because the absorber does not have a condenser nor a reboiler the recycled stream from the rectifier (RECLIQ1) and stripper (STRVAP2) were fed on stage 1 and 40 respectively (Figure 4.10). If this is not done, Aspen reports that specifications are not complete.

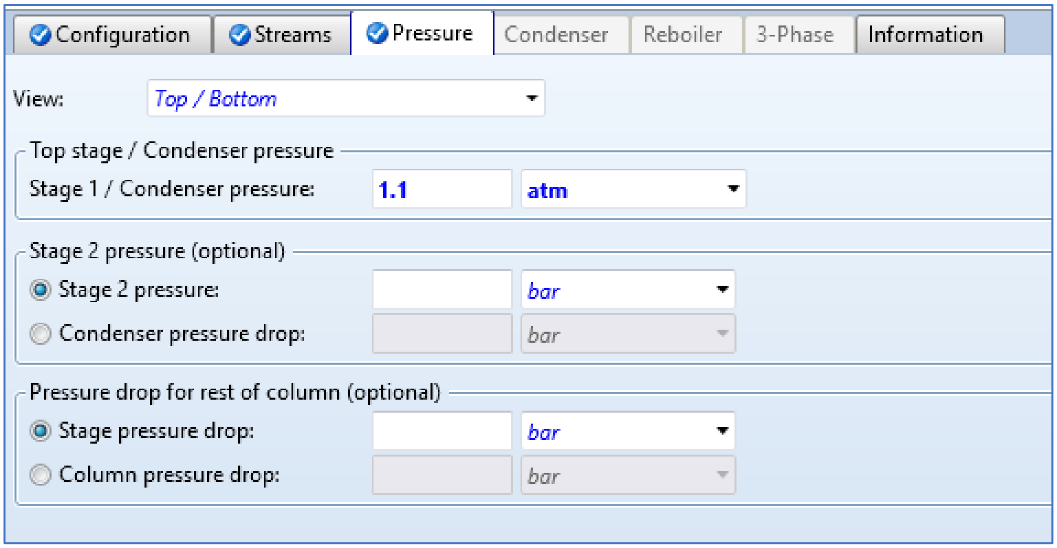

View: *Top / Bottom*

Top stage / Condenser pressure

Stage 1 / Condenser pressure: **1.1** **atm**

Stage 2 pressure (optional)

● Stage 2 pressure: *bar*

○ Condenser pressure drop: *bar*

Pressure drop for rest of column (optional)

● Stage pressure drop: *bar*

○ Column pressure drop: *bar*

Figure 4.11. Pressure Specification for the Absorber Column

Absorber 2 (Column C-2)

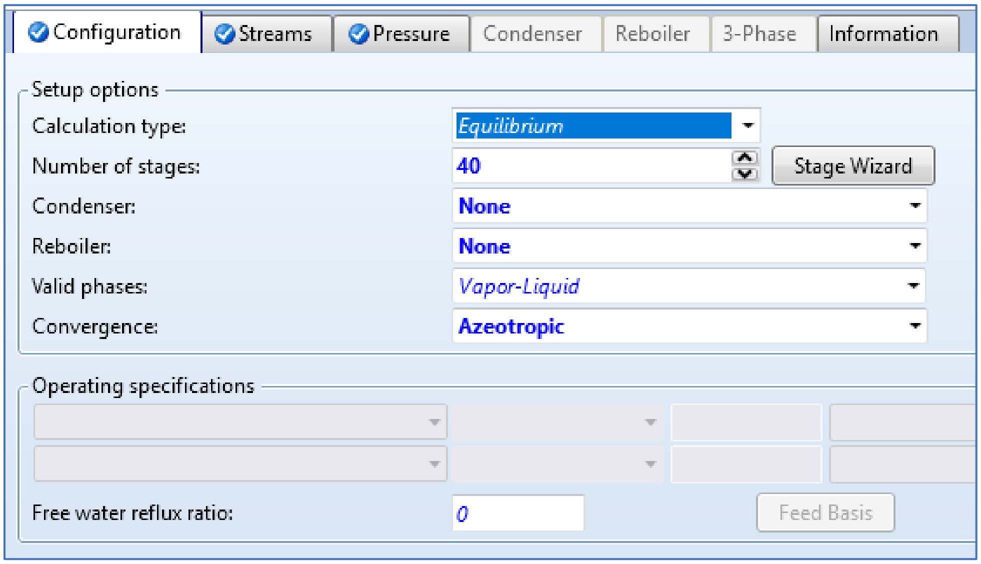

Setup options

Calculation type: *Equilibrium*

Number of stages: **40**

Condenser: **None**

Reboiler: **None**

Valid phases: *Vapor-Liquid*

Convergence: **Azeotropic**

Operating specifications

Free water reflux ratio: *0*

Figure 4.12. Configuration Specifications for Absorber Column 2

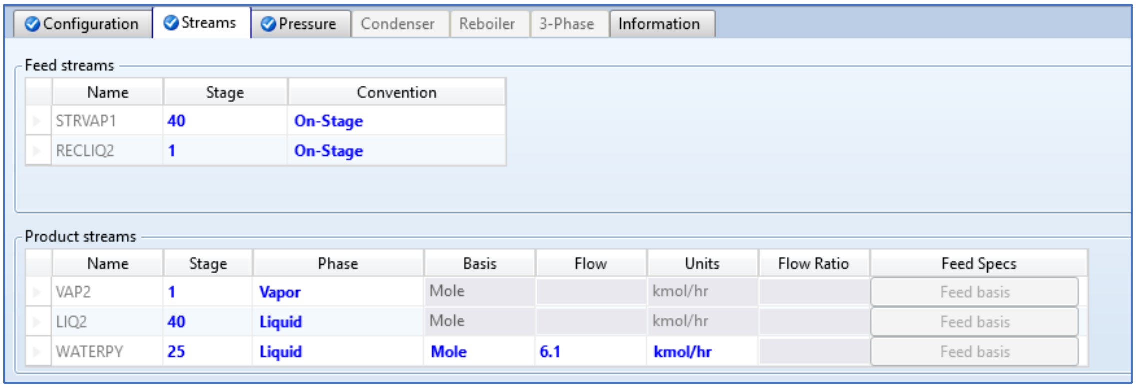

Feed streams

Name	Stage	Convention
STRVAP1	40	On-Stage
RECLIQ2	1	On-Stage

Product streams

Name	Stage	Phase	Basis	Flow	Units	Flow Ratio	Feed Specs
VAP2	1	Vapor	Mole		kmol/hr		Feed basis
LIQ2	40	Liquid	Mole		kmol/hr		Feed basis
WATERPY	25	Liquid	Mole	6.1	kmol/hr		Feed basis

Figure 4.13. Inlet and product streams specifications for absorber column 2

The first and second absorbers (C-1 and C-2 in Figure 4.7) represent the midsection of the DWC. C-1 represents one side of the wall while C-2 represents the other side of the wall. Therefore, their number of stages are equal. Like the first absorber, the second absorber also requires that the first (stage 1) and last stage (stage 40) have feeds. The feed from the stripper split is fed onto the 40th stage and the feed from the rectifier split is fed onto the 1st stage. Lastly the mid boiling product is specified to be withdrawn on the 25th stage. This stage was found by trial and error.

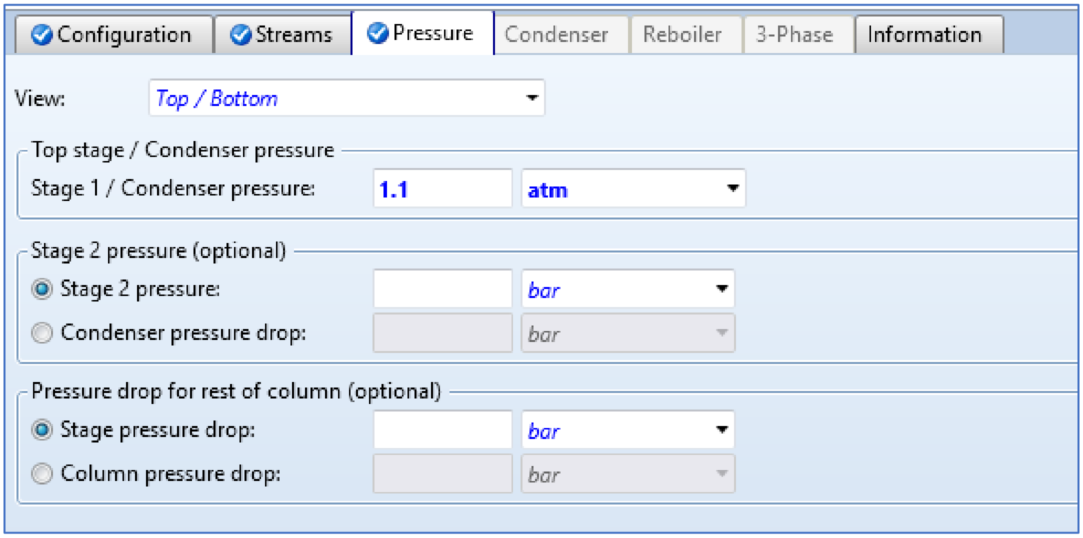

View: Top / Bottom

Top stage / Condenser pressure

Stage 1 / Condenser pressure: 1.1 atm

Stage 2 pressure (optional)

● Stage 2 pressure: bar

○ Condenser pressure drop: bar

Pressure drop for rest of column (optional)

● Stage pressure drop: bar

○ Column pressure drop: bar

Figure 4.14. Pressure Specification for Absorber Column 2

Rectifier (column C-4)

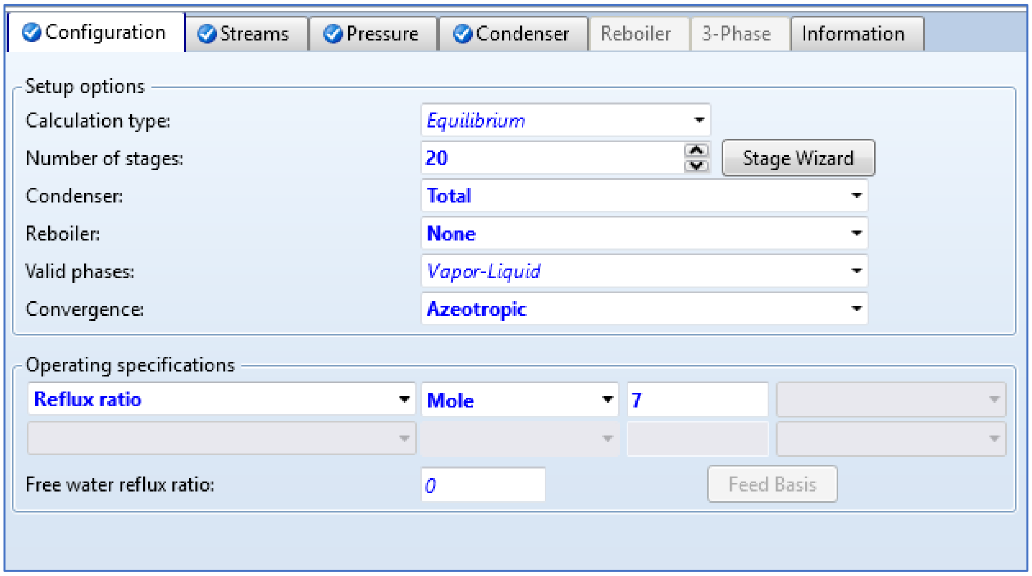

Setup options

Calculation type: Equilibrium
Number of stages: 20
Condenser: Total
Reboiler: None
Valid phases: Vapor-Liquid
Convergence: Azeotropic

Operating specifications

Reflux ratio Mole 7

Free water reflux ratio: 0

Figure 4.15. Configuration Specifications for the Rectifier

The rectifier has got no reboiler therefore the reboiler is specified as none in the specifications (Figure 4.15)

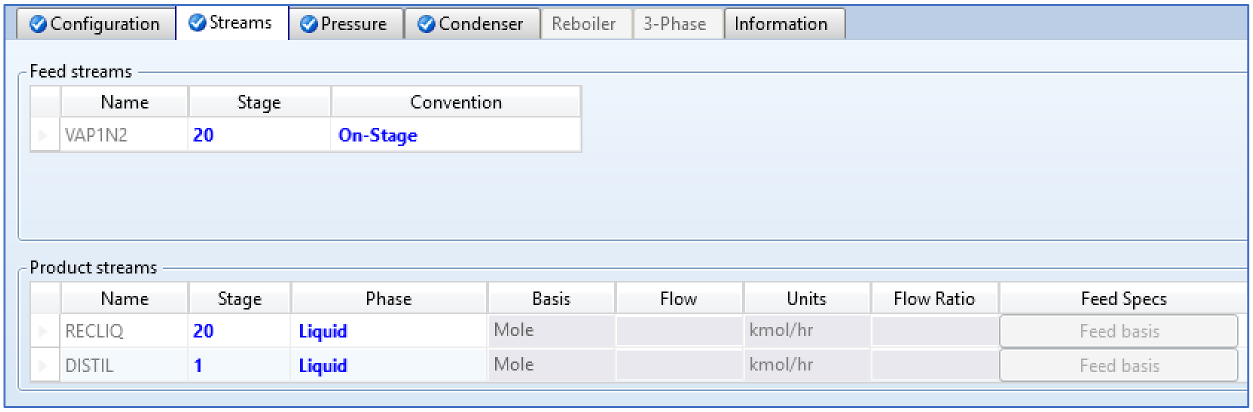

Feed streams

Name	Stage	Convention
VAP1N2	20	On-Stage

Product streams

Name	Stage	Phase	Basis	Flow	Units	Flow Ratio	Feed Specs
RECLIQ	20	Liquid	Mole		kmol/hr		Feed basis
DISTIL	1	Liquid	Mole		kmol/hr		Feed basis

Figure 4.16. Inlet and Product Streams Specifications

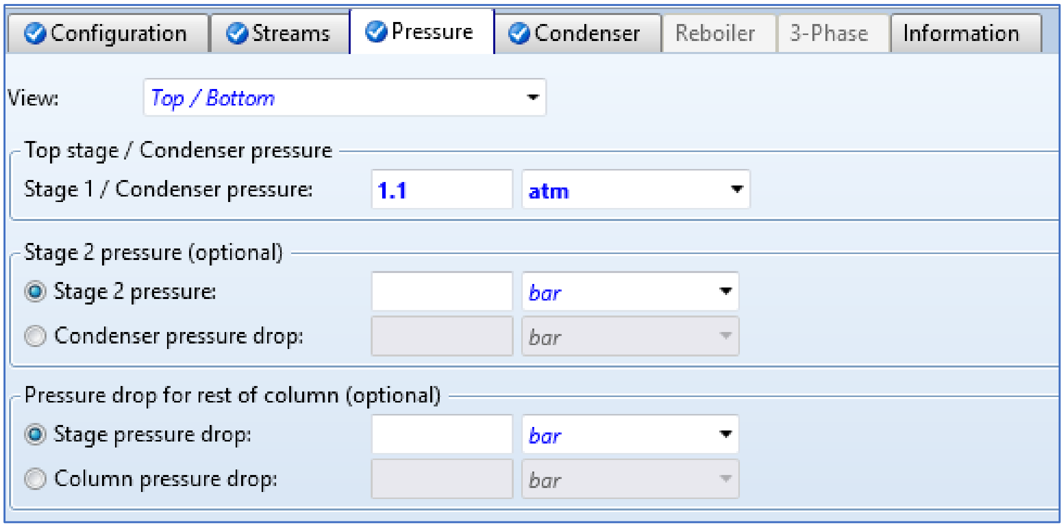

View: *Top / Bottom*

Top stage / Condenser pressure

Stage 1 / Condenser pressure: **1.1** **atm**

Stage 2 pressure (optional)

● Stage 2 pressure: *bar*

○ Condenser pressure drop: *bar*

Pressure drop for rest of column (optional)

● Stage pressure drop: *bar*

○ Column pressure drop: *bar*

Figure 4.17. Pressure Specifications

Stripper (column C-3)

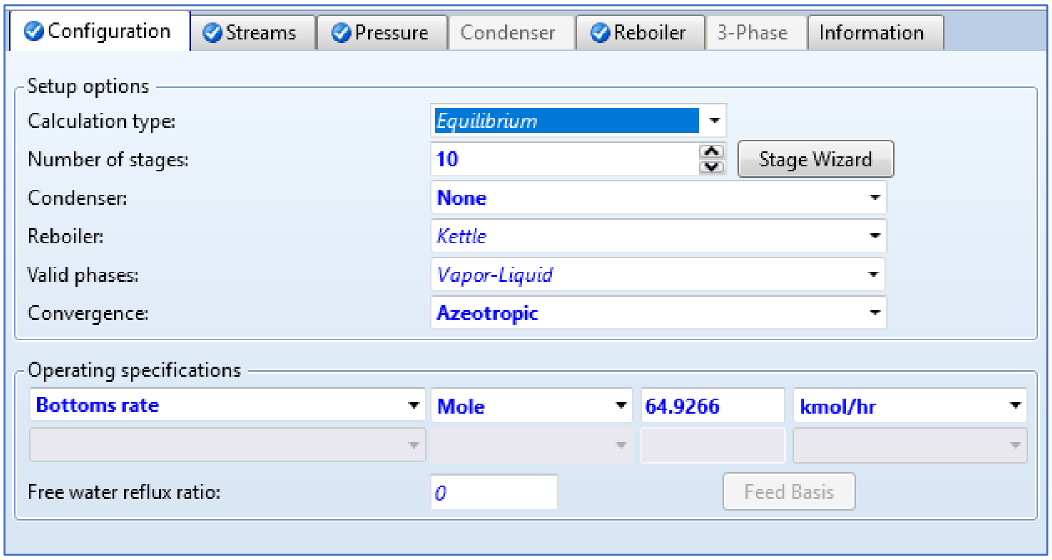

Setup options

Calculation type: *Equilibrium*

Number of stages: **10**

Condenser: **None**

Reboiler: *Kettle*

Valid phases: *Vapor-Liquid*

Convergence: **Azeotropic**

Operating specifications

Bottoms rate **Mole** **64.9266** **kmol/hr**

Free water reflux ratio: *0*

Figure 4.18. Stripper configuration specifications

A stripper is used to represent the bottom section of the DWC since it has the reboiler and no condenser which is what the bottom of the DWC looks like. The bottoms rate specified is equal to the bottoms rate from in C-2 of the original design (Figure 4.6).

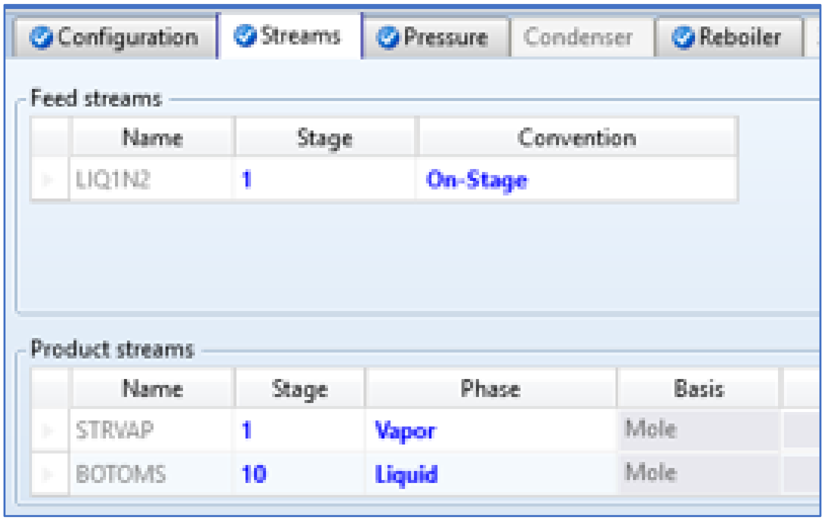

Feed streams

Name	Stage	Convention
LIQ1N2	1	On-Stage

Product streams

Name	Stage	Phase	Basis
STRVAP	1	Vapor	Mole
BOTOMS	10	Liquid	Mole

Figure 4.19. Inlet and Product Streams Specifications

Since the stripper is without a condenser, the feed stream to this column is fed onto the first stage.

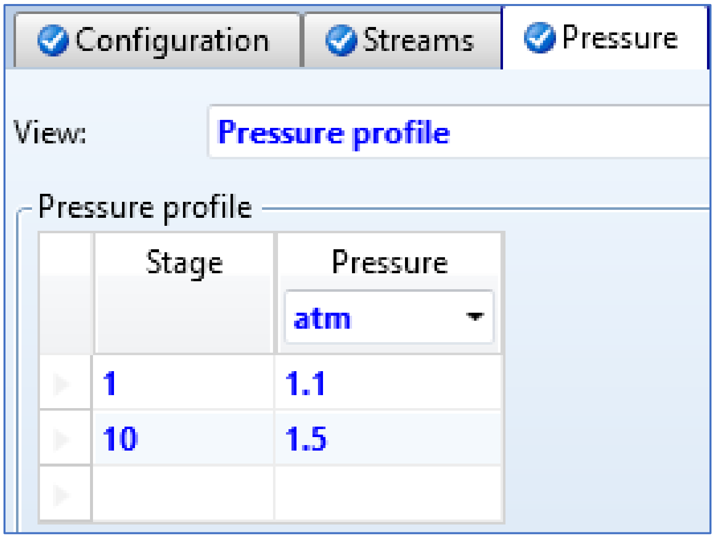

View: Pressure profile

Pressure profile

Stage	Pressure atm
1	1.1
10	1.5

Figure 4.20. Pressure Profile Specifications

4.3. Discussions

The initial simulation of the DWC resulted in severe errors on all units. Then steps outlined below were followed to overcome the errors. Some of the recommendations were acquired from open literature [13] and some were initiated in this research work (section 4.31, i & iii). Whilst all the blocks ran without problems, the mixers had issues converging the material balance thereby affecting the material balance of the whole unit. Consequently, the material balance is off by 0.6%.

4.3.1. Troubleshooting Recommendations to Deal with Convergence Issues

Convergence problems are common when simulating a complex unit as a Dividing Wall Column [13]. They may be brought about by an increased number of recycles, multiple feeds on the columns and the extent to which the mixture is far from ideality. A single cause of convergence problems may not be known in advance, usually a trial and error approach should be followed. Some of the steps that can be taken are as follows:

i. Ensure realistic and sensible withdrawal flowrates.

While it would be easier to determine the withdrawal flowrates for a ternary ideal mixture, it is difficult to determine the flowrates for azeotropic and other non-ideal mixtures. In such cases, it may prove worthwhile to first simulate an indirect or direct separation sequence of the mixture to get proper initial estimates of the flowrates of withdrawal streams.

ii. Change convergence of the column [13].

Depending on the type of mixture being separated the column convergence may have to be changed from default standard to either azeotropic, non-ideal, petroleum or cryogenic.

iii. Minimize the number of streams feeding columns.

The distillates from the two absorbers are both fed to the last stage of the rectifier, so instead of feeding these streams individually on this stage mix them first using the mixer unit on Aspen Plus library, then feed the combined stream to the rectifier. The same should be done for the bottoms product of the two absorbers that feed on the first stage of the stripper column. Using the three recommendations, one should at least be able to get the simulation to run sensibly. As a last resort, one may consider changing the solver method. The default solver in Aspen Plus is Wegstein method and it is possible to change this to Newton [13]. Increasing the number of iterations should be considered after everything else has failed. In the plots to follow only pyridine, water and acetonitrile compositions profile are plotted. Acetonitrile represents the trends observed in all other light components (MEK, MIK, and acetone). The profiles for the first absorber are depicted in Figure 4.21.

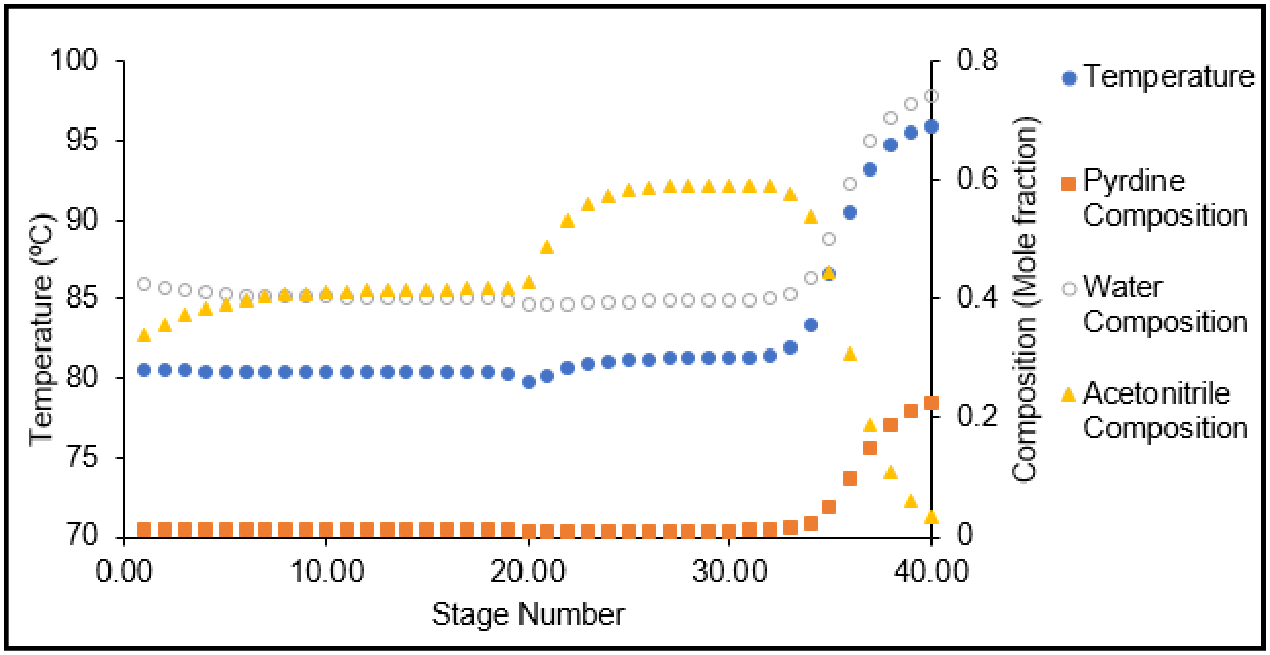

Figure 4.21. Profiles in Absorber 1

Temperature increases with increasing number of stages over the entire range. On the 20th stage, there occurs a trough on the temperature profile. This phenomenon occurs because the feed is fed onto the 20th stage and the feed is at a lower temperature (Figure 4.21). Acetonitrile composition increases with increasing number of stages and thus increasing temperature for the first 25 stages. On the 20th stage, the acetonitrile composition increases abruptly. This increase is due to the feed being fed on this stage. From the 26th stage, the composition reaches a plateau at about 62mol% acetonitrile. Unsurprisingly, this composition is close to that of water-acetonitrile azeotrope (67mol% acetonitrile and 33mol% water). Consequently, acetonitrile cannot concentrate any further than this composition. This serves to corroborate the assumption made that the components do not act as individuals but follow azeotropic properties due to massive presence of water in the feed. Moreover, beyond the 33rd stage the acetonitrile composition starts decreasing due to elevated temperatures that are higher than the boiling point of acetonitrile-water azeotrope (76.53˚C). After being vaporized by elevated temperatures, the water-acetonitrile azeotrope is entrained upwards resulting in decreased composition in the lower part of the column until it is very close to zero on the 40th stage.

Since water is the heaviest component, it is expected not to find large presence of water on the upper part of the column. The presence of water in the first stages of the column may be due to azeotropic formations with light components like MEK, MIK and acetonitrile. Unlike water, pyridine does not form azeotropes with light components in the waste and hence its composition remains close to zero until the 33rd stage. Its composition increases up to about 22mol% on the 40th stage which is also closer to water-pyridine azeotrope. On this stage, the water composition is 75mol% (Figure 4.21). Water-pyridine azeotrope is the heaviest of all azeotropes boiling at 91˚C. A closer look at water and pyridine compositions shows that the profiles are the same showing that the two components act as a unit, especially beyond the 33rd stage. This may be because of the water-pyridine azeotrope formation. The profiles observed in the second absorber (column C) are shown in Figure 4.22.

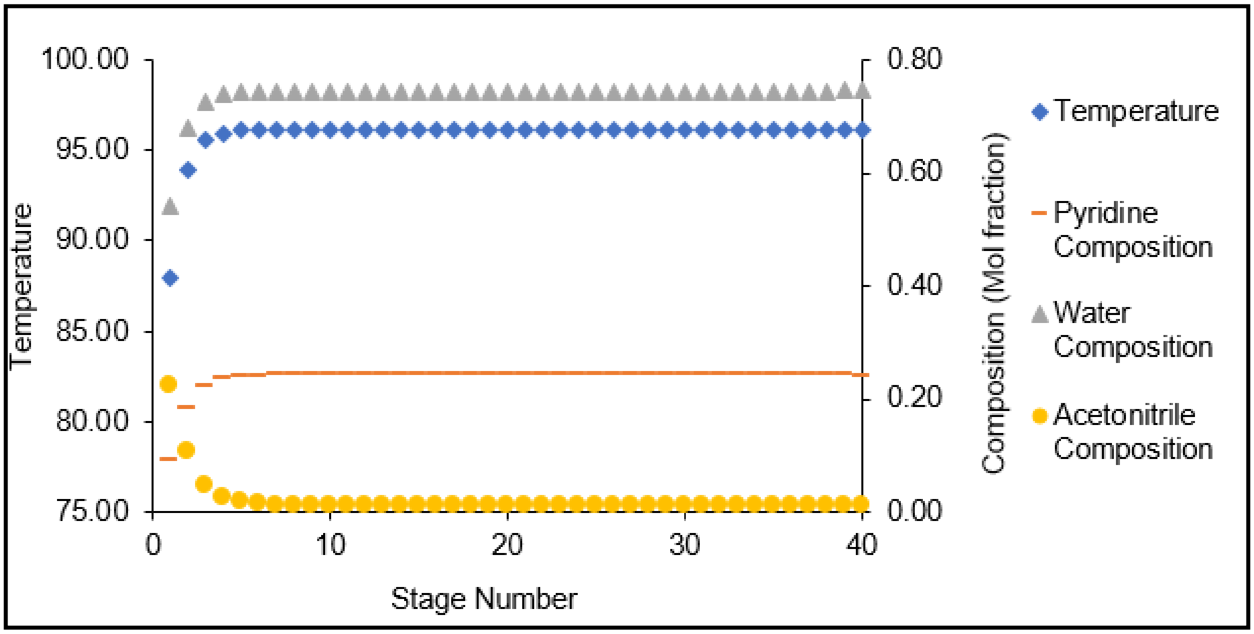

Figure 4.22. Pyridine and water composition profiles and temperature profile in the second absorber

The minimum temperature in the second absorber is 88˚C and the maximum is 97˚C; this is because the streams feeding the second absorber (one from stripper and the other from the rectifier) enter at these temperatures respectively, and since the absorber has no condenser or reboiler, heat exchange can only be within the two ranges. The temperature increases with increasing number of stages up to the sixth stage (Figure 4.22). At this point, it is noteworthy that the stages are numbered from top to bottom. As shown in Figure 4.22 acetonitrile composition decreases with increasing number of stages and hence temperature; at around the fifth stage the composition of acetonitrile approaches zero. This is because at the fifth stage temperature is over 95˚C and this is beyond the acetonitrile boiling point. Furthermore, the water and pyridine compositions start to stabilize around the fifth stage at 75mol% and 25mol% respectively.

The increase in number of stages and doesn’t seem to affect these compositions. This is because these compositions represent azeotropic point between the two components. Since the primary aim was to recover this azeotrope, the knowledge of the stage at which these compositions are reached helps with the decision of where to withdraw the middle product. In this column, other light components such acetone and

MEK are present but are not depicted in Figure 4.22, all the light fractions are represented by acetonitrile since they exhibit similar trends. This is also shown by the fact that as the number of stages increase the mole fractions of water and pyridine summation approaches 1 showing that that they are the only components left. The fact that stabilizations of almost all components occur at the fifth stage does no warrant reducing the number of stages of the column since in reality the second absorber along with the first represent the middle section therefore the number of stages which is directly related to the height must be equal. Stripper profiles are depicted in Figure 4.23.

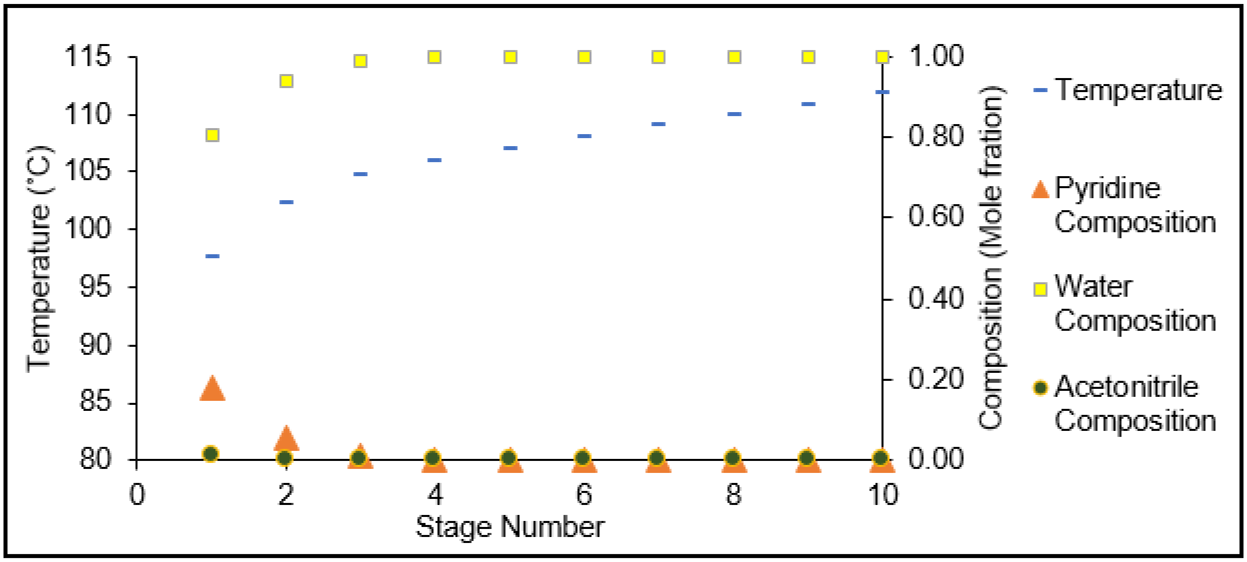

Figure 4.23. Stripper profiles

The theory behind the operation of the Dividing Wall Column suggests that all the light components are entrained upwards and recovered as the distillate while the mid-boiling component is entrained both upwards and downwards with the light and heavy components respectively. The composition profiles in the stripper (bottom section) support this notion as the only light component present in this part of the column is acetonitrile at less than 1mol% composition (Figure 4.23). In the top section of the column, pyridine and water composition sum up to 1 with acetonitrile being negligible; in stage 1, pyridine composition is about 20mol% and that of water is 80mol%. From the 4th stage the composition of water stabilizes at 100mol% while pyridine composition goes to 0. As the heavy component, water is recovered in its pure form from the bottom of this column. The profiles found in the rectifier column (top part of the DWC) are illustrated in Figure 4.24.

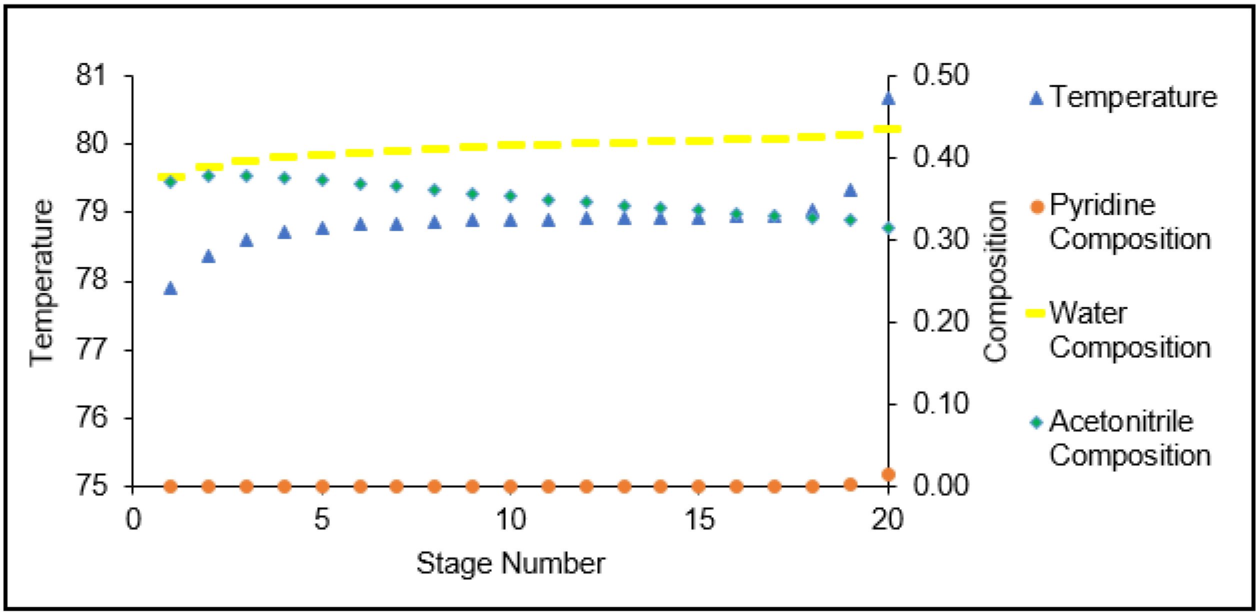

Figure 4.24. Rectifier Profiles

Figure 4.24 shows that light fractions dominate the top section of the rectifier. This is expected since it is where they are recovered as a distillate. Pyridine-water azeotrope was evidently entrained upwards and downwards as pyridine trace amount can be seen on the 20th stage of the rectifier where the combination of the distillates from absorbers is fed. Pyridine composition is small because it is the pyridine-water azeotrope that is entrained and not pyridine alone and even in the azeotrope the pyridine composition is still low at 25mol%.

4.4. Results Implications

Figure 4.25 depicts the overall material balance around the Dividing Wall Column (detailed material balance presented in Appendix C.3-C.6). The intermediate product (water-pyridine azeotrope) is almost pure at 24.7mol% pyridine 74.7mol% water, as it is closer to the water-pyridine azeotrope (75mol% water and 25mol% pyridine) than the composition achieved by the original design (23.6mol% pyridine and 75.5mol% water with the difference being acetonitrile).

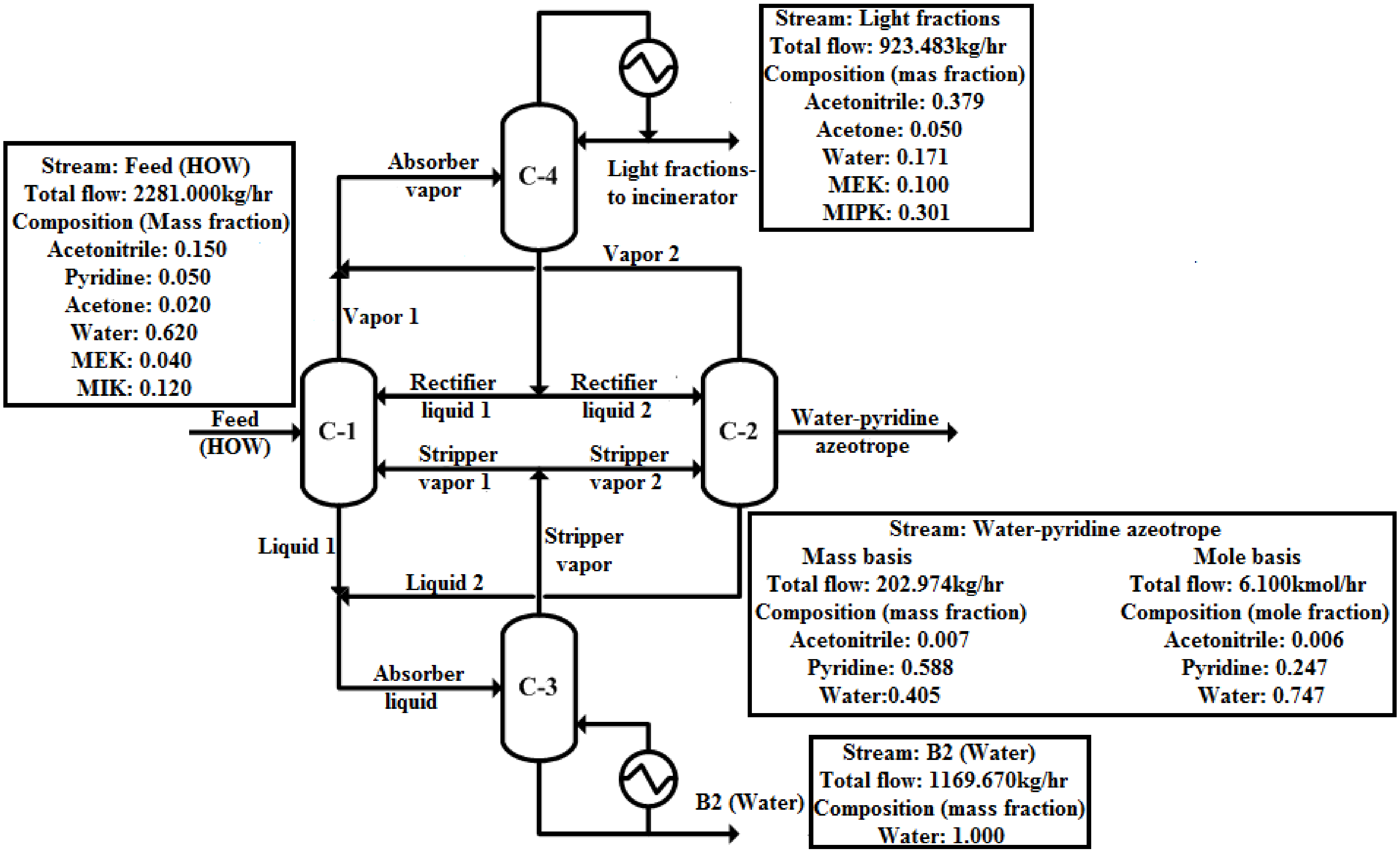

Figure 4.25. Overall material balance of the Dividing Wall Colum

Liquid-liquid Extraction Unit plus Regeneration Column Overall Balance

The summary of the material balance around the extraction unit and the regeneration column is given in Figure 4.26.

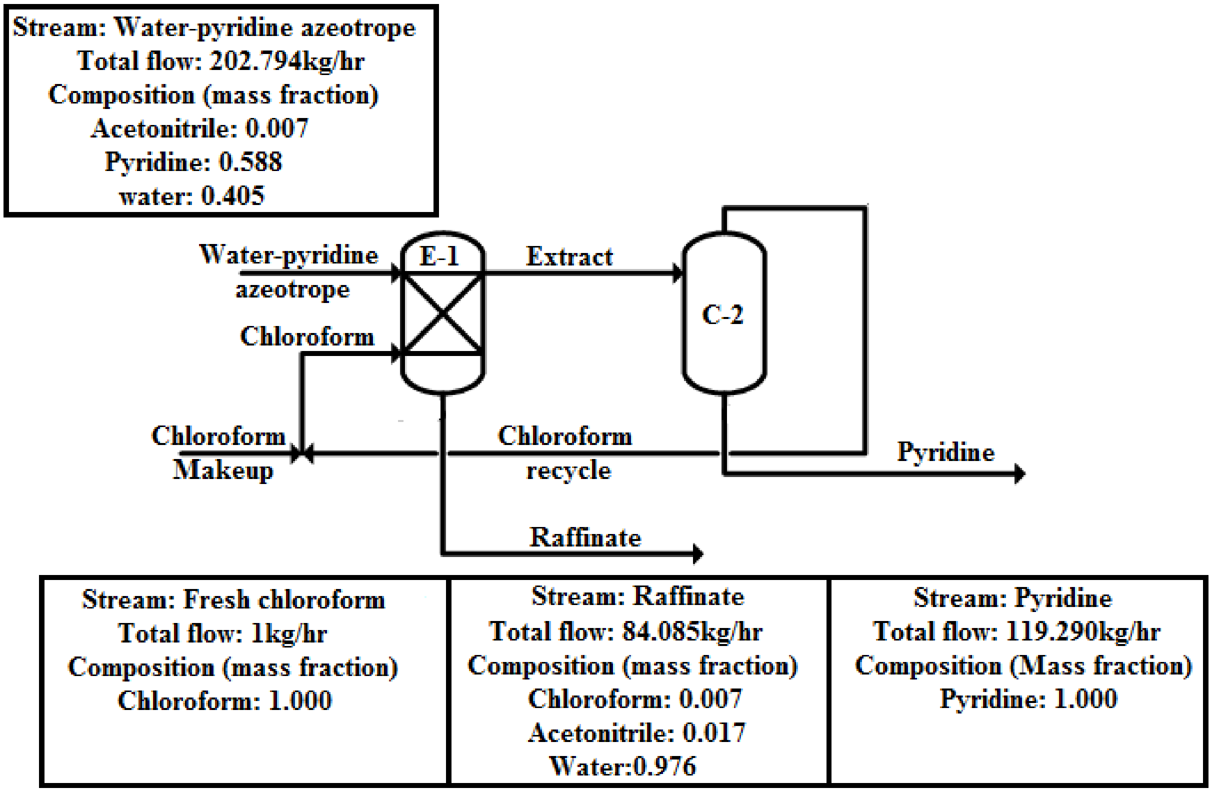

Figure 4.26. Overall Material balance around the liquid-liquid extraction and regeneration column

The comparison of Dividing Wall column and the original two-column design is summarized in Table 4.5. As mentioned in Chapter 3, the acetonitrile present in the bottoms stream of the distillation column (C-1) was the main impurity in the pyridine stream from the regeneration column. The implementation of DWC has reduced the acetonitrile impurity in the water-pyridine azeotrope stream by around 36mol% (from 0.055kmol/hr to 0.036kmol/hr). This made an enormous difference in the purity of pyridine recovered; the purity has increased from 98mass% to over 99mass% matching closely the industry specification of pyridine. These results agree with what has been reported in the open literature that the DWC technique has the potential to enhance the purity of products [64]. Although the original design does not recover all the pyridine, the loss to the light fraction stream is extremely small (about 5kg/year), however, the DWC system has 100% pyridine recovery. Results also show that the application of the DWC technique reduces the condenser and reboiler heat duties by 10% and 9% respectively (Table 4.5). This reduction in the reboiler and condenser duties is lower than the ones that have been reported in the open literature. Between 20 and 40% reduction in energy consumption have been reported by many authors [10-12].

Table 4.5. Comparison between the original two-column system and DWC the system

Parameter	**Original two-column System**	**Dividing Wall Column System**
Chloroform Makeup Flowrate (kg/hr)	1.000	1.000
Total Condenser Heat Duty (kW)	-1909.279	-1719.600 (-9.935%)
Total Reboiler Heat duty (kW)	2076.19	1885.000 (-9.209%)
Pyridine Purity (mass%)	97.72	99.957
Pyridine Recovery (%)	99.997	100

4.5. Conclusions

The objective in this chapter was to use DWC process integration technique to integrate the first two 2 distillation columns in the previously proposed recovery process using the principle of Dividing Wall Column. This was done to improve energy utilization. The more realistic four-column model was used to model the Petlyuk column equivalent of the DWC. Some of the convergence errors that are usually encountered in simulation of the DWC were overcome using mixers to reduce the number of recycle streams feeding onto the rectifier and the stripper. It was found that the implementation of DWC reduced both the reboiler and condenser by 10% each. This energy was relatively lower than 30% that has been reported in the open literature. However, the reduction in capital and other operational costs such as control costs justify the implementation of the technique.

Moreover, DWC implementation improved the purity of the recovered pyridine from 97mass% to over 99.9mass% matching industry specifications for reusable pyridine.

References

[1] M. T. D. Nguyen, “Conceptual Design, Simulation and Experimental Validation of Divided Wall Column: Application for Nonreactive and Reactive Mixture,” Toulouse Institute of Technology, 2015.

[2] S. Becht, R. Franke, A. Geißelmann, and H. Hahn, “An industrial view of process intensification,” *Chem. Eng. Process. Process Intensif.*, vol. 48, no. 1, pp. 329–332, Jan. 2009.

[3] K. Khushalani, A. Maheshwari, and N. Jain, “Separation of mixture by divided wall column using Aspen Plus,” *Int. J. Emerg. Technol. Adv. Eng.*, vol. 4, no. 8, pp. 563–571, 2014.

[4] M. A. Schultz, D. G. Stewart, J. M. Harris, S. P. Rosenblum, M. S. Shakur, and D. E. O’Brien, “Reduce costs with dividing-wall columns,” *Chem. Eng. Prog.*, vol. 98, no. 5, pp. 64–71, 2002.

[5] I. Dejanović, L. Matijašević, and Ž. Olujić, “Dividing wall column-A breakthrough towards sustainable distilling,” *Chem. Eng. Process. Process Intensif.*, vol. 49, no. 6, pp. 559–580, 2010.

[6] V. K. Sangal, V. Kumar, and I. M. Mishra, “Optimization of a Divided Wall Column for the Separation of C4-C6 Normal Paraffin Mixture using Box-Behken design,” *Chem. Ind. Chem. Eng. Q.*, vol. 19, no. 1, pp. 107–119, 2013.

[7] C. Bravo-Bravo, J. G. Segovia-Hernández, C. Gutiérrez-Antonio, A. L. Durán, A. Bonilla-Petriciolet, and A. Briones-Ramírez, “Extractive dividing wall column: design and optimization,” *Ind. Eng. Chem. Res.*, vol. 49, no. 8, pp. 3672–3688, 2010.

[8] R. K. Dohare, K. Singh, and R. Kumar, “Modeling and model predictive control of dividing wall column for separation of Benzene–Toluene- *o* -Xylene,” *Syst. Sci. Control Eng.*, vol. 3, no. 1, pp. 142–153, 2015.

[9] M. Illner and M. R. bin O. Othman, “Modeling and simulation of a dividing wall column for fractionation of fatty acid in oleochemical industries,” *Iran. J. Chem.*

Eng., vol. 12, no. 1, pp. 60–67, 2015.

[10] A. A. Kiss and R. R. Rewagad, “Energy efficient control of a BTX dividing-wall column,” *Comput. Chem. Eng.*, vol. 35, no. 12, pp. 2896–2904, 2011.

[11] Y. C. Wu, H. Lee, H. Huang, and I. Chien, “Energy-Saving Dividing-Wall Column Design and control for Heterogeneous Azeotropic Distillation Systems Energy-Saving Dividing-Wall Column Design and Control for Heterogeneous Azeotropic Distillation Systems,” 2014.

[12] Ö. Yildirim, A. A. Kiss, and E. Y. Kenig, “Dividing wall columns in chemical process industry: A review on current activities,” *Sep. Purif. Technol.*, vol. 80, no. 3, pp. 403–417, 2011.

[13] W. L. Luyben and I.-L. Chien, *Design and control of distillation systems for separating azeotropes*, vol. 53, no. 9. 2013.

[14] Y. C. Wu and I. L. Chien, “Design and control of heterogeneous azeotropic column system for the separation of pyridine and water,” *Ind. Eng. Chem. Res.*, vol. 48, no. 23, pp. 10564–10576, 2009.

[15] P. Prayoonyong, “Conceptual design of heterogeneous azeotropic distillation process for ethanol dehydration using 1-butanol as entrainer,” *Maejo Int. J. Sci. Technol.*, vol. 8, no. 3, pp. 334–347, 2014.

Chapter 5 : Entropy Generation Analysis of the Regeneration Column

After the pre-concentration section (C-1 and C-2) of the process proposed in **Chapter 3** (Figure 5.1)**,** the regeneration unit (C-3) is likely to be the most energy intensive part of the process. In Chapter 4, energy integration using DWC was implemented on the pre-concentration section to abate energy consumption. Therefore, in this chapter, a method of entropy generation analysis across a distillation column proposed by Benyounes et al. [1] was adopted to determine if the separation efficiency in Column (C-3) was within acceptable range. If not, to establish if there were an area that warranted improvement.

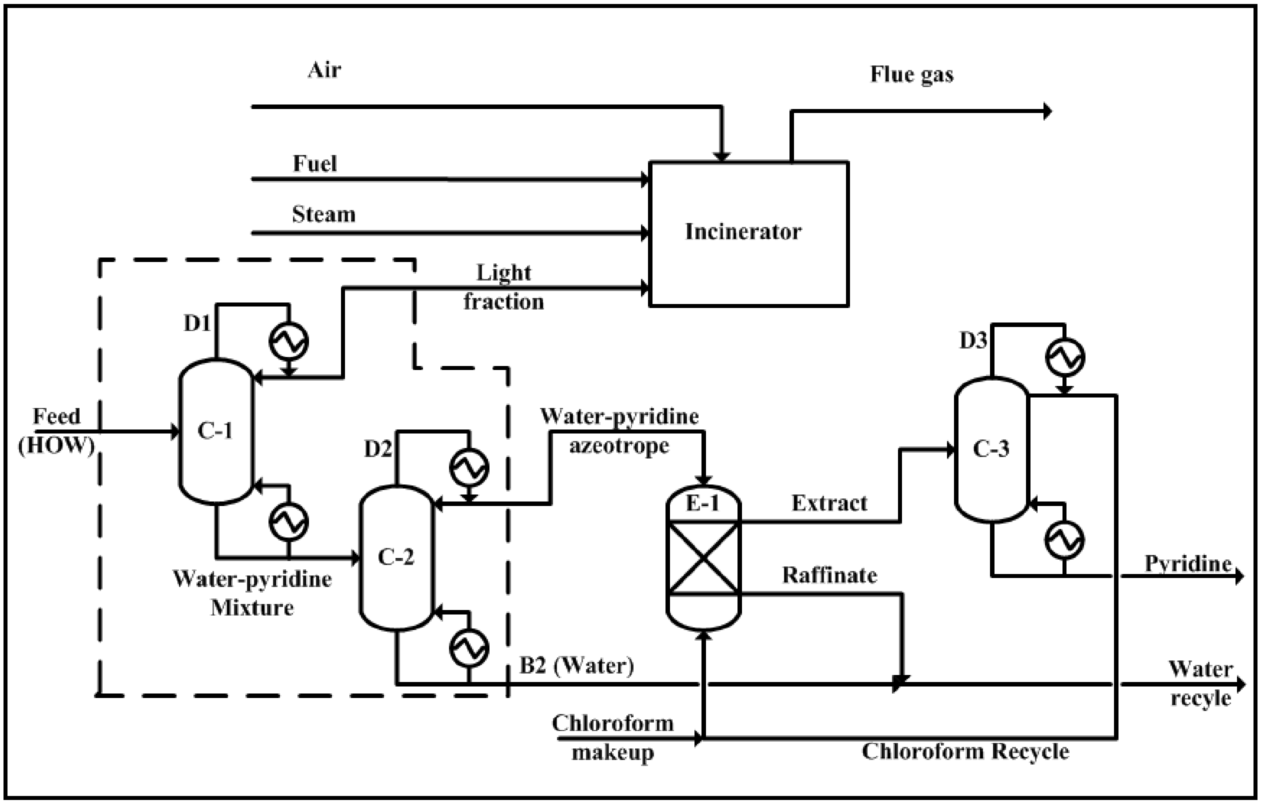

Figure 5.1. Proposed pyridine recovery process

5.1. Introduction

Traditionally, overall energy consumption of separation processes is used to determine the efficiency of separation. However, in recent years an innovative approach to evaluate efficiencies of separation processes which uses the thermodynamic second law has been proposed. The main advantage of the thermodynamic second law analysis over the first law is that the latter approach follows a section by section energy analysis of the distillation column. There are 2 ways to make a thermodynamic second law analysis; one is entropy generation and the other is exergy destruction. Exergy destruction is equivalent to entropy generation. Exergy is the maximum amount of work obtainable from a reversible process given by equation (5.1) [2]. The exergy lost due to distillation can be determined by doing an exergy balance around the column (equation (5.2)).

$$E = (H - H_0) - T_0(S - S_0) \qquad (5.1)$$

Where:

E: Exergy

H_0: Enthalpy at standard state (298.15K, 1 atm)

T_0: Standard state temperature

S: Entropy

S_0: Entropy at standard state

$$\dot{E}_{loss} = L_{j-1}E_{j-1}^{L} + V_{j+1}E_{j+1}^{V} + F_jE_j^{F} - V_jE_j^{F} - S_jE_j^{V} - \dot{E}_j \qquad (5.2)$$

Where:

j: stage number

$\dot{E}$: Rate of exergy

L: Liquid flowrate

E^L: Exergy of the liquid stream

E^V: Exergy of the vapor stream

In this chapter, entropy generation analysis as proposed by Benyounes et al. [1] is made on the regeneration column (C-3). This approach is discussed and applied in the subsequent sections. Like with the exergy analysis, the entropy generation analysis is made on the trays, reboiler and condenser independently [1]. This way, it is possible to determine the area of greater inefficiency and suitable modifications can be made to improve the performance of the distillation column [3].

5.2. Entropy Generation Analysis

Assumptions:

1. The column is operated adiabatically;
2. All the heat is provided by the reboiler;
3. All the cooling is provided by the condenser.

The entropy of the liquid and vapor stream on the j^th stage is given by equation (5.3) and (5.4) respectively. The number of stages are calculated from the top to bottom.

$$S_j^L = L_j \left[\sum \left(x_{ij} (S_i^{OL} + C_{Pi}^L ln \left(\frac{T_j}{T_0} \right) \right) - R \sum x_{ij} ln(\gamma_{xij} x_{ij}) \right] \tag{5.3}$$

$$S_j^V = V_j \left[\sum y_{ij} \left(S_i^{0V} + C_{Pi}^V ln \left(\frac{T_j}{T_0} \right) \right) + R ln \left(\frac{P_i^0}{P_T} \right) - R \sum y_{ij} ln \left(y_{ij} \frac{P_T}{P_0} \right) \right] \tag{5.4}$$

Where:

S_j^L: Entropy of the liquid stream of the j^th stage

S_j^V: Entropy of the vapor stream of the j^th stage.

L_j: Liquid stream flowrate from the j^th stage

V_j: Vapor stream flowrate from the jth stage

x_{ij}: Mole fraction component i in the liquid phase from the jth stage

y_{ij}: Mole fraction component i in the vapor phase from the jth stage

S_i^{OL}: Entropy of a pure component i at standard state (298.15K, 1 atm)

S_i^{0V}: Entropy of a pure component i at standard state

C_{Pi}^{L}: Specific heat capacity of liquid component i

γ_{xij}: Liquid activity coefficient of component i

T_j: Temperature in the jth stage

T_0: Standard state temperature (298.15K)

R: Gas constant (8.314Kj/Kmol-K)

P_i^0: Partial pressure of component i at standard state.

P_T: Vapor pressure of the vapor stream at the stage temperature.

P_0: Standard state pressure

In this work, the stage-wise vapor and liquid entropy were obtained from Aspen Plus. The entropy values for the first 6 stages are depicted in Table 5.1, the rest of the entropy values can be found in Appendix F, Table F.1.

Table 5.1. Entropy values from Aspen Plus

Stage	liquid stream Entropy (kJ/kmol-K)	Vapor stream Entropy (KJ/kmol-K)
1	-42.678	0.000
2	-45.904	-19.258
3	-45.944	-22.22
4	-45.889	-22.498
5	-45.904	-22.453
6	-46.79	-22.353

The entropy of streams exiting the jth stage was calculated using equation (5.5) and equation (5.6) was used to calculate the entropy of streams entering the jth stage. The entropy production within each stage was determined using equation (5.7) to be 23.486kW/K. The entropy production in each stage data is depicted in Appendix F, Table F.2.

$$S_{out,j} = S_{separation} = S_j^V + S_j^V \tag{5.5}$$

$$S_{in,j} = S_{mix,j} = S_{j-1}^L + S_{j+1}^V \tag{5.6}$$

$$\Delta S_j = S_{separation} - S_{mix,j} \tag{5.7}$$

$$\Delta S_{trays} = \sum \Delta S_j \tag{5.8}$$

Entropy production in the reboiler was determined using equation (5.9) and data depicted in Table 5.2 to be 525.755kW/K. Vapor and liquid stream flowrates from each tray were extracted from Aspen Plus (depicted in Appendix F, Table F.2).

$$\Delta S_B = V_B S_B^V + W S_B^L - L_n S_n^L - \frac{Q_B}{T_B} \tag{5.9}$$

Where:

$\varDelta S_B$: Entropy generation in the reboiler.

V_B: Vapor flowrate from the reboiler

W: Bottoms flowrate

L_n: Liquid stream flowrate from the last stage of the column

S_n^L: Entropy of the liquid stream from the last stage

Q_B: Reboiler heat duty

T_B: Reboiler temperature.

Using equation (5.10), the entropy production within the condenser was found to be 35.105kW/K. The result from the entropy generation analysis of the distillation column stages, reboiler and condenser are summarized in Table 5.2. Lost work which is proportional to energy inefficiency can then be calculated for each section using equation (5.11) [1].

$$\varDelta S_C = V_1\,(S_C^L - S_1^V) + \frac{Q_C}{T_C} \tag{5.10}$$

$$LW = T_0 \varDelta S_{column\ section} \tag{5.11}$$

Where:

$\varDelta S_C$: Entropy generation in the condenser

V_1: Vapor flowrate from stage 1

S_C^L: Entropy of the liquid stream from the condenser

S_1^V: Entropy of vapor from stage 1

Q_C: Condenser duty

T_C: Condenser temperature

LW: Lost Work

$\Delta S_{column\ section}$: Refers to entropy generation in any section of the column (trays, condenser or reboiler)

Table 5.2. Summary of the parameters in the regeneration column (C-3)

Parameter	Reboiler	Condenser	Column Trays	Total
Q (kW)	80.911	82.042	-	162.953
T(K)	378.187	315.226	-	-
ΔS (kW/K)	525.755	35.105	23.486	584.347
Lost work (LW)	156675.070	10461.227	6998.969	174135.266

Minimum work can be calculated from equation (5.12). The calculated minimum work in this work was 8044.870kW. The data required for the calculation can be found in Appendix F, Table F.3.

$$W_{min,T_0} = RT_0 \left[F \sum \left(x_{iF} ln(\gamma_{iF} x_{iF})\right) - D \sum x_{iD} ln(\gamma_{iD} x_{iD}) - W \sum x_{iW} ln(\gamma_{iW} x_{iW})\right] \quad (5.12)$$

Finally, thermodynamic second law efficiency was calculated as 4.62% from equation (5.13).

$$\eta = \frac{W_{min,T_0}}{W_{min,T_0} + LW} \quad (5.13)$$

5.3. Results Discussion and Recommendations

Results show that the reboiler is the main source of entropy generation contributing 90% to the total entropy produced and the trays produce the lowest entropy (Table 5.2). Therefore, the inefficiency of the regeneration column is largely due to the reboiler. This coincides with observations reported by Benyounes et al. [1]. The calculated efficiency for the regeneration column (4.6%) was within the anticipated range of second law thermodynamic efficiencies (5-20%) of distillation columns [3]. Kim [2] obtained a second law efficiency of 5.8% for the separation of toluene and upon implementation of double effect distillation system, Kim [2] was able to improve the second law efficiency from 5.8% to 24.3% which was a major improvement (Figure 5.2).

The double effect is a distillation heat integration technique in which a reboiler of one distillation column is paired with a condenser of another column within the process. Therefore, we recommend the assessment of a similar technique to integrate the heat between the condenser of the proposed Dividing Wall Column (DWC) and the reboiler of the regeneration column. One way in which this could be achieved is through the application of the pinch technology. It is anticipated that the implementation of such a system would result in improved efficiency since the entropy generation analysis showed that the reboiler is the main source of inefficiency, followed by the condenser in the regeneration column. The entropy generation analysis is indeed a better alternative to analyze thermodynamic efficiency since the analysis is done by section and shows the areas of greater inefficiency. The knowledge of the areas of greater inefficiencies is valuable for the purpose of proposition solutions to improving energy usage within the column; for instance, in the current work, the implementation of diabatic distillation in which there is heat exchange within trays to optimize energy usage would have insignificant impact on the overall efficiency because the main source of inefficiency is the reboiler followed by the condenser.

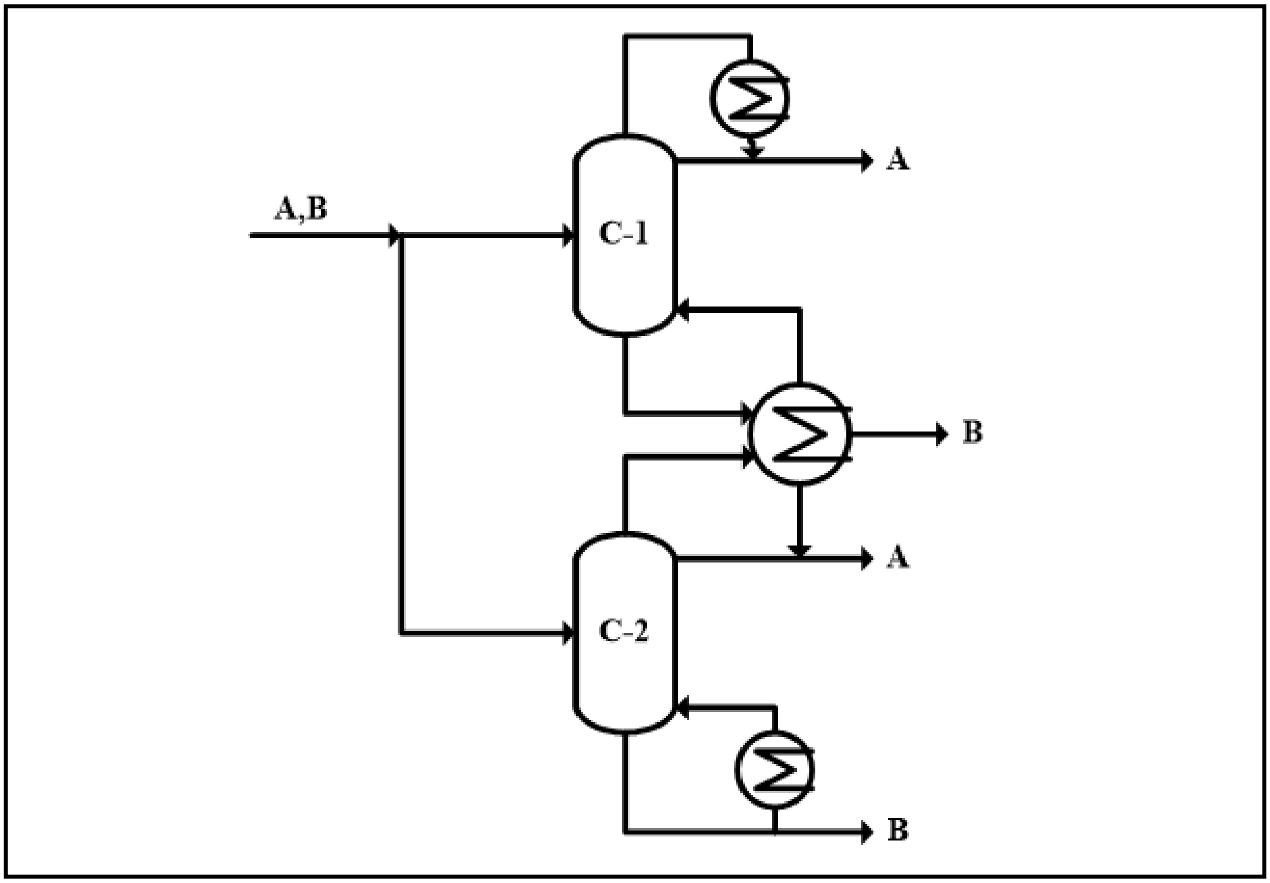

Figure 5.2. Double effect distillation system [2]

5.4. Conclusions

In this chapter we aimed to do an entropy generation analysis on the regeneration column. This was done to locate the area of greater inefficiency an explore possible ways to improve energy utilization in the column. The column was found to have a thermodynamic second law efficiency of 4.6%, which is typical of a distillation column according to the open literature. It was established that the reboiler was a major contributor of entropy generation, i.e. about 90% of lost work is due to the reboiler. Tray by tray separation was found to be the least contributor to entropy generation of the column. As a result, it is recommended for future work to assess the heat integration between the DWC condenser and the regeneration column reboiler through a method of pinch technology.

References

[1] H. Benyounes, W. Shen, and V. Gerbaud, “Entropy Flow and Energy Efficiency Analysis of Extractive Distillation with a Heavy Entrainer,” *ACS*, pp. 4778–4791, 2014.

[2] Y. H. Kim, “Energy saving and thermodynamic efficiency of a double-effect distillation column using internal heat integration,” *Korean J. Chem. Eng.*, vol. 29, pp. 1680–1687, 2012.

[3] G. De Koeijer and S. Kjelstrup, “Minimizing entropy production rate in binary tray distillation,” *Int. J. Thermodyn.*, vol. 3, pp. 105–110, 2000.

Chapter 6 : Incineration Evaluation and Process Economics

Currently the HOW stream is incinerated without energy recovery. In this chapter we present a simplified incinerator model from Aspen Plus. Two options are considered and compared: incineration of all the HOW stream as is currently practiced at Sasol versus the incineration of only the light fractions from the pre-concentration section (D1) as shown in our proposed process (Figure 6.1). Heat recovery in the form of steam generation is assessed for both options. Furthermore, economic evaluation of the proposed process is made to assess its economic performance. Economic evaluation was done using Aspen Plus economic analyzer. Since there was no reliable technique found in literature for the costing of the Diving Wall Column (DWC), the economic evaluation was done on the process proposed in **Chapter 3** (Figure 6.1) and it is expected that the economic performance will be improved by the implementation of DWC proposed in **Chapter 4.**

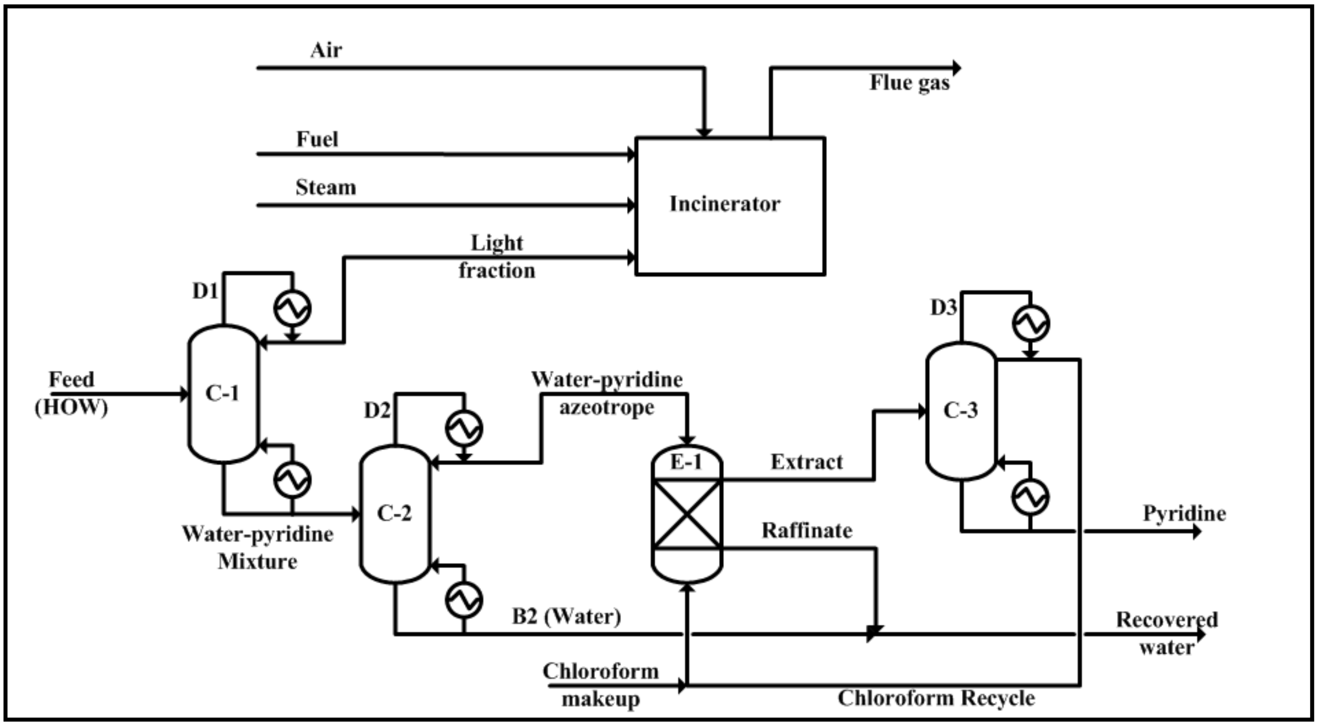

Figure 6.1. The proposed pyridine recovery process

6.1. Introduction

Incineration is a combustive thermal waste treatment technique. It is mostly used to minimize landfilling of waste; it is recorded that this technique can reduce the solid waste by up to 90%. On the other hand, there has been compelling arguments against incineration and related thermal waste treatment techniques i.e. the harmful gases emissions [1]. Although modern incinerators can be operated with emissions control devices, most operators may be unwilling to fit them because of the additional capital and operational costs [1]. Zero waste production lobbyists have argued that thermal treatment techniques act as barriers to the objective of waste minimization through valuable resources recycling and as a result, stands in the way of economic growth [2,,3]. Connett [3] argued recycling and reusing of waste components uses 4 times less energy than incineration. Nonetheless, it is only fair to acknowledge that zero waste may not be feasible and there would always be residual even after intensive recycling; consequently, incineration of waste may be inevitable to a certain extent. Also, there are instances whereby the incineration of waste may be more beneficial than recycling, one such example is the treatment of medical waste.

At Sasol the HOW stream is incinerated without energy recovery using 2 incinerator compartments (Figure 6.2). In this chapter, quantification of the incinerator impact was made and the energy recovery through steam generation was assessed. It is also proposed that the water recovered in the pyridine enrichment section be used for steam generation.

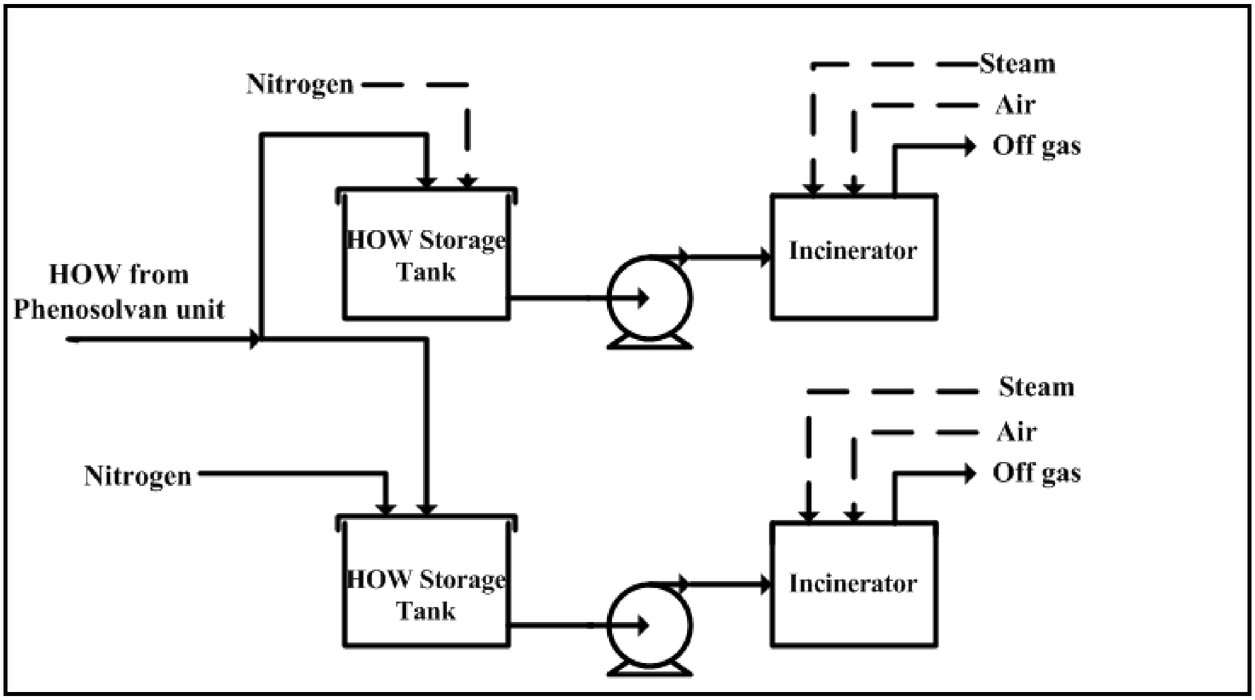

Figure 6.2. Schematic diagram of incineration unit as carried out by Sasol

6.2. Incineration of the whole HOW stream Versus Incineration of Light Fraction Only

6.2.1. Simulation of Incinerator Units on Aspen Plus

Assumptions:

- i. The incinerator is operated at 1300˚C and 1atm;
- ii. The HOW does not contain particulate matter;
- iii. The air composition is 79mol% nitrogen and 21mol% Oxygen;
- iv. The fuel added to keep the incinerator burning was not accounted for;
- v. The incineration model has only 1 compartment.

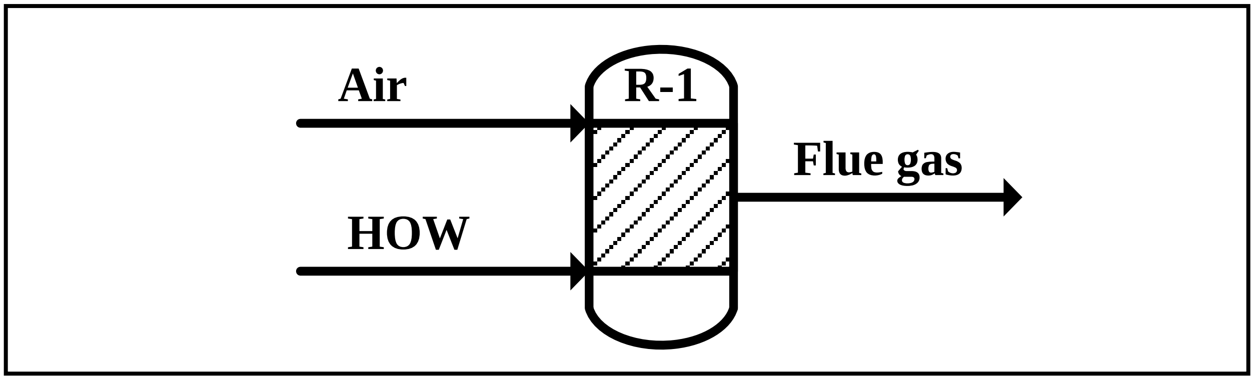

Figure 6.3. Simplified schematic diagram of the incineration unit (Status Quo)

A simplified incineration unit was modelled on Aspen Plus using an RGibbs reactor model on Aspen library. The use of RGibbs reactor for the combustion reaction taking place in an incinerator was proposed by Cimini et al. [4]. The setup of the simulation is depicted in Figure 6.3. The reactor was specified to operate at 1300ºC and 1.1 bar (Figure 6.4). This reactor model is mostly used when the kinetics of reactions are unknown or complex as is the case with kinetics of the combustion of the HOW stream. The RGibbs model uses Gibb's free energy minimization to predict possible products (Figure 6.5).

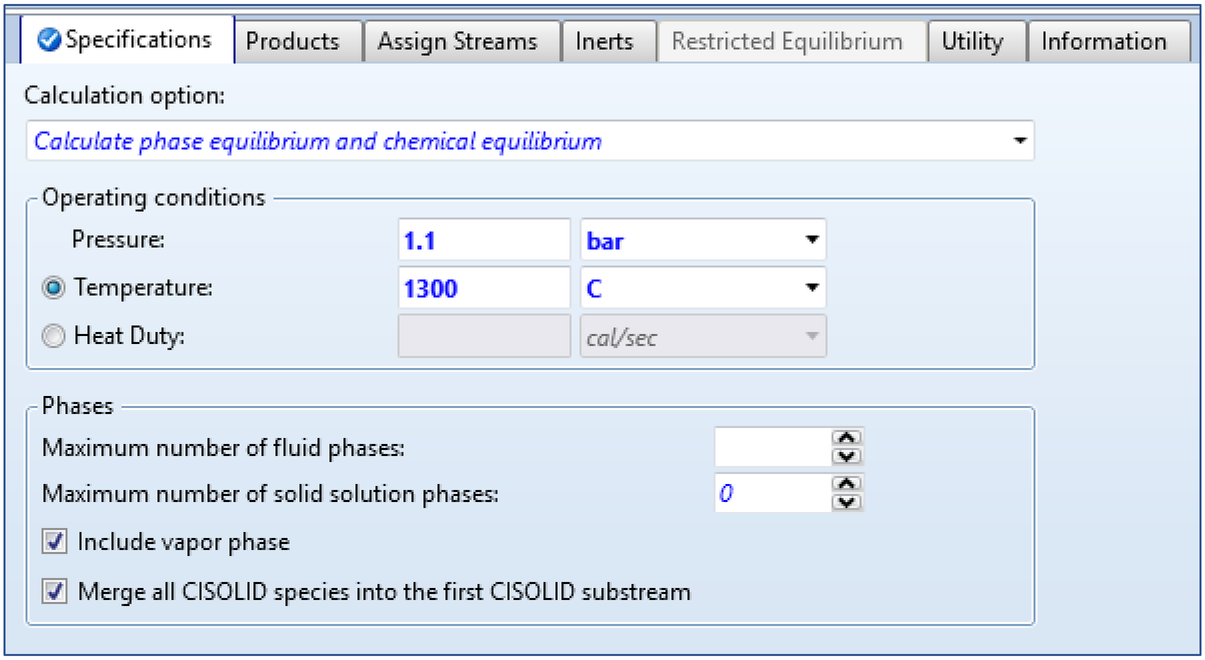

Calculation option:

Calculate phase equilibrium and chemical equilibrium

Operating conditions

Pressure: 1.1 bar

● Temperature: 1300 C

○ Heat Duty: *cal/sec*

Phases

Maximum number of fluid phases:

Maximum number of solid solution phases: *0*

☑ Include vapor phase

☑ Merge all CISOLID species into the first CISOLID substream

Figure 6.4. RGibbs reactor specifications

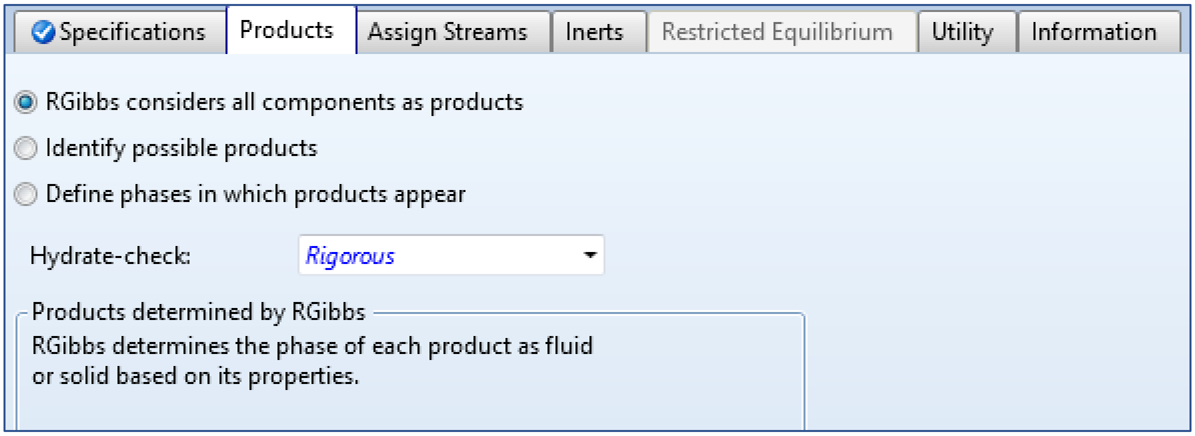

● RGibbs considers all components as products

○ Identify possible products

○ Define phases in which products appear

Hydrate-check: *Rigorous*

Products determined by RGibbs

RGibbs determines the phase of each product as fluid or solid based on its properties.

Figure 6.5. RGibbs reactor specifications continued

Option i. Incineration of all the HOW

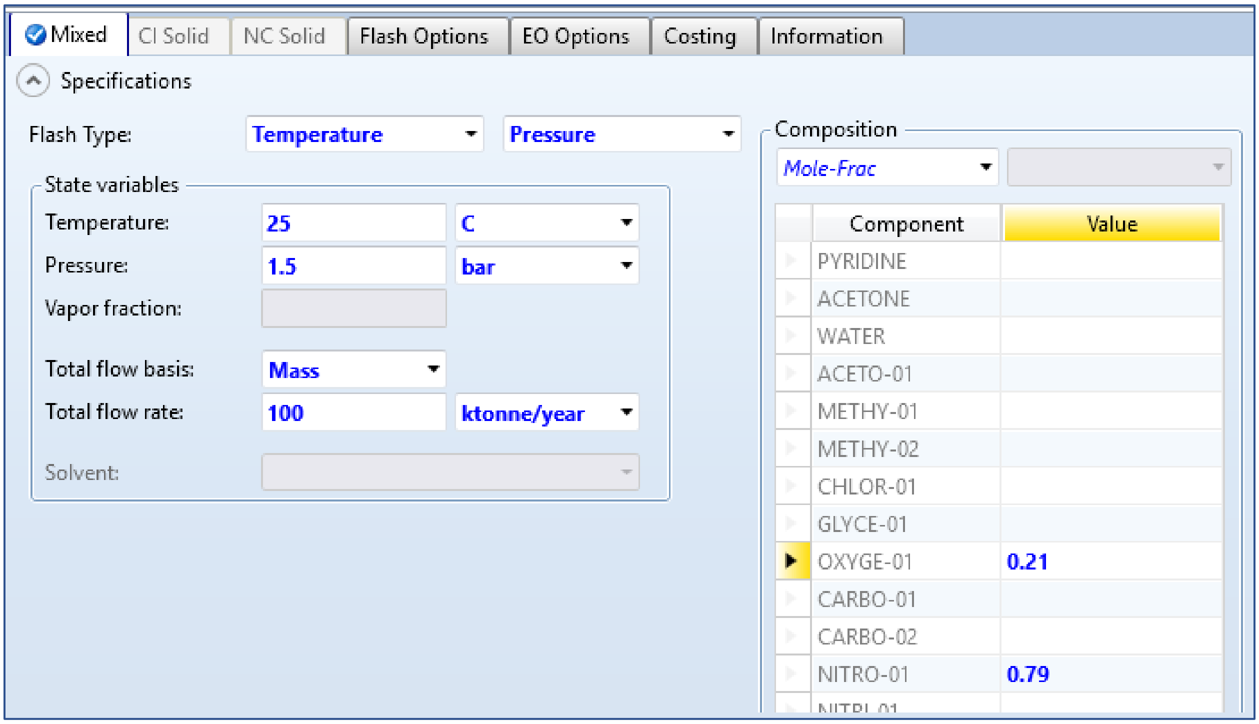

Flash Type: **Temperature** **Pressure**

State variables

Temperature: **25** **C**

Pressure: **1.5** **bar**

Vapor fraction:

Total flow basis: **Mass**

Total flow rate: **100** **ktonne/year**

Solvent:

Composition

Mole-Frac

Component	Value
PYRIDINE	
ACETONE	
WATER	
ACETO-01	
METHY-01	
METHY-02	
CHLOR-01	
GLYCE-01	
OXYGE-01	**0.21**
CARBO-01	
CARBO-02	
NITRO-01	**0.79**

Figure 6.6. Air stream specifications

The air stream flowrate was determined using trial and error approach via sensitivity analysis function on Aspen Plus. The objective of the sensitivity analysis was to determine the amount of air flowrate that favored the formation of CO2 over that of CO. While this required higher air flowrates, it was undesired to have unreacted oxygen in the flue gas stream. The first assumption of the air flowrate was 100kton/year (Figure 6.6). The results of this trial run are depicted in Table 2.1

Table 6.1. Incineration of all the HOW mass balance

Parameter	HOW	AIR	Flue gas
Total flowrate(kg/hr)	2281.542	11407.710	13689.250
Mass Fraction			
Methyl Isopropyl Ketone	0.290	0.000	0.000
Methyl Ethyl Ketone	0.081	0.000	0.000
Carbon monoxide	**0.000**	**0.000**	**0.148**
Carbon dioxide	**0.000**	**0.000**	**0.049**
Acetonitrile	0.173	0.000	0.000
Acetone	0.033	0.000	0.000
Pyridine	0.111	0.000	0.000
Nitrogen	0.000	0.767	0.652
Oxygen	0.000	0.233	0.000
Water	0.313	0.000	0.151

When the flowrate of the air stream was set at 100kton/year (11407.170kg/hr), all the oxygen was used up and more carbon monoxide (CO) than carbon dioxide (CO_2) was formed (Table 2.1)This meant that there was no oxygen left to convert the CO to CO_2, which is undesirable because carbon monoxide is more environmentally harmful than carbon dioxide. Therefore, sensitivity analysis was done to determine the flowrate that minimizes the CO formation and maximizes CO_2 formation, while also minimizing the oxygen flowrate in the emissions stream. The sensitivity analysis is depicted in Figure 6.7.

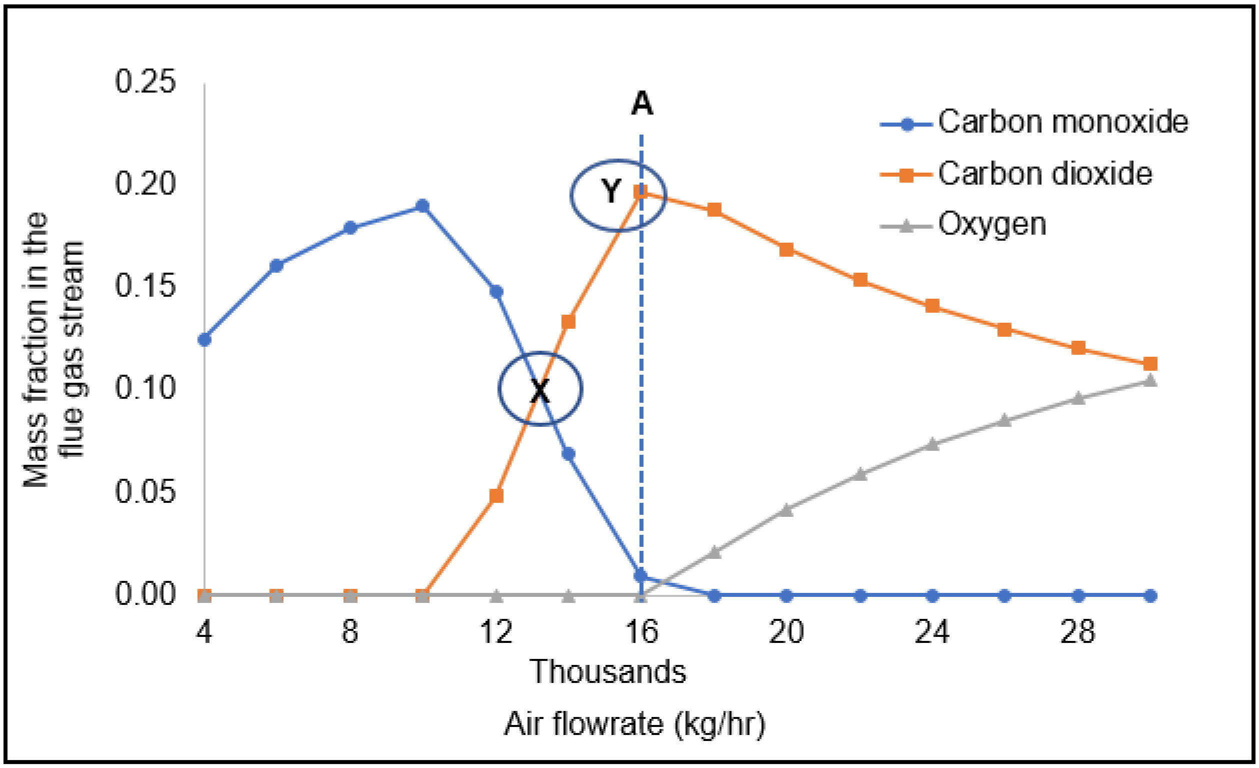

Figure 6.7. Sensitivity of O2, CO, and CO2 to air flowrate

Carbon monoxide formation increases with increasing air flowrate up to 10,000kg/hr then starts decreasing with a further increment in the air flowrate (Figure 6.7). The opposite trend is observed for CO_2 formation; CO_2 composition remains zero up to 10,000kg/hr, after which it increases rapidly with the increasing air flowrate, almost as fast as CO composition is decreasing (Figure 6.7). This is probably due to the conversion of CO to CO_2 beyond 10,000kg/hr air stream flowrate. At point **X** (around 13,000kg/hr) (Figure 6.7), CO composition is equal to CO_2 composition. Beyond **X**, CO_2 becomes more dominant than CO. The most desired phenomenon occurs at 16,000kg/hr (line **A**, Figure 6.7). 16,000kg/hr represents maximum dominance of CO_2 over CO. Beyond line **A,** CO composition reaches zero and CO_2 composition starts decreasing; this occurs at the expense of having unreacted oxygen in the emissions stream, which is undesirable. Therefore, 16,000kg/hr was used as the air flowrate. The corresponding mass balance is given in Table 6.2.

Table 6.2. Incineration of the whole HOW stream after implementation of sensitivity results

Parameter	**HOW**	**Air**	**Flue gas**
Total flowrate(kg/hr)	2281.542	16000.000	18281.540
Mass Fraction			
Methyl Isopropyl Ketone	0.290	0.000	0.000
Methyl Ethyl Ketone	0.081	0.000	0.000
Carbon monoxide	**0.000**	**0.000**	**0.009**
Carbon dioxide	**0.000**	**0.000**	**0.197**
Acetonitrile	0.173	0.000	0.000
Acetone	0.033	0.000	0.000
Pyridine	0.111	0.000	0.000
Nitrogen	0.000	0.767	0.681
Oxygen	0.000	0.233	0.000
Water	0.313	0.000	0.113

Feeding air at 16,000kg/hr results in the composition of CO and CO_2 in the flue gas stream being 0.9mass% and 19.7mass% respectively (Table 6.2). This corresponds to the anticipated composition as indicated by point **Y** in Figure 6.7. The CO_2 composition was equivalent to 86,558 tons/day and CO composition to 3,827tons/day.

Option ii. Incineration of the Light Fractions from Distillation Column (C-1)

Because the topology of the sensitivity analysis curves for the 2 options are similar (Figure 6.7 and Figure 6.8), a similar approach and reasoning to determine the air flowrate for the incineration of the whole HOW stream, was used to determine the ideal air flowrate for the incineration of the light fractions. The required airflow was determined to be 7420kg/hr (line **A** in Figure 6.8) for the incineration of the part of the HOW stream (light fractions). The resulting material balance is depicted in Table 6.3.

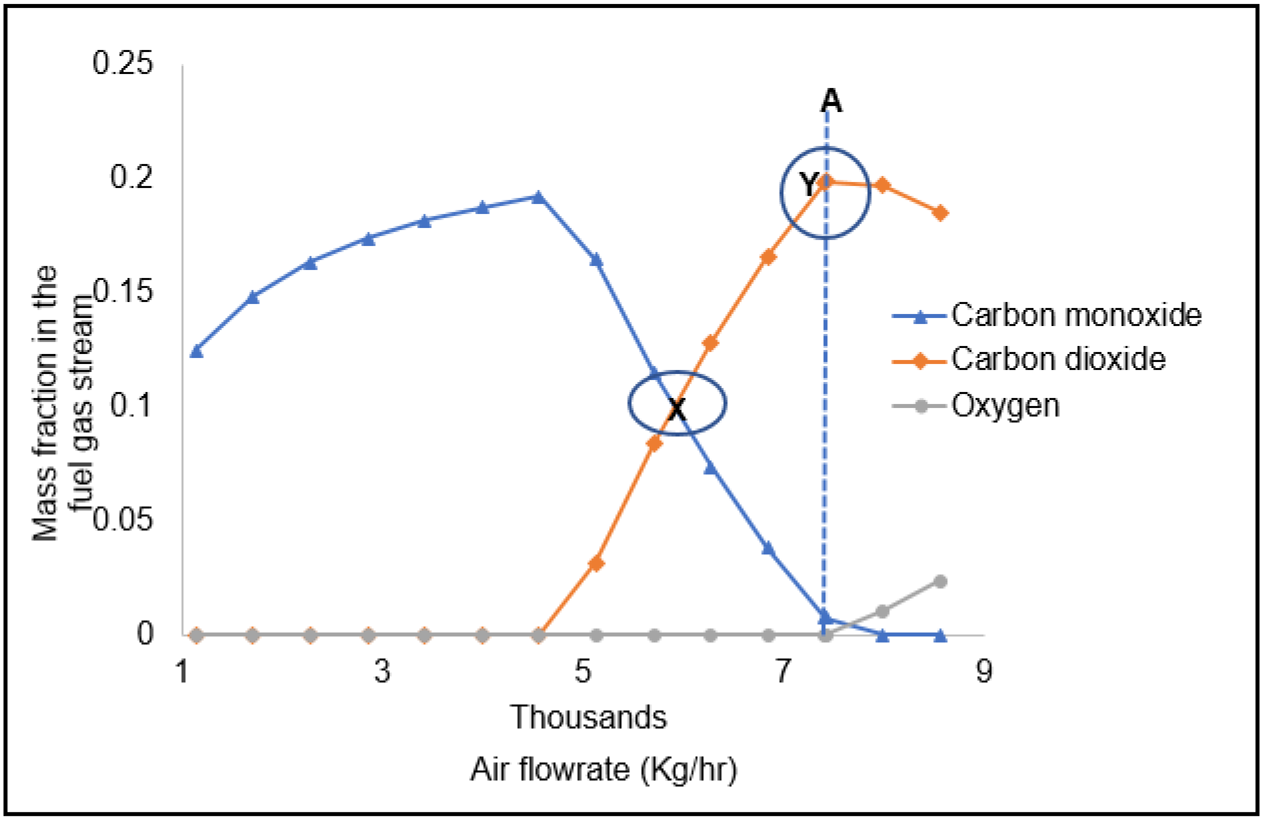

Figure 6.8. Sensitivity analysis to determine the ideal air flowrate

The CO_2 emissions flowrate from the incineration of light fractions from the proposed process (Figure 6.1) is reported by the simulation to be 39.755tons/day and the CO emissions 1.503tons/day. For both CO_2 and CO, the flowrates in the flue gas is over 2 times less than the values reported for the incineration of the whole HOW stream.

Table 6.3. Incineration of light fractions only mass balance

Parameter	**Light fraction**	**Air**	**Flue gas**
Total flowrate(kg/hr)	912.617	7420.000	8332.617
Mass Fraction			
Methyl Isopropyl Ketone	0.300	0.000	0.000
Methyl Ethyl Ketone	0.100	0.000	0.000
Carbon monoxide	**0.000**	**0.000**	**0.008**
Carbon dioxide	**0.000**	**0.000**	**0.199**
Acetonitrile	0.373	0.000	0.000
Acetone	0.050	0.000	0.000
Nitrogen	0.000	0.767	0.697
Oxygen	0.000	0.233	0.000
Water	0.177	0.000	0.097

6.2.2. Energy Recovery through Steam Production

The incinerator is operated at 1300ºC; therefore, the fuel gas is expected to exit the incinerator at the same temperature. Therefore, the flue gas can be used to produce superheated steam through heat exchange with the water. The steam can then be used for power generation and other steam requirements within the process. In the subsequent sections, the quantity of steam produced by each of the 2 options being considered in this chapter (incineration of all the HOW versus incineration of only the light fractions from the column C-1 (D1, in Figure 6.1). It is noteworthy that, the incineration of all the HOW will require external water source for steam generation purposes. On the other hand, in the proposed process, it is suggested that the water recovered in the pyridine enrichment section be recycled for steam generation (water recycle stream in Figure 6.9). This promotes water utilization efficiency in the plant which could align with some of the water efficiency strategies implemented in 2011 at the Sasol Secunda plant [5].

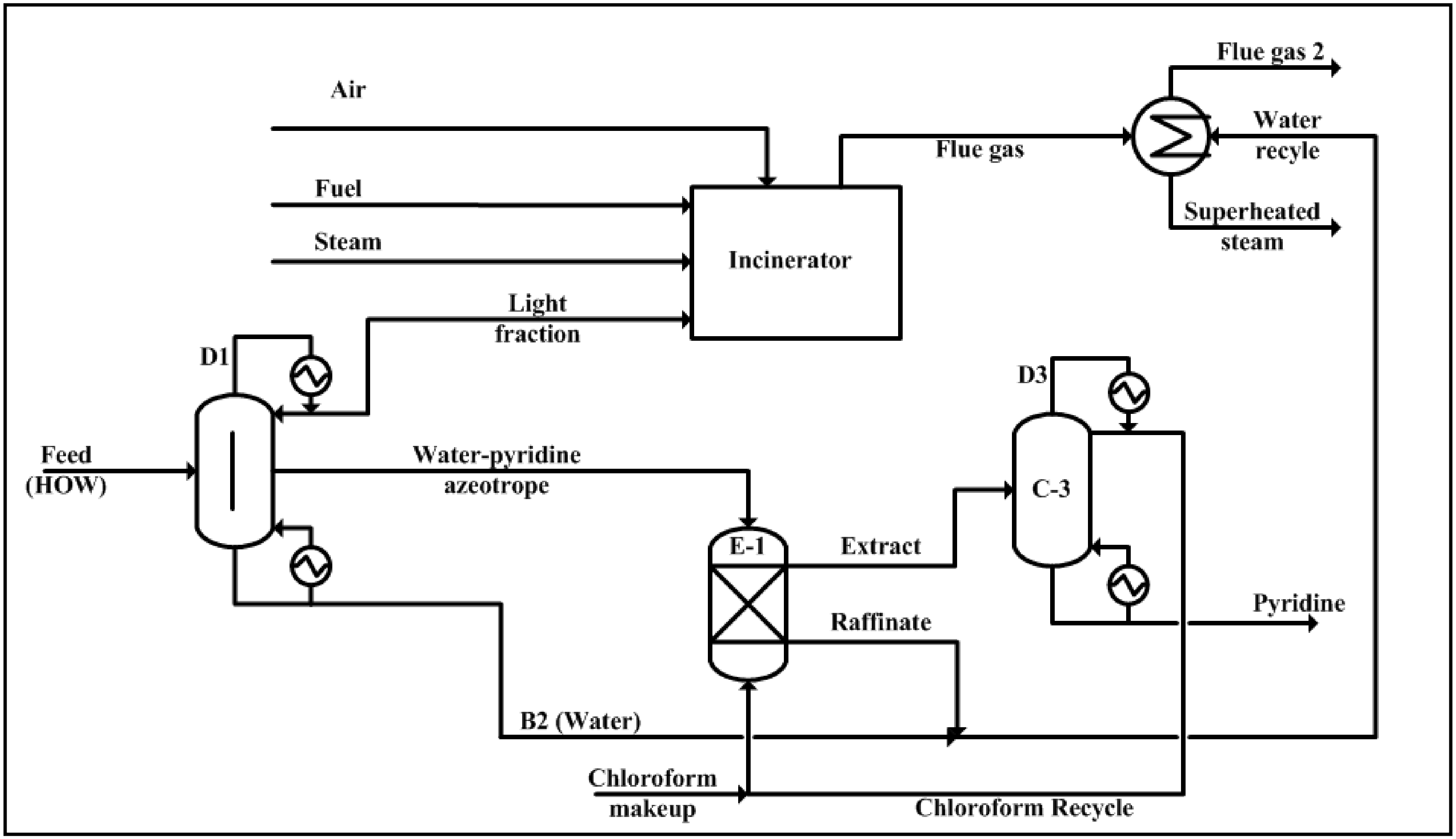

Figure 6.9. Proposed utilization of recovered water (B2 and Raffinate)

Estimation of the Steam Generation Capacity

In both the options, it was assumed that the superheated steam target temperature was 1200ºC (Figure 6.10) and heat recovery takes place in a simple heat exchanger. A shortcut, cross current heat exchanger model from Aspen Plus library was used for heat recovery assessment. If we also assume that all the heat flow (enthalpy) of the flue gas is consumed by the water stream to reach a temperature of 1200ºC, then the amount of water that can be superheated can be calculated using equation (6.1). According to equation (6.1), the water is first heated to the boiling point, then vaporization occurs and finally, the water vapor is heated from the boiling temperature of water to 1200ºC. It is assumed that the water is at 25ºC and that water boils at 100ºC. Data required for equation (6.1) is depicted in Table 6.4.

The enthalpy of the flue gas and heat capacity of the water were extracted from Aspen Plus. The mass flowrate to be determined from this calculation may not achievable in application due to heat transfer coefficients and other heat transfer limitations of the heat exchange device. Nevertheless, the calculation will provide good initial estimation which can then be adjusted through trial and error in simulation. The amount of water at 25ºC that could be converted to superheated steam at 1200ºC was found to be 6282.722kg/hr. However, from simulation the amount of water that could be converted to steam was 5800kg/hr. This gave a percentage relative error of 8% from the calculated value.

$$\dot{Q} = \dot{m}(C_{p,l}\Delta T_1 + \Delta H_V + C_{p,v}\Delta T_2) \tag{6.1}$$

Where:

$\dot{Q}$: Enthalpy flow of the flue gas;

ΔH_V: Heat of vaporization;

$\dot{m}$: Water mass flowrate;

$C_{p,l}$: liquid water heat capacity;

$C_{p,l}$: Water vapor steam capacity;

ΔT: Change in temperature of the water from the initial temperature to 1200ºC.

A similar approach was followed to determine the amount of recycled water from the pyridine enrichment section (Figure 6.9) using data in Table 6.4. The potential amount of water that could be superheated from the pyridine enrichment temperature (93ºC) to 1200ºC was calculated to be 2784.336kg/hr. On the other hand, the water recycle flowrate is 1253.189kg/hr; therefore, the recycled water cannot fully exploit the heat available from the flue gas. This was indicated by the fact that the flue gas exited the heat exchanger at over 700ºC, indicating that a lot of heat energy is still contained in the stream. For comparison sake, the flue gas from the incineration of the whole HOW stream exits the heat exchanger at 59ºC. There are 2 things that could be done to maximize heat recovery from the flue gas resulting from light fractions only incinerations: 1) supplement the recycled water with external source water before heat exchange with the flue gas or 2) use external source water to recover some of the energy from the flue gas after heat exchange with the recycled water.

Figure 6.10. Heat exchange

Table 6.4. Parameters required to calculate the amount of steam generation

Parameter	Whole Incineration	Light fractions only
$C_{p,l}$ (kJ/kg-K)	4.199	4.199
$C_{p,v}$ (kJ/kg-K)	1.996	1.996
ΔH_v (kJ/kg)	2,260	2,260
$\dot{Q}$ (kJ/hr)	30,000,000	12,500,000
ΔT_1 (K)	(100-25)	(100-93)
ΔT_2 (K)	(1200-100)	(1200-100)

Table 6.5. Proposed process versus incineration of all the HOW: Summary

Parameter	Proposed Process	HOW incineration
Superheated Steam (kg/hr)	1253.189	5800.000
Enthalpy flow (kJ/hr)	12,500,000	30,800,000
CO_2 emissions (tpd)	39.755	86.558
CO emissions (tpd)	1.503	3.827

*tpd: tons per day

The enthalpy flow of the flue gas for the incineration of the whole HOW was 8,556kW (30,800,000kJ/hr) and enthalpy flow of the flue gas from the light fraction only incineration only 40% of this value at 3,471kW. This is equivalent to 1684.99kJ/kg and 1499kJ/kg for the flue gas from full HOW incineration and light fraction only incineration respectively. Even though the enthalpy remains higher on per unit mass basis, the difference is not that significant. For instance, if the light fraction had the same flowrate as the whole HOW, then its enthalpy flow would be 27,415,851.48kJ/hr, 89% of the value of the enthalpy flow of the full incineration flue gas.

6.2. Economic Evaluation of the Proposed Process

Economic evaluation is used to assess the potential of process to be profitable. Net Present Value (NPV), Internal Rate of Return (IRR) and payback period are the most widely used financial indicators for assessing profitability of processes. Net Present Value records the difference between the present values cash inflows and outflows. The IRR is the interest rate at which the NPV is zero. A higher IRR is desired for a lucrative investment project. If for instance, there exists another investment option yielding interest rate higher than the IRR, then one is better off investing in that option than investing in the project. The payback period is the number of years it will take to recover the invested capital. Payback period may be an effective comparison tool between two seemingly profitable investment in which the one resulting in shorter payback period would be favored.

Assumptions

The following assumptions form the basis of the economic evaluation carried out by Aspen Plus:

i. Plant life = 10 years;
ii. Pyridine can be resold at 5 USD/kg [6];
iii. Chloroform can be purchased at 0.5 USD/kg [7];
iv. Interest rate=5%;
v. Tax rate=40%;
vi. The process will be built at Sasol Secunda plant and thus there is no need to buy land.

The main costs of the process are specified in Table 6.6 to Table 6.8. The total operating profit was calculated to be 3,261,790USD/year (44,360,344 ZAR/year using an exchange rate of 1 USD:13.60).

Table 6.6. Major Equipment Capital and Installation Costs

Unit	Equipment Cost [USD]	Installation Cost [USD]
C-1	800,400	1,719,000
C-2	323,500	843,300
C-3	385,100	917,800

Table 6.7. Process Utility Costs of the distillation columns

Unit	Steam [USD/hr]	Cooling Water [USD/hr]	Electricity [USD/hr]
C-1	21.777186	1.30752	0.058125
C-2	6.500189	0.50412	0.014725
C-3	2.528699	0.20148	0.028675

Table 6.8. Total Costs Summary

Parameter	Total
Capital Cost [USD]	10,102,400
Operating Cost [USD/Year]	1,853,870
Raw Materials Cost [USD/Year]	4,382.17
Product Sales [USD/Year]	5,115,660
Utilities Cost [USD/Year]	324,948
Equipment Cost [USD]	1,510,100
Total Installed Cost [USD]	3,437,200

Cash flow data depicted in Table 6.9 was extracted from aspen plus. The Present Value for each cash flow was calculated using equation (6.2) and the Net Present Value (NPV) was calculated from the Present Value data using equation (6.3) (Table 6.9). The NPV was determined to be 5,775,740USD indicating that the process could potentially be a profitable investment. Internal Rate of Return (IRR) was determined from the cash flow data in Table 6.9 as 19.597%. Excel IRR function was used to calculate IRR. A higher value of IRR is a characteristic of a profitable investment.

$$PV = \frac{CF}{(1+i)^n} \quad (6.2)$$

Where:

PV: Present Value for cash flow at the nth year;

CF: Cash Flow;

i: Interest rate;

n: Number of years.

$$NPV = \sum PV \quad (6.3)$$

Cumulative cash flow curve (Figure 6.11) found by the cumulative summation of the cash flows (collected payback in Table 6.9) shows that the breakeven point occurs between 4 and 5 years meaning that it would take about 4.5 years to recover the invested capital. After the breakeven point the process starts to be profitable.

Table 6.9. Cash flow, present value and collected payback

Number of years	**Cash flow (USD)**	**PV (USD)**	**Collected payback (USD)**
0	-11,654,300	-11,654,300	-11,654,300
1	1,812,190	1,647,445	-9,842,110
2	2,575,180	2,128,248	-7,266,930
3	2,711,780	2,037,400	-4,555,150
4	2,855,930	1,950,639	-1,699,220
5	3,008,040	1,867,756	1,308,820
6	3,168,520	1,788,547	4,477,340
7	3,337,830	1,712,835	7,815,170
8	3,516,410	1,640,431	11,331,580
9	6,264,450	2,656,738	17,596,030

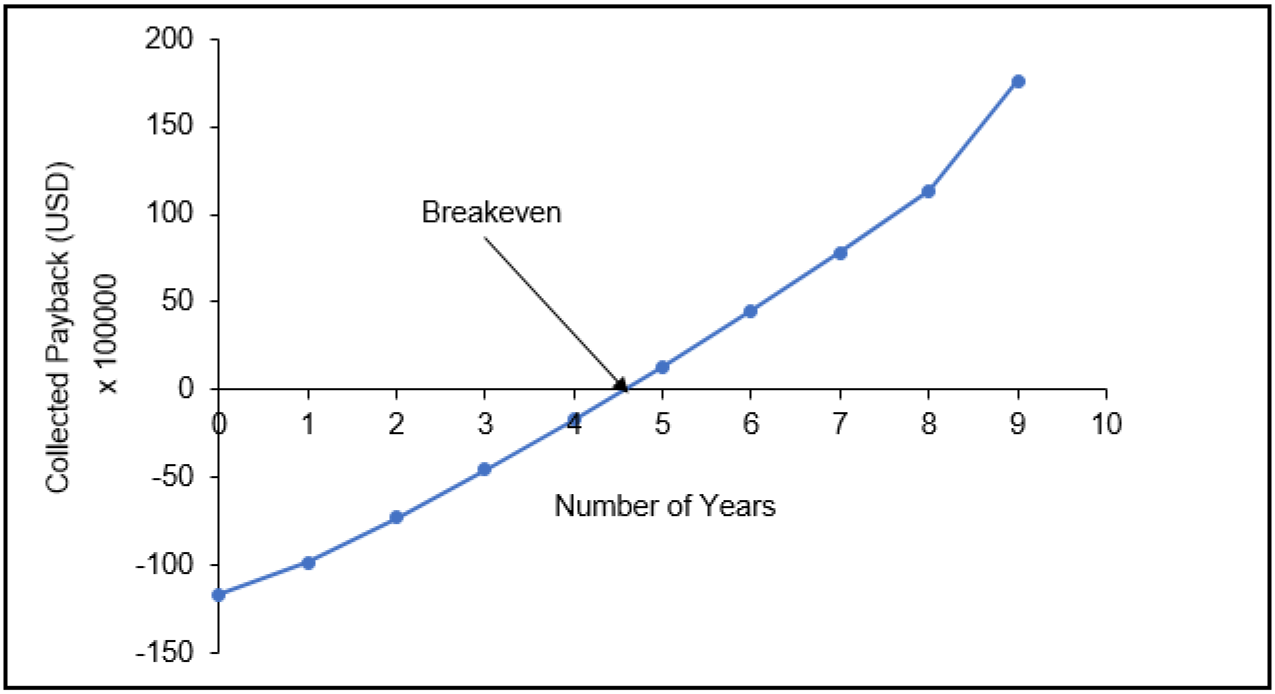

Figure 6.11. Cumulative cash flow for the proposed process

6.3. Conclusions

The incineration of whole HOW stream emits over 2 times CO and CO_2 as flue gas. We acknowledge the limitation of the simplified model, as the incinerator as currently applied for the incineration of the HOW stream may be more complex. One of the key aspects of incineration that was not accounted for in this work, is the addition of fuel to keep the incinerator running. Furthermore, it is expected that the flue gas will have a diverse range of gases, whereas in this work, CO and CO_2 were the main products of consideration. On this basis, the simplified model represents minimum impact of the whole HOW stream incineration. Still, it may be a good basis for the argument against the incineration of the whole HOW. The economic evaluation shows that the pyridine recovery yields a payback period of 4.5 years and an Internal Rate of Return of 19.576%.

References

[1] European Commission, “Reference document on the Best Available Techniques for Waste Incineration,” *Integr. Pollut. Prev. Control*, no. August, pp. 1–638, 2006.

[2] “Energy from Waste: Part 1 -The Myths Debunked - YouTube,” 2007.

[3] P. Connett, “Zero waste: A global perspective,” 2006. [Online]. Available: https://web.archive.org/web/20080406085208/http://www.recycle.ab.ca/2006Proceedings/PaulConnett_Zero_waste.pdf. [Accessed: 23-Oct-2017].

[4] S. Cimini, M. Prisciandaro, and D. Barba, “Simulation of a waste incineration process with flue gas cleaning and heat recovery sections using Aspen Plus,” *Waste Manag.*, vol. 25, pp. 171–175, 2005.

[5] Sasol, “Sasol online sustainable development information: responding to environmental challenges,” 2015.

[6] “Pyridine Price, Pyridine Price Suppliers and Manufacturers at Alibaba.com.” [Online]. Available: https://www.alibaba.com/showroom/pyridine-price.html. [Accessed: 18-Oct-2017].

[7] “Chloroform Price, Chloroform Price Suppliers and Manufacturers at Alibaba.com.” [Online]. Available: https://www.alibaba.com/showroom/chloroform-price.html. [Accessed: 18-Oct-2017].

Chapter 7 : Conclusions and Recommendations

The objective in this work was to recover pyridine from a petrochemical waste stream, namely, the High Organic Waste (HOW) stream produced at Sasol Secunda plant. The proposed recovery process was divided into 2 sections: water-pyridine mixture separation from the rest of the HOW using simple distillation and pyridine enrichment section. In the latter, thermodynamic tools were used to assess different entrainers and techniques that can separate the water-pyridine azeotropic mixture. Methyl Isobutyl Ketone (MIBK) and chloroform were compared as potential entrainers and it was shown that chloroform was a better entrainer. Even so, the conventional design of the chloroform-water-pyridine system had a very high Entrainer to azeotropic mixture (EA=4:1; calculated from the RCM). This was deemed inappropriate for waste treatment facility which was meant to recover pyridine but also reducing the incinerator load.

A separation process that incorporates liquid-liquid extraction into the system was synthesized based on the Residue Curve Map (RCM) topology and this resulted in a 90% reduction of the EA from 4:1 to 0.36:1 (calculated from the RCM). The EA calculated from the simulation material balance was 0.32:1 and the percentage relative error between the EA from the RCM and the EA from simulation material balance was calculated to be 13%. The entrainer performance of the proposed system was compared to the classical toluene-water-pyridine system and it was established that the proposed process required 1.6 times less entrainer than the toluene system. The proposed process had the added benefit of lower energy consumption due to the reduced load to the azeotropic distillation column as liquid-liquid extraction unit removed over 80% of the water originally in the azeotrope. Over 99% recovery of pyridine and over 80% of water was achieved using the proposed process. The water and pyridine had purities of 99.9mol% and 96mol% respectively.

To reduce the number of distillation columns in the proposed process and consequently improve energy utilization, a Diving Wall Column (DWC) technique was proposed for the integration of the two pre-concentration distillation columns as in the initial proposed process. The DWC implementation reduced the reboiler and condenser heat duties by

10% each. Furthermore, it improved the recovered pyridine purity from 96mol% to over 99.9mol% matching up to industry specification of reusable pyridine. Therefore, despite the low energy saving, DWC was still advocated for in this work.

As an extension of energy integration in the proposed process, entropy generation analysis was done on the regeneration column to evaluate its thermodynamic second law efficiency and to recommend an energy integration strategy if the efficiency is low. The calculated second law efficiency was 4.6% which is typical of a distillation column according to literature. It was also found that the reboiler in the regeneration column was the major source of inefficiency, being responsible for over 90% of the total lost work. Consequently, it was recommended that heat integration between the DWC condenser and regeneration column reboiler be assessed using pinch technology in future work.

Incineration of the whole HOW as currently practiced at Sasol Secunda plant was compared with the incineration of only the light fractions from the proposed pyridine and water recovery process. It was established that the proposed process reduced the CO and CO_2 emissions by 50%. Although the incineration of the HOW stream is currently executed without energy recovery, heat recovery was assessed for both the incineration of the whole HOW and light fractions. The enthalpy of the flue gas due to incineration of the whole stream 1685kJ/kg and that of the flue gas resulting from the incineration of the light fractions only was 1499kJ/kg. The steam produced from the incineration of the whole stream was 5800kg/hr versus 1253kg/hr for the incineration. However, the flue gas emanating from the heat exchanger for light fractions only incineration had a temperature over 700ºC showing that it still contained significant energy.

In future work, the recycled water could be supplemented with external water source for maximum heat recovery. We acknowledge the limitation of the simplified model, as the incinerator as currently applied for the incineration of the HOW stream may be more complex. One of the key aspects of incineration that was not accounted for in this work, is the addition of fuel to keep the incinerator running. Furthermore, it is expected that the flue gas will have a diverse range of gases, whereas in this work, CO and CO_2 were the main products of consideration. On this basis, the simplified model represents minimum impact of the whole HOW stream incineration. Still, it may be a good basis for the argument against the incineration of the whole HOW.

Finally, preliminary economic evaluation of the proposed recovery process was done using Aspen Plus economic analyzer. Ideally, the evaluation should have been done on the improved design incorporating DWC, however a reliable technique for DWC costing has not been established yet. Therefore, the process economic evaluation was done on the original design including heat recovery through steam generation. The process was found to be profitable with the Net Present Value of over 5 million USD and an Internal Rate of Return of about 20%. The payback period of the project was calculated from the cash flows to be 4.5 years.

Appendices

Appendix A: Conference Paper

Recovery of pyridine and water from a petrochemical organic rich waste stream: thermodynamic constraints and alternatives analysis

Moratwe Molote[1] and Jean Mulopo[2]

(1), (2) Sustainable Energy and Environment Research Group, School of Chemical Engineering, University of Witwatersrand PO Box 3, Johannesburg, Wits 2050, South Africa. Phone: +27 11 717-7507; Fax: +27 11 717-7604;

[*] *Corresponding Author email: moratwe.molote@gmail.com*

ABSTRACT. The South African waste industry is currently worth over 15 billion ZAR (1 GBP=17.34 ZAR), employing 29,000 people. Recent research has shown that of the 108 million tons of waste generated per annum (all types of waste), only 10% is recycled. Consequently, the development of sustainable waste management strategies remains a critical area of concern in South Africa. In most cases, industrial liquid waste streams are usually very dilute so that it is often economically inviable to recover targeted valuable chemicals. The use of process simulators may be the fastest way to check for the feasibility of separation and chemical processes in general. However, over the past 2 decades, process simulators have grown in complexity and robustness resulting in a detachment between process engineers and the processes they design. On the other hand, the use of thermodynamic tools, i.e. residue curve maps (RCM) and iso-volatility curves have proven valuable in providing unique insight into the synthesis and design of complex separation processes. The objective of this work is therefore twofold i) to use simple thermodynamic analysis tools to assess the recovery of pyridine from an organic rich industrial waste stream and ii) to validate the thermodynamic prediction using Aspen Plus process simulator. It is shown that the combination of thermodynamic tools and rigorous process simulation resulted in a process that reduces the waste and the corresponding CO_2 emissions from the incinerator by 60% and 50% respectively compared to the current incineration practice and stands to save $3 million from pyridine reuse.

1 Introduction

Recent economic and industrial expansion across the globe (Indonesia, China, South Africa and India) and the development of urban cities (megacities) has resulted in massive waste generation; a phenomenon which has grown to be one of the major challenges of the 21st century [1]. Lack of strategic plans for waste management has undesirable consequences such as pollution and loss of lives as could be seen with the accident that took place in Quezon in the year 2000 wherein a stack of waste collapsed [86]. Due to lack of policy enforcement in South Africa, dilute industrial waste streams are often discarded onto large water bodies and sewage systems for companies located inland [25]. The latter results in difficulty in treating sewage waste. One of the most widespread, global strategies to treat waste is incineration; although this practice reduces the volume of waste, it is not always the best approach to waste treatment as it could also contribute to global warming through greenhouse gases emissions and could also result in loss of valuable chemicals [4]. There is thus a need to do away with "treat to discard" mentality and start focusing on the opportunities presented by waste generation [87].

Waste valorization through implementation of appropriate waste management strategies has the potential to alleviate the socio-economic stresses such as unemployment and high resource consumption rate in South Africa. For instance, the SA waste industry was reported to be worth 15.8 billion ZAR (0.51% GDP of the country) in 2012, employing over 29,000 people [4]. It is estimated that a further 20% and 60%

recycle of industrial waste and domestic waste respectively could result in a further 17 billion ZAR revenue and potential job creation for 30,000 more people. Consequently, the SA government has recently developed a new green policy and regulatory framework for waste management which emphasize minimization of waste production and resource consumption [National Environmental Management: Waste Act (Act 59 of 2008))] [4]. This paper focuses on the aqueous waste stream produced in SASOL Secunda composed of low boiling organic components such as acetonitrile, pyridine, and methyl ethyl ketone. Currently the stream is incinerated with energy recovery in the form of steam generation. This practice produces about 13 tons per day of CO_2 emission which serves to exacerbate the already alarming CO_2 emissions from this plant that emanates from power generation part of the plant.

Separation of pyridine from water and other components is an ongoing research [6]. This can be attributed to the fact that pyridine is a versatile chemical solvent that has found application in a variety of industries including textile, paint and agrochemical industries [6,7]. Currently the pyridine market is worth over 450 million USD; it is projected that this will increase to about 650 million USD by 2021 [5]. Moreover, its demand is expected to grow by 9.95% compound annual growth rate between now and 2025 [6]. Besides the azeotrope formed between pyridine and water, pyridine recovery from spent streams is further made difficult by the dilute nature of the waste streams in which it is found [39]. Luyben and Chien (2013) [39] proposed the use of heterogeneous azeotropic distillation using toluene as an entrainer, Burroughs Wellcome Co implemented liquid-liquid extraction for the recovery of pyridine from a waste stream and made 1.5 million USD per annum worth of savings in the early 1990s [37].

Pervaporation, and other membrane based techniques have been proposed as techniques for the separation of azeotropic mixtures [11-14], however industry has shown more preference toward distillation processes because of their simplicity, ability to deal with complex mixtures and to yield purer products and perpetual improvements it receives [15-18]. More importantly, distillation is preferred because its separation is based on VLE (Vapor Liquid Equilibrium) which can be rigorously predicted using thermodynamic models such as Wilson, Non-Random Two Liquid (NRTL) and others [53].

In its ordinary form, distillation cannot separate azeotropic mixtures, as a result, modified distillation techniques such as azeotropic distillation (homogeneous and heterogeneous) and pressure swing distillation (PSD) are used [19,20]. Pressure swing distillation cannot be used for the separation of water-pyridine azeotrope since this mixture is not pressure sensitive [16,21]. Of interest, is the heterogeneous azeotropic distillation in which the entrainer introduces one or more azeotrope(s) and liquid-liquid immiscibility to the original mixture [55]. The addition of a solvent (entrainer) in azeotropic distillation is a cause for concern especially for the application of waste minimization; in some applications, the entrainer to mixture ratio can be as high as 8, as in the dehydration of ethanol using 1-butnaol [55]. The higher the solvent requirement the more redundant the treatment becomes since the chief aim is to reduce waste while the recovery of valuable chemicals serves as motivation. The entrainer reduction techniques were studied by Hilal et al (2002) [40], but have generally not been addressed adequately in the past; therefore this work aims to expand on the subject.

The objective of this work is therefore to assess the applicability of separation processes to the recovery of pyridine from a low boiling organic waste stream produced at Sasol Secunda plant using Aspen Plus process simulator in conjunction with thermodynamic tools. Hitherto, no other solvent apart from toluene has been studied in detail for the separation of water and pyridine azeotrope. In this work, Methyl Isobutyl Ketone (MIK) and chloroform were compared as potential entrainers for the same. We illustrate using chloroform-pyridine-water system how the design of heterogeneous azeotropic distillation can be modified to reduce the entrainer to azeotropic mixture ratio. The proposed process’ solvent consumption was then compared with the classical example of toluene-water-pyridine system proposed by Wu and Chien (2009) [27].

2 Thermodynamic Analysis of Separation Processes

2.1 Background

Thermodynamic analysis of separation processes has been proposed to gain insight of separation processes. The most used thermodynamics tools used for separation processes are residue curve maps and iso-volatility curves discussed below. These are commonly applied for distillation processes [23-25]. Although the curves are useful, their use have been extremely limited in the past due to the tedious process of producing them mathematically [65]. Today, computer software such as Aspen Plus and Matlab can generate these curves with relative ease. The amount of solvent required is largely influenced by the topology of the residue curve map and can de deduced from the residue curve map plot. In conjunction with residue curve maps, iso-volatility curves can be used to enhance entrainer selection criteria.

2.2 Residue Curve Maps

Residue curve maps are primarily used for the preliminary design of distillation sequence and to assess the feasibility of separation, but their use can be easily extrapolated to the assessment of the effectiveness potential entrainers as shown [21,24]. Other uses include column troubleshooting and control [65] . A residue curve represents composition of a liquid remaining in a simple batch distillation process [57]. This can be represented mathematically by equation 1 below [55]. The plot of a residue curve may be done on an equilateral triangle or right-angled triangle. In this work, Aspen Plus was used to generate the residue curve maps. Figure 1 below shows graphically how a residue curve is generated experimentally.

$$\frac{dx_i}{d\xi} = x_i - y_i \qquad (1)$$

Where x_i: Liquid composition of component i

y_i: Vapor composition of component i

ξ: Dimensionless time

A residue curve starts at an unstable node (lowest boiling component) and approaches the saddle point (intermediate boiling component) then ends up at the stable node (highest boiling component) (see Figure 1 below). Residue curve maps generated for heterogeneous azeotropic distillation will typically have at least one distillation boundary. It is practically impossible to separate components located in different distillation regions using distillation; however, liquid-liquid separation such as decanting and liquid-liquid extraction may be used to cross the boundary when there is liquid-liquid immiscibility within the mixture.

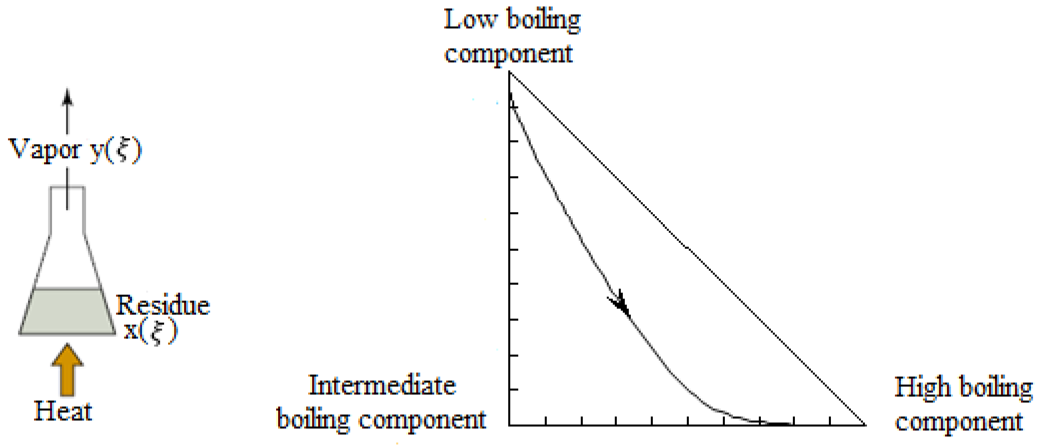

Figure 1. Experimental development of a residue curve [65].

2.3 Iso-volatility Curves

The iso-volatility curve tracks the composition in which the relative volatility of the mixture is 1 [39]. The superimposition of iso-volatility curve on the residue curve map can help with the comparison of the effectiveness of potential entrainers for azeotropic distillation. Although, they are mainly used for when heavy entrainers are concerned [39], their use can be extended to light entrainers application as illustrated in this work. The iso-volatility curve starts at the azeotrope and ends at the intersection where the composition of one of the components in the original binary mixture is zero (from point A to B in Figure 2 below); the number of azeotropes present in the mixture will match the number of iso-volatility curves. The entrainer whose point B is farther from the entrainer is regarded as the most effective entrainer for separation using azeotropic distillation [39].

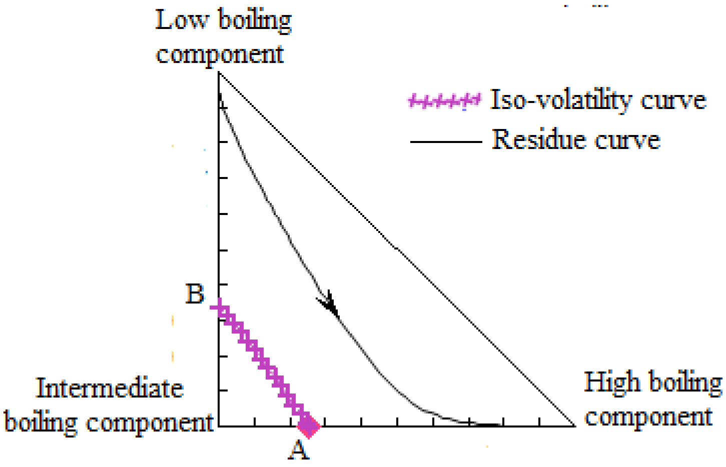

Figure 2. Superimposition of iso-volatility curve on a residue curve map.

3 Process Analysis Application

A waste stream under consideration consists mainly of low boiling organic components is produced at SASOL Secunda plant. Amongst the components contained in the waste is pyridine; one of the most versatile solvents in industry. A large fraction of the stream is made up of water. The stream composition is given in Table 1 (a) below. The waste stream flow rate is reported to vary between 20 and 30 kilo tons per year. As can be seen from Table 1(a), water is common in all the azeotropes formed except for the acetonitrile-methyl ethyl ketone azeotrope. Moreover, pyridine is the highest boiling component, followed by water and Methyl Isobutyl Ketone. Also, water-pyridine azeotrope is the highest boiling azeotrope in the feed mixture; the difference between the boiling points allows for the isolation of water-pyridine azeotrope using simple distillation. This can be done without the loss of pyridine because pyridine forms azeotrope with water only. From these observations, the generic process flow diagram depicted in Figure 2 below was proposed for the recovery of pyridine from this waste stream.

Table 1 (a). Waste stream composition, existing azeotropes and boiling points.

Component	Mass Fraction	BP(C)	Azeotropes Formed	Azeotrope BP(C)
Pyridine	0.05	115.16	W-P	93.71
Acetone	0.02	56.14	W-A	76.53
Water	0.62	100.02	W-A-MIK	76.32
Acetonitrile	0.15	81.48	W-MEK	79.34
Methyl Ethyl Ketone	0.04	79.34	W-MIK	77.61
Methyl Iso Propyl Ketone	0.12	94.08	A-MEK	79.09

Table 1(b). Explanation of keys used in Table 1 (a).

Abbreviation	**Explanation**
W-P	Water-Pyridine
W-A	Water-Acetonitrile
W-A-MIK	Water-Acetonitrile-Methyl Isopropyl Ketone
W-MEK	Water-Methyl Ethyl Ketone
W-MIK	Water-Methyl Isopropyl Ketone

A-MEK	Acetonitrile-Methyl Ethyl Ketone

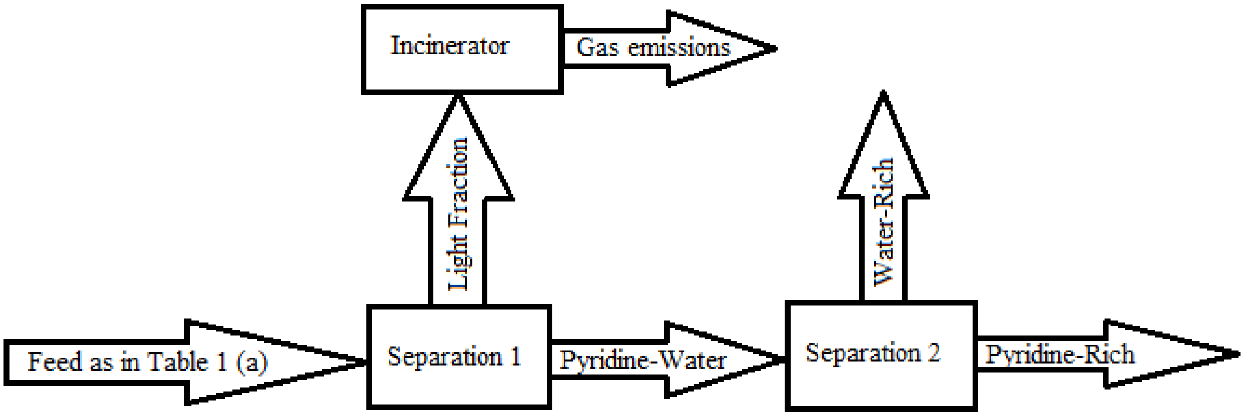

Figure 3. Generic proposed separation process flow.

The system being studied in the sections to follow is the pyridine-water stream in Figure 3 above.

Assumptions

4. The waste stream flow rate is 20 kilo tons per year.
5. Pressure drop is insignificant in all distillation columns.
6. NRTL property method was used across all process units: Aspen plus uses the modified Antoine equation given as equation 2 below to calculate the liquid activity coefficients using binary parameters.

$$\ln \gamma_i = \frac{\sum_j x_j \tau_{ji} G_{ji}}{\sum_k G_{ki}} + \sum_j \frac{x_j G_{ij}}{\sum_k G_{kj}} \left[\tau_{ij} \frac{\sum_m x_m \tau_{mj} G_{mj}}{\sum_k x_k G_{kj}} \right] \qquad (2)$$

$$G_{ij} = \exp(-\alpha_{ij} \tau_{ij}) \qquad (2a)$$

$$\tau_{ij} = a_{ij} + \frac{b_{ij}}{T} + e_{ij} lnT \qquad (2b)$$

$$\alpha_{ij} = c_{ij},\ \tau_{ii} = 0,\ G_{ii} = 1 \qquad (2c)$$

Entrainer selection is the single most crucial step in azeotropic distillation. This is because the entrainer dictates feasible separation sequence and number of columns required to realize the desired separation. Consequently, the entrainer plays a key role in the economics of the process and its energy consumption thereof. Any design made is within the constraints imposed by the entrainer, i.e. distillation boundary. In azeotropic distillation, entrainer performance should also be gauged by the ease with which they can enhance the relative volatility of an azeotropic mixture (indicated by the iso-volatility curves). Some of the factors to consider when selecting the entrainer are: its cost relative to the cost of the targeted chemical, availability within the area of the process and its toxicity. The choice of Chloroform and methyl isobutyl ketone as potential entrainers was informed by literature [10,28].

Chloroform

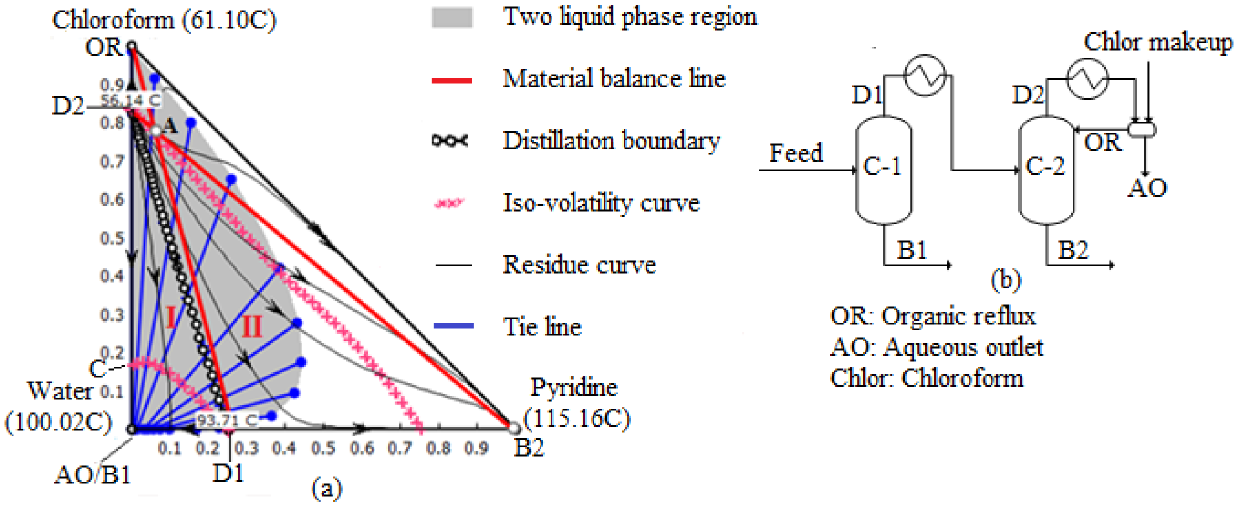

Figure 4. (a): Chloroform-water-pyridine residue curve map showing liquid-liquid envelope, iso-volatility curves, distillation boundary and material balance lines; (b): Corresponding synthesized process flow diagram.

The addition of chloroform to the water-pyridine mixture introduces one more azeotrope to the system (water-chloroform) as depicted in Figure 4(a) above. The resulting residue curve map is divided into 2 regions with a large liquid-liquid immiscibility region, thus allowing for natural liquid-liquid separation to take place. In both regions, the water-chloroform azeotrope is the lowest boiling point (unstable node). The feed is in Region I and the objective is to move into Region II wherein pyridine is found. This can be done by taking advantage of the liquid-liquid equilibrium phenomenon to cross the boundary. In Region II pyridine is the stable node. Therefore, it follows naturally that once in this region, an indirect split approach will be followed to sample pyridine as a bottoms product (B2) of a distillation column. The process flow diagram corresponding to this residue curve is depicted in Figure 4(b).

Methyl Isobutyl Ketone

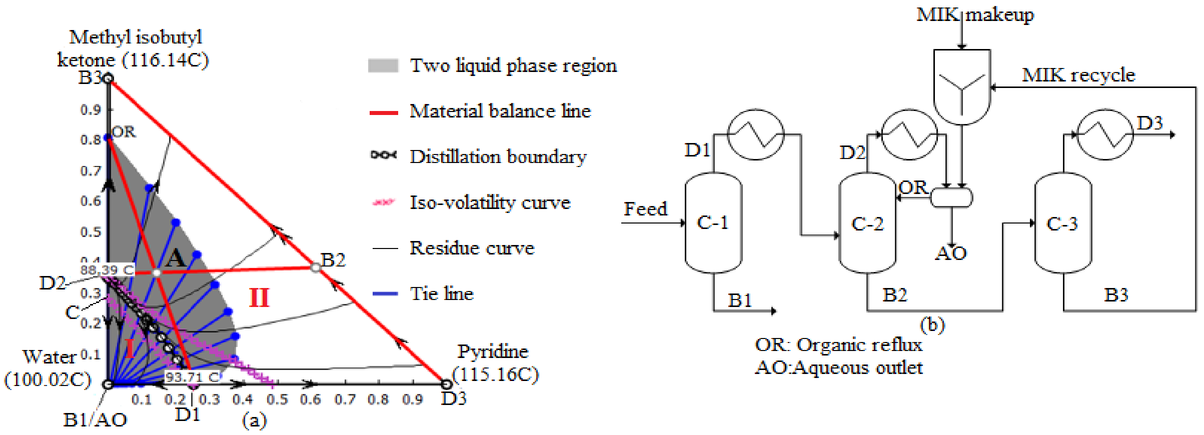

Figure 5. (a): MIK-water-pyridine residue curve map showing liquid-liquid envelope, iso-volatility curves, distillation boundary and material balance lines; (b): Corresponding Synthesized process flow diagram.

The residue curve map is divided into 2 regions and as required for heterogeneous azeotropic distillation, there exists a liquid-liquid immiscibility region (see Figure 5 (a) above). The feed is found in Region I and as in the last analysis the aim is to move to region 2 wherein pyridine is found. The feed is first concentrated to azeotropic composition using a distillation column. The azeotropic composition (D1) leaves the first distillation column (C-1) as a distillate and pure water leaves this column as the bottoms product. D1 is mixed with the organic reflux in the next distillation column (C-2) where the MIK-water azeotrope is a distillate product and the mixture of pyridine and MIK are sampled as a bottoms product. The bottoms product of C-2 are further distilled to separate into pure pyridine and MIK as a distillate and bottoms product respectively in distillation column C-3. The process flow diagram corresponding to this synthesis is depicted in Figure 5(b). The residue curve formed by the addition of methyl isobutyl ketone to the water-pyridine system necessitates the use of 3 distillation columns. consequently, the operational costs will be much higher than the 2-column process on the chloroform system in terms of energy intensity and control costs. Moreover, the difference between boiling points of pyridine and MIK is insignificant, therefore separation in column 3 may not be feasible at all.

From the discussion above, it follows that chloroform is the more suitable entrainer for the separation of pyridine-water azeotrope. furthermore, the iso-volatility curves in Figure 5 and 4 above also shows that chloroform is a more effective entrainer; the iso-volatility curve in the chloroform-water-pyridine intersects the water-chloroform axis at 0.18 whereas the intersection is at 0.30 for the MIK system (see point C in Figures 4 & 5 respectively). The chloroform system process however requires large sums of entrainer in the azeotropic distillation column. This is seen by point A in Figure 4 (a) wherein chloroform composition is approximately 80mol% of the ternary mixture.

4 Can We Do Better?

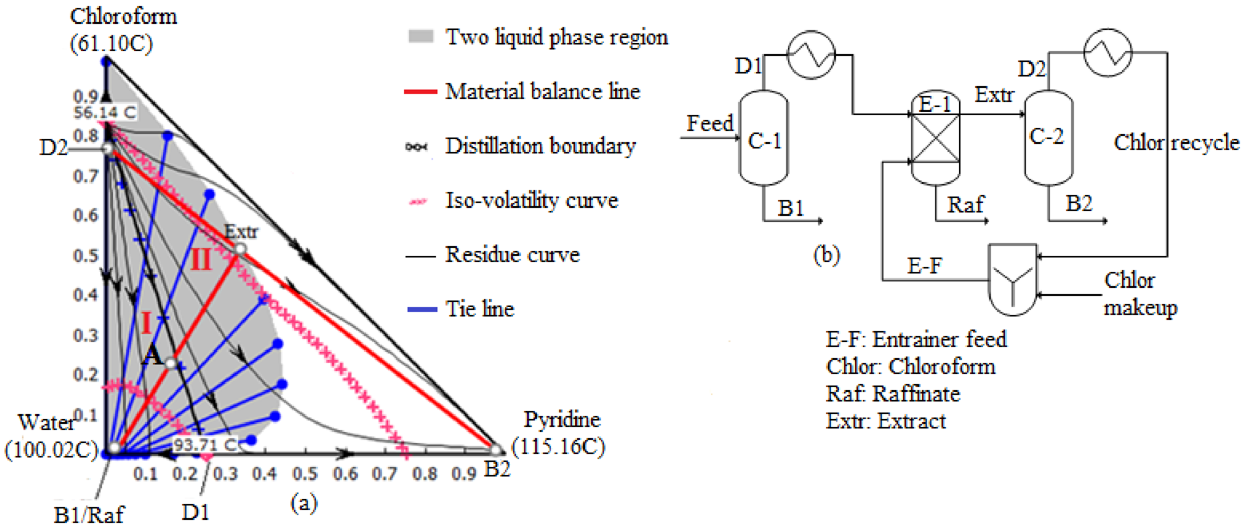

Figure 6. (a): Chloroform-water-pyridine residue curve map showing liquid-liquid envelope, iso-volatility curves, distillation boundary and material balance lines; (b): Improved process flow diagram including liquid-liquid extraction.

The idea is to add just enough entrainer to move point D1 to point A (see Figure 6(a) above) to the distillate of the pre-concentrator (D1). Once the composition in A is attained, liquid-liquid extraction is used to separate the mixture into an organic rich phase (extract) and an organic lean phase (raffinate). The extract is a ternary mixture of pyridine, water and chloroform (see Extract in Figure 6 (a) above). It is then taken to the azeotropic distillation column (C-2) where pyridine is sampled as a bottoms product. The distillate of C-2 (D2) is the composed of mainly chloroform (about 77mol%), and water (23mol%) (see point D2 in Figure 6(a) above) and it is recycled back to the liquid-liquid extraction column. To avoid the loss of pyridine and because chief fraction of D2 is chloroform (the entrainer); it is recycled back to the liquid-liquid extraction column as it is. This process was simulated in Aspen Plus with the NRTL binary parameters and equipment design parameters given in Table 2 and 3 respectively.

Table 2. Binary parameters of the chloroform-water-pyridine mixture.

Comp* i Comp* j	Pyridine Water	Pyridine Chloroform	Water Chloroform
a_{ij}	0.138	2.671	8.844
a_{ji}	5.118	-4.517	-7.352
b_{ij}	-197.679	-1225.041	-1140.115
b_{ji}	-735.747	1595.533	3240.688
c_{ij}	0.300	0.300	0.200

Comp*: Component

Table 3. Summary of columns used for pyridine dehydration.

	C-1	C-2	E-4
Reflux Ratio	2.000	2.500	-
Total number of stages	20.000	30.000	10
Condenser duty	-205.316	-81.837	-

Reboiler duty	207.987	80.882	-

The main difference between the design in Figure 6 and the conventional analysis proposed in Figure 4 above is that liquid-liquid separation in the conventional analysis, liquid-liquid separation is used for entrainer regeneration and water-pyridine separation takes place mainly in the distillation column; whereas, in the improved design separation of pyridine-water mixture takes place both in the liquid-liquid extraction column and the distillation column, thereby taking advantage of the both LLE (Liquid-Liquid Equilibrium) and VLE (Vapor Liquid Equilibrium) for separation of the same mixture. The result is a dramatic reduction of entrainer to mixture ratio (from 80mol% to 22mol% in the total mixture (see point A in Figure 4(a) and Figure 6(a) respectively). Liquid-liquid extraction removes just enough water to enable distillation to sample pure pyridine from the ternary mixture. Therefore, distillation column C-2 serves 2 purposes: solvent regeneration as well as pyridine recovery. The former approach is equivalent to mixing the entrainer and the azeotropic mixture then distilling to sample the target component. That way, to move from D1 to a point in Region II where pyridine can be effectively sampled using distillation requires the addition of a large amount of entrainer; separation would only be feasible if the entrainer makes up about 80mol% (point A in Figure 4(a)) of the total mixture (entrainer plus azeotropic mixture), anything below this will either result in pyridine loss, unnecessary recycles or more unduly number of columns. Substantial amounts of entrainer to azeotropic mixture ratio results in higher energy consumption, increases raw materials costs significantly and large recycle flowrates which can be very costly. More importantly, it makes the waste treatment redundant in light of sustainable development.

Pyridine recovery of over 99wt% at 98wt% (96mol%) purity is possible using the proposed design. The mass balance for the recovery process is given in Table 4 below. There is good agreement between the simulation composition depicted in Table 4 below and the ones predicted in the residue curve map in Figure 6(a). The differences between these can be attributed to the presence of acetonitrile as an impurity in the feed stream that is unaccounted for in the residue curve map. It is noteworthy that the main impurity in the pyridine stream (B2) is acetonitrile (see Table 4 below) and not water. This signifies that the proposed system is effective in breaking water-pyridine azeotrope in that in the absence of acetonitrile impurity, purity over 99mol% could potentially be attained.

Table 4. Material balance of the proposed process.

	Feed	B1	D1	E-F	Raffinate	Extract	B2	D2	Fresh Chloroform
Component	**Mole Fraction**								
Pyridine	0.020	0.000	0.236	0.000	0.000	0.341	0.961	0.000	0.000
Water	0.979	1.000	0.755	0.282	0.000	0.182	0.000	0.283	0.000
Acetonitrile	0.001	0.000	0.009	0.001	0.999	0.014	0.036	0.001	0.000
Chloroform	0.000	0.000	0.000	0.717	0.001	0.463	0.002	0.716	1.000
Units	**Mole Flow Rate**								
kmol/hr	71.027	64.927	6.100	2.736	4.608	4.228	1.500	2.727	0.008

The process proposed by Wu and Chien (2009) [27] and its mass balance are depicted in Figure 7 and Table 5 respectively. The residue curve produced for this system has 2 distillation boundaries resulting in 3 distillation regions. Fresh feed is mixed with the aqueous outlet from the decanter (see Figure 7(a)). The mixture is distilled to concentrate the mixture closer to azeotropic composition; this is done to avoid using excessive amounts of solvents in the azeotropic column [39]. The azeotropic mixture (D2) is recycled back to the heterogeneous azeotropic distillation column (C-1). From C-1, pure pyridine is recovered as the bottoms product as per mass balance line shown in Figure 7 (a). Liquid-liquid separation (decanter in this case) is used to cross the boundary to separate the organic rich phase from the organic lean phase (Aqueous Outlet). The organic rich phase is recycled back into the column.

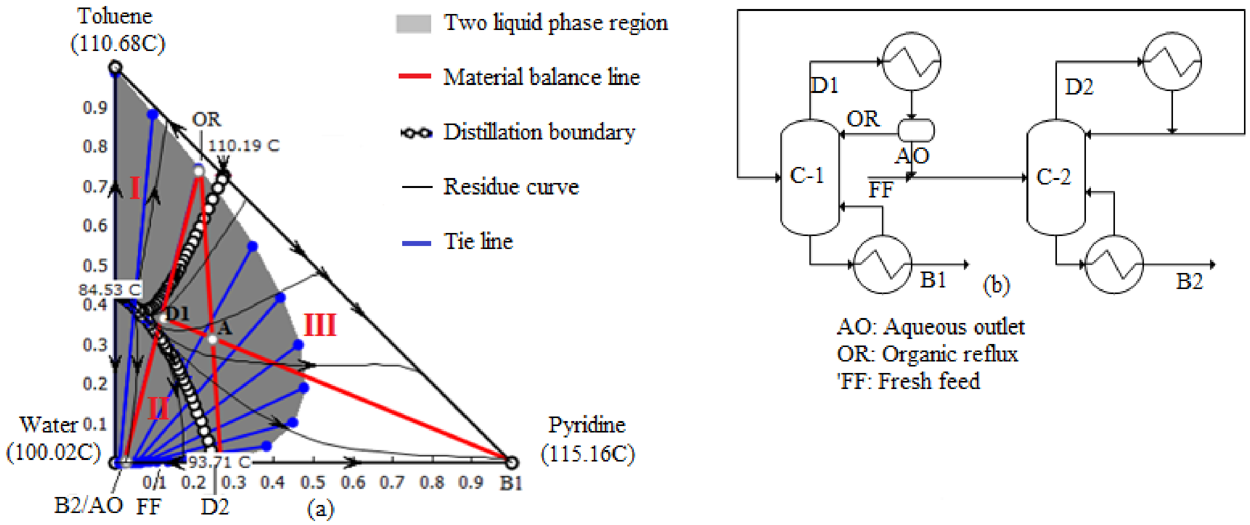

Figure 7. (a) Water-pyridine-toluene system residue curve map; (b) Azeotropic distillation process flow diagram for pyridine dehydration using toluene [66].

Table 5. Material balance for the toluene-water-pyridine system [66].

	Fresh Feed	AO	D2	B2	D1	B1	OR
Component	**Mole fraction**						

Pyridine	0.100	0.010	0.210	0.001	0.071	0.999	0.150
Water	0.900	0.990	0.790	0.999	0.561	0.001	0.011
Toluene	0.000	0.000	0.000	0.000	0.368	0.000	0.839
Units	**Mole Flow Rate**						
kmol/hr	1000.000	391.200	490.400	900.800	696.300	99.200	305.100

The entrainer to azeotropic mixture ratio is 0.285 for the chloroform system and 0.474 for the toluene system [66] (see Table 6 below). The compositions of the entrainers for the chloroform and toluene system are 0.221 and 0.321 respectively in the total mixture. These compositions can be predicted preliminary using residue curve maps systems (see Figure 6(a) and Figure 7(a) above). Therefore, the proposed design uses 1.7 times less solvent as used in the toluene system. This translates to the toluene system using over 16,000 kmol/year more than the chloroform system. The reduced amount of entrainer means smaller equipment for storage and processing and thus lower capital costs. Therefore, in terms of entrainer consumption, the chloroform process proposed in this work is better than the status-quo toluene azeotropic distillation system. Chloroform has the added benefit of being cheaper than toluene at 0.5 USD/kg versus 1USD/kg. The fact that separation is divided between the liquid-liquid extraction and distillation has good implications on the energy requirements of the system because distillation is more energy intensive than liquid-liquid extraction so the reduction of the load to be processed by the distillation column is bound to result in less energy consumption of the separation process.

Table 6. Comparison of toluene and chloroform as entrainers.

	Chloroform	Toluene
Composition in the total mixture	0.222	0.321

Entrainer to mixture ratio	0.285	0.474

5 Let us Consider the Bigger Picture

Currently the feed stream under consideration is incinerated with energy recovery in the form of steam generation that in turn helps in the production of electricity as shown in Figure 8 below. This practice produces at least 36tons/day of CO_2; this can be deduced from Table 7 below. The treatment facility depicted in Figure 9 reduces the waste stream by 60%. Presently, 20kt/year is fed to the incinerator but with the proposed treatment, only 8kt/year is fed to the incinerator. This reduces the carbon dioxide emissions from the incinerator by 50wt% (from 36 to 18 tons per day) with the benefit of recovering pyridine. The 40% remaining is incinerated as per current practice. This is advantageous in a sense that the current facility would still be used and will not become redundant. Moreover, over 90wt% of the water present in the feed was recovered and reused for steam generation using the heat from the stream exiting the incinerator (see Figure 9). Chloroform required to achieve pyridine using the proposed design is about 0.5mol% of the pyridine in the original feed; so, even in the bigger scheme of things, particularly in light of sustainable development the proposed process is sensible. Table 8 below summarizes the economic evaluation of the treatment plant.

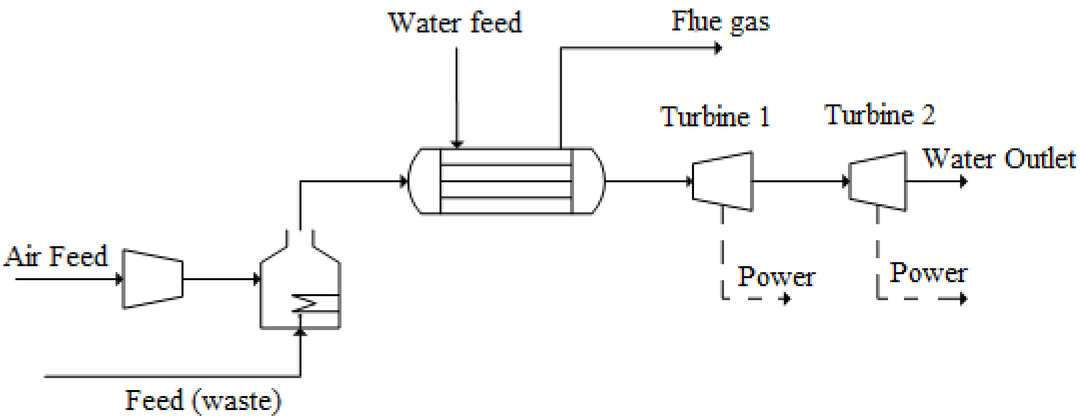

Figure 8. Simplified waste incineration treatment plant (Status Quo)

Table 7. Incineration Material Balances

	Feed (waste)	Air feed	Water feed	Steam	Flue gas
	Mass Fraction				
Acetone	0.020	0.000	0.000	0.000	0.000
Acetonitrile	0.150	0.000	0.000	0.000	0.000
Pyridine	0.050	0.000	0.000	0.000	0.000
Methyl ethyl ketone	0.040	0.000	0.000	0.000	0.000
ethyl isopropyl ketone	0.120	0.000	0.000	0.000	0.000
Water	0.620	0.000	1.000	1.000	0.207
Oxygen	0.000	0.233	0.000	0.000	0.000
Carbon monoxide	0.000	0.000	0.000	0.000	0.034
Carbon dioxide	0.000	0.000	0.000	0.000	0.149
Nitric oxide	0.000	0.000	0.000	0.000	0.000
Hydrogen cyanide	0.000	0.000	0.000	0.000	0.000
Nitrogen	0.000	0.767	0.000	0.000	0.610
Units	**Mass flow rate**				
kg/hr	2281.542	7985.398	4449.008	4449.008	10266.940

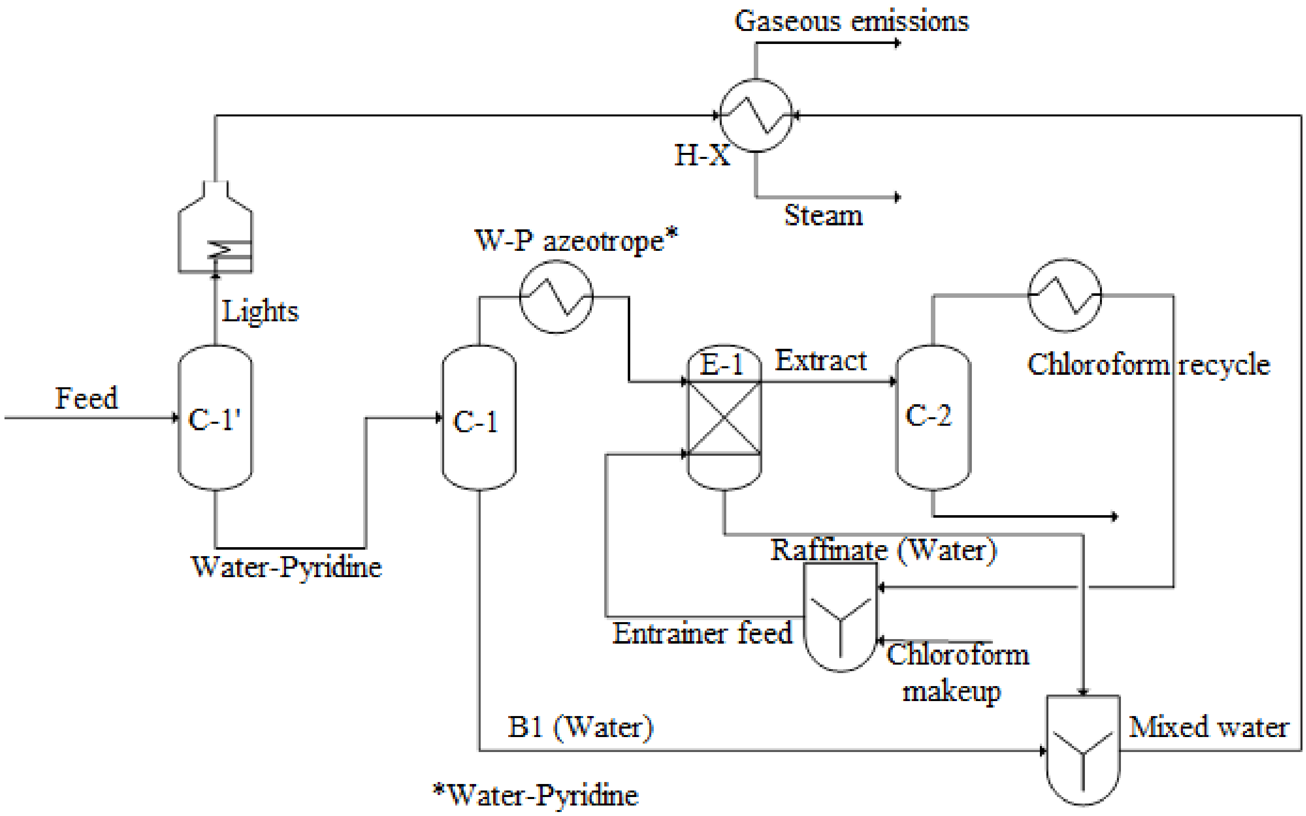

Figure 9. Full treatment plant.

Table 8. Preliminary economic analysis summary of the chloroform system.

Currency	(USD)
Pyridine cost (per kg)	5
Chloroform cost (per kg)	0.5
Utility cost (pa)	324,948
Capital cost (pa)	10,102,400
Operating profit (pa)	3,621,790

As shown in Table 8 above, the proposed chloroform process provides a good financial incentive operating at a profit of over 3 million USD per annum. With the capital cost being 10 million USD, the payback period is just over 3 years. The implementation of this process by SASOL would therefore be a fruitful investment.

Conclusions

Simulation results were in agreement with the predicted compositions by the residue curve maps showing that RCMs are a handy tool to be used along with process simulators for separation systems. Pyridine recovery from dilute waste streams is a profitable undertaking and chloroform was shown be the most effective entrainer for this endeavor up to so far. Future work will be based on energy optimization the process proposed in this work.

Acknowledgements

The authors would like to express their gratitude to Sasol and National Research foundation for their financial support to carry out this work.

References

[1] D. Hoornweg, P. Bhada-Tata, and C. Kennedy, “Environment: waste production must peak this century,” *Nature*, vol. 502, no. 7473, pp. 615–617, Oct. 2013.

[2] B. Vrede, “Department of Geography and Environmental Studies petroleum waste disposal challenges in selected African contries - policy, practice and prospects,” no. November, 2014.

[3] E. C. S. Nunes and A. N. Haddad, “Waste Management in the Oil and Gas Industry by Brazilian Guideline for Environmental Audits - DZ-056-R.3,” *Am. J. Environ. Prot.*, vol. 2, no. 6, p. 170, 2013.

[4] GreenCape, “Waste economy: market intelligence report 2016,” no. April, pp. 1–55, 2015.

[5] Marketsandmarkets, “Pyridine & amp; pyridine derivatives market worth 656.3 Million USD by 2021,” 2017. [Online]. Available: http://www.marketsandmarkets.com/PressReleases/pyridine-derivatives.asp. [Accessed: 13-Jul-2017].

[6] “Pyridine market: global industry size, share and forecast period 2015 -2025.” [Online]. Available: http://www.persistencemarketresearch.com/market-research/pyridine-market.asp. [Accessed: 28-Jun-2017].

[7] P. Sébastien, M. Silvère, G. Vincent, B. Olivier, B. Philippe, and J. Xavier, “Heterogeneous batch distillation processes: Real system optimisation,” *Comput. Aided Chem. Eng.*, vol. 20, no. C, pp. 1081–1086, 2005.

[8] R. Cheng, C.-H. Cho, S. Kirby, and B. Lim, “Economic recovery of pyridine and 3-methylpyridine,” 2010.

[9] Z. Zhu, D. Xu, X. Liu, Z. Zhang, and Y. Wang, “Separation of acetonitrile/methanol/benzene ternary azeotrope via triple column pressure-swing distillation,” *Sep. Purif. Technol.*, vol. 169, pp. 66–77, 2016.

[10] M. K. Mandal and P. K. Bhattacharya, “Poly(ether-block-amide) membrane for pervaporative separation of pyridine present in low concentration in aqueous solution,” *J. Memb. Sci.*, vol. 286, no. 1–2, pp. 115–124, 2006.

[11] I. F. McConvey, D. Woods, M. Lewis, Q. Gan, and P. Nancarrow, “The importance of acetonitrile in the pharmaceutical industry and opportunities for its recovery from waste,” *Org. Process Res. Dev.*, vol. 16, no. 4, pp. 612–624, 2012.

[12] C. Bravo-Bravo, J. G. Segovia-Hernández, C. Gutiérrez-Antonio, A. L. Durán, A. Bonilla-Petriciolet, and A. Briones-Ramírez, “Extractive dividing wall column: design and optimization,” *Ind. Eng. Chem. Res.*, vol. 49, no. 8, pp. 3672–3688, 2010.

[13] M. Illner and M. R. bin O. Othman, “Modeling and simulation of a dividing wall column for fractionation of fatty acid in oleochemical industries,” *Iran. J. Chem. Eng.*, vol. 12, no. 1, pp. 60–67, 2015.

[14] V. Julka, M. Chiplunkar, and L. O. Young, “Selecting entrainers for azeotropic distillation,” *Aiche*, no. March, pp. 47–53, 2009.

[15] Y. Wang, Z. Zhang, D. Xu, W. Liu, and Z. Zhu, “Design and control of pressure-swing distillation for azeotropes with different types of boiling behavior at different pressures,” *J. Process Control*, vol. 42, pp. 59–76, 2016.

[16] K. Khushalani, A. Maheshwari, and N. Jain, “Separation of mixture by divided wall column using Aspen Plus,” *Int. J. Emerg. Technol. Adv. Eng.*, vol. 4, no. 8, pp. 563–571, 2014.

[17] A. A. Kiss and R. R. Rewagad, “Energy efficient control of a BTX dividing-wall column,” *Comput. Chem. Eng.*, vol. 35, no. 12, pp. 2896–2904, 2011.

[18] Y. C. Wu, H. Lee, H. Huang, and I. Chien, “Energy-Saving Dividing-Wall Column Design and control for Heterogeneous Azeotropic Distillation Systems Energy-Saving Dividing-Wall Column Design and Control for Heterogeneous Azeotropic Distillation Systems,” 2014.

[19] G. M. De Koeijer and S. Kjelstrup, “Application of irreversible thermodynamics to distillation,” *Int. J. Thermodyn.*, vol. 7, no. 3, pp. 107–114, 2004.

[20] “Sustainability reporting, sasol,” 2016.

[21] Z. Zhu, D. Xu, X. Liu, Z. Zhang, and Y. Wang, “Separation of acetonitrile/methanol/benzene ternary azeotrope via triple column pressure-swing distillation,” *Sep. Purif. Technol.*, vol. 169, pp. 66–77, 2016.

[22] “Aspen Technology,” 2017. [Online]. Available: http://home.aspentech.com/products/engineering/aspen-plus/. [Accessed: 22-Aug-2017].

[23] Department of Environmental Affairs, “National Waste Information Baseline Report,” no. November, 2012.

[24] “Waste management.”

[25] “Environmental Outlook,” pp. 1987–1996, 2001.

[26] T. Majozi and P. Veldhuizen, “The chemicals industry in South Africa,” *Am. Inst. Chem. Eng.*, no. July, pp. 46–51, 2015.

[27] “Sasol produces 1,5 billion barrels of synthetic fuel from coal in fifty years | Sasol,” 2005. [Online]. Available: http://www.sasol.com/media-centre/media-releases/sasol-produces-15-billion-barrels-synthetic-fuel-coal-fifty-years. [Accessed: 22-Aug-2017].

[28] “Operations / Locations | Sasol.” [Online]. Available: http://www.sasol.com/about-sasol/regional-operating-hubs/southern-africa-operations/secunda-synfuels-operations. [Accessed: 28-Aug-2017].

[29] “The chemical industry: Sasol.” [Online]. Available: http://archive.cnx.org/contents/4733ff32-a845-42bb-b98d-37a346da5cce@1/the-chemical-industry-sasol. [Accessed: 28-Aug-2017].

[30] Sasol, “Sasol 50 years of Innovation,” *Sasol Ltd. 50th Anniv. J.*, 2000.

[31] H. S. Samanta and S. K. Ray, “Pervaporative recovery of acetone from water using mixed matrix blend membranes,” *Sep. Purif. Technol.*, vol. 143, pp. 52–63,

2015.

[32] L. Burger, R. von Gruenewaldt, and T. Bird, “Atmospheric impact report : Sasol Secunda facility,” vol. 27, no. 11. 2014.

[33] A. Y. Sazonova and V. M. Raeva, “Recovery of acetonitrile from aqueous solutions by extractive distillation – effect of entrainer,” *Int. J. Chem. Mol. Nucl. Mater. Metall. Eng.*, vol. 9, no. 2, pp. 288–291, 2015.

[34] P. Das and S. Kumar, “Synthesis of highly water selective copolymer membranes for pervaporative dehydration of acetonitrile,” *J. Memb. Sci.*, vol. 507, pp. 81–89, 2016.

[35] M. K. Mandal, S. B. Sant, and P. K. Bhattacharya, “Dehydration of aqueous acetonitrile solution by pervaporation using PVA-iron oxide nanocomposite membrane,” *Colloids Surfaces A Physicochem. Eng. Asp.*, vol. 373, no. 1–3, pp. 11–21, 2010.

[36] N. R. Singha, P. Das, and S. K. Ray, “Recovery of pyridine from water by pervaporation using filled and crosslinked EPDM membranes,” *J. Ind. Eng. Chem.*, vol. 19, no. 6, pp. 2034–2045, 2013.

[37] C. Crew and T. Schafer, “Recovery of pyridine saves $1.5 million per year,” 1993.

[38] Sasol, “Sasol online sustainable development information: responding to environmental challenges,” 2015. .

[39] W. L. Luyben and I.-L. Chien, *Design and control of distillation systems for separating azeotropes*, vol. 53, no. 9. 2013.

[40] N. Hilal, G. Yousef, and P. Langston, “The reduction of extractive agent in extractive distillation and auto-extractive distillation,” *Chem. Eng. Process.*, vol. 41, no. 8, pp. 673–679, 2002.

[41] “Minimum requirements for the handling, classification and disposal of hazardous waste,” 1998.

[42] “Atmospheric emissions licence.”

[43] “Sasol online sustainable development information 2015: responding to environemntal challenges,” 2015. .

[44] E. Lladosa, J. B. Montón, and M. Burguet, “Separation of di-n-propyl ether and n-propyl alcohol by extractive distillation and pressure-swing distillation: computer simulation and economic optimization,” *Chem. Eng. Process. Process Intensif.*, vol. 50, no. 11–12, pp. 1266–1274, 2011.

[45] A. Kaewchada, S. Tubslingkra, and A. Jaree, “Separation of toluene from heptane via liquid–liquid extraction in microtube contactor using triethylene glycol,” *Chem. Eng. Res. Des.*, vol. 117, pp. 784–791, 2017.

[46] A. B. Pereiro and A. Rodríguez, “Ternary (liquid + liquid) equilibria of the azeotrope (ethyl acetate + 2-propanol) with different ionic liquids at T = 298.15 K,” *J. Chem. Thermodyn.*, vol. 39, no. 12, pp. 1608–1613, 2007.

[47] M. Królikowski, “Liquid-liquid extraction of p-xylene from their mixtures with alkanes using 1-butyl-1-methylmorpholinium tricyanomethanide and 1-butyl-3-methylimidazolium tricyanomethanide ionic liquids,” *Fluid Phase Equilib.*, vol. 412, pp. 107–114, 2016.

[48] M. Khayet, C. Cojocaru, and G. Zakrzewska-Trznadel, “Studies on pervaporation separation of acetone, acetonitrile and ethanol from aqueous solutions,” *Sep. Purif. Technol.*, vol. 63, no. 2, pp. 303–310, 2008.

[49] E. Drioli, S. Zhang, and A. Basile, “Recovery of pyridine from aqueous solution by membrane pervaporation,” *J. Memb. Sci.*, vol. 80, no. 1, pp. 309–318, 1993.

[50] A. Y. Pulyalina, G. A. Polotskaya, K. Y. Veremeychik, M. Y. Goikhman, I. V. Podeshvo, and A. M. Toikka, “Ethanol purification from methanol via pervaporation using polybenzoxazinoneimide membrane,” *Fuel Process. Technol.*, vol. 139, pp. 178–185, 2015.

[51] S. Xia, X. Dong, Y. Zhu, W. Wei, F. Xiangli, and W. Jin, “Dehydration of ethyl acetate-water mixtures using PVA/ceramic composite pervaporation membrane,” *Sep. Purif. Technol.*, vol. 77, no. 1, pp. 53–59, 2011.

[52] A. A. Kiss and R. R. Rewagad, “Energy efficient control of a BTX dividing-wall column,” *Comput. Chem. Eng.*, vol. 35, no. 12, pp. 2896–2904, 2011.

[53] J. Gmehling and C. Mollman, “Synthesis of Distillation Processes Using Thermodynamic Models and the Dortmund Data Bank,” *Am. Chem. Soc.*, vol. 5885, no. 97, pp. 3112–3123, 1998.

[54] L. Berg and Z. Yang, “Separation of pyridine from water using extractive distillation,” 1992.

[55] P. Prayoonyong, “Conceptual design of heterogeneous azeotropic distillation process for ethanol dehydration using 1-butanol as entrainer,” *Maejo Int. J. Sci. Technol.*, vol. 8, no. 3, pp. 334–347, 2014.

[56] P. Langston, N. Hilal, S. Shingfield, and S. Webb, “Simulation and optimisation of extractive distillation with water as solvent,” *Chem. Eng. Process. Process Intensif.*, vol. 44, no. 3, pp. 345–351, 2005.

[57] W. F. Shen, H. Benyounes, and J. Song, “Thermodynamic topological analysis of extractive distillation of maximum boiling azeotropes,” *Brazilian J. Chem. Eng.*, vol. 32, no. 4, pp. 957–966, 2015.

[58] G. De Koeijer and S. Kjelstrup, “Minimizing entropy production rate in binary tray distillation,” *Int. J. Thermodyn.*, vol. 3, no. 3, pp. 105–110, 2000.

[59] P. Salamon, G. Siragusa, M. Schaller, and K. H. Hoffmann, “Comparison of entropy production rate minimization methods for binary diabatic distillation,” pp. 5826–5834, 2002.

[60] R. Rivero, “Exergy simulation and optimization of adiabatic and diabatic binary distillation,” vol. 26, pp. 561–593, 2001.

[61] Ö. Yildirim, A. A. Kiss, and E. Y. Kenig, “Dividing wall columns in chemical process industry: A review on current activities,” *Sep. Purif. Technol.*, vol. 80, no. 3, pp. 403–417, 2011.

[62] R. Delgado-Delgado, S. Hernández, F. O. Barroso-Muñoz, J. G. Segovia-Hernández, and V. Rico-Ramírez, “Some operational aspects and applications of dividing wall columns: energy requirements and carbon dioxide emissions,” *Clean Technol. Environ. Policy*, vol. 17, no. 3, pp. 657–665, 2015.

[63] R. K. Dohare, K. Singh, and R. Kumar, “Modeling and model predictive control of dividing wall column for separation of Benzene–Toluene- *o* -Xylene,” *Syst. Sci. Control Eng.*, vol. 3, no. 1, pp. 142–153, 2015.

[64] M. T. D. Nguyen, “Conceptual Design, Simulation and Experimental Validation of Divided Wall Column: Application for Nonreactive and Reactive Mixture,” Toulouse Institute of Technology, 2015.

[65] W. E. De Villiers, R. N. French, and G. J. Koplos, “Navigate phase equilibria via residue curve maps,” *Chem. Eng. Prog.*, vol. 98, no. 11, pp. 66–71, 2002.

[66] Y. C. Wu and I. L. Chien, “Design and control of heterogeneous azeotropic column system for the separation of pyridine and water,” *Ind. Eng. Chem. Res.*, vol. 48, no. 23, pp. 10564–10576, 2009.

[67] H. Benyounes, W. Shen, and V. Gerbaud, “Entropy Flow and Energy Efficiency Analysis of Extractive Distillation with a Heavy Entrainer,” *ACS*, pp. 4778–4791, 2014.

[68] S. Xia, X. Dong, Y. Zhu, W. Wei, F. Xiangli, and W. Jin, “Dehydration of ethyl acetate-water mixtures using PVA/ceramic composite pervaporation membrane,” *Sep. Purif. Technol.*, vol. 77, no. 1, pp. 53–59, 2011.

[69] E. R. Gilliland, “Multicomponent Rectification- Estimates of the Number of Theoretical Plates as a Function of the Reflux Ratio,” *Ind. Eng. Chem.*, vol. 32, no. 9, pp. 1220–1223, 1940.

[70] M. A. Soliman, “A shortcut method for binary distillation column design,” in *Towards Engineering Environment to Merge in a Competitive Global Economy*, 2007.

[71] G.-J. A. F. Fien and Y. A. Liu, “Heuristic synthesis and shortcut design of separation Processes using residue curve maps: A review,” *Ind. Eng. Chem. Res.*, vol. 33, no. 11, pp. 2505–2522, 1994.

[72] “Chloroform Price, Chloroform Price Suppliers and Manufacturers at Alibaba.com.” [Online]. Available: https://www.alibaba.com/showroom/chloroform-price.html. [Accessed: 18-Oct-2017].

[73] “Pyridine Price, Pyridine Price Suppliers and Manufacturers at Alibaba.com.” [Online]. Available: https://www.alibaba.com/showroom/pyridine-price.html. [Accessed: 18-Oct-2017].

[74] S. Becht, R. Franke, A. Geißelmann, and H. Hahn, “An industrial view of process intensification,” *Chem. Eng. Process. Process Intensif.*, vol. 48, no. 1, pp. 329–332, Jan. 2009.

[75] M. A. Schultz, D. G. Stewart, J. M. Harris, S. P. Rosenblum, M. S. Shakur, and D. E. O’Brien, “Reduce costs with dividing-wall columns,” *Chem. Eng. Prog.*, vol. 98, no. 5, pp. 64–71, 2002.

[76] V. K. Sangal, V. Kumar, and I. M. Mishra, “Optimization of a Divided Wall Column for the Separation of C4-C6 Normal Paraffin Mixture using Box-Behken design,” *Chem. Ind. Chem. Eng. Q.*, vol. 19, no. 1, pp. 107–119, 2013.

[77] I. Dejanović, L. Matijašević, and Ž. Olujić, “Dividing wall column-A breakthrough towards sustainable distilling,” *Chem. Eng. Process. Process Intensif.*, vol. 49, no. 6, pp. 559–580, 2010.

[78] Y. H. Kim, “Energy saving and thermodynamic efficiency of a double-effect distillation column using internal heat integration,” *Korean J. Chem. Eng.*, vol. 29, no. 12, pp. 1680–1687, 2012.

[79] “Briefing Main EU Directives on Waste.”

[80] European Commission, “Reference document on the Best Available Techniques for Waste Incineration,” *Integr. Pollut. Prev. Control*, no. August, pp. 1–638, 2006.

[81] “Energy from Waste: Part 1 -The Myths Debunked - YouTube,” 2007.

[82] P. Connett, “Zero waste: A global perspective,” 2006. [Online]. Available: https://web.archive.org/web/20080406085208/http://www.recycle.ab.ca/2006Proceedings/PaulConnett_Zero_waste.pdf. [Accessed: 23-Oct-2017].

[83] S. Cimini, M. Prisciandaro, and D. Barba, “Simulation of a waste incineration process with flue gas cleaning and heat recovery sections using Aspen Plus,” *Waste Manag.*, 2005.

[84] “Net Present Value - NPV.” [Online]. Available: http://www.investopedia.com/terms/n/npv.asp. [Accessed: 26-Oct-2017].

[85] “NPV and IRR in Excel 2010 - YouTube.” [Online]. Available: https://www.youtube.com/watch?v=qAhV3xG0i8s. [Accessed: 26-Oct-2017].

[86] United Nations, “Waste,” *State Environ. Asia Pacific*, pp. 170–194, 2000.

[87] M. Loizidou, “Waste Valorization and Management,” *Waste and Biomass Valorization*, vol. 7, no. 4, pp. 645–648, 2016.

Appendix B: Shortcut Models Specifications

Appendix B.1. Shortcut Model Specifications for the water-pyridine mixture separation from the HOW

The light key is defined the component whose presence is in the residue is substantial but components lighter than it are present in small concentrations. On the other hand, is the components with a recognizable presence in the distillate but components with higher boiling points have negligible concentrations in the distillate

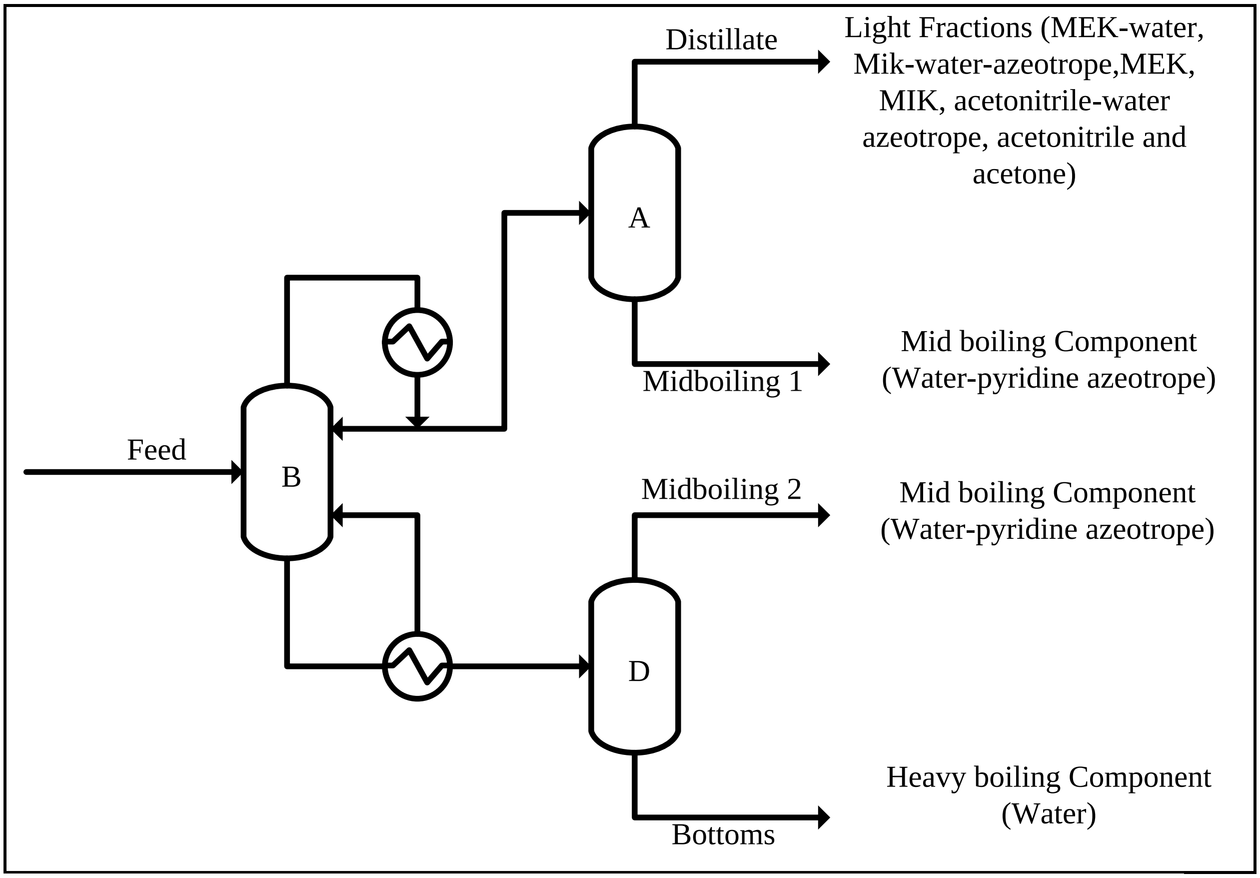

Figure B.1. DWC shortcut model

4.5.1.1. Specifications on Aspen Plus for the Shortcut Model

In the following specifications, the pressure of the column is the same, this is mainly because the columns represent one Dividing Wall Column. Furthermore, the absorbers have the same number of stages since they both represent the middle section of the column. Absorber 1 represents one side of the wall while the second absorber represents the other side of the wall. The shortcut model is purely trial and error process to achieve the desired results. Consequently, the recovery specifications in the shortcut model were established through trial and error to achieve the desired results.

Column B

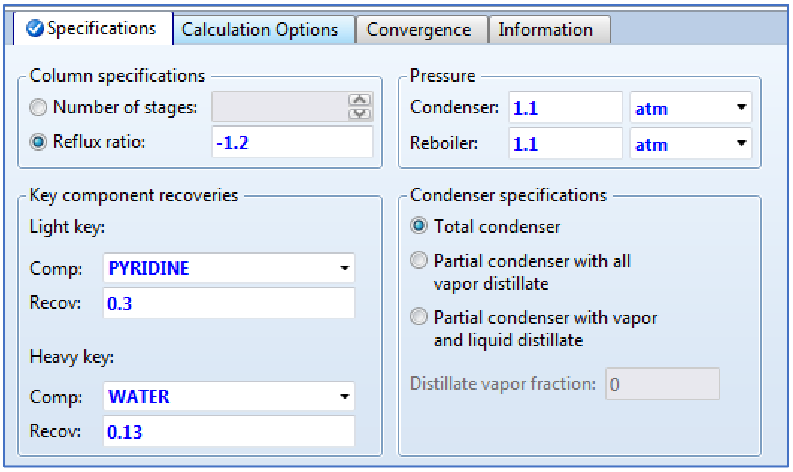

Column specifications
○ Number of stages:
● Reflux ratio: -1.2

Pressure
Condenser: 1.1 atm
Reboiler: 1.1 atm

Key component recoveries
Light key:
Comp: PYRIDINE
Recov: 0.3
Heavy key:
Comp: WATER
Recov: 0.13

Condenser specifications
● Total condenser
○ Partial condenser with all vapor distillate
○ Partial condenser with vapor and liquid distillate
Distillate vapor fraction: 0

Figure B.2. Column B specifications

The reflux ration is specified as -1.2 (Figure B.2). This is interpreted by Aspen to mean 1.2 times the minimum reflux ratio. The value 1.2 is justified because of the specification itself relate to the Fenske equation assumptions. The column is assumed to be run at 1.1atm and total condenser is chosen. The recovery refers to the fraction of a particular component that reports to the distillate. Conventionally, pyridine is heavier than water but because in this case pyridine has formed an azeotrope with water and the azeotrope's boiling point is lower than that of water, pyridine is taken as the light fraction and water taken as the heavy component.

Column A

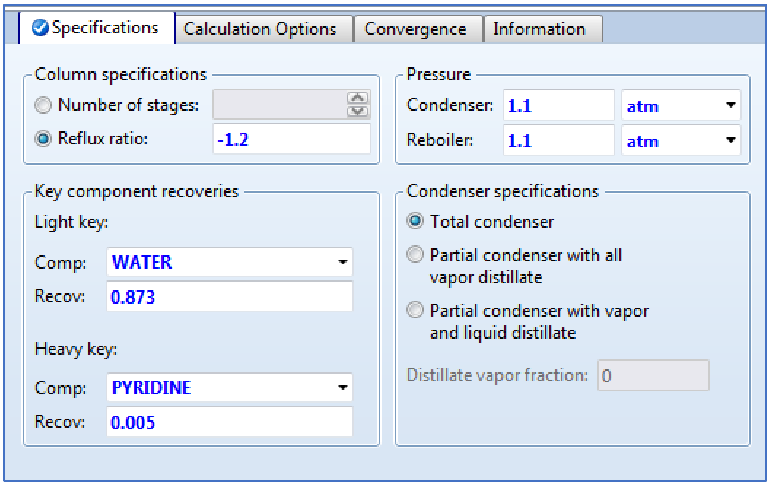

Column specifications
○ Number of stages:
● Reflux ratio: -1.2

Pressure
Condenser: 1.1 atm
Reboiler: 1.1 atm

Key component recoveries
Light key:
Comp: WATER
Recov: 0.873
Heavy key:
Comp: PYRIDINE
Recov: 0.005

Condenser specifications
● Total condenser
○ Partial condenser with all vapor distillate
○ Partial condenser with vapor and liquid distillate
Distillate vapor fraction: 0

Figure B.3. Column A specifications.

In the specifications of column A, recovery of water is assumed to be 87% and that of pyridine to be 0.5%. Ideally, the recovery of pyridine must be 0 but then Aspen Plus does not run when this is done so the closest value to zero is taken instead. The recovery of water in this column is very high because only a small fraction of the original quantity was entrained to this column. The water in this column is specified as the light component because a fraction of water will report to the distillate along with light components in the stream. This occurs because water also forms azeotropes with light components and these azeotropes boiling at a lower temperature and all of them boil at a lower temperature than the water-pyridine azeotrope. Therefore, this specification is justified.

Column D

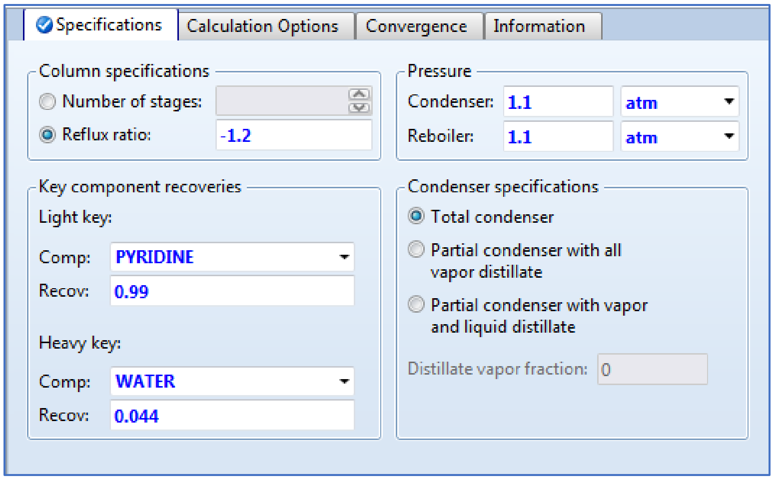

Column specifications

○ Number of stages:

● Reflux ratio: -1.2

Pressure

Condenser: 1.1 atm

Reboiler: 1.1 atm

Key component recoveries

Light key:

Comp: PYRIDINE

Recov: 0.99

Heavy key:

Comp: WATER

Recov: 0.044

Condenser specifications

● Total condenser

○ Partial condenser with all vapor distillate

○ Partial condenser with vapor and liquid distillate

Distillate vapor fraction: 0

Figure B.4. Column D specifications

In the stripper section (column D) the recovery of pyridine is stated as 0.99 to minimize losses to the bottoms product. In this column pyridine is again the light component because all of it along with some of the water (water-pyridine azeotrope) report to the distillate.

Appendix C: Detailed Material balances

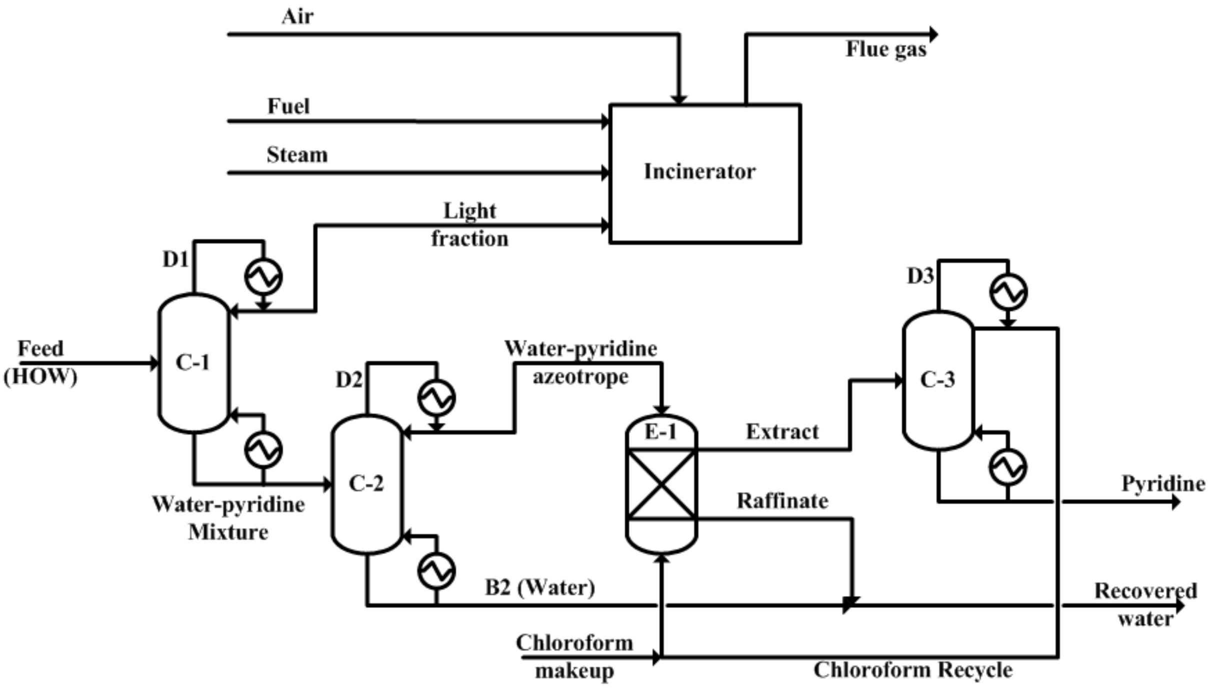

Figure C.1. Proposed pyridine recovery process

Appendix C.1. Pyridine Enrichment Section Material Balances

Table C.1. Extraction Column (E-1) detailed material balances

Parameter	**Water-pyridine azeotrope**	**Chloroform**	**Extract**	**Raffinate**
Mole Basis				
Total Flow (kmol/hr)	**6.1**	**2.736**	**4.227345**	**4.608372**
Composition (Mole Fraction)				
Pyridine	0.236	0.000	0.341	0.000
Acetone	0.000	0.000	0.000	0.000
Water	0.755	0.282	0.182	0.999
Acetonitrile	0.009	0.001	0.014	0.000
Methyl Ethyl Ketone	0.000	0.000	0.000	0.000
Methyl Isopropyl Ketone	0.000	0.000	0.000	0.000
Chloroform	0.000	0.717	0.463	0.001
Mass Basis				
Total Flow (kg/hr)	**199.252**	**248.200**	**363.936**	**83.516**
Composition (Mass Fraction)				
Pyridine	0.573	0.000	0.313	0.000
Acetone	0.000	0.000	0.000	0.000
Water	0.416	0.056	0.038	0.993
Acetonitrile	0.011	0.000	0.006	0.000
Methyl Ethyl Ketone	0.000	0.000	0.000	0.000
Methyl Isopropyl Ketone	0.000	0.000	0.000	0.000
Chloroform	0.000	0.944	0.642	0.007

Table C.2. Regeneration Column (B4) Detailed Material Balances

Parameter	**Extract**	**Chloroform recycle**	**Pyridine**
Mole Basis			
Total Flow (kmol/hr)	**4.227**	**2.727**	**1.500**
Composition (Mole Fraction)			
Pyridine	0.341	0.000	0.961
Acetone	0.000	0.000	0.000
Water	0.182	0.283	0.000
Acetonitrile	0.014	0.001	0.036
Methyl Ethyl Ketone	0.000	0.000	0.000
Methyl Isopropyl Ketone	0.000	0.000	0.000
Chloroform	0.463	0.716	0.002
Mass Basis			
Total Flow (kg/hr)	**363.936**	**247.200**	**116.736**
Composition (Mass Fraction)			
Pyridine	0.313	0.000	0.977
Acetone	0.000	0.000	0.000
Water	0.038	0.056	0.000
Acetonitrile	0.006	0.001	0.019
Methyl Ethyl Ketone	0.000	0.000	0.000
Methyl Isopropyl Ketone	0.000	0.000	0.000
Chloroform	0.642	0.943	0.004

Appendix C.2. Dividing Wall Column Material Balances

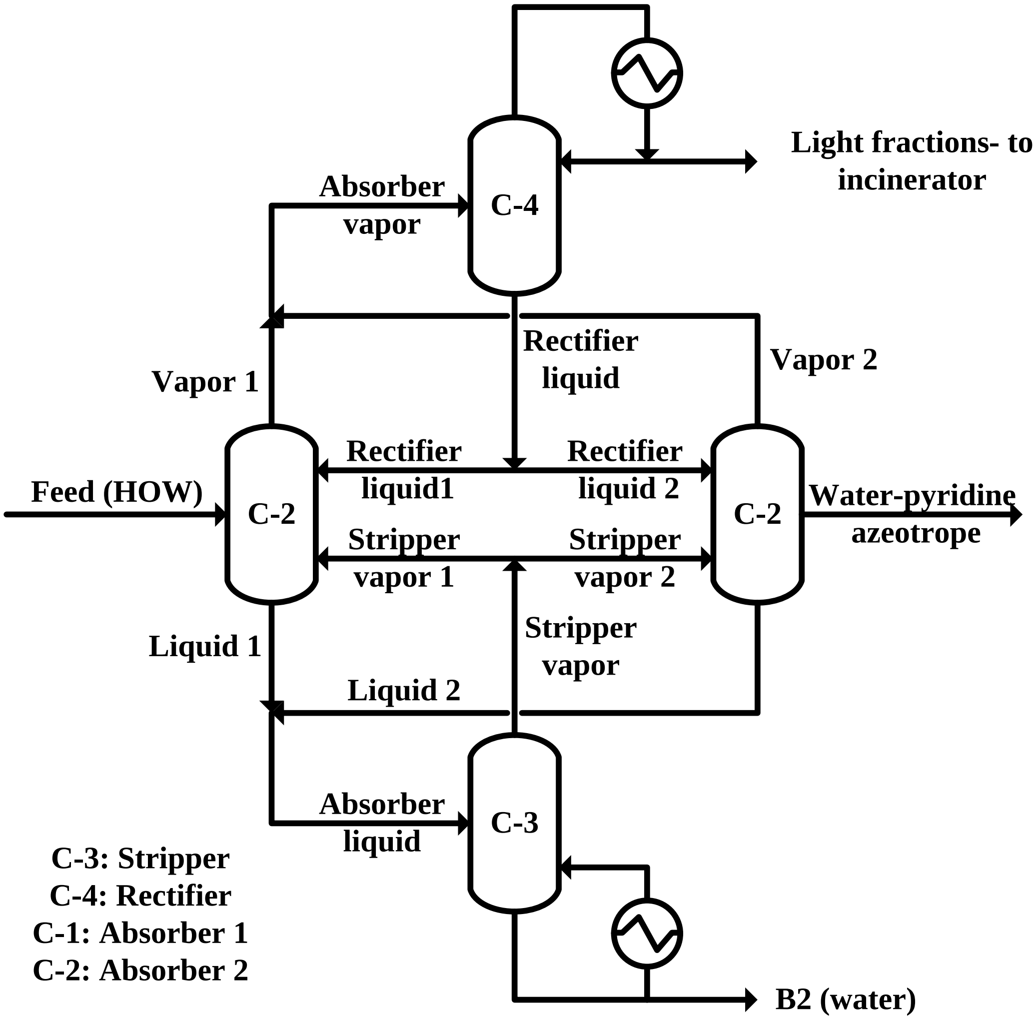

Figure C.2. Dividing Wall Column setup as modelled on Aspen Plus

Table C.3. Absorber 1 detailed material balance

Parameter	**Feed**	**Stripper vapor1**	**Rectifier liquid 1**	**Stripper vapor 1**	**Liquid 1**
Mole Basis					
Total Flow (kmol/hr)	**93.528**	**82.007**	**74.498**	**80.796**	**169.237**
Composition (Mole Fraction)					
Pyridine	0.015	0.183	0.063	0.013	0.118
Acetone	0.008	0.000	0.003	0.013	0.000
Water	0.840	0.807	0.502	0.425	0.873
Acetonitrile	0.089	0.010	0.264	0.339	0.009
Methyl Ethyl Ketone	0.014	0.000	0.022	0.036	0.000
Methyl Isopropyl Ketone	0.034	0.000	0.146	0.174	0.000
Mass Basis					
Total Flow (kg/hr)	**2281.542**	**2411.301**	**2919.123**	**3308.026**	**4303.940**
Composition (Mass Fraction)					
Pyridine	0.050	0.491	0.126	0.026	0.368
Acetone	0.020	0.000	0.005	0.018	0.000
Water	0.620	0.495	0.231	0.187	0.619
Acetonitrile	0.150	0.014	0.277	0.340	0.014
Methyl Ethyl Ketone	0.040	0.000	0.041	0.064	0.000
Methyl Isopropyl Ketone	0.120	0.000	0.321	0.366	0.000

Table C.4. Rectifier detailed material balances

Parameter	**Absorber vapor**	**Rectifier liquid**	**Light fractions**
Mole Basis			
Total Flow (kmol/hr)	**171.593**	**148.995**	**22.598**
Composition (Mole Fraction)			
Pyridine	0.054	0.063	0.000
Acetone	0.007	0.003	0.035
Water	0.487	0.502	0.389
Acetonitrile	0.279	0.264	0.377
Methyl Ethyl Ketone	0.027	0.022	0.056
Methyl Isopropyl Ketone	0.145	0.146	0.143
Mass Basis			
Total Flow (kg/hr)	**6761.729**	**5838.245**	**923.483**
Composition (Mass Fraction)			
Pyridine	0.109	0.126	0.000
Acetone	0.011	0.005	0.050
Water	0.223	0.231	0.171
Acetonitrile	0.291	0.277	0.379
Methyl Ethyl Ketone	0.049	0.041	0.100
Methyl Isopropyl Ketone	0.318	0.321	0.301

Table C.5. Stripper detailed material balances

Parameter	Absorber liquid	Stripper vapor	B2(Water)
Mole Basis			
Total Flow (kmol/hr)	**228.940**	**164.014**	**64.927**
Composition (Mole Fraction)			
Pyridine	0.131	0.183	0.000
Acetone	0.000	0.000	0.000
Water	0.862	0.807	1.000
Acetonitrile	0.007	0.010	0.000
Methyl Ethyl Ketone	0.000	0.000	0.000
Methyl Isopropyl Ketone	0.000	0.000	0.000
Mass Basis			
Total Flow (kg/hr)	**5992.274**	**4822.603**	**1169.671**
Composition (Mass Fraction)			
Pyridine	0.395	0.491	0.000
Acetone	0.000	0.000	0.000
Water	0.593	0.495	1.000
Acetonitrile	0.011	0.014	0.000
Methyl Ethyl Ketone	0.000	0.000	0.000
Methyl Isopropyl Ketone	0.000	0.000	0.000

Table C.6. Absorber 2 detailed material balances

Parameter	**Stripper vapor 2**	**Rectifier liquid 2**	**Vapor 2**	**Liquid 2**	**Water-pyridine azeotrope**
Mole Basis					
Total Flow (kmol/hr)	**82.007**	**74.498**	**90.073**	**60.332**	**6.100**
Composition (Mole Fraction)					
Pyridine	0.183	0.063	0.091	0.164	0.247
Acetone	0.000	0.003	0.003	0.000	0.000
Water	0.807	0.502	0.543	0.831	0.747
Acetonitrile	0.010	0.264	0.225	0.004	0.006
Methyl Ethyl Ketone	0.000	0.022	0.018	0.000	0.000
Methyl Isopropyl Ketone	0.000	0.146	0.121	0.000	0.000
Mass Basis					
Total Flow (kg/hr)	**2411.301**	**2919.123**	**3428.981**	**1698.650**	**202.794**
Composition (Mass Fraction)					
Pyridine	0.491	0.126	0.189	0.462	0.588

Acetone	0.000	0.005	0.004	0.000	0.000
Water	0.495	0.231	0.257	0.532	0.405
Acetonitrile	0.014	0.277	0.242	0.006	0.007
Methyl Ethyl Ketone	0.000	0.041	0.035	0.000	0.000
Methyl Isopropyl Ketone	0.000	0.321	0.273	0.000	0.000

Appendix D: Binary Parameters

Table D.10: Binary parameters for the pre-concentration section

Comp i	Comp j	AIJ	AJI	BIJ	BJI	CIJ	TLower (C)	TUpper(C)
Pyridine	Acetone	-5.854	5.573	1966.062	-1793.400	0.300	30.000	115.300
Pyridine	Water	0.138	5.118	-197.679	-735.747	0.300	50.000	115.500
Acetone	Water	6.398	0.054	-1808.991	419.972	0.300	20.000	95.100
Acetone	Acetonitrile	0.000	0.000	-53.460	53.285	0.300	45.000	80.400
Acetone	MEK	-8.099	5.103	2364.934	-1083.496	0.300	56.200	79.500
Water	Acetonitrile	1.057	-0.116	283.409	256.459	0.300	60.000	94.900
Water	MEK	0.000	0.000	1087.744	201.301	0.300	73.300	100.000
Water	MIK	10.721	-3.839	-2071.876	1378.792	0.200	20.000	30.000
Acetonitrile	MEK	0.000	0.000	224.274	-143.421	0.300	55.000	60.520
MEK	MIK	0.000	0.000	-220.770	278.458	0.300	78.000	93.850
Pyridine	Acetonitrile	0.000	0.000	669.600	-455.011	0.300	25.000	25.000
Pyridine	MEK	0.000	0.000	180.649	-125.756	0.300	25.000	25.000
Pyridine	MIK	0.000	0.000	253.748	-191.946	0.300	25.000	25.000
Acetone	MIK	0.000	0.000	138.794	-114.406	0.300	25.000	25.000
Acetonitrile	MIK	0.000	0.000	315.820	-189.130	0.300	25.000	25.000

Table D.2. Binary parameters of the chloroform-water-pyridine mixture

Comp* i **Comp* j**	**Pyridine** **Water**	**Pyridine** **Chloroform**	**Water** **Chloroform**
a_{ij}	0.138	2.671	8.844
a_{ji}	5.118	-4.517	-7.352
b_{ij}	-197.679	-1225.041	-1140.115
b_{ji}	-735.747	1595.533	3240.688
c_{ij}	0.300	0.300	0.200

Comp*: Component

Appendix E: Calculations

Calculation 1: Chloroform system

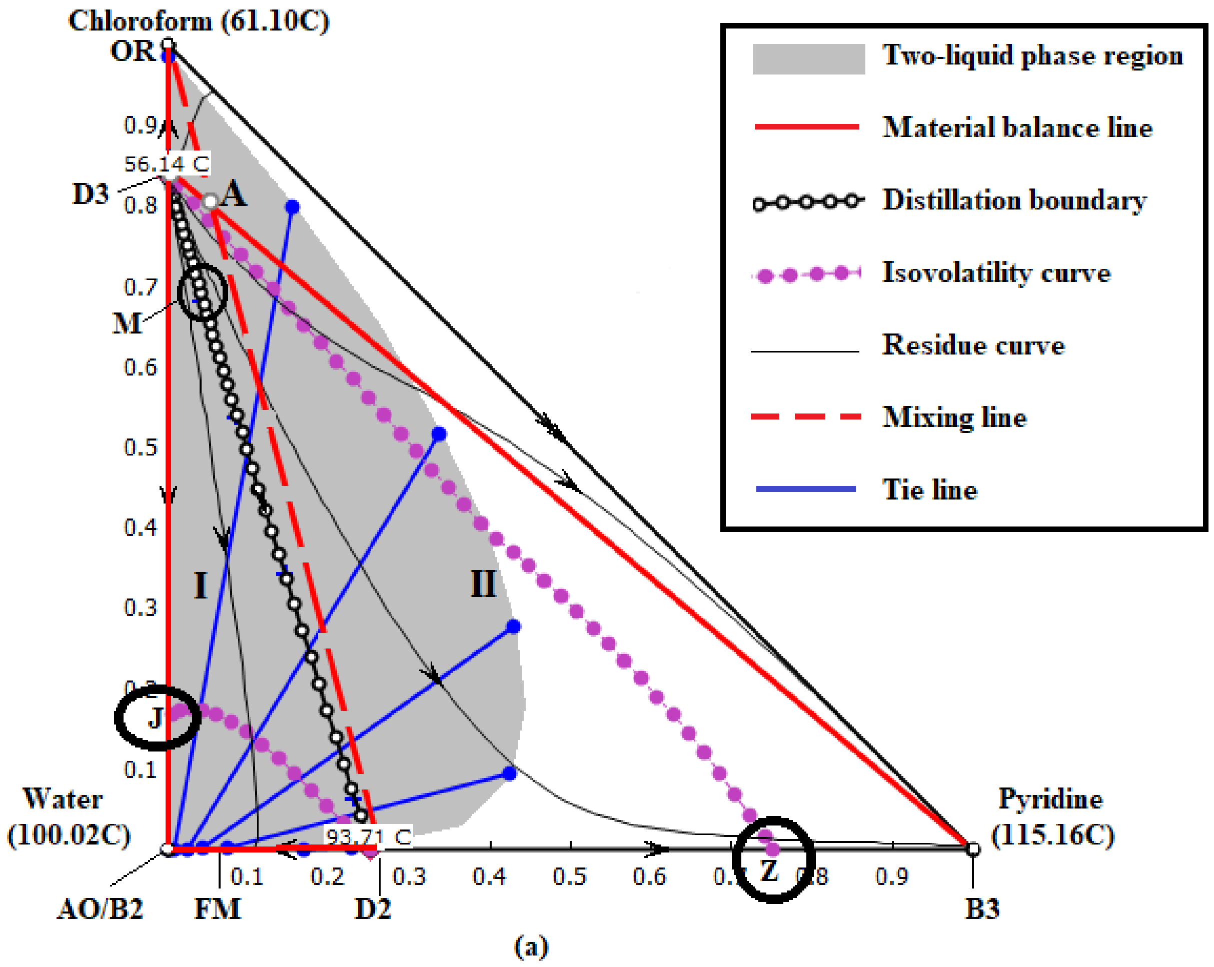

Figure E.1. Water-pyridine-chloroform residue curve map

The composition of the chloroform in the ternary mixture required for feasible separation is 80mol% (point **A** in the RCM above). If we assume the ternary mixture flowrate of 1kmol/hr, it is established that the chloroform flowrate is 0.8kmol/hr and the azeotropic mixture is 0.2kmol/hr. Therefore, the entrainer to azeotropic mixture is calculated as thus:

$$EA = \frac{Entrainer\ flowrate}{Azeotropic\ mixture\ flowrate} \qquad (E.1)$$

$$EA = \frac{0.8 kmol/hr}{0.2 kmol/hr} = 4.000$$

The entrainer to azeotropic mixture ratio is therefore 4.000:1.000.

The ratio for the improved design was calculated using the same procedure and it was found that the ratio was 0.360:1.

(a) The entrainer to azeotropic mixture ratio from simulation material balance

$$Chloroform\ flowrate\ entering\ extraction\ column\ C-1 = 0.717 \times 2.736 \frac{kmol}{hr}$$

$$= 1.961 \frac{kmol}{hr}$$

$$water - pyridine\ azeotropic\ mixture\ flowrate = 6.100 \frac{kmol}{hr}$$

Therefore, using equation E.1, the chloroform to water-pyridine azeotropic mixture is calculated as:

$$Entrainer\ to\ azeotropic\ mixture\ ratio = \frac{1.961\ kmol/hr}{6.1\ kmol/hr} = 0.320$$

Therefore, the chloroform to water-pyridine azeotropic mixture was 0.320:1.

(b) Relative error calculation for the for the predicted chloroform to water-pyridine azeotropic mixture

$$percentage\ relative\ error = \frac{|x - x_0|}{x} \times 100 \qquad E.2$$

Where:

x: entrainer to mixture ratio from the simulation material balance

x_0: entrainer to azeotropic mixture ratio predicted from the RCM

$$percentage\ relative\ error = \frac{0.320 - 0.360}{0.320} \times 100 = 12.500\%$$

Calculation 2: Toluene system

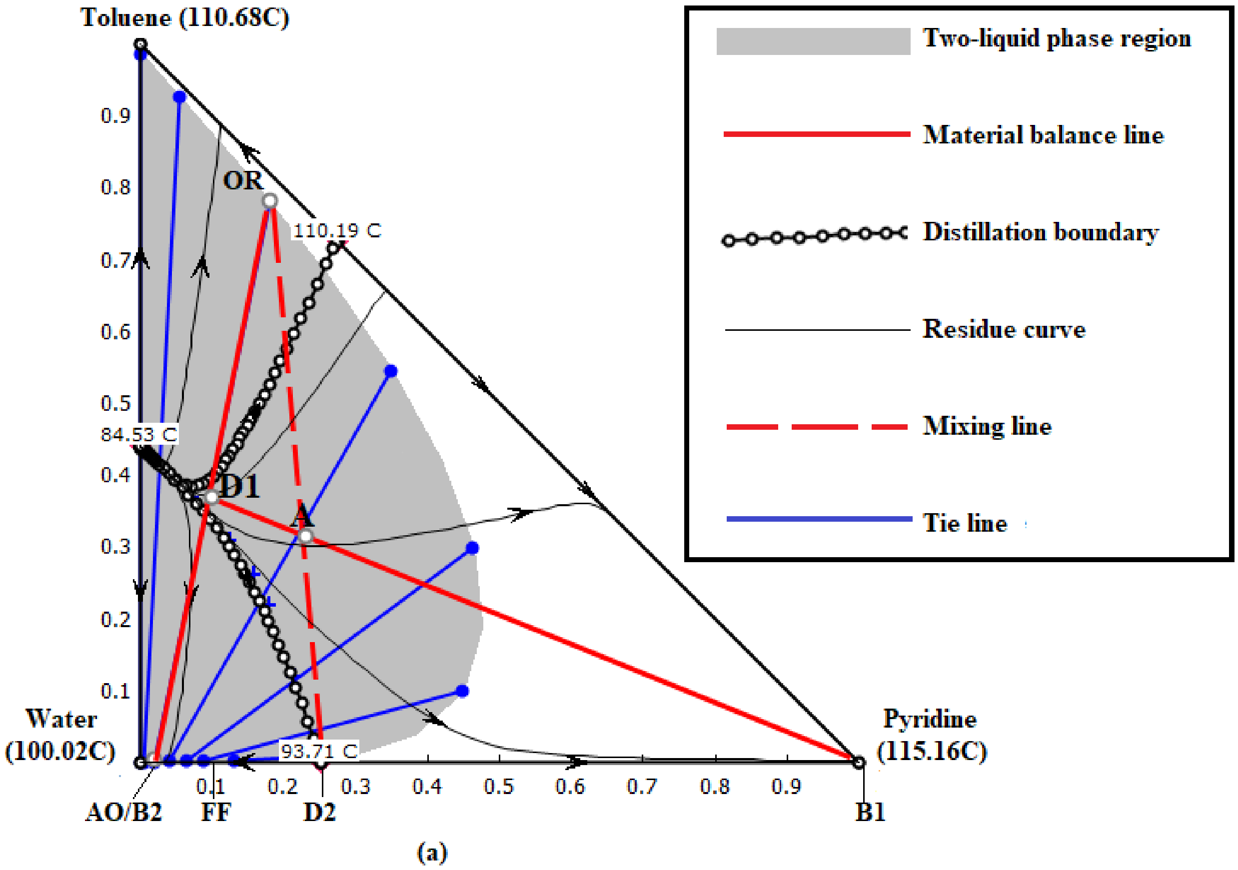

Figure E.2. Toluene-water-pyridine system residue curve map

(a) Predictive calculation of toluene to water-pyridine azeotropic mixture ratio from RCM

The same procedure used in *calculation 1a* above was used to determine the toluene to azeotropic mixture ratio from the RCM. The ratio was calculated to be **0.471:1**.

(b) Toluene to water-pyridine azeotropic mixture ratio calculated from simulation results.

$$Toluene\ flowrate\ entering\ azeotropic\ distillation\ column\ C-1 = 305.1\frac{kmol}{hr} \times 0.839$$

$$= 255.978\frac{kmol}{hr}$$

$$Water - pyridine\ azeotropic\ mixture\ flowrate = 490.4\ kmol/hr$$

Using equation E.1, the toluene to water-pyridine azeotropic mixture was calculated as thus:

$$entrainer\ to\ mixture\ ratio = \frac{255.978 kmol/hr}{490.400 kmol/hr} = 0.522$$

Therefore, toluene to azeotropic mixture is ratio is 0.522:1.

Appendix F: Entropy Generation Data

Table F.1. Vapor and liquid streams entropy

Stage	liquid stream Entropy (kJ/kmol-K)	Vapor stream Entropy(Kj/kmol-K)
1	-42.678	0.000
2	-45.904	-19.258
3	-45.944	-22.220
4	-45.889	-22.498
5	-45.904	-22.453
6	-46.790	-22.353
7	-46.758	-23.501
8	-46.618	-23.655
9	-46.349	-23.493
10	-45.890	-23.125
11	-45.176	-22.496
12	-44.178	-21.539
13	-42.948	-20.249
14	-41.621	-18.737
15	-40.364	-17.195
16	-39.302	-15.820
17	-38.493	-14.730
18	-37.928	-13.953
19	-37.567	-13.448
20	-37.373	-13.148
21	-37.339	-13.002
22	-37.536	-12.994
23	-38.162	-13.178
24	-39.574	-13.743
25	-42.083	-15.067
26	-45.506	-17.571

27	-49.150	-21.215
28	-52.291	-25.315
29	-54.497	-29.007
30	-55.779	-31.696

Table F.2. Entropy generated on each stage, liquid and vapor stream flowrates

stage	Entropy generation (KW/K)	Liquid flow (kmol/hr)	Vapor flow(kmol/hr)
1	3.433	6.818	0.000
2	0.256	6.939	9.546
3	0.050	7.030	9.666
4	-7.123	7.026	9.758
5	-174.681	6.875	9.753
6	0.392	10.734	9.173
7	0.145	10.793	9.234
8	0.199	10.787	9.293
9	0.365	10.756	9.287
10	0.603	10.703	9.256
11	0.853	10.628	9.203
12	1.029	10.544	9.128
13	1.077	10.472	9.044
14	1.005	10.430	8.972
15	0.855	10.423	8.930
16	0.673	10.443	8.923
17	0.497	10.477	8.943
18	0.350	10.513	8.977
19	0.239	10.543	9.013
20	0.162	10.564	9.043
21	0.127	10.568	9.063
22	0.202	10.546	9.068
23	0.548	10.477	9.046
24	1.210	10.336	8.977
25	1.797	10.131	8.836
26	1.944	9.924	8.631
27	1.713	9.775	8.424

28	1.272	9.695	8.274
29	184.294	9.668	8.194
30	23.486	1.500	8.167

Table F.3. Components compositions and activity coefficients in trays

	Activity coefficient (γ)			Liquid composition (x)				
Stage	Pyridine	Water	Acetonitrile	Chloroform	Pyridine	Water	Acetonitrile	Chloroform
1	0.084	11.234	0.762	1.430	0.000	0.330	0.000	0.670
2	0.246	75.184	1.069	1.005	0.000	0.283	0.001	0.716
3	0.301	79.957	1.152	1.000	0.000	0.102	0.002	0.896
4	0.305	78.668	1.155	1.000	0.000	0.085	0.004	0.912
5	0.321	68.349	1.119	1.001	0.001	0.084	0.005	0.910
6	0.461	28.646	0.923	0.982	0.011	0.076	0.008	0.905
7	0.479	29.479	0.951	0.976	0.012	0.014	0.011	0.963
8	0.479	28.977	0.961	0.976	0.012	0.002	0.017	0.969
9	0.474	27.770	0.973	0.977	0.013	0.000	0.027	0.960
10	0.465	25.717	0.993	0.980	0.013	0.000	0.047	0.941
11	0.455	22.706	1.020	0.981	0.013	0.000	0.082	0.905
12	0.448	18.994	1.052	0.979	0.014	0.000	0.139	0.848
13	0.453	15.195	1.079	0.971	0.015	0.000	0.222	0.763
14	0.474	11.897	1.093	0.954	0.018	0.000	0.327	0.655

15	0.516	9.364	1.091	0.932	0.022	0.000	0.445	0.533
16	0.573	7.569	1.077	0.908	0.028	0.000	0.560	0.412
17	0.636	6.358	1.059	0.886	0.035	0.000	0.661	0.304
18	0.698	5.564	1.041	0.866	0.042	0.000	0.742	0.216
19	0.750	5.046	1.026	0.850	0.048	0.000	0.803	0.149
20	0.792	4.706	1.015	0.836	0.054	0.000	0.845	0.101
21	0.824	4.467	1.007	0.820	0.060	0.000	0.873	0.067
22	0.851	4.267	1.000	0.793	0.068	0.000	0.888	0.044
23	0.877	4.033	0.994	0.743	0.083	0.000	0.887	0.030
24	0.911	3.696	0.984	0.656	0.117	0.000	0.862	0.020
25	0.954	3.251	0.966	0.547	0.188	0.000	0.797	0.015
26	0.991	2.811	0.941	0.453	0.310	0.000	0.678	0.012